No. 327
September 1994

An Experimental Study for Slamming Flow and Green Water on Deck
Final Report

This research was carried out in part under the Office of Naval Research Applied Hydrodynamic Research Program, Contract No. DOD-G-N00014-90-J-1818. Reproduction in whole or in part is permitted for any purpose of the United States Government.

An Experimental Study for Slamming Flow and Green Water on Deck
Final Report

A.W. Troesch
Minglun Wang

Department of Naval Architecture
and Marine Engineering

An Experimental Study for Slamming Flow and Green Water on Deck

Final Report

by
Armin W. Troesch
Minglun Wang

Department of Naval Architecture and Marine Engineering
The University of Michigan

August 1994

ABSTRACT

The results of an experimental investigation on large-amplitude oscillations of an axisymmetric flared body in a free surface are presented here, the goal being to generate sets of quality experimental data, e.g. time-history measurements, for the study of slamming flows and green water on deck, as well as comparison with time-domain numerical codes. The measured data include time histories of the prescribed displacement, the acceleration, the resultant force, and the wave elevation at several locations away from the body. Both the deck dry condition and green-water-on-deck cases are studied. A range of oscillation frequencies and amplitudes are covered to investigate steep waves, local wavebreaking, and spray sheets. Video recordings were also taken in each run to provide qualitative photographs for breaking wave profiles and contact line dynamics.

Contents

1 Introduction **3**

2 Experimental Setup **5**

3 Task Matrix for the Experiments **7**

4 Formulation of Motion Equations **12**
4.1 Deck Dry Condition 12
4.2 Green Water on Deck 13

5 Results and Analysis **14**

6 Summary and Conclusions **45**

7 Acknowledgments **47**

A Description of Experimental Data **50**

B Figures of Time Histories and the FFT Analyses **52**

C Tables of Fourier Coefficients **141**

Chapter 1

Introduction

Increasing demand for understanding the complexity of nonlinear free-surface flows, such as bottom and bow flare slamming and green water on deck, necessitates the experimental investigation on large-amplitude motion of an idealized axisymmetric flared body. Of particular interest are the nonlinear hydrodynamic phenomena of the flare-slamming and deck-wetness flows during large-amplitude oscillations. Among the many slamming experiments performed in attempting to investigate the forced vertical oscillations of different models are early slamming researches of segmented ship models, rectangular and circular cylinders, wedges with different dead rise angels, and so forth (e.g. Tasai and Koterayama, 1976 and Radev and Beukelman, 1992). This experimental program is primarily designed to generate sets of quality experimental data, e.g. time-history measurements, for comparison with time-domain numerical codes, as well as video recordings to provide qualitative information for breaking wave profiles and contact line dynamics.

The experimental tests were performed at the University of Michigan Marine Hydrodynamics Laboratory (MHL) to measure the time histories of the prescribed motions including the prescribed displacement and the acceleration, the wave elevation, and the resultant forces. The MHL's vertical motion mechanism (VMM) is used to conduct such large-amplitude oscillation experiments. The axisymmetric flared body was forced to oscillate sinusoidally with different frequencies and amplitudes so that different wave profiles, such as steep waves, local wavebreaking, spray sheets, and so on, could be observed. The flared body was previously used by Troesch and Kang (1986

and 1988) and Kang (1988) in drop tests where impact forces were measured and the experimental results showed mixed agreement with their highly nonlinear impact theory. In this experiment, the measured data include time histories of the prescribed displacement, the resultant force, and the wave elevation at several locations away from the body. Video recordings were also taken in each run for qualitative photographs. The experimental measurements will be compared with the numerical calculations carried out by USAERO/FSP (see Maskew, 1992 and Maskew, Wang and Troesch, 1994), a time-domain panel code with nonlinear treatment of the free-surface boundary conditions. Also, these results are prepared for the future comparison with other numerical codes.

Chapter 2

Experimental Setup

In order to conduct the vertical forced oscillation tests on the idealized flared body, the VMM dynamometer, an accelerometer, wave probes, and a video recorder were set up in MHL's towing tank to record time histories of prescribed displacement, acceleration, load cell forces, wave elevation and video information, respectively. The description of the experimental setup is shown in the schematic illustration of Figure 2.1.

The VMM dynamometer was originally designed to determine the unsteady vertical forces acting on planing hulls (see Ashcroft, Troesch and Sullivan, 1990). The dynamometer is designed to uncouple all forces and moments so that only pure vertical force and associated moments are measured. Two of the four load cells, which were originally configured to measure vertical forces and roll moments, were used in this test. The sum of the two load cells gives the net vertical force, while the difference of the two load cells can be used to estimate the error of the experiment due to unbalanced mechanical vibration. The prescribed motions were sinusoidal oscillations with a starting ramp function. Four wave probes were installed to measure the wave elevation at different positions away from the body. In addition two wave probes were fixed on the deck of the body for the study of green water on deck. Finally, the video camera was set up to record wave profiles and observe the behavior of the free-surface intersection lines.

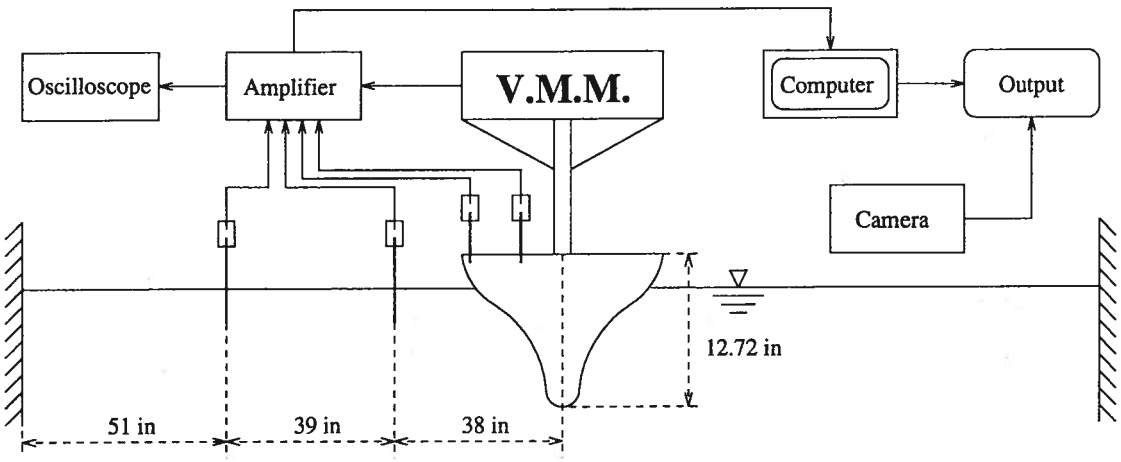

Forward Elevation

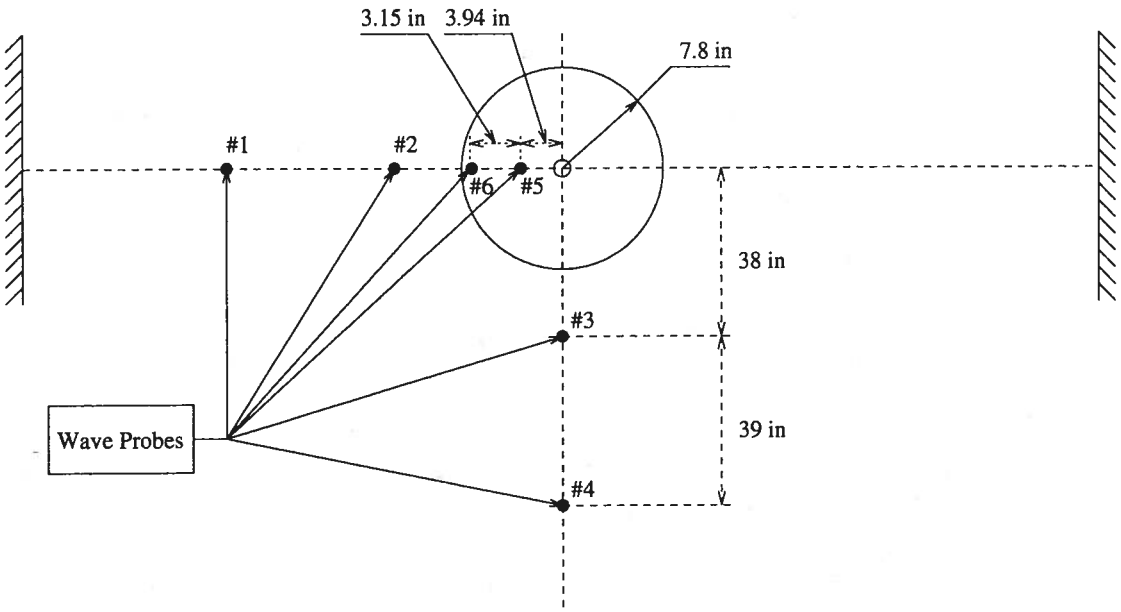

Plan View

Figure 2.1: Schematic Setup of the Experiment

Chapter 3

Task Matrix for the Experiments

As mentioned previously in the introduction, two types of large-amplitude oscillation experiments were conducted to investigate the slamming and deck-wetness of the flared body oscillating in a free surface. Here these two cases are referred to as "deck dry condition" and "green water on deck", respectively. A range of oscillation frequencies and amplitudes were covered, whose details are shown in Table 3.1. The VMM is capable of driving a stroke of ± 4 inches at a rate of ± 3 inches per second. Therefore, the frequency and amplitude shown in Table 3.1 were selected to demonstrate the dominance of hydrostatic forces in the slow-frequency oscillation, steep wave profiles in the moderate-frequency oscillation, and the local breaking waves and spray sheets in the high-frequency oscillation. However, for the green water on deck cases, the general parameters were carefully selected to prevent the spray sheets from damaging the wave probes or hitting the upper supporting structure.

The comparative study indicated a large discrepancy between the calculated and the previously measured loads, which led up to the recently repeated experiments. The repeated experiments determined that the experimental load cell forces were incorrect due to malfunctioning load cells in the previous tests. Table 3.1 shows the new repeated twenty-six tests with run numbers from 06 to 30. The missing run numbers were either calibration tests or bad runs which have been discarded here. The time histories of the

prescribed vertical displacement, the acceleration, Load Cells 1 and 2, the sum and difference of the load cells, four wave probes in the deck dry condition and six wave probes in the green water on deck condition have been recorded with individual run times equal to 40 seconds. Three thousand samples were taken in each run, i.e. the sampling interval $\Delta t = 0.01333333$ seconds. Before the analog signals were digitized, they were passed through a multiple electronic filter bank with a cut-off frequency of $25.6\,Hz$.

In Table 3.1, the freeboard values were also selected in each run so that different drafts were used for the deck dry condition and green water on deck experiments, respectively. The information shown in the fourth column of Table 3.1 is provided for the numerical filter treatment of the experimental results by a Fast Fourier Transform (FFT) analysis. These results are shown in Appendix C. The "FFT Range" denotes the time segments of each run that was Fourier analyzed. Table 3.2 gives the offsets of the flared body whose isometric view is shown in Figure 3.1. The flared body used in the experiments was a wooden and aluminum structure with thin yellow waterproof coating and black measuring marks. The total weight of the flared body plus the upper supporting structure is $22.8\,lbs$ $(101.5\,N)$. This represents the total inertia accelerated by the load cells. The photograph in Figure 3.2 shows the oscillating object, the wave profiles, and part of the upper supporting structure.

Table 3.1: Task Matrix for the Experiments

Run Tests	Frequency (Hz)	Amplitude (in)	FFT Range $(sec.)$	Freeboard (in)
Deck Dry Condition				
06	0.907	0.976	10.0 - 36.471	3.0
07	0.598	0.903	10.0 - 36.787	3.0
08	0.895	1.873	10.0 - 36.832	3.0
09	0.598	2.056	10.0 - 36.783	3.0
10	1.220	1.087	10.0 - 36.259	3.0
11	0.719	0.908	12.0 - 34.271	3.0
12	1.221	1.357	10.0 - 36.216	3.0
13	0.720	1.997	10.0 - 37.795	3.0
14	1.213	1.471	10.0 - 36.389	3.0
15	0.718	1.393	20.0 - 36.723	3.0
16	0.599	1.623	10.0 - 36.743	3.0
17	0.909	1.503	10.0 - 32.011	3.0
Green Water on Deck				
18	0.908	1.732	10.0 - 36.453	0.0
19	1.221	1.435	10.0 - 36.216	0.0
20	0.720	1.908	10.0 - 37.811	0.0
21	0.598	1.632	10.0 - 36.765	0.0
22	1.223	0.848	10.0 - 36.173	0.0
23	0.905	1.110	10.0 - 36.538	0.0
24	0.719	0.825	10.0 - 37.834	0.0
25	0.598	1.257	10.0 - 36.778	0.0
26	1.222	1.455	10.0 - 36.195	0.0
28	0.719	2.189	10.0 - 37.819	0.0
29	0.597	2.372	10.0 - 36.801	0.0
30	0.905	1.858	10.0 - 36.515	0.0

Table 3.2: Offset Table of the Flared Body

Radius R (*in*)	Height Z (*in*)	Radius R (*in*)	Height Z (*in*)
0.0000	0.0000	2.9023	5.9070
0.3849	0.0285	3.1071	6.3008
0.7550	0.1186	3.3434	6.6946
1.0961	0.2950	3.5836	7.0884
1.3951	0.5141	3.8632	7.4822
1.6404	0.7969	4.1546	7.8760
1.8228	1.1505	4.4854	8.2698
1.9350	1.4614	4.8733	8.6636
1.9729	1.5752	5.2691	9.0574
2.0084	1.9690	5.7219	9.4512
2.0360	2.3628	6.1866	9.8450
2.0576	2.7566	6.6119	10.2389
2.0970	3.1504	6.9309	10.6327
2.1659	3.5442	7.2223	11.0265
2.2447	3.9380	7.4784	11.4202
2.3392	4.3318	7.6752	11.8141
2.4534	4.7256	7.7854	12.4692
2.5973	5.1194	7.7933	12.7251
2.7290	5.5132		

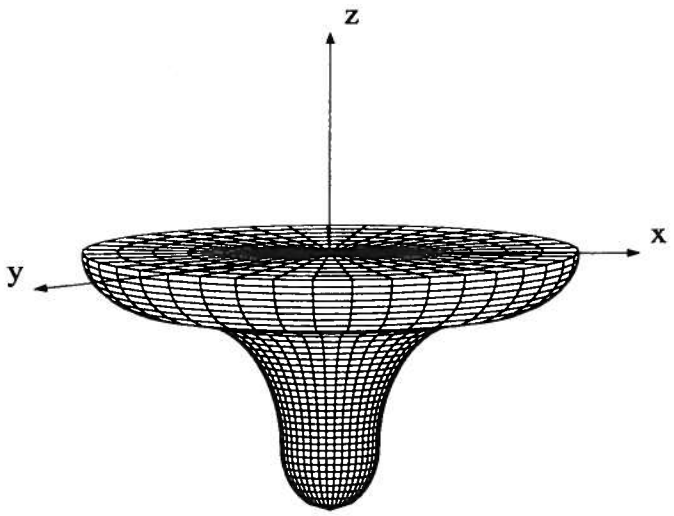

Figure 3.1: Schematic of Coordinate Systems and Geometry of the Body

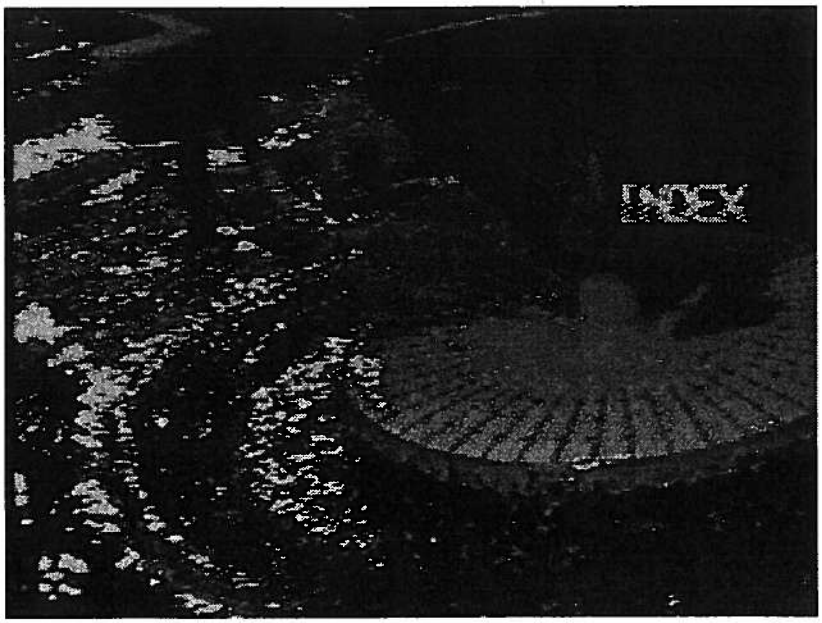

Figure 3.2: Photograph of the Oscillating Body and its Supporting Structure

Chapter 4

Formulation of Motion Equations

An inertial Cartesian coordinate system $Oxyz$ with the origin on the still water surface and the $z-$axis pointing upwards is shown in Figure 3.1. It is assumed that the body strictly undergoes forced vertical motions under the action of load cells, hydrodynamic action, and gravitational force, where the upward acting forces are defined as positive. The equations of motion can be set up by equating the above forces to the inertial force associated with acceleration of the body mass m. Here the motion equations representing the body moving in a vertical direction are presented for the deck dry condition and green water on deck, respectively.

4.1 Deck Dry Condition

For the deck dry condition, the equations of motion can be expressed as

$$F_{lc}(t) + F_{hy}(t) - mg = m\ddot{z} \tag{4.1}$$

where $F_{lc}(t)$ represents the load cells measured by VMM; $F_{hy}(t)$ denotes the total hydrodynamic force which for potential flow is given by Bernoulli's equation as follows

$$F_{hy}(t) = \int_{S(t)} \rho(-\Phi_t - \frac{1}{2}\nabla\Phi \cdot \nabla\Phi - gz)n_3 ds. \tag{4.2}$$

The hydrodynamic force can be separated into dynamic and static terms, $F_{dy}(t)$ and $F_{st}(t)$ respectively, defined by

$$F_{dy}(t) = \int_{S(t)} \rho(-\Phi_t - \frac{1}{2}\nabla\Phi \cdot \nabla\Phi) n_3 ds \tag{4.3}$$

and

$$F_{st}(t) = \int_{S(t)} \rho(-gz) n_3 ds \tag{4.4}$$

with $S(t) = S_0(t) + \Delta S_\zeta$. The transient wetted body surface $S(t)$ consists of the mean surface $S_0(t)$ below the $z = 0$ plane which varies with the oscillation of the body and the difference ΔS_ζ between the transient wetted surface and the mean surface, which is due to the wave elevation; Φ is the velocity potential; mg is the gravitational force equal to $22.8\,lbs$ $(101.5\,N)$, and $\ddot{z}$ is the vertical acceleration of the oscillating body.

4.2 Green Water on Deck

Two different approaches can be used to deal with the case of green water on deck. One is to treat the green water as added mass which is called the control volume integration method. Equation 4.1 can be rewritten as

$$F_{lc}(t) + F_{hy}(t) - mg = M\ddot{z} + \dot{M}\dot{z} \tag{4.5}$$

where M is the total mass consisting of the mass of the body and the added mass of the green water on deck; the dot indicates the differentiation with respect to time. The right hand side of the above equation represents the time rate of change of the momentum of the body including the added mass contributed by the green water on deck. Another approach is the total surface integration which treats the action of the green water on deck as an external force. Its equation of motion has the same form as Equation 4.1. For the convenience of the comparison with numerical simulations, we adopt Equation 4.1 to calculate the cases of green water on deck. Equations 4.3 and 4.4 are used to separate the components of the total forces. Because we don't have the information of the intersection line between water surface and flared body from the experimental results, the hydrostatic forces are computed with respect to $S_0(t)$.

Chapter 5

Results and Analysis

Based upon Equation 4.1, we know that the load cells F_{lc} can be viewed as the combination of hydrodynamic force F_{dy} which is only contributed by the dynamic terms, hydrostatic force F_{st}, inertial force F_{in}, and gravitational force. Here the gravitational force is known as $22.8\,lbs$ and the hydrostatic force can be readily obtained by Equation 4.4. The inertial force can be obtained from the prescribed displacement measured in the experiment with a special treatment.

In order to obtain accurate inertial forces, three different methods were tried to calculate the vertical acceleration of the oscillating body, as described below:

- Assume the prescribed displacement is given by perfect sinusoidal oscillation, then the vertical acceleration can be calculated by $\ddot{z}(t) = -\omega^2 z(t)$;
- Based upon the prescribed displacement measured in experiment, the finite difference scheme is directly applied to calculate the vertical acceleration by differentiating twice;
- The FFT $\mathcal{F}^+$ and $\mathcal{F}^-$, i.e. the Fourier transform and the inverse Fourier transform, respectively, can be employed to calculate the vertical acceleration, as follows:

$$\ddot{z} = \mathcal{F}^-\{-\omega^2 \mathcal{F}^+[z(t)]\}. \tag{5.1}$$

The first two methods suffer from inaccuracy due to the noise induced by the high-frequency and small-amplitude mechanical vibration of VMM. Only the third method can easily be used to filter the unwanted noise and yield the more accurate results by zeroing the FFT above frequencies of $\omega_c = \alpha\omega_0$ where ω_c is the cutoff frequency, ω_0 is the fundamental frequency of the sinusoidal oscillation, and α is the cutoff frequency coefficient. In order to minimize the the unwanted mechanical noise, an accelerometer was installed to measure the acceleration of the body in the later repeated tests. The inertial forces obtained by using the same numerical filter technique are greatly improved.

By using the acceleration data measured, the inertial force was calculated assuming a value $\alpha = 6$. The results of the force components, i.e. F_{hy}, F_{dy}, F_{st}, F_{lc}, and F_{in}, are shown in two separate figures, see Figures 5.1 to 5.24, where the oscillation amplitudes sweep from 1.0 to $2.5\,in$ and the oscillation frequencies sweep from 0.597 to $1.22\,Hz$. In general, these figures illustrating the deck dry conditions show large nonlinearities in all force components, which are caused by the significant third harmonic contributions. Similar to the deck dry conditions, Figures 5.13 to 5.24 show the corresponding comparisons of the cases of green water on deck. By comparison of the load cells between the cases of the deck dry condition and the green water on deck, after the starting ramp period, the load cells jump down in the deck dry conditions while jump up in the deck wet conditions. It is because the load cells are shifted down mainly by the mean of the nonlinear hydrostatic forces in deck dry conditions while lifted up greatly by the contribution of the added weight of the green water on deck. This phenomenon is demonstrated in the time histories of the load cells, which are shown in Appendix B, see Figures B.1 to B.88.

Originally, the experimental tests were designed to conduct forced vertical sinusoidal oscillations. However, VMM suffers from its limitation to follow a perfect sine wave input signal. Tables C.1 to C.24 are designed here to demonstrate the contribution of the high-frequency oscillations given by VMM. The Fourier coefficients of the force components including F_{hy}, F_{dy}, F_{st}, F_{lc}, and F_{in} are listed here in magnitude and argument forms, so that the time history, $x(t)$ accurate through the sixth harmonic, can be regenerated

by

$$x(t) = \sum_{j=0}^{j=6} X_j cos(\omega_j t - \phi_j) \tag{5.2}$$

where X_j and ϕ_j are the magnitude and phase of the j-th harmonic, respectively. The coefficients are nondimensionalized where the displacement amplitude A is divided by the diameter of the flared body $D = 15.59\,in$, the radian frequency ω divided by $\sqrt{g/D}$, and the force components divided by $\rho g D^3$, respectively.

Figures 5.25 to 5.28 qualitatively demonstrate the wave progress and green water progress on deck during one period, where Figures 5.27 and 5.28 are selected to illustrate the wave profiles in both deck dry and deck wet conditions. By careful observation of these figures, we can see that among the large steep or even breaking waves there are some tiny waves located in front of the wavefront. These tiny waves had been originally thought to be just capillary waves generated by the water surface tension. However, the numerical results show that these tiny waves are partially induced by the high-frequency oscillations.

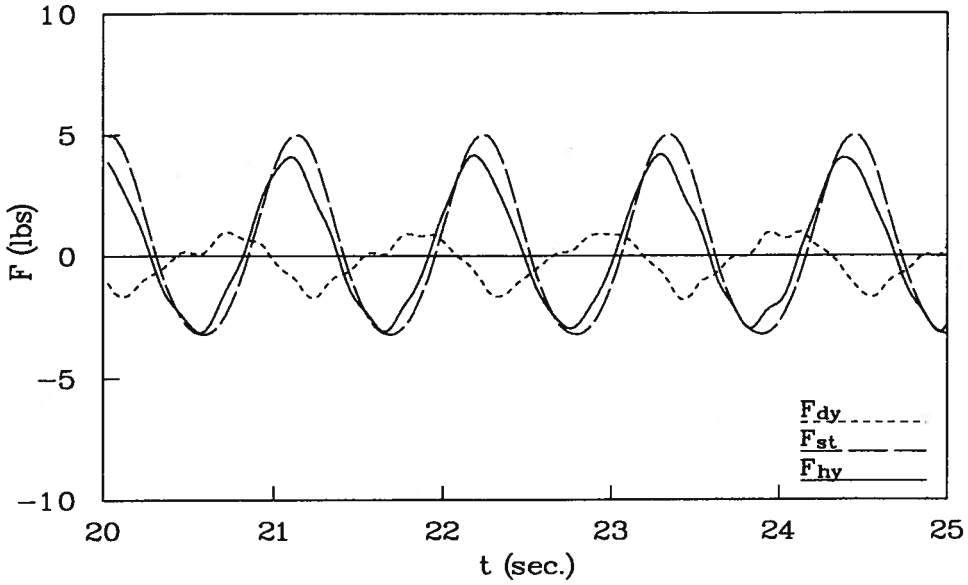

(a) Analyzed Hydrodynamic Forces

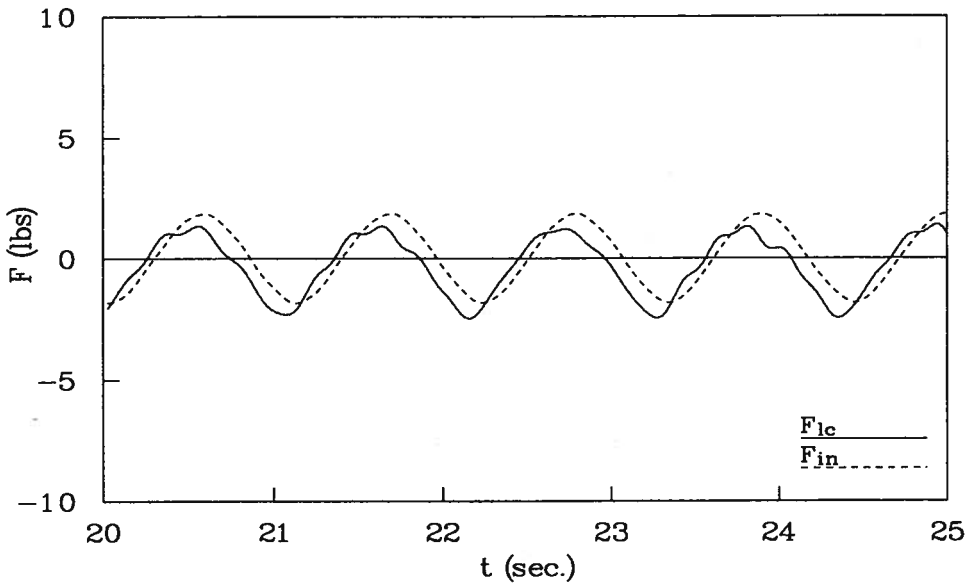

(b) Analyzed Load Cell and Inertial Forces

Figure 5.1: Run 06, $f_1 = 0.907\,Hz$, $A_1 = 0.976\,in$, $\alpha = 6$

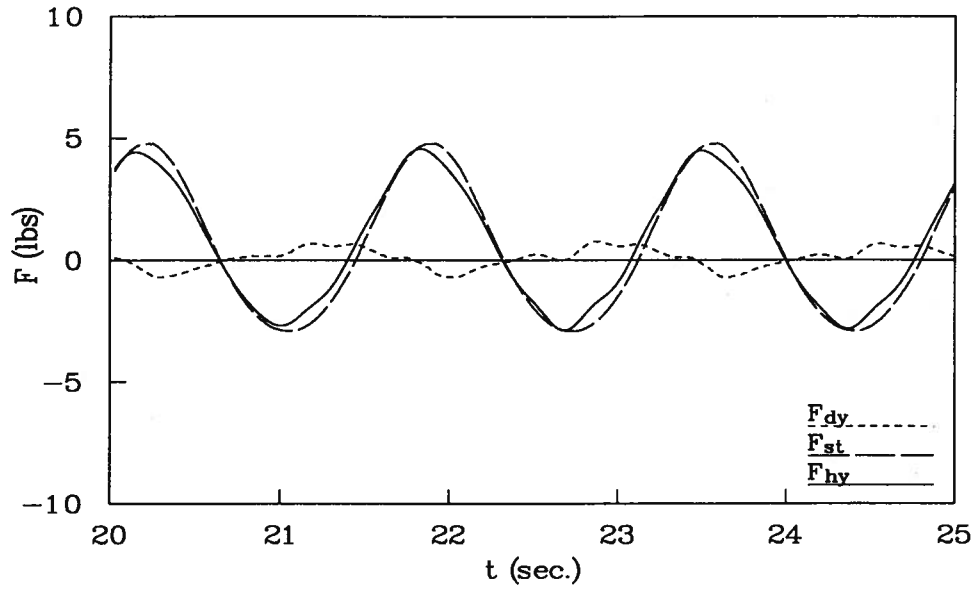

(a) Analyzed Hydrodynamic Forces

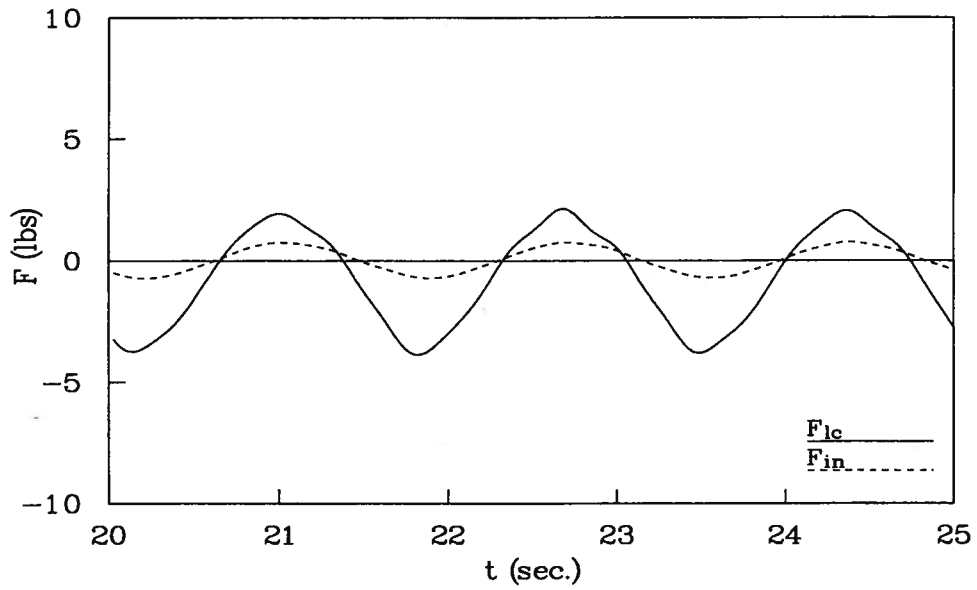

(b) Analyzed Load Cell and Inertial Forces

Figure 5.2: Run 07, $f_1 = 0.598\,Hz$, $A_1 = 0.903\,in$, $\alpha = 6$

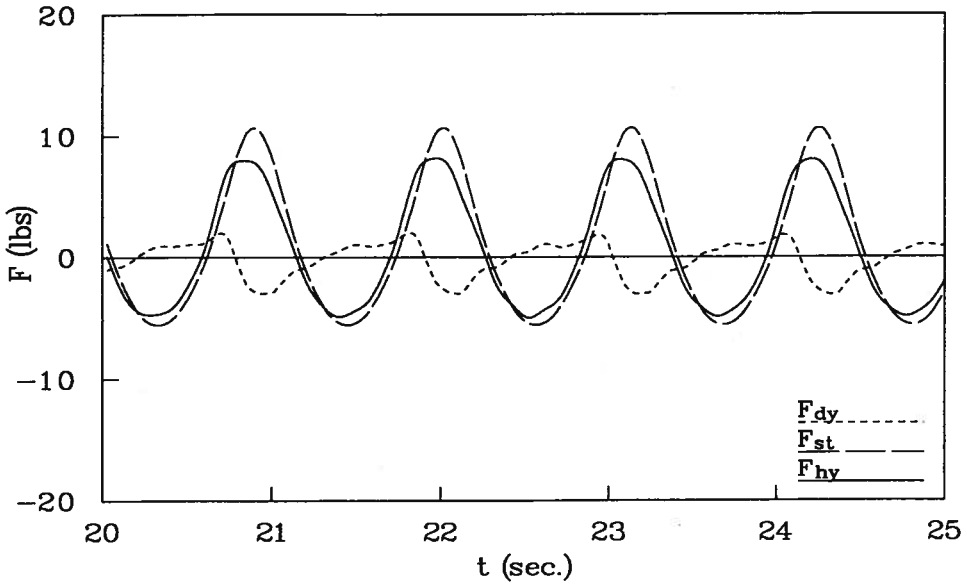

(a) Analyzed Hydrodynamic Forces

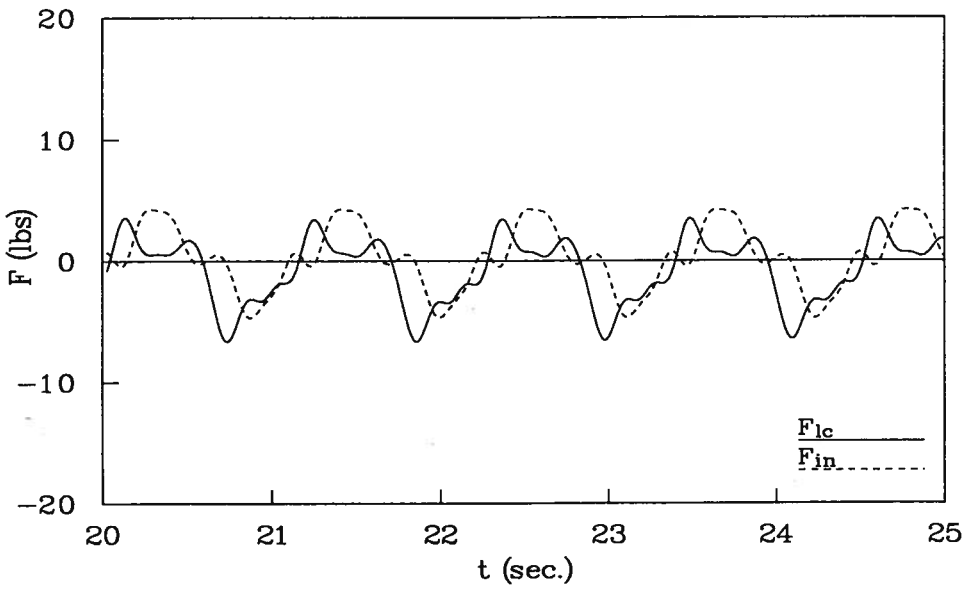

(b) Analyzed Load Cell and Inertial Forces

Figure 5.3: Run 08, $f_1 = 0.895\,Hz$, $A_1 = 1.873\,in$, $\alpha = 6$

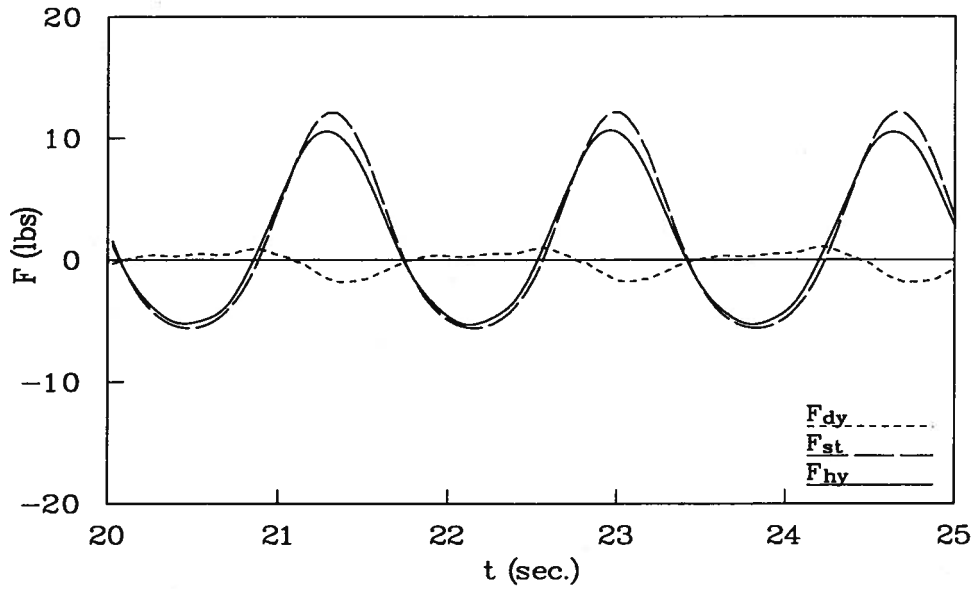

(a) Analyzed Hydrodynamic Forces

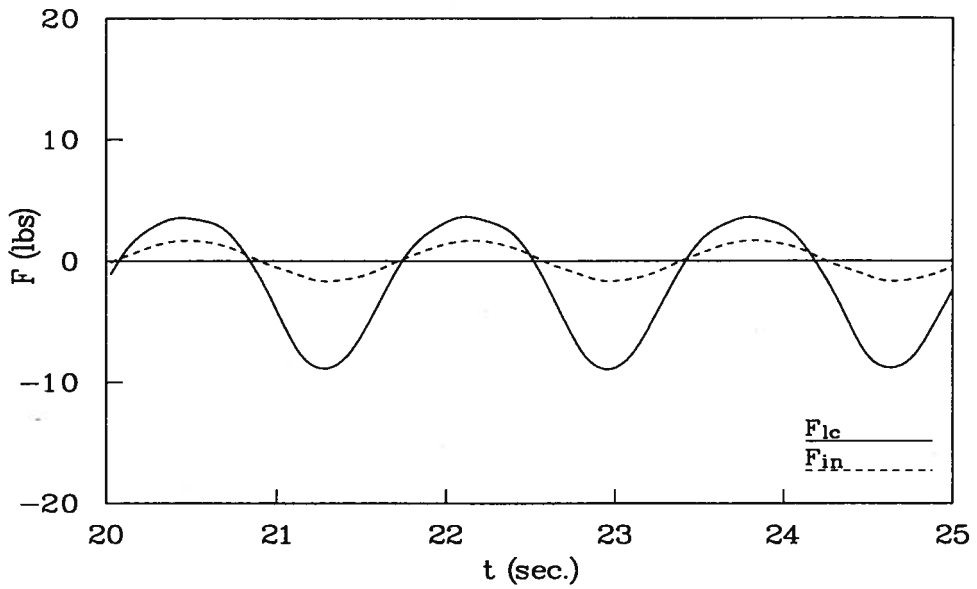

(b) Analyzed Load Cell and Inertial Forces

Figure 5.4: Run 09, $f_1 = 0.598\,Hz$, $A_1 = 2.056\,in$, $\alpha = 6$

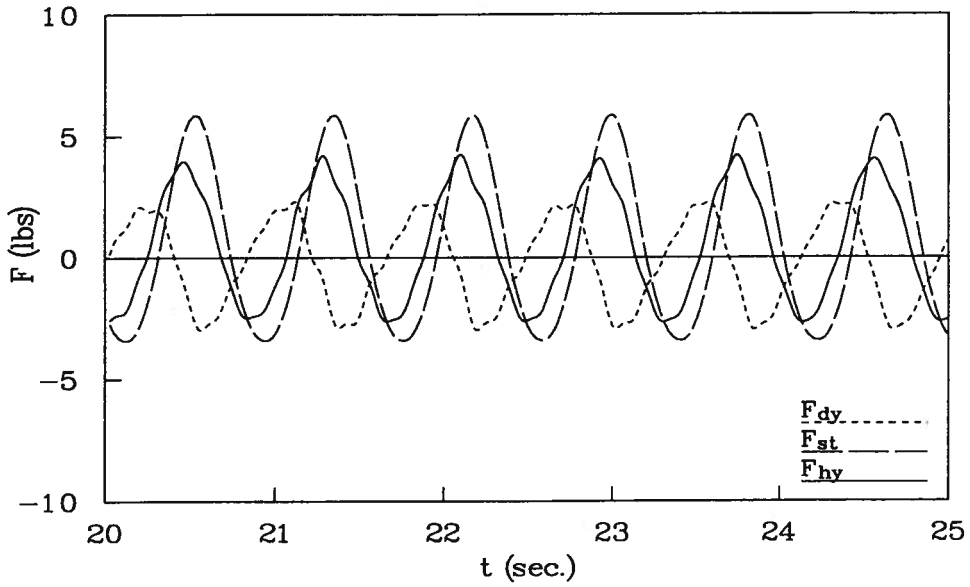

(a) Analyzed Hydrodynamic Forces

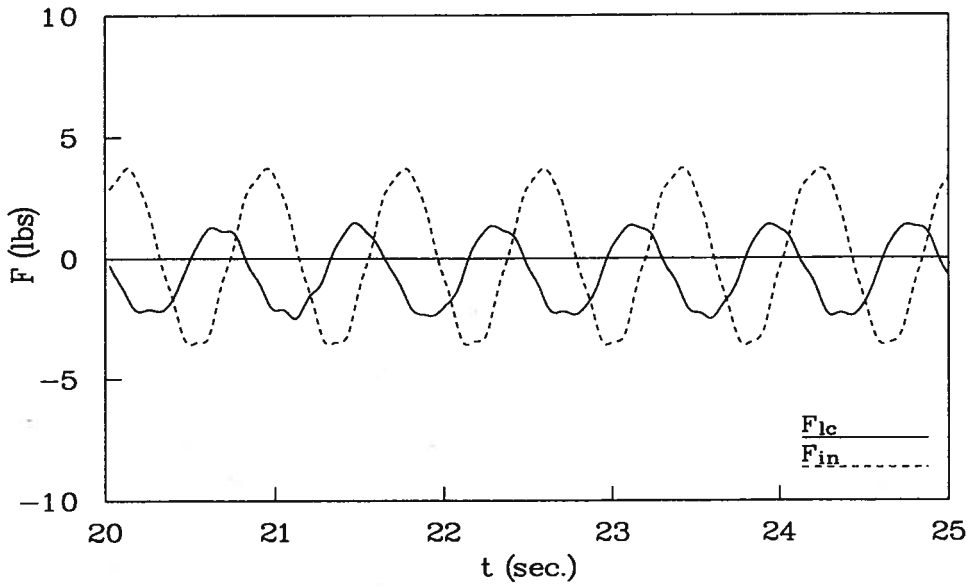

(b) Analyzed Load Cell and Inertial Forces

Figure 5.5: Run 10, $f_1 = 1.220\,Hz$, $A_1 = 1.087\,in$, $\alpha = 6$

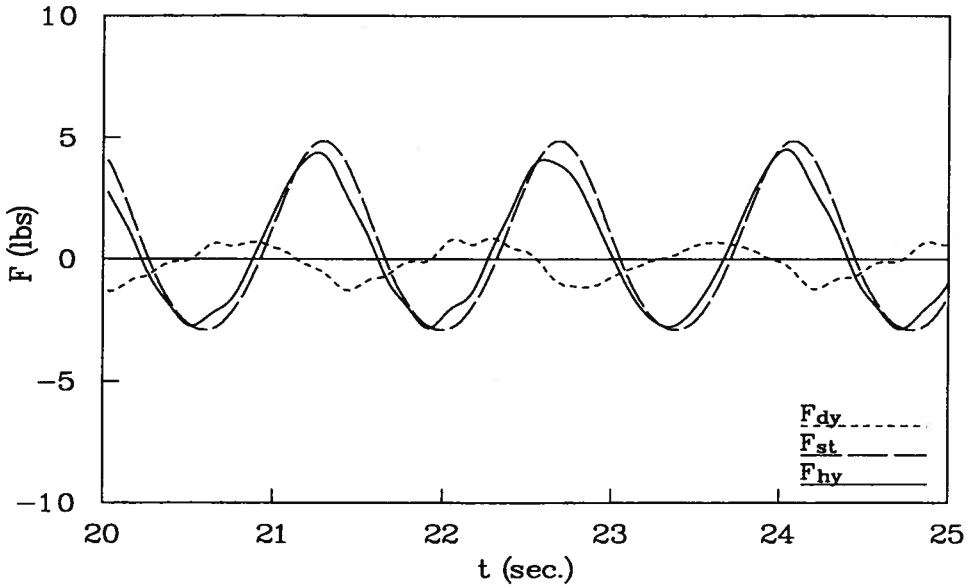

(a) Analyzed Hydrodynamic Forces

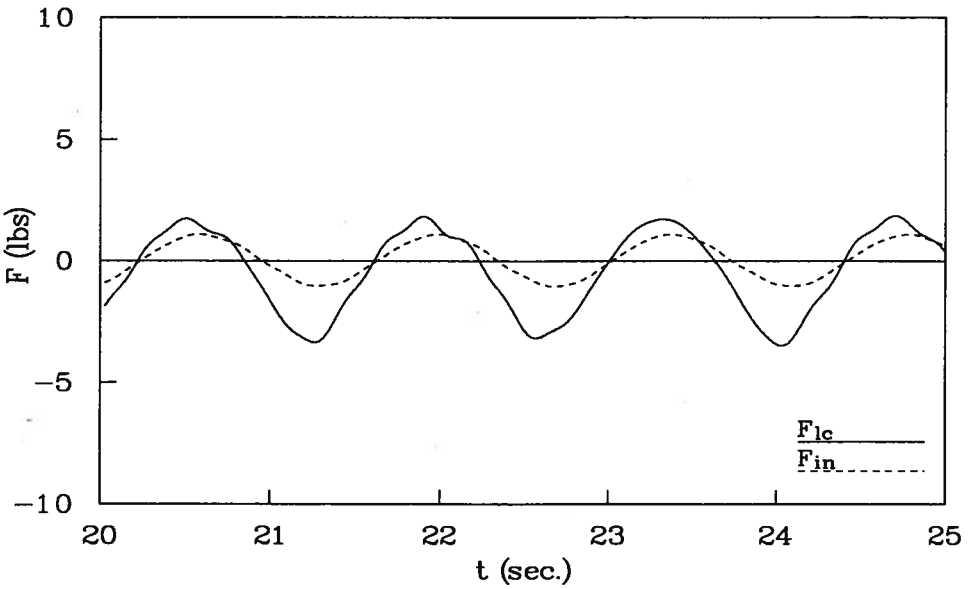

(b) Analyzed Load Cell and Inertial Forces

Figure 5.6: Run 11, $f_1 = 0.719\,Hz$, $A_1 = 0.908\,in$, $\alpha = 6$

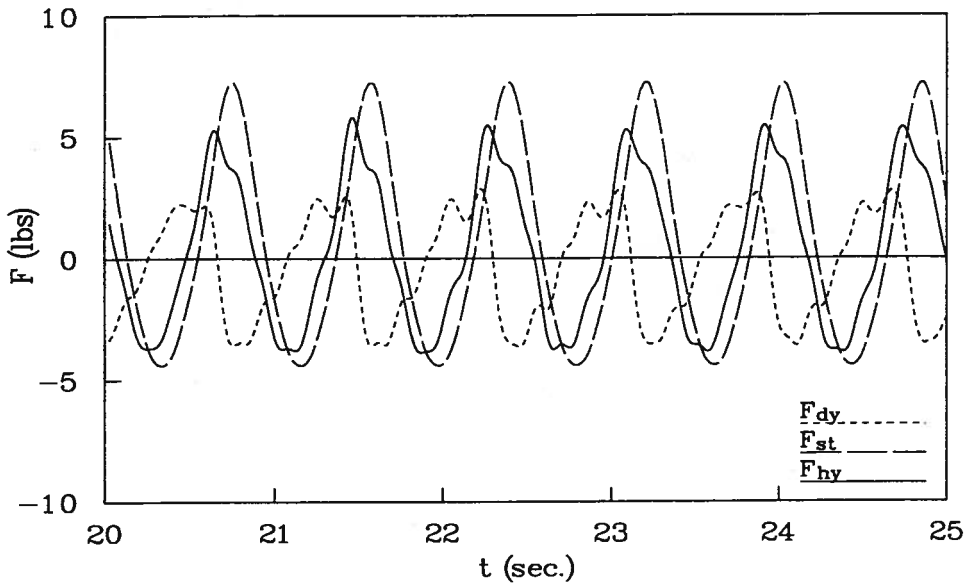

(a) Analyzed Hydrodynamic Forces

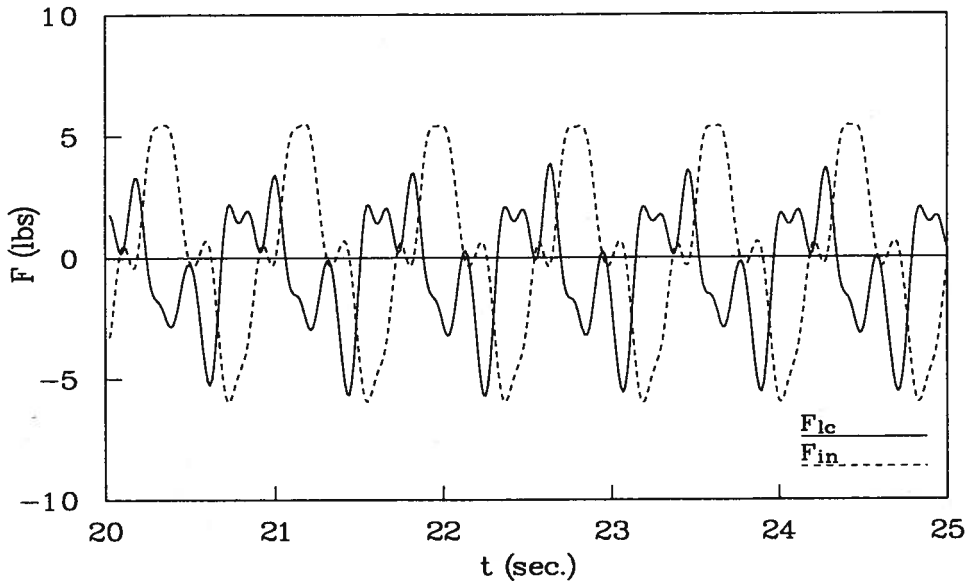

(b) Analyzed Load Cell and Inertial Forces

Figure 5.7: Run 12, $f_1 = 1.221\,Hz$, $A_1 = 1.357\,in$, $\alpha = 6$

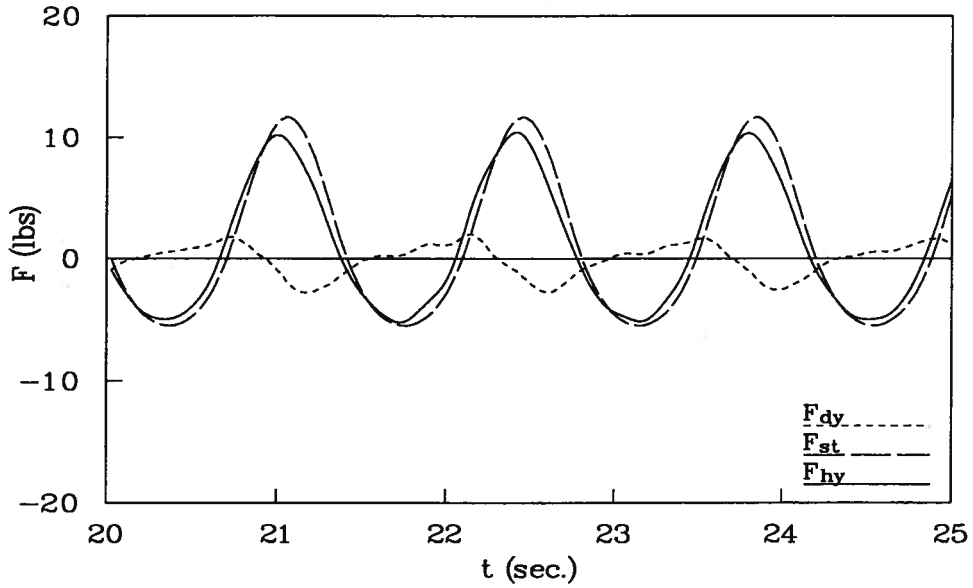

(a) Analyzed Hydrodynamic Forces

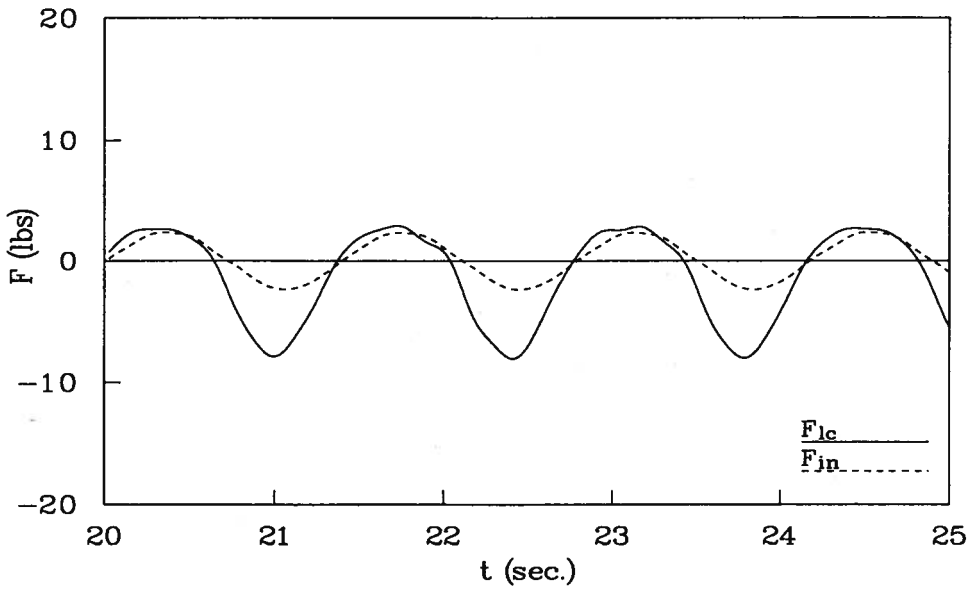

(b) Analyzed Load Cell and Inertial Forces

Figure 5.8: Run 13, $f_1 = 0.720\,Hz$, $A_1 = 1.997\,in$, $\alpha = 6$

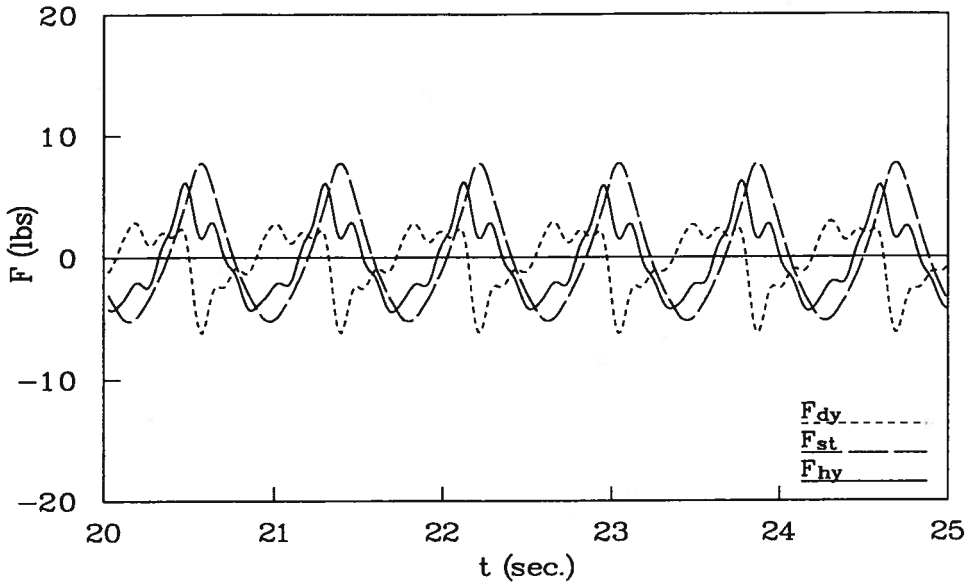

(a) Analyzed Hydrodynamic Forces

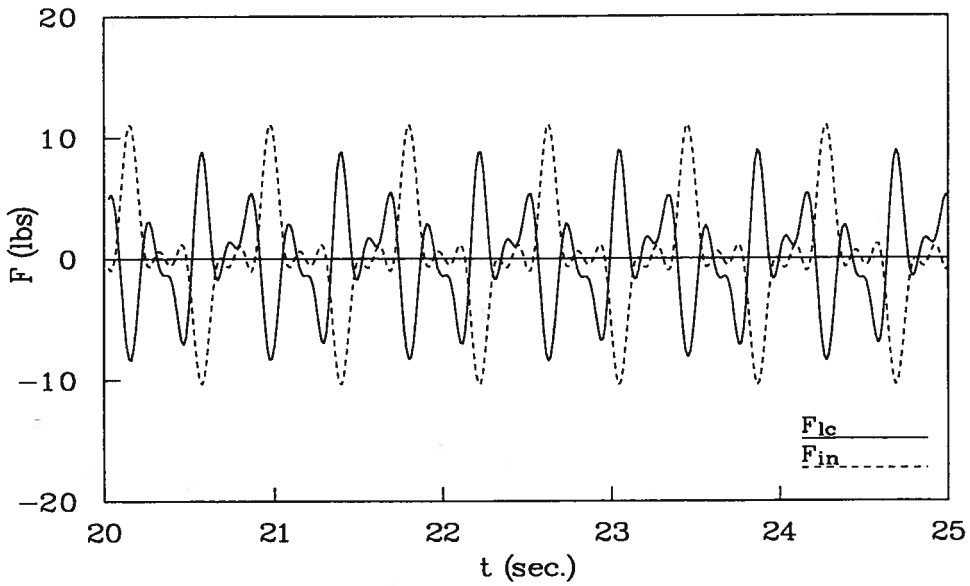

(b) Analyzed Load Cell and Inertial Forces

Figure 5.9: Run 14, $f_1 = 1.213\,Hz$, $A_1 = 1.471\,in$, $\alpha = 6$

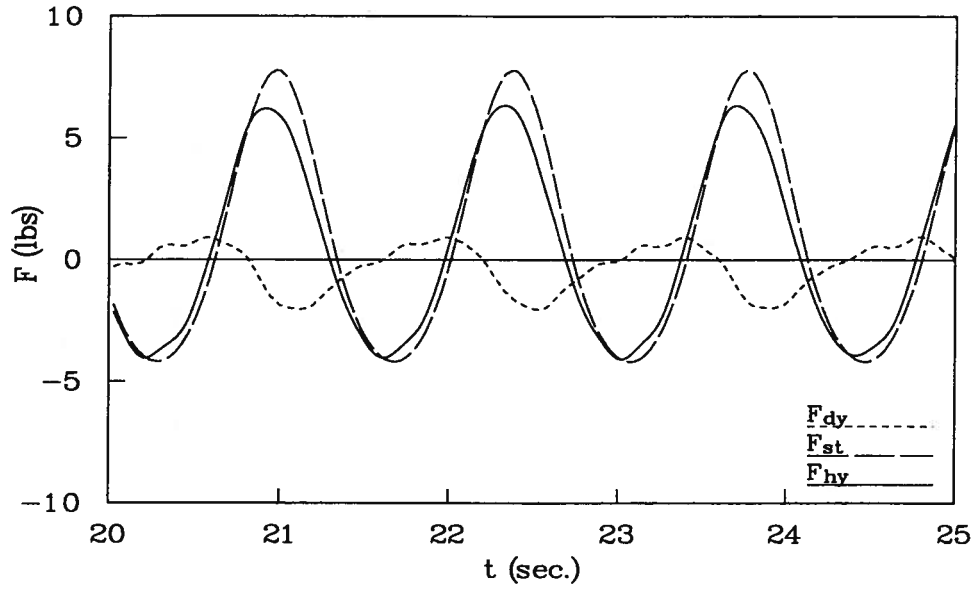

(a) Analyzed Hydrodynamic Forces

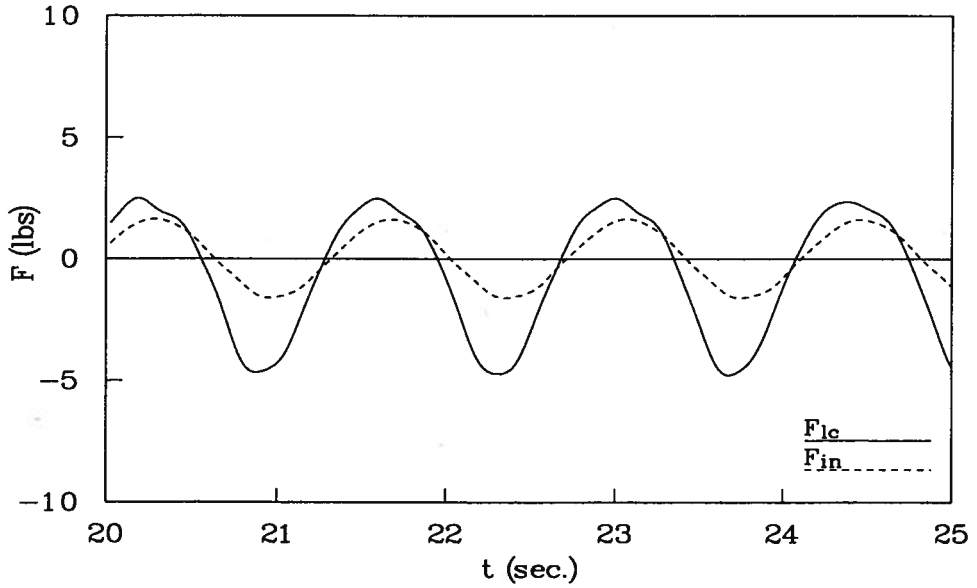

(b) Analyzed Load Cell and Inertial Forces

Figure 5.10: Run 15, $f_1 = 0.718\,Hz$, $A_1 = 1.393\,in$, $\alpha = 6$

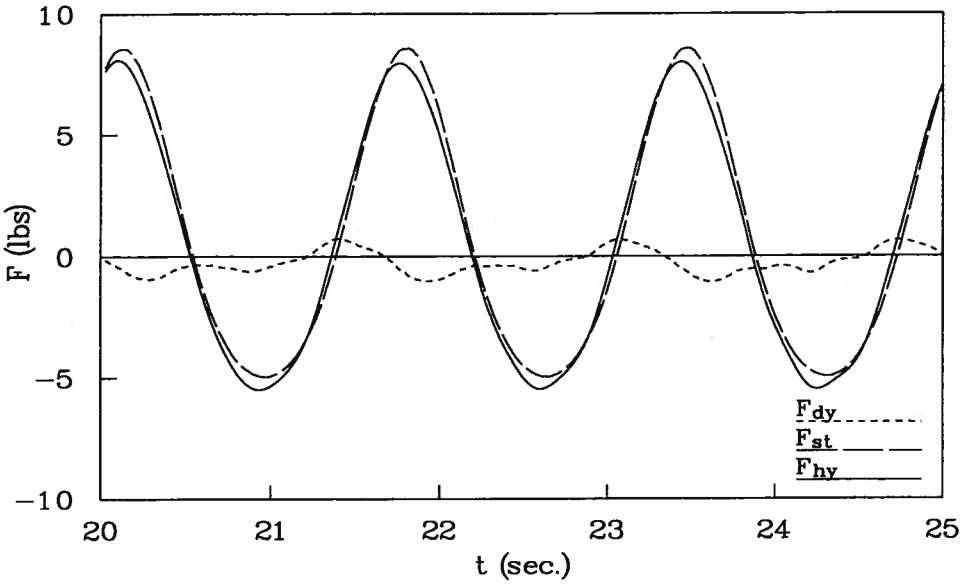

(a) Analyzed Hydrodynamic Forces

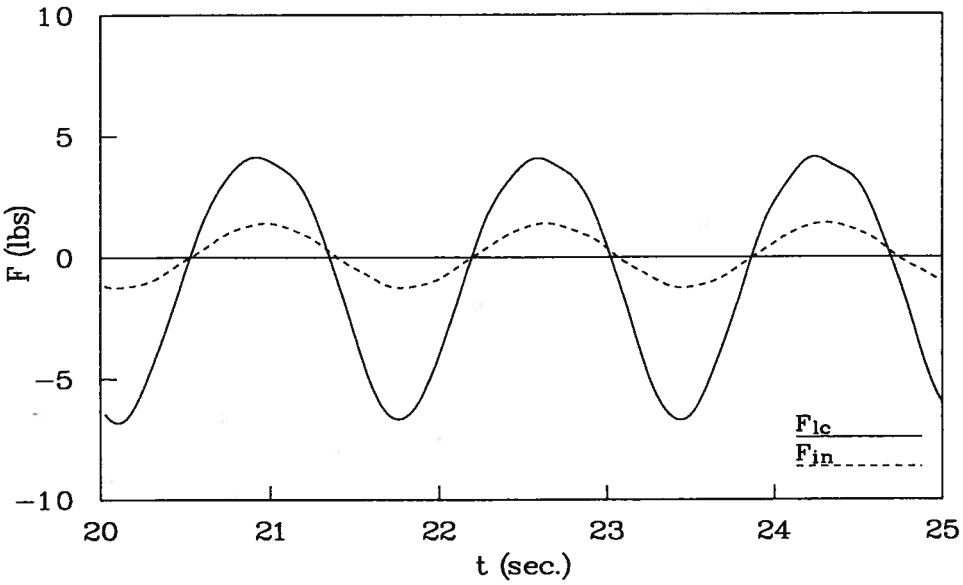

(b) Analyzed Load Cell and Inertial Forces

Figure 5.11: Run 16, $f_1 = 0.599\,Hz$, $A_1 = 1.623\,in$, $\alpha = 6$

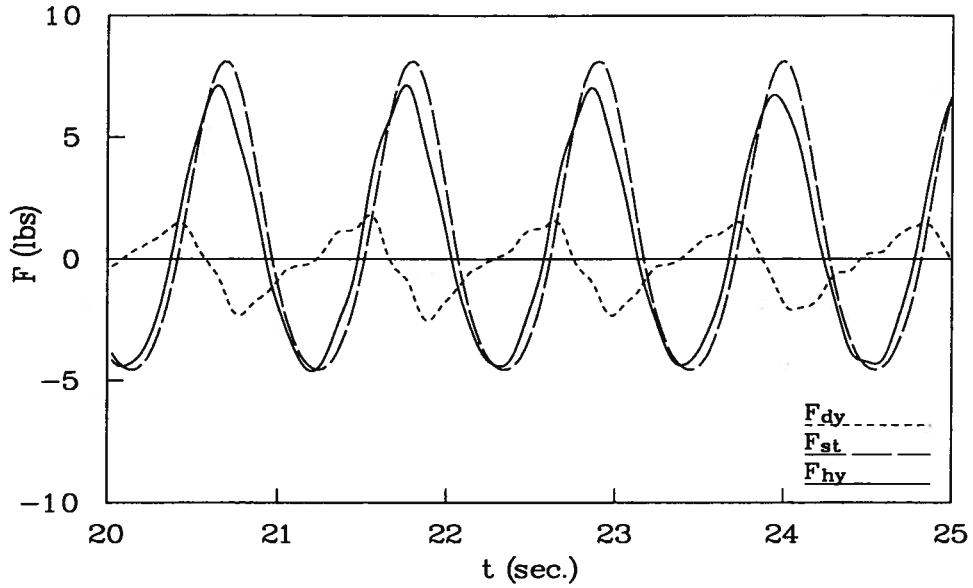

(a) Analyzed Hydrodynamic Forces

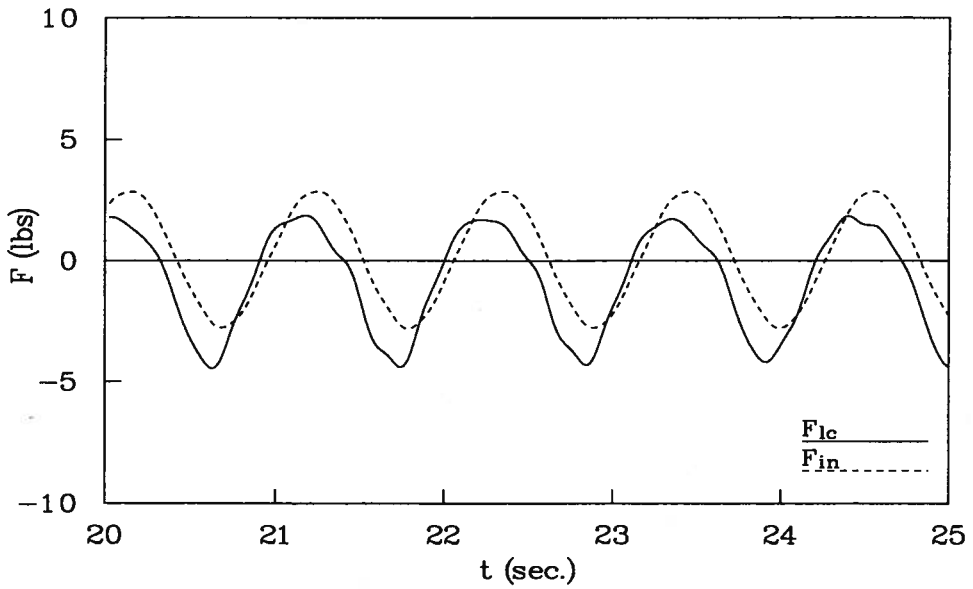

(b) Analyzed Load Cell and Inertial Forces

Figure 5.12: Run 17, $f_1 = 0.909\,Hz$, $A_1 = 1.503\,in$, $\alpha = 6$

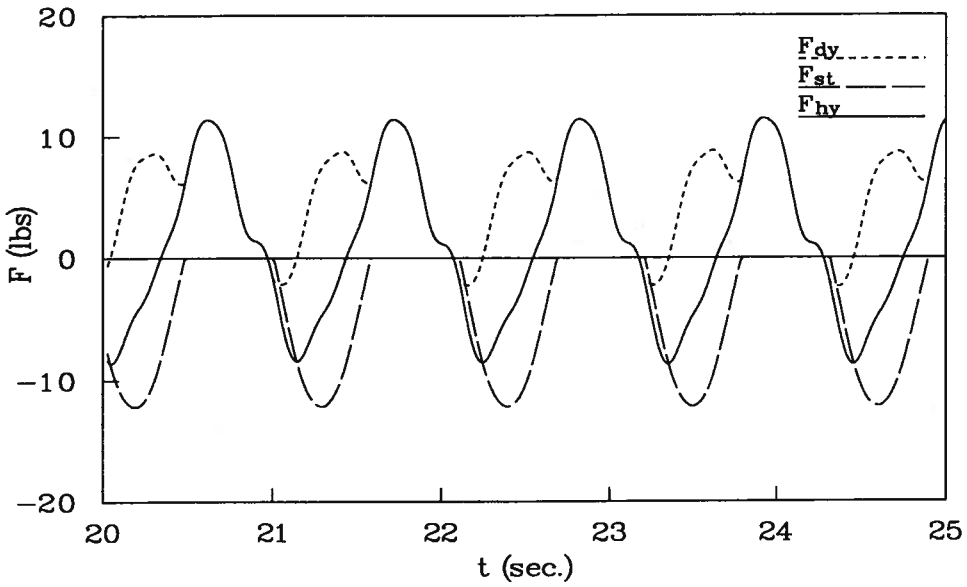

(a) Analyzed Hydrodynamic Forces

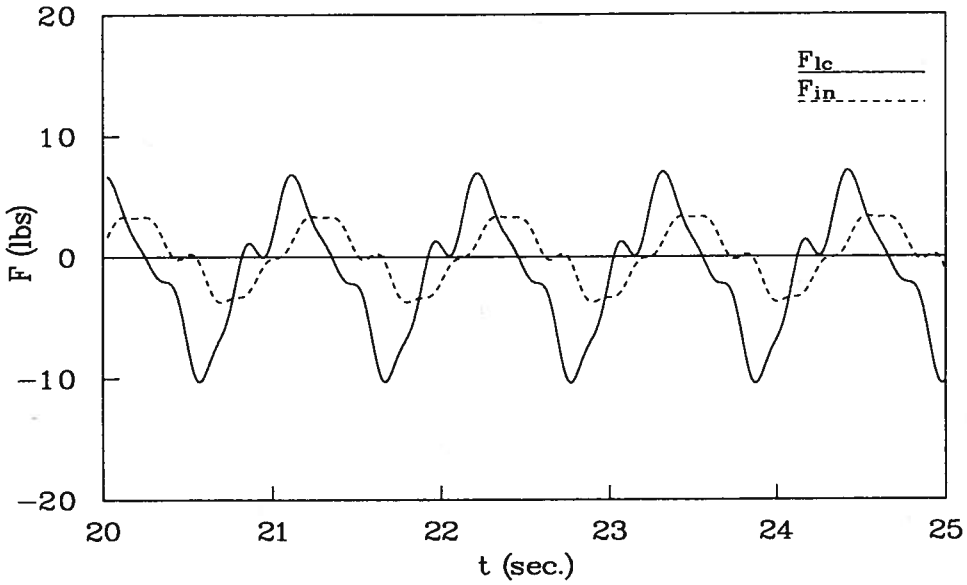

(b) Analyzed Load Cell and Inertial Forces

Figure 5.13: Run 18, $f_1 = 0.908\,Hz$, $A_1 = 1.732\,in$, $\alpha = 6$

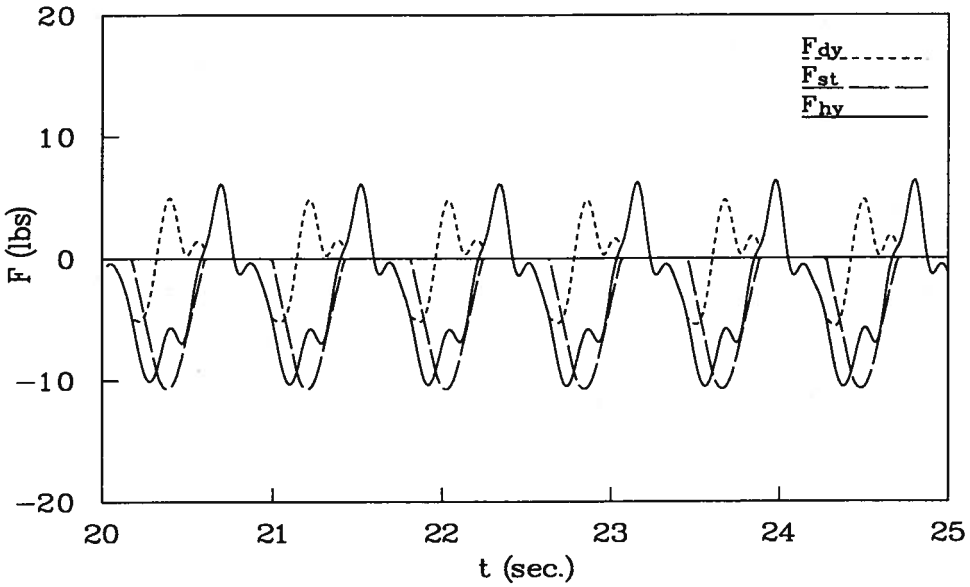

(a) Analyzed Hydrodynamic Forces

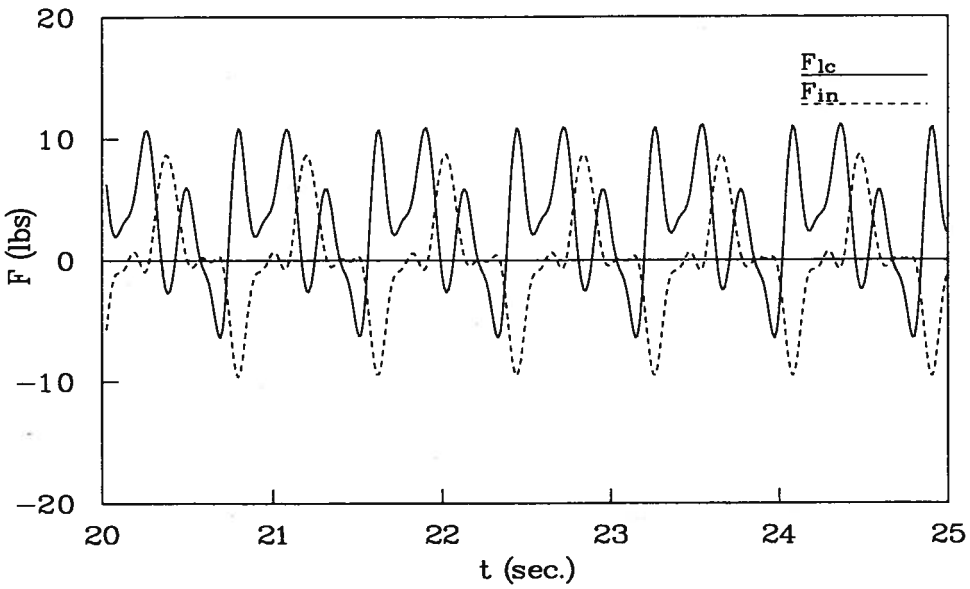

(b) Analyzed Load Cell and Inertial Forces

Figure 5.14: Run 19, $f_1 = 1.221\,Hz$, $A_1 = 1.435\,in$, $\alpha = 6$

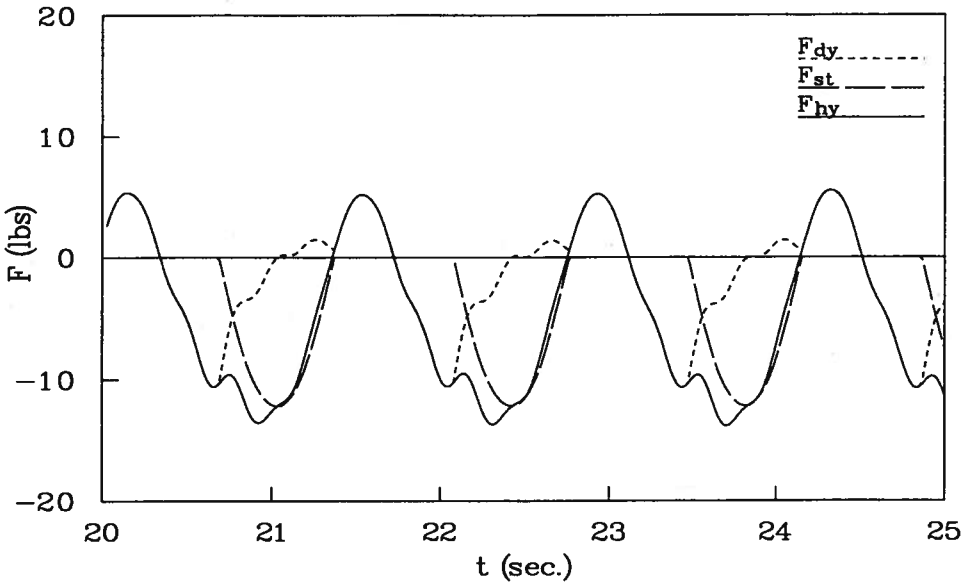

(a) Analyzed Hydrodynamic Forces

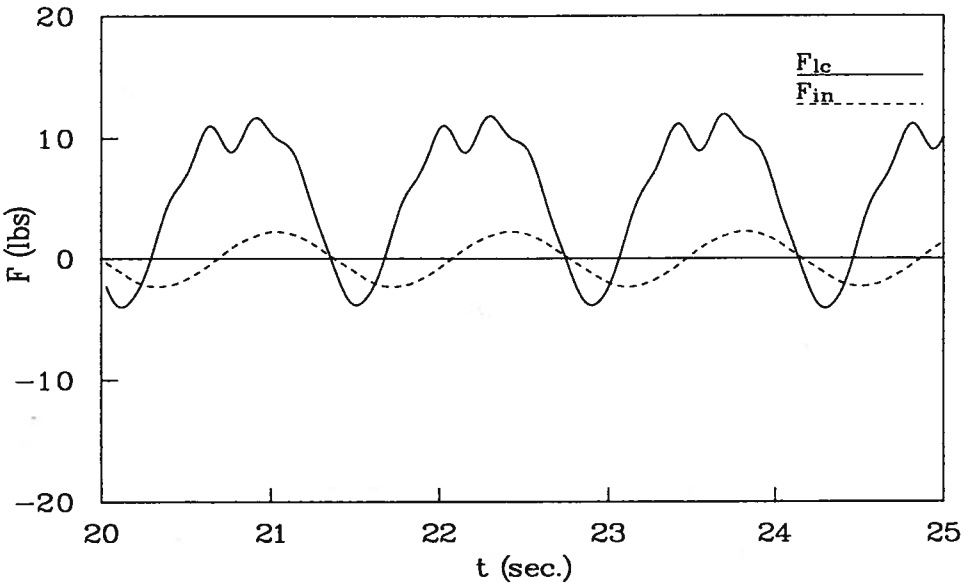

(b) Analyzed Load Cell and Inertial Forces

Figure 5.15: Run 20, $f_1 = 0.720\,Hz$, $A_1 = 1.908\,in$, $\alpha = 6$

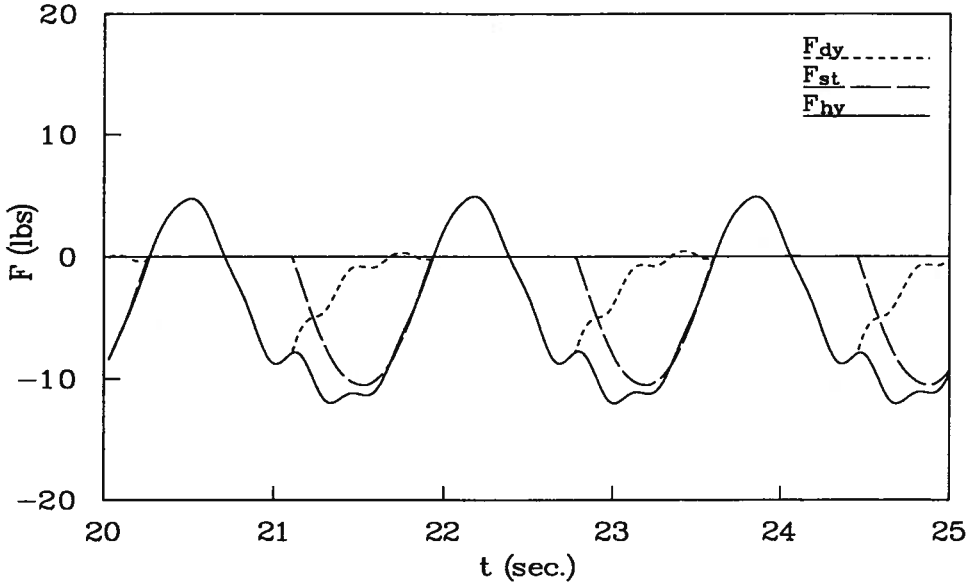

(a) Analyzed Hydrodynamic Forces

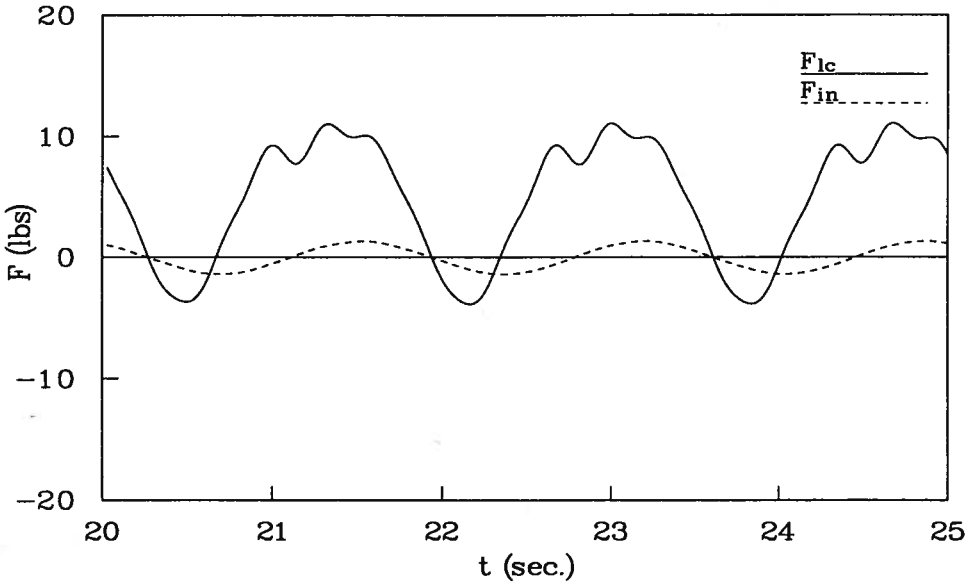

(b) Analyzed Load Cell and Inertial Forces

Figure 5.16: Run 21, $f_1 = 0.598\,Hz$, $A_1 = 1.632\,in$, $\alpha = 6$

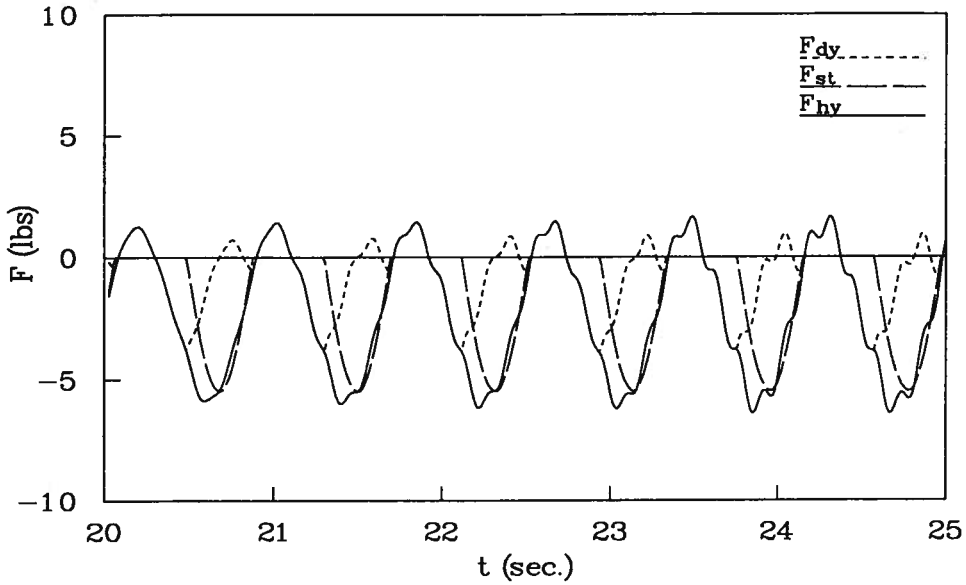

(a) Analyzed Hydrodynamic Forces

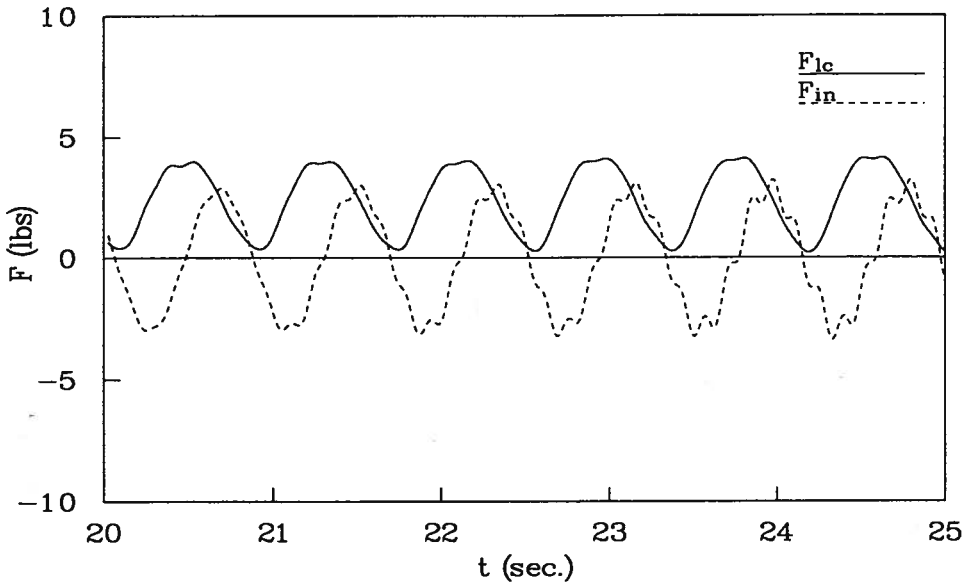

(b) Analyzed Load Cell and Inertial Forces

Figure 5.17: Run 22, $f_1 = 1.223\,Hz$, $A_1 = 0.848\,in$, $\alpha = 6$

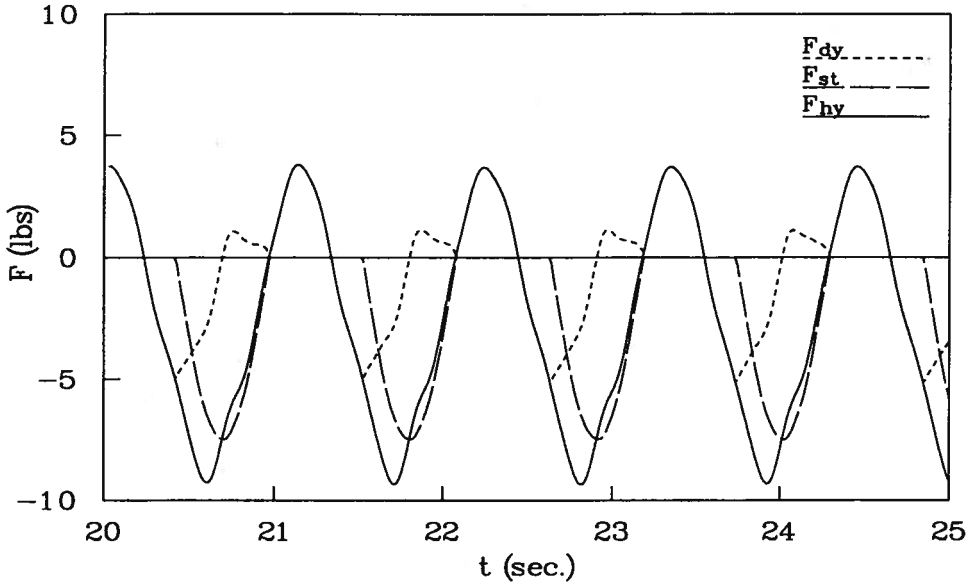

(a) Analyzed Hydrodynamic Forces

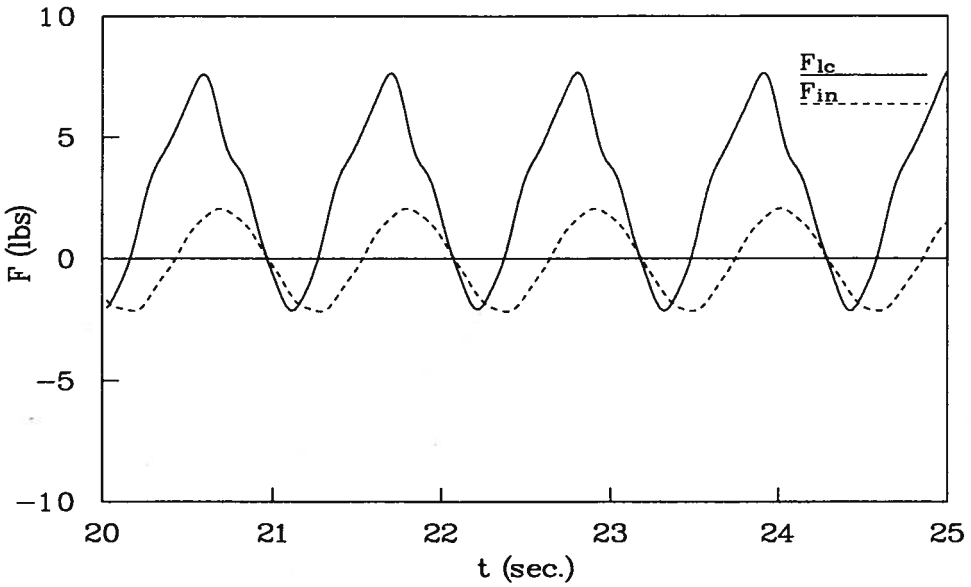

(b) Analyzed Load Cell and Inertial Forces

Figure 5.18: Run 23, $f_1 = 0.905\,Hz$, $A_1 = 1.110\,in$, $\alpha = 6$

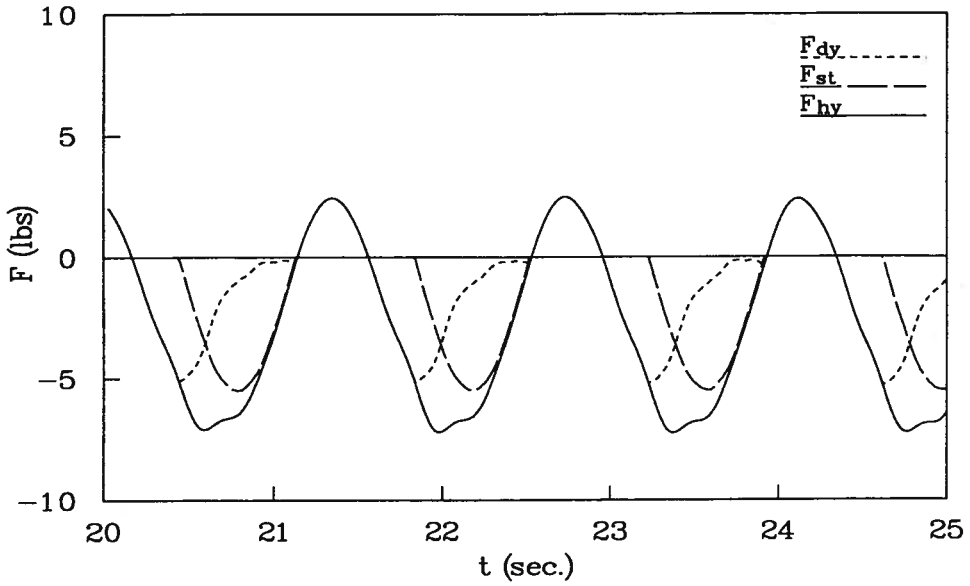

(a) Analyzed Hydrodynamic Forces

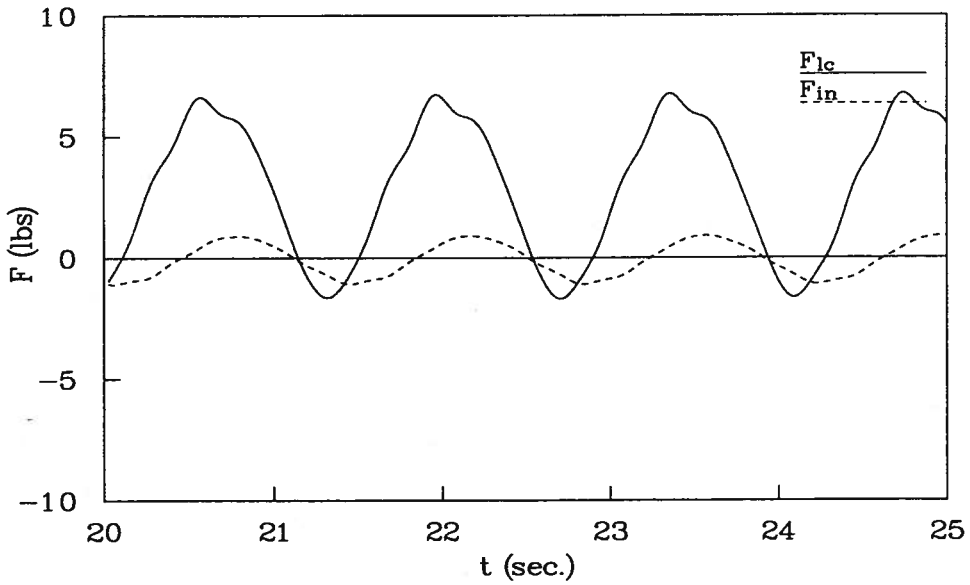

(b) Analyzed Load Cell and Inertial Forces

Figure 5.19: Run 24, $f_1 = 0.719\,Hz$, $A_1 = 0.825\,in$, $\alpha = 6$

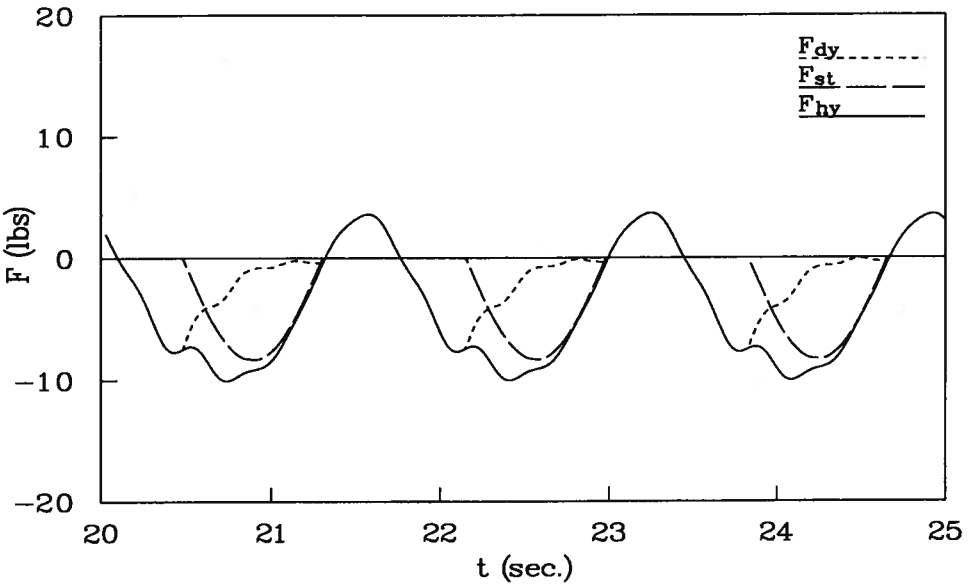

(a) Analyzed Hydrodynamic Forces

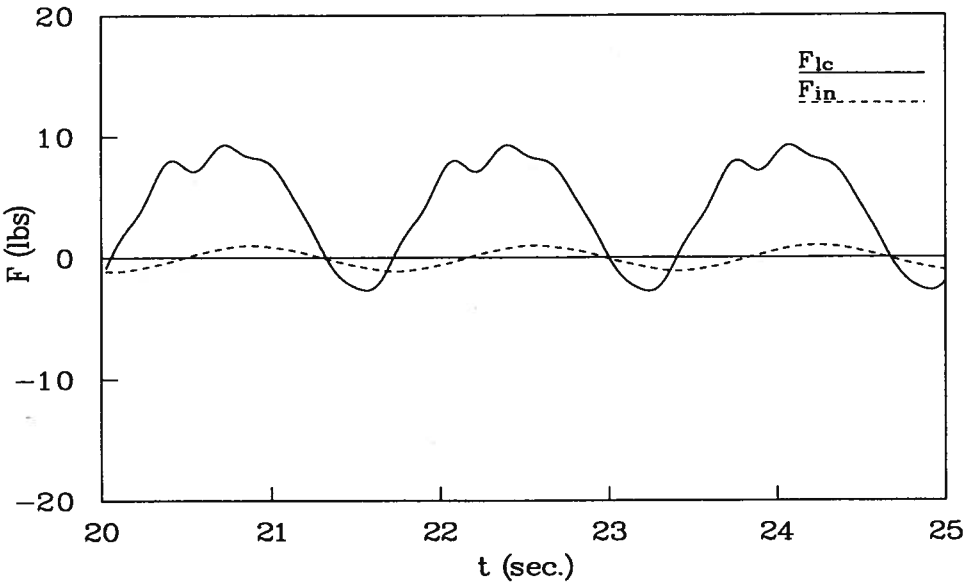

(b) Analyzed Load Cell and Inertial Forces

Figure 5.20: Run 25, $f_1 = 0.598\,Hz$, $A_1 = 1.257\,in$, $\alpha = 6$

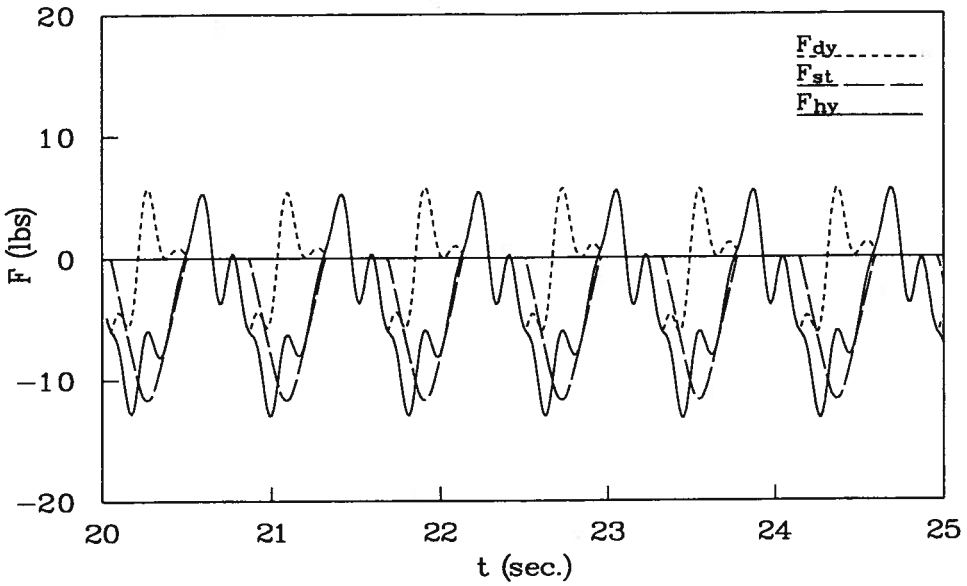

(a) Analyzed Hydrodynamic Forces

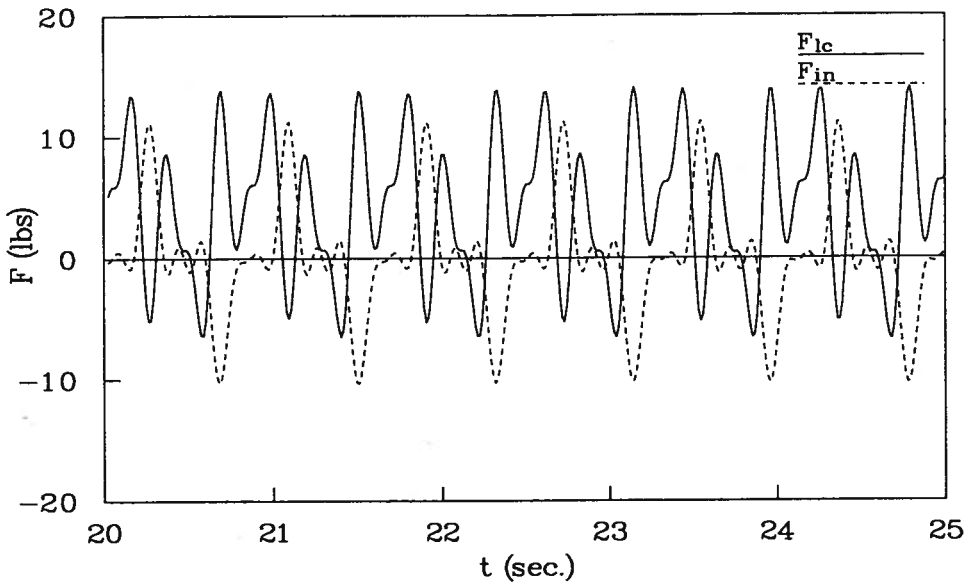

(b) Analyzed Load Cell and Inertial Forces

Figure 5.21: Run 26, $f_1 = 1.222\,Hz$, $A_1 = 1.455\,in$, $\alpha = 6$

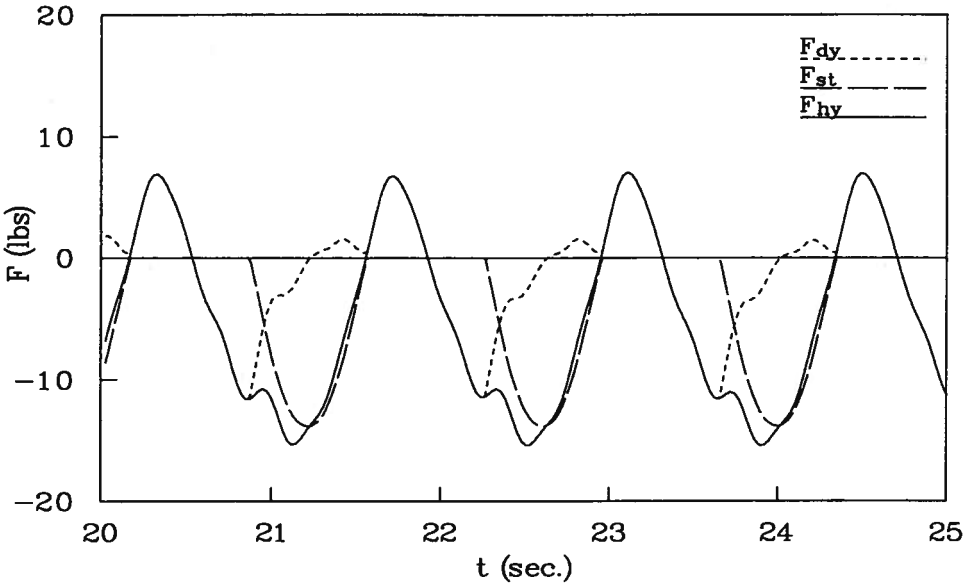

(a) Analyzed Hydrodynamic Forces

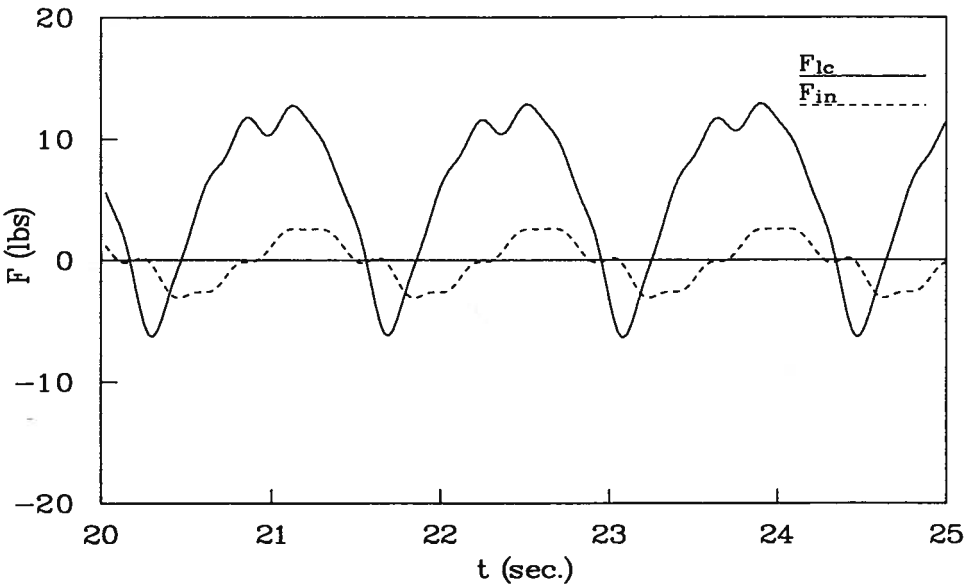

(b) Analyzed Load Cell and Inertial Forces

Figure 5.22: Run 28, $f_1 = 0.719\,Hz$, $A_1 = 2.189\,in$, $\alpha = 6$

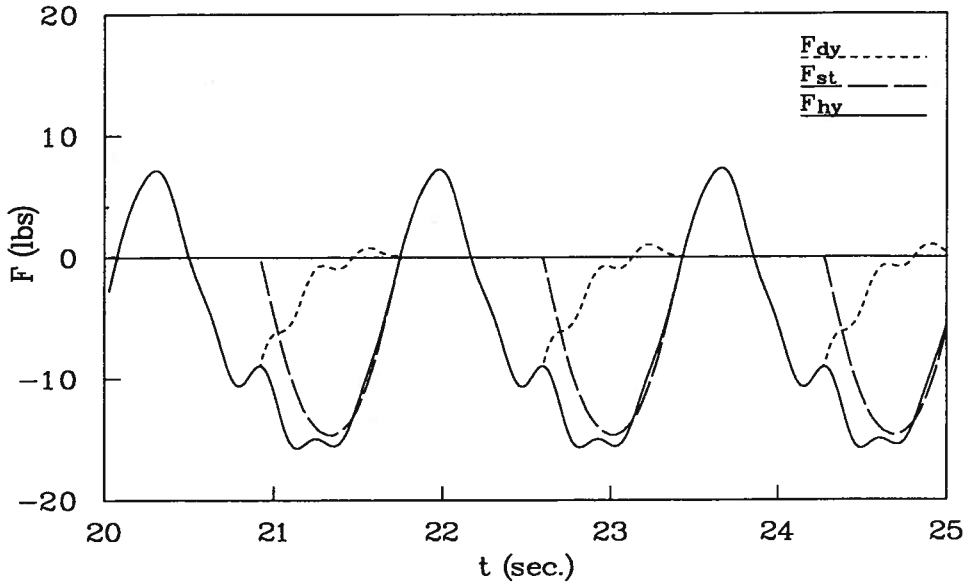

(a) Analyzed Hydrodynamic Forces

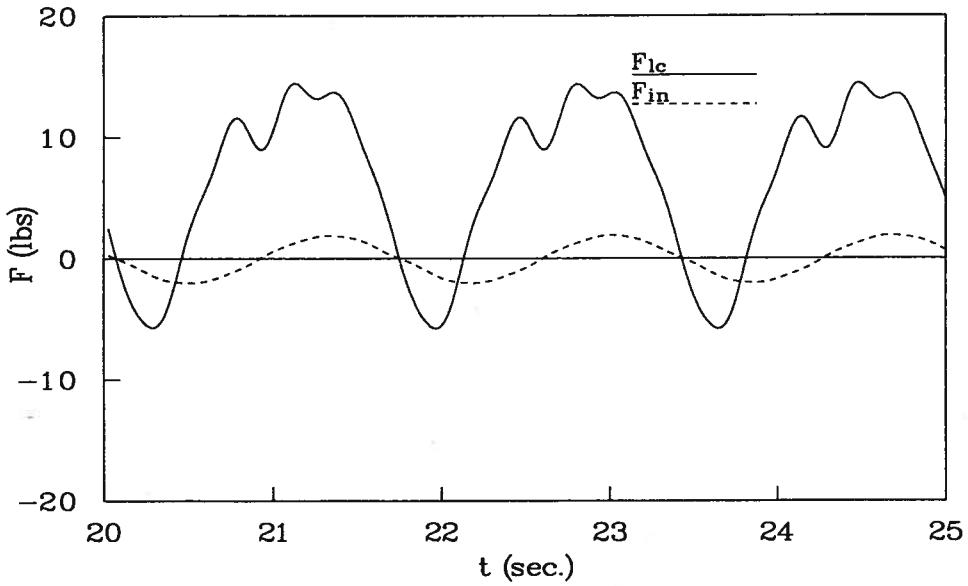

(b) Analyzed Load Cell and Inertial Forces

Figure 5.23: Run 29, $f_1 = 0.597\,Hz$, $A_1 = 2.372\,in$, $\alpha = 6$

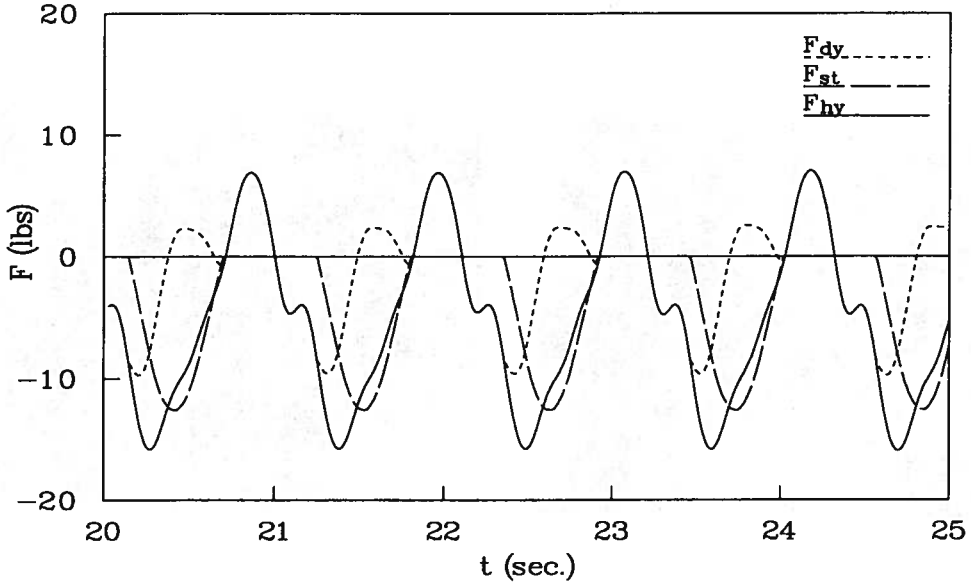

(a) Analyzed Hydrodynamic Forces

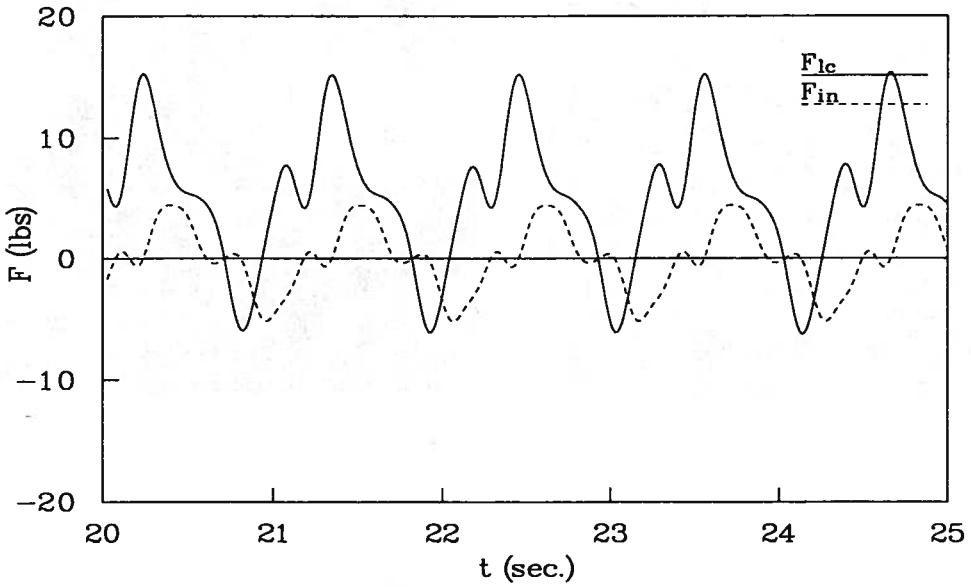

(b) Analyzed Load Cell and Inertial Forces

Figure 5.24: Run 30, $f_1 = 0.905\,Hz$, $A_1 = 1.858\,in$, $\alpha = 6$

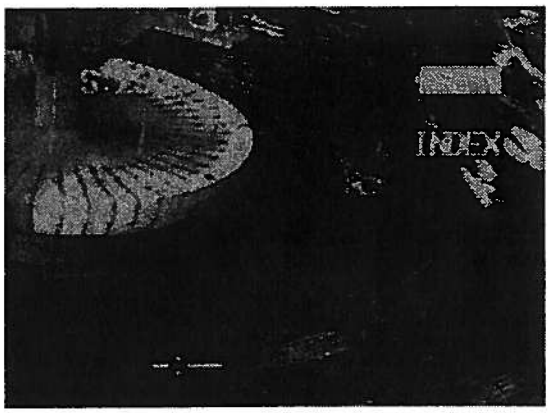

(a) $t = \frac{1}{4}T$

(b) $t = \frac{1}{2}T$

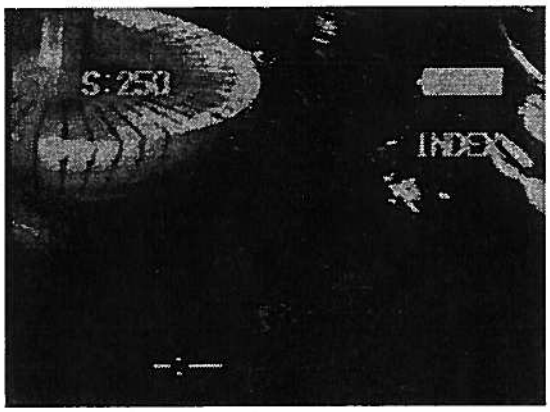

(c) $t = \frac{3}{4}T$

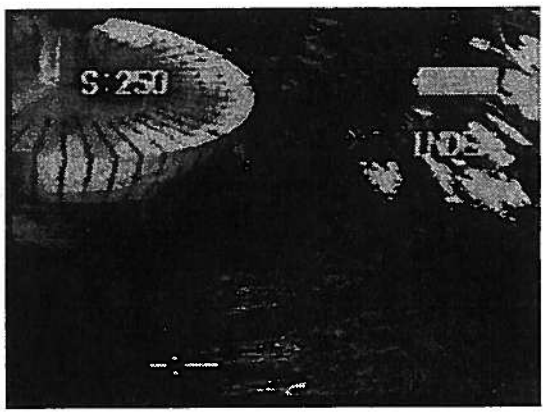

(d) $t = T$

Figure 5.25: Run 12, Wave Progress in Deck Dry Condition During One Period

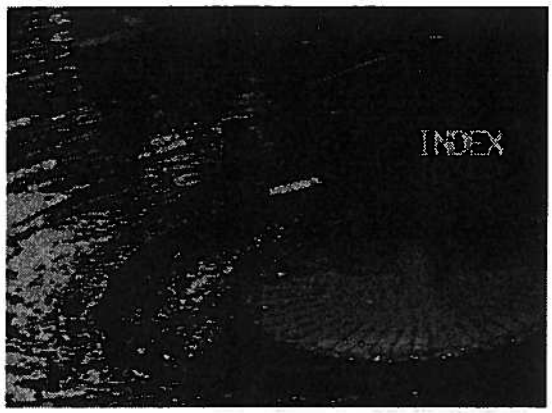

(a) $t = \frac{1}{4}T$

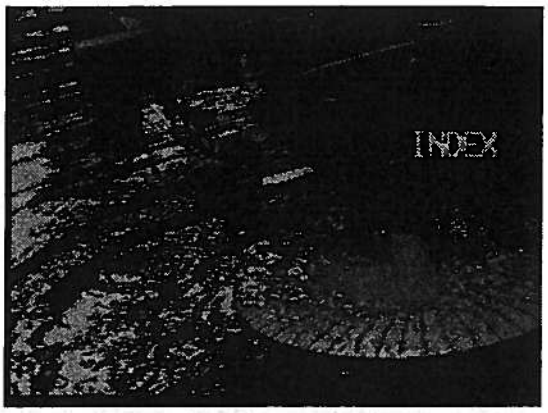

(b) $t = \frac{1}{2}T$

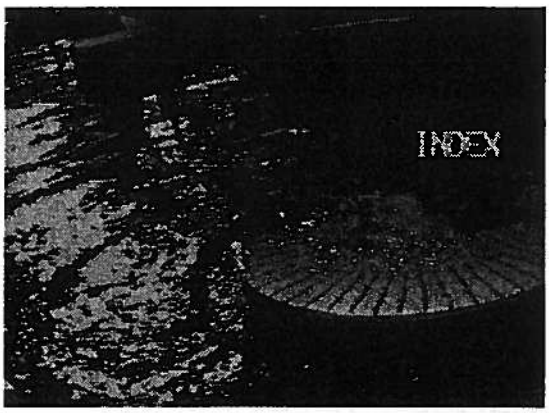

(c) $t = \frac{3}{4}T$

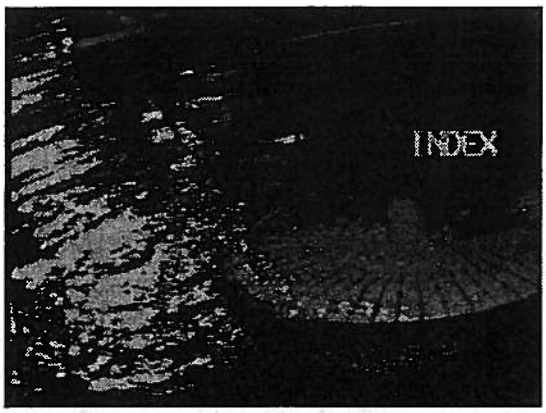

(d) $t = T$

Figure 5.26: Run 19, Green Water Progress on Deck During One Period

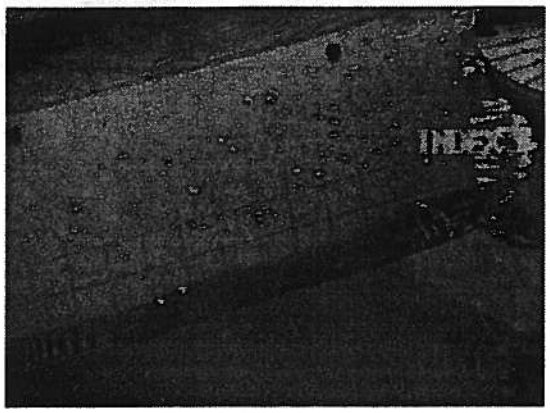

(a) $t = \frac{1}{4}T$

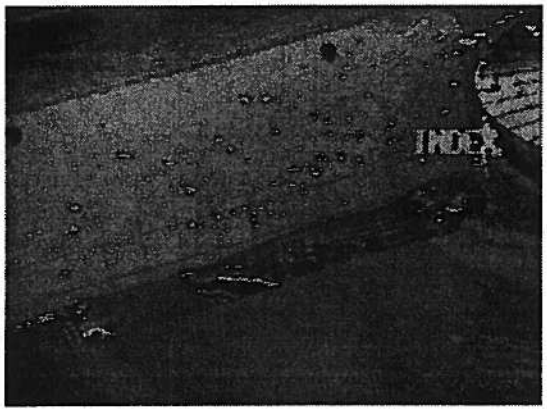

(b) $t = \frac{1}{2}T$

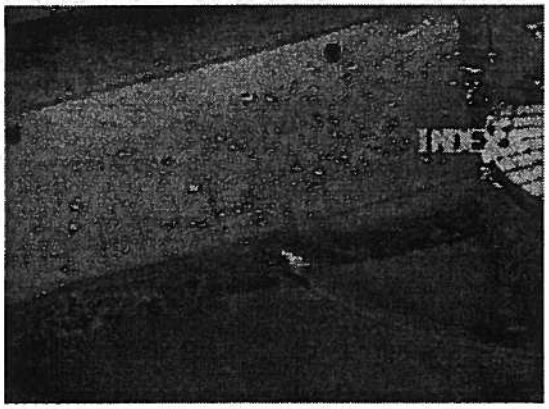

(c) $t = \frac{3}{4}T$

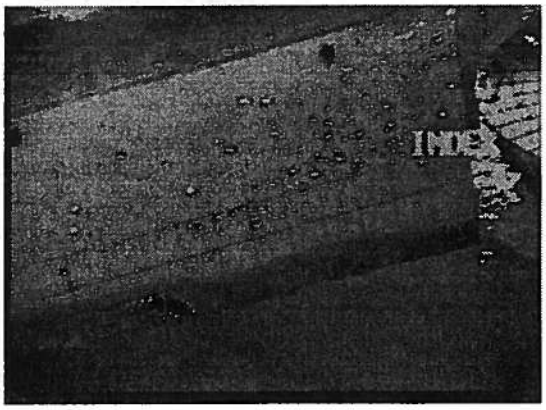

(d) $t = T$

Figure 5.27: Run 12, Wave Profiles in Deck Dry Condition During One Period

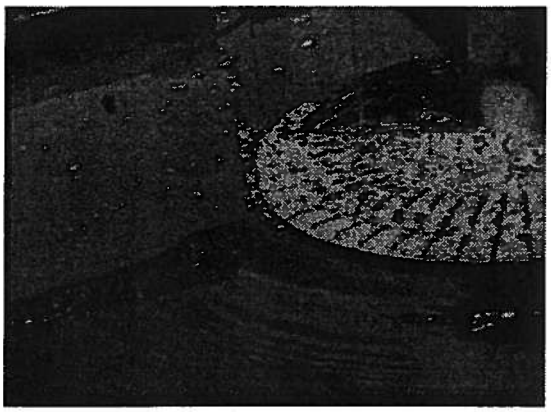

(a) $t = \frac{1}{4}T$

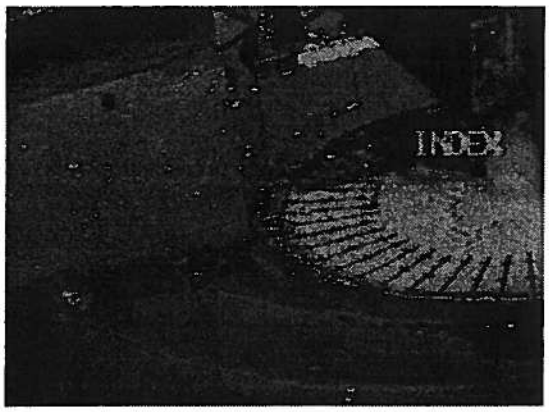

(b) $t = \frac{1}{2}T$

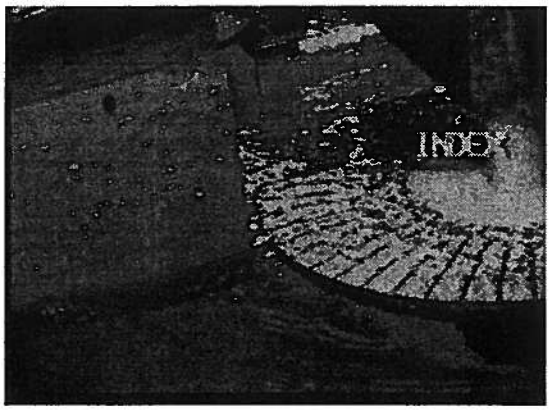

(c) $t = \frac{3}{4}T$

(d) $t = T$

Figure 5.28: Run 19, Wave Profiles of Green Water on Deck During one Period

Chapter 6

Summary and Conclusions

Some remarkable tendencies can be seen from the above analysis of the test results, which deliver the following conclusions:

- The nonlinear hydrostatic force acting as a stiffening spring produces a net positive offset for the deck dry condition and a net negative offset for green water on deck condition. This is the dominant component of the mean shift for the deck dry condition. Conversely, the increased mass associated with the green water on deck case offsets the hydrodynamic force, the net result being a negative mean offset.

- Highly nonlinear hydrodynamic phenomena have been observed from the components shown in Figures 5.1 to 5.24. The nonlinearities have been numerically described in Tables C.1 to C.24.

- Some tiny waves could be observed in front of the wavefront in some cases, see Figures 5.25 to 5.28, which may be contributed by both the water surface tension and the high-frequency oscillations induced by VMM. Further numerical studies (see Maskew, Wang and Troesch, 1994) are recommended to verify this conclusion. These tiny waves may also provide useful information for contact-line problems.

- Critical issues that are being addressed in the ongoing study include contact line behavior, jet development, sharp bow flow.

- This experiment is primarily designed to generate sets of quality experimental data for comparison with time-domain codes. These time-history acquisitions can be useful to develop a rational technology for evaluating a naval vessel's nonlinear hydrodynamics.

Chapter 7

Acknowledgments

The results presented here are from studies supported by the Office of Naval Research, Contract DOD-G-N00014-90-J-1818.

Bibliography

[1] Tasai, F. and W. Koterayama, 1976, "Nonlinear Hydrodynamic Forces Acting on Cylinders Heaving on the Surface of a Fluid" Reports of Research Institute for Applied Mechanics Vol. XXIV, No. 77.

[2] Radev, D. and W. Beukelman, 1992, "Slamming on Forced Oscillating Wedges at Forward Speed, Part I-Test Results", Int. Shipbuild. Progr., Vol. 39, No. 420, pp. 399-422, January.

[3] Troesch, A.W. and C.G. Kang, 1986, "Hydrodynamic Impact Loads on Three-dimensional bodies," 16th Symposium on Naval Hydrodynamics, U.C. Berkeley, CA.

[4] Troesch, A.W. and C.G. Kang, 1988, "Evaluation of Impact Loads Associated with Flare Slamming," SNAME Spring Meeting/STAR Symposium, Pittsburgh, PA.

[5] Kang, C.G., 1988, "Bow Flare Slamming and Nonlinear Free Surface-Body Interaction in the Time Domain," Ph.D Thesis, Dept. of NAME, Univ. of Michigan.

[6] Maskew, B., 1992, "Prediction of Nonlinear Wave/Hull Interactions on Complex Vessels," 19th Symposium on Naval Hydrodynamics, Seoul, Korea.

[7] Maskew, B., M. Wang and A.W. Troesch, 1994, "Comparison of Calculated and Measured Loads on a Flared Body Oscillating in a Free Surface," Presented at 20th Symposium on Naval Hydrodynamics, U.C. Santa Barbara, CA.

[8] Ashcroft, F.H., A.W. Troesch and P. Sullivan, 1989, "Design, Construction, and Initial Testing of a Vertical Motion Mechanism," Proc. 22nd ATTC, St. John's, NF, Aug. 8-11, pp. 204-210.

Appendix A

Description of Experimental Data

The attached floppy disk package includes the time histories of load cells, vertical motions including prescribed displacements and accelerations, and wave elevations of the vertical forced oscillation tests on the idealized flared body in MHL's towing tank, whose run tests are summarized in Table 3.1. All the time-history acquisitions and their FFT results are plotted and listed in Appendix B where 'disp' and 'acc' indicates the prescribed displacement and the acceleration of the vertical motions, respectively; 'lc1', 'lc2', 'sum lc' and 'diff lc' denote Load Cell 1, Load Cell 2, the sum and the difference of two load cells, respectively; 'w1', 'w2', 'w3', 'w4', 'w5' and 'w6' represent the wave elevations measured by the corresponding wave probes, respectively; the prefix 'FTG' define the gain of Fourier coefficients. We adopt the British unit system here, that is, the unit of load cells is 'lbs' and the length unit is inch. Appendix C shows the tables of the first six harmonic Fourier coefficients including gains and phases with the same units as above.

In this package, there are a total of seven $3\frac{1}{2}''$ floppy disks which are Macintosh formatted. Each of the enclosed floppies includes a description file named README. The three floppies named DECK DRY CONDITION include the data files of deck dry condition cases and the other four floppies named GREEN WATER ON DECK include the data files of deckwetness cases. Both previous and new repeated experimental data are included in the floppy disks. The previous results only contain prescribed displacement and

wave elevations measured at different positions. The repeated experimental results consist of load cells, prescribed displacement, acceleration and the wave elevation located at the position of No. 2 wave probe but 16.8 inches away from the center of the flared body. See their README and Table 3.1 for details.

The format of the data files is a sequential real format in which the arrays are stored one after the other. The format is illustrated as the following Fortran write statements which will produce the correct format:

```
      write(4,*) '*REAL*'
      write(4,1000) TITLE
1000  format(a80)
      write(4,1001) LABEL,VT1,VARDT,NPTS
1001  format(a12,2(1x,1pe12.5),1x,i5)
      write(4,1002) (TH(j),j=1,NPTS)
1002  format(10(1x,1pe12.5))
```

where

REAL	used to separate arrays in original program;
TITLE	80 character title of the array;
LABEL	12 character of the array;
VT1	starting time of frequency;
VARDT	incremental time;
NPTS	number of points in the array of time-history record;
TH(j)	values of the time-history arrays, 10 values per line.

Appendix B

Figures of Time Histories and the FFT Analyses

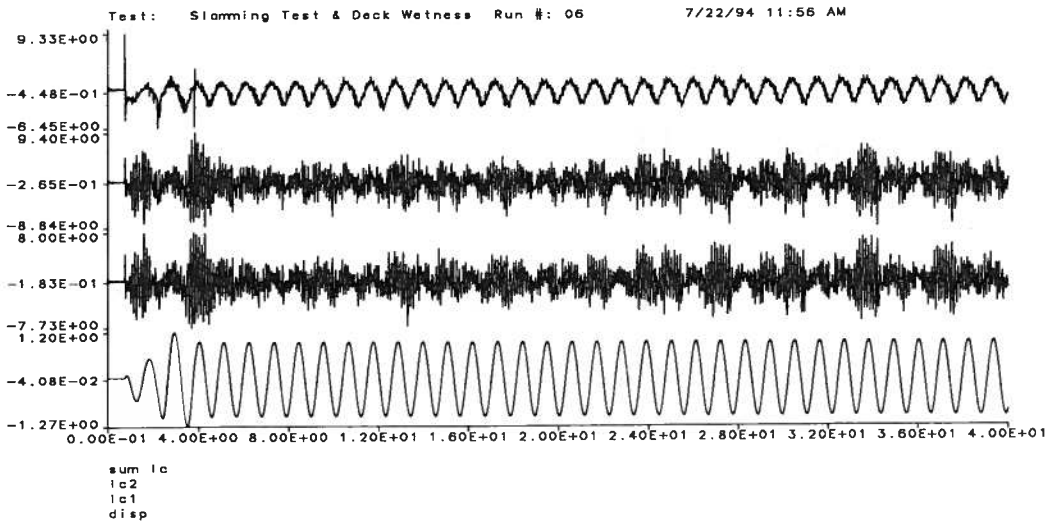

(a) Time-History Acquisitions

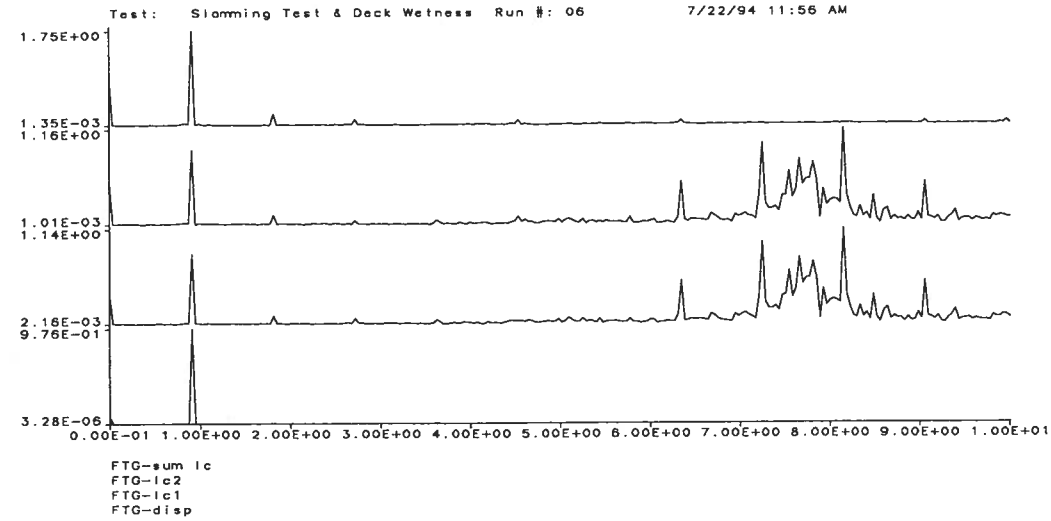

(b) Gains of the FFT Analyses

Figure B.1: Run 06, $f_1 = 0.907\,Hz$, $A_1 = 0.976\,in$, $\alpha = 6$

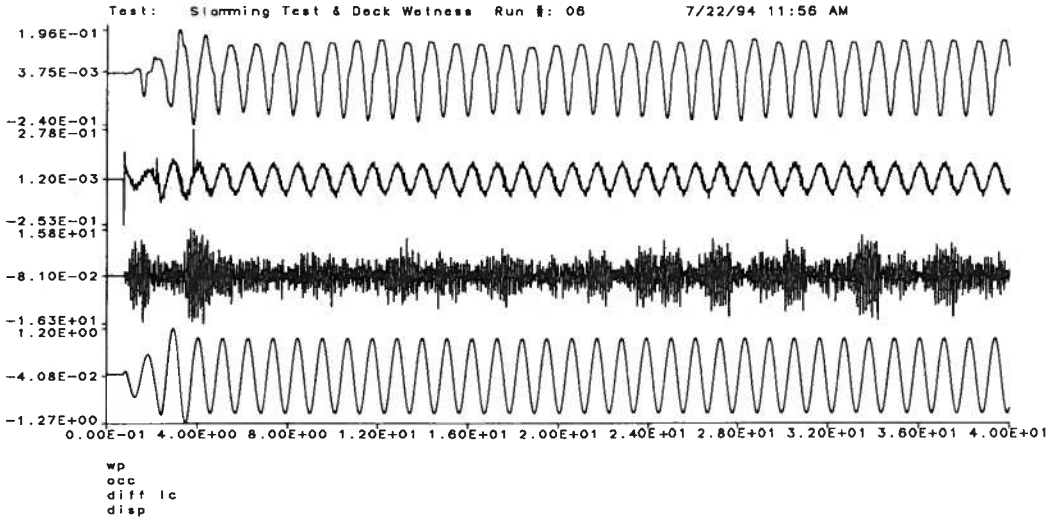

(a) Time-History Acquisitions

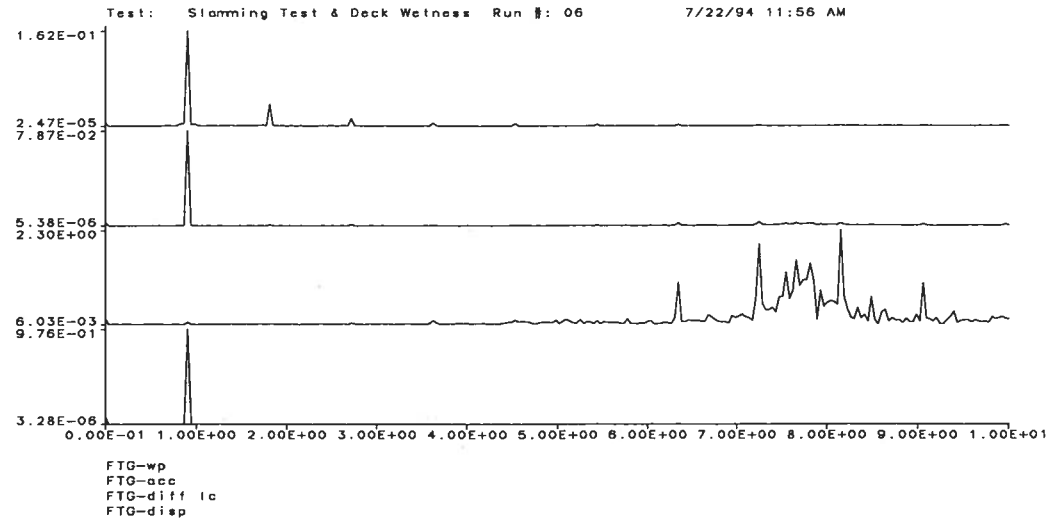

(b) Gains of the FFT Analyses

Figure B.2: Run 06, $f_1 = 0.907\,Hz$, $A_1 = 0.976\,in$, $\alpha = 6$

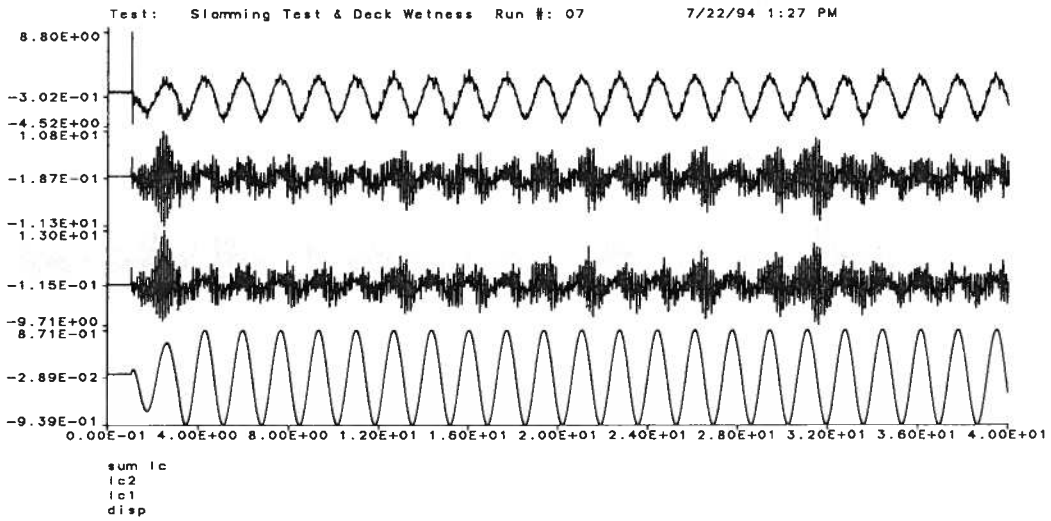

(a) Time-History Acquisitions

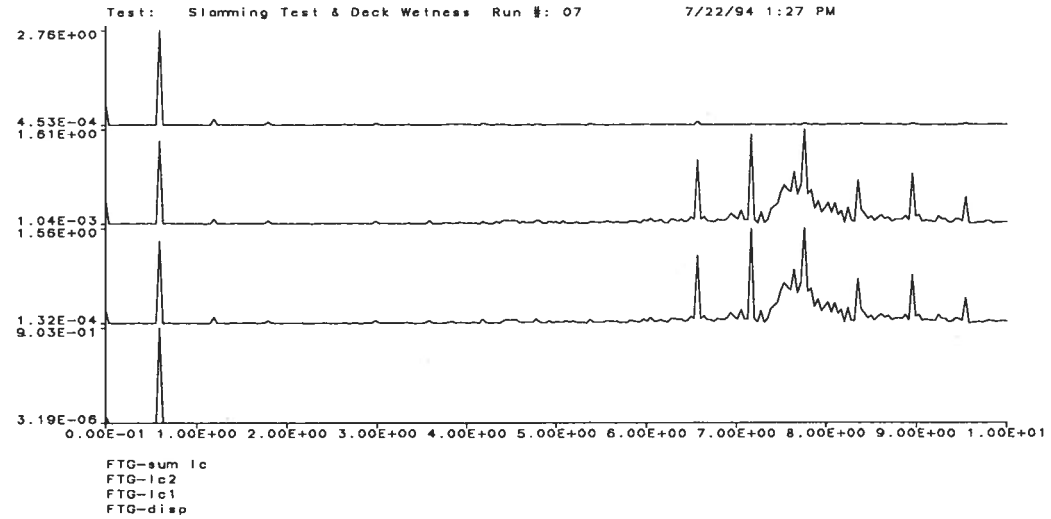

(b) Gains of the FFT Analyses

Figure B.3: Run 07, $f_1 = 0.598\,Hz$, $A_1 = 0.903\,in$, $\alpha = 6$

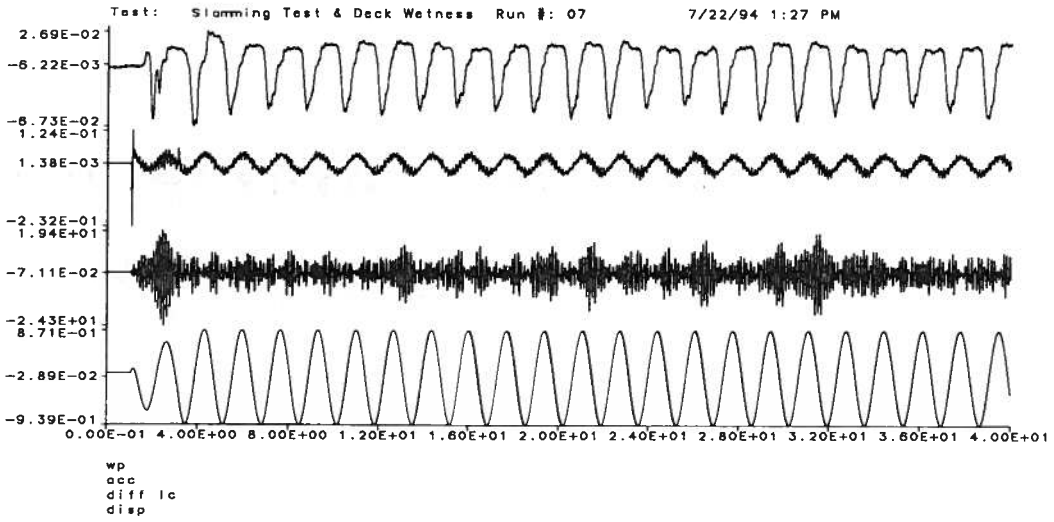

(a) Time-History Acquisitions

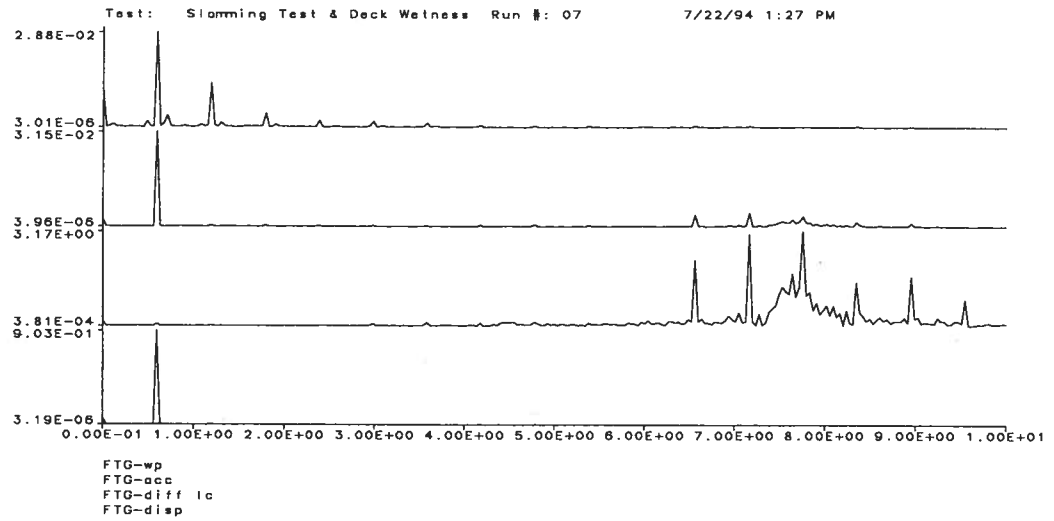

(b) Gains of the FFT Analyses

Figure B.4: Run 07, $f_1 = 0.598\,Hz$, $A_1 = 0.903\,in$, $\alpha = 6$

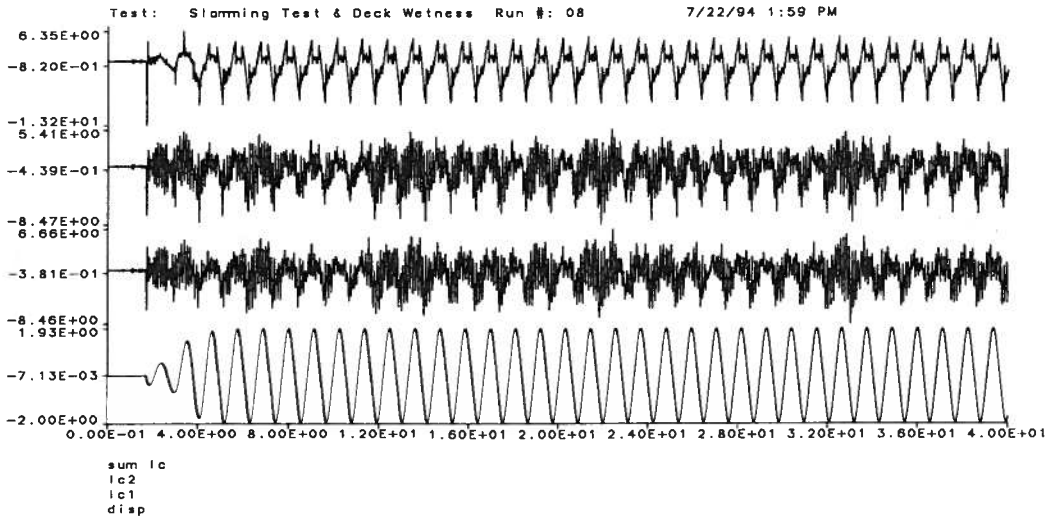

(a) Time-History Acquisitions

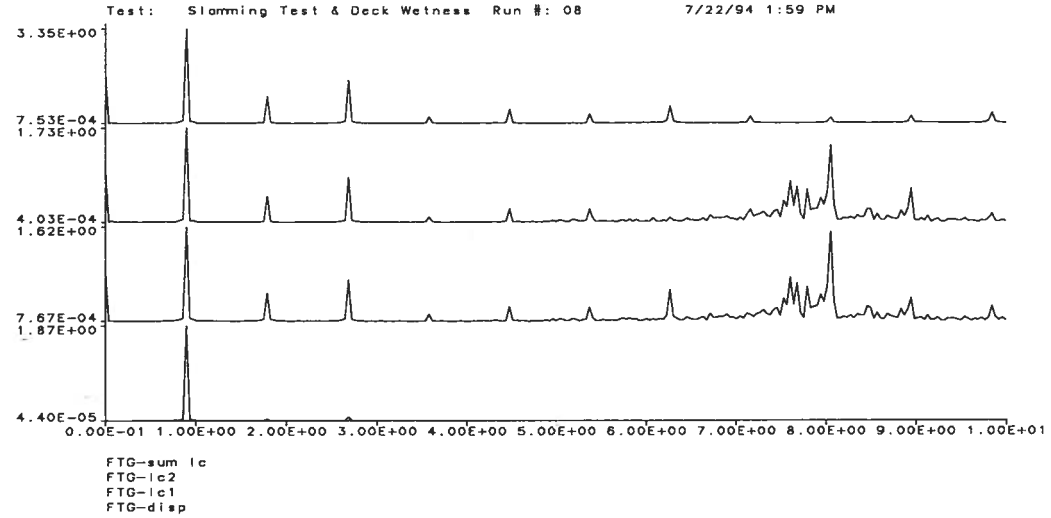

(b) Gains of the FFT Analyses

Figure B.5: Run 08, $f_1 = 0.895\,Hz$, $A_1 = 1.873\,in$, $\alpha = 6$

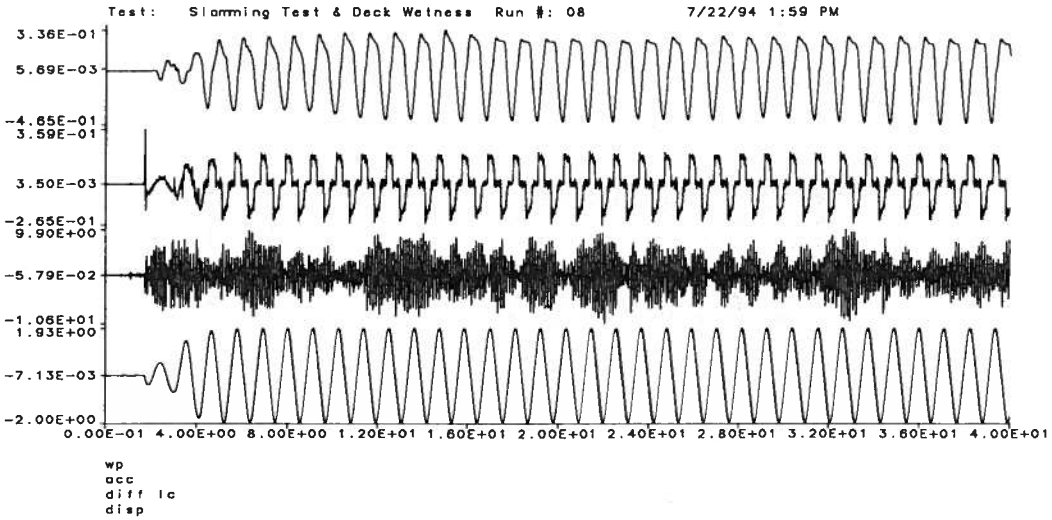

(a) Time-History Acquisitions

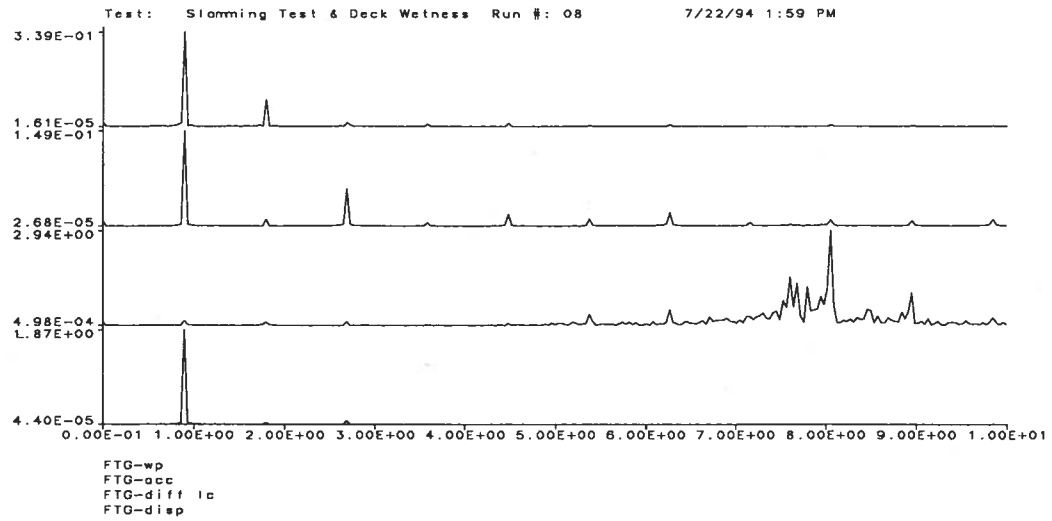

(b) Gains of the FFT Analyses

Figure B.6: Run 08, $f_1 = 0.895\,Hz$, $A_1 = 1.873\,in$, $\alpha = 6$

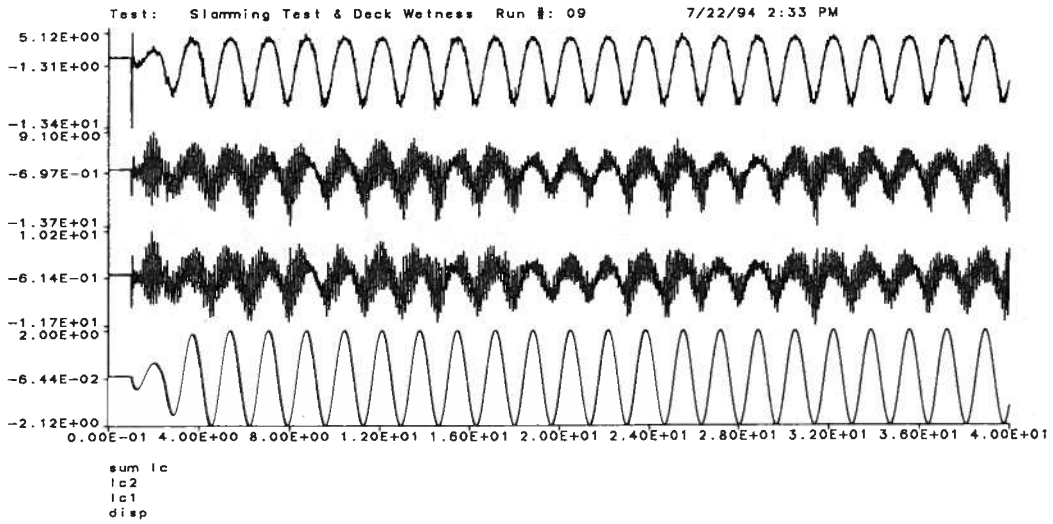

(a) Time-History Acquisitions

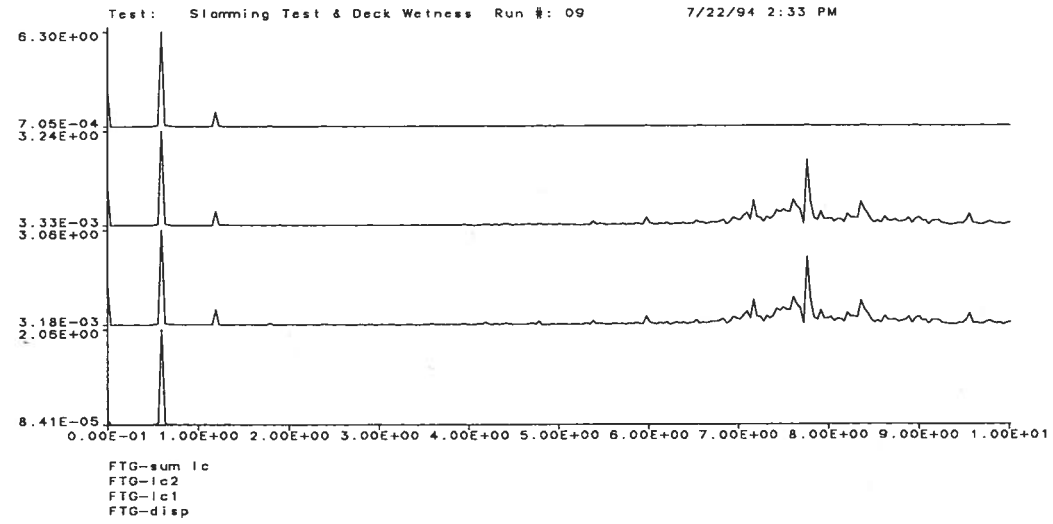

(b) Gains of the FFT Analyses

Figure B.7: Run 09, $f_1 = 0.598\,Hz$, $A_1 = 2.056\,in$, $\alpha = 6$

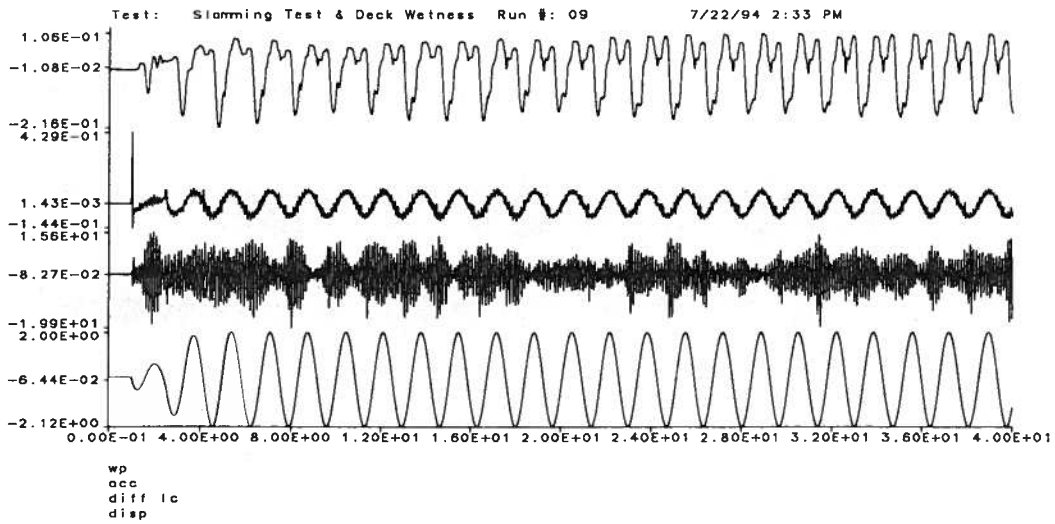

(a) Time-History Acquisitions

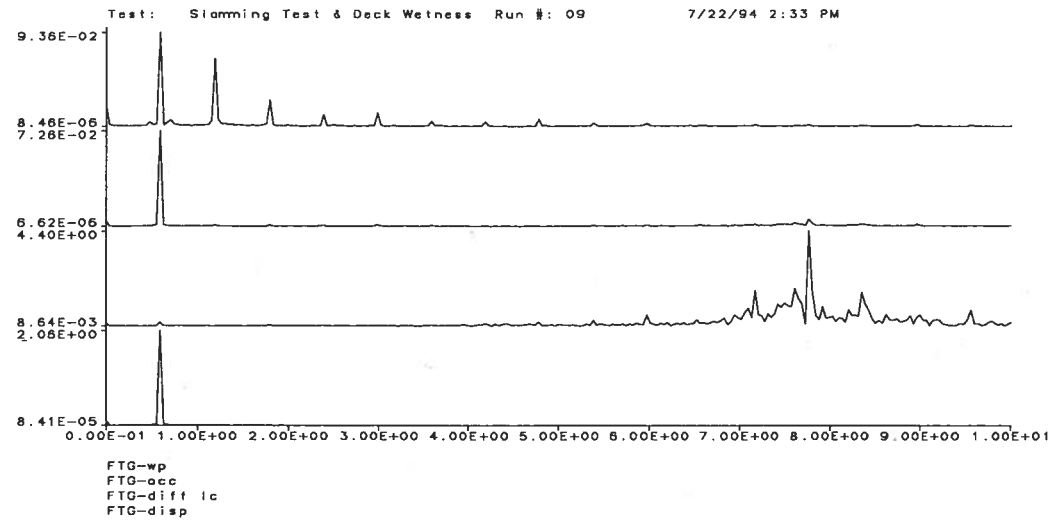

(b) Gains of the FFT Analyses

Figure B.8: Run 09, $f_1 = 0.598\,Hz$, $A_1 = 2.056\,in$, $\alpha = 6$

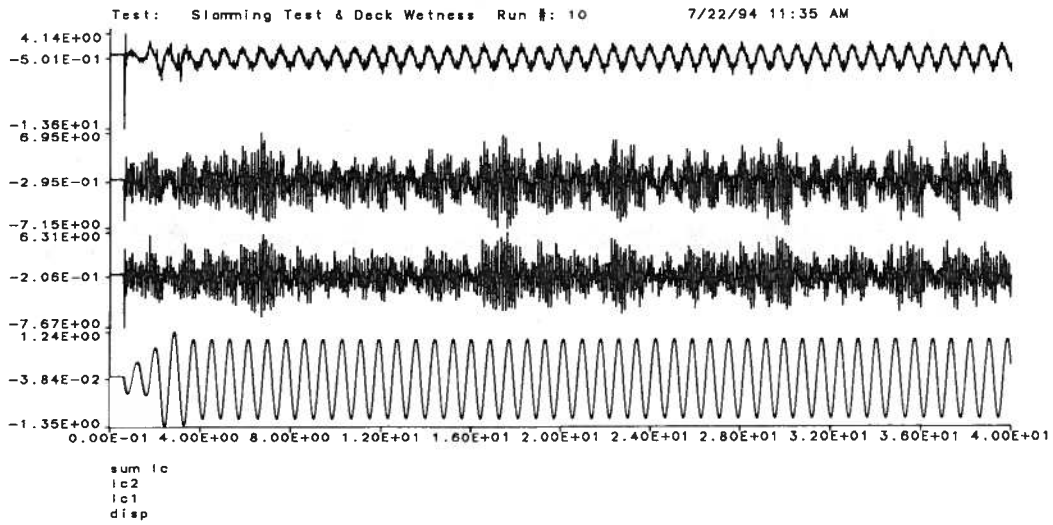

(a) Time-History Acquisitions

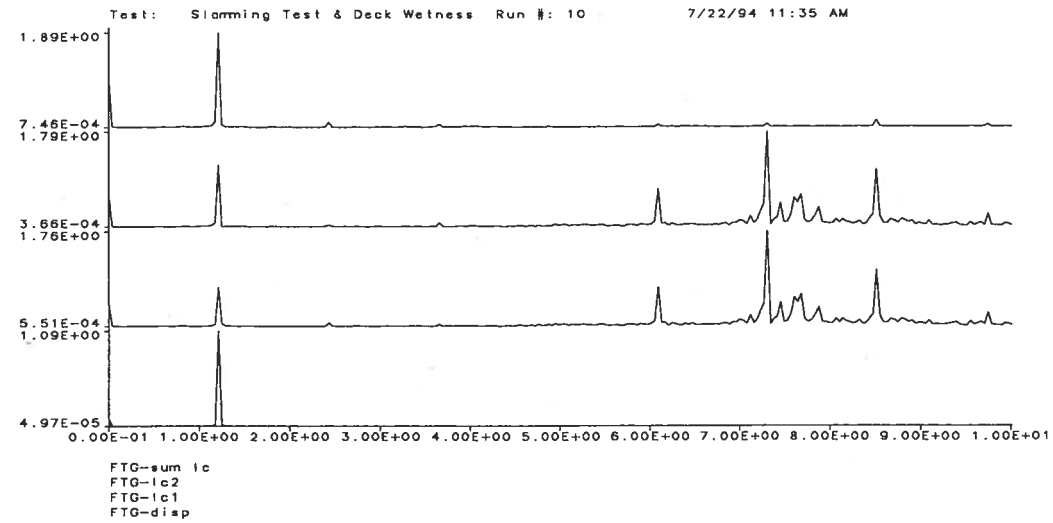

(b) Gains of the FFT Analyses

Figure B.9: Run 10, $f_1 = 1.220\,Hz$, $A_1 = 1.087\,in$, $\alpha = 6$

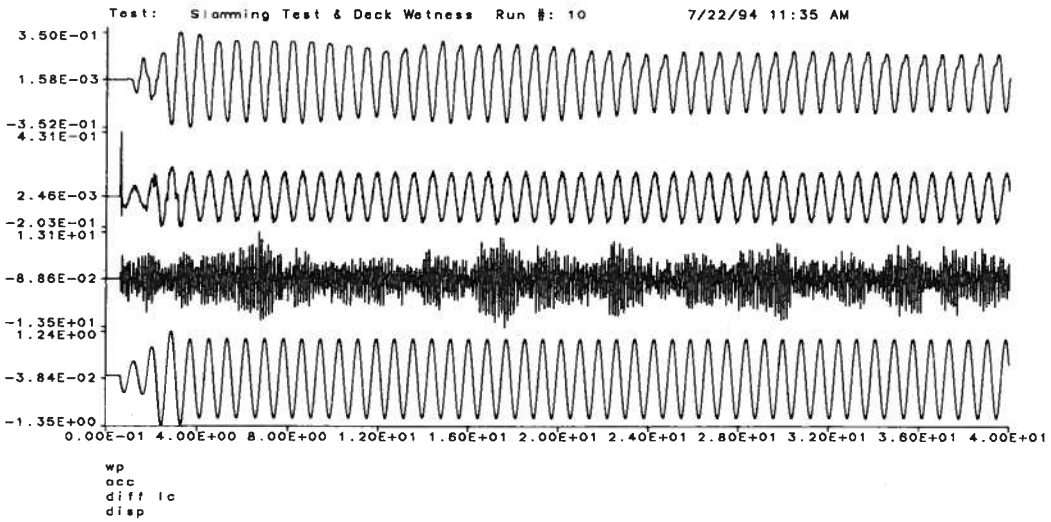

(a) Time-History Acquisitions

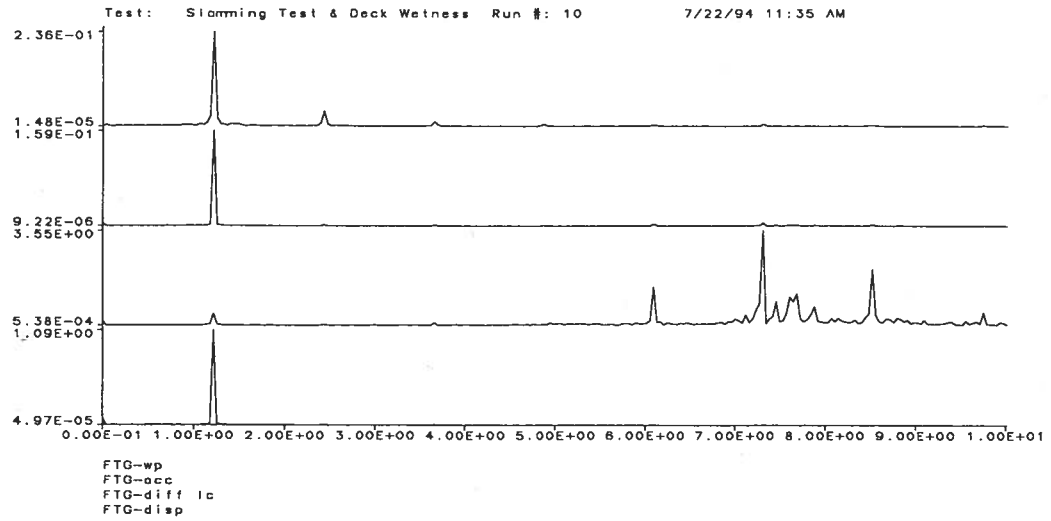

(b) Gains of the FFT Analyses

Figure B.10: Run 10, $f_1 = 1.220\,Hz$, $A_1 = 1.087\,in$, $\alpha = 6$

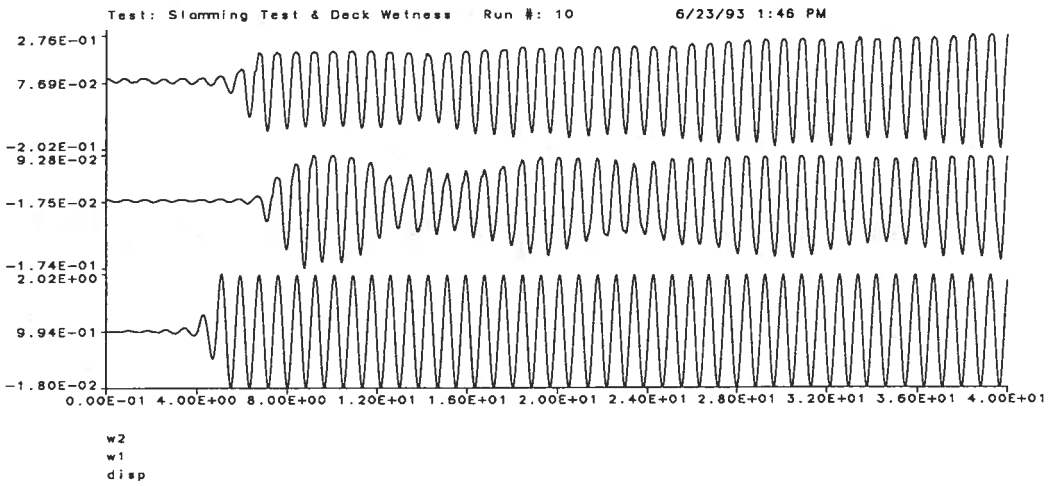

(a) Time-History Acquisitions

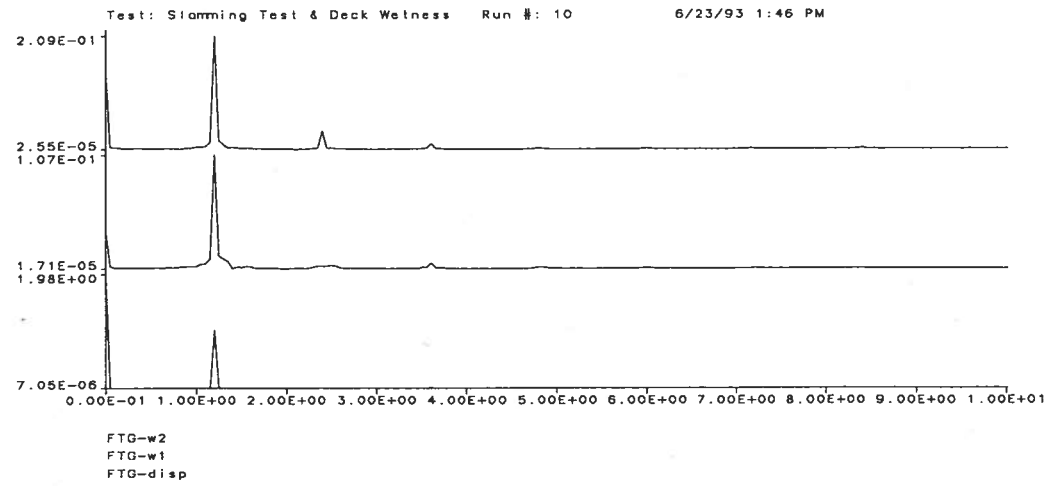

(b) Gains of the FFT Analyses

Figure B.11: Run 10, $f_1 = 1.202\,Hz$, $A_1 = 1.001\,in$, $\alpha = 6$

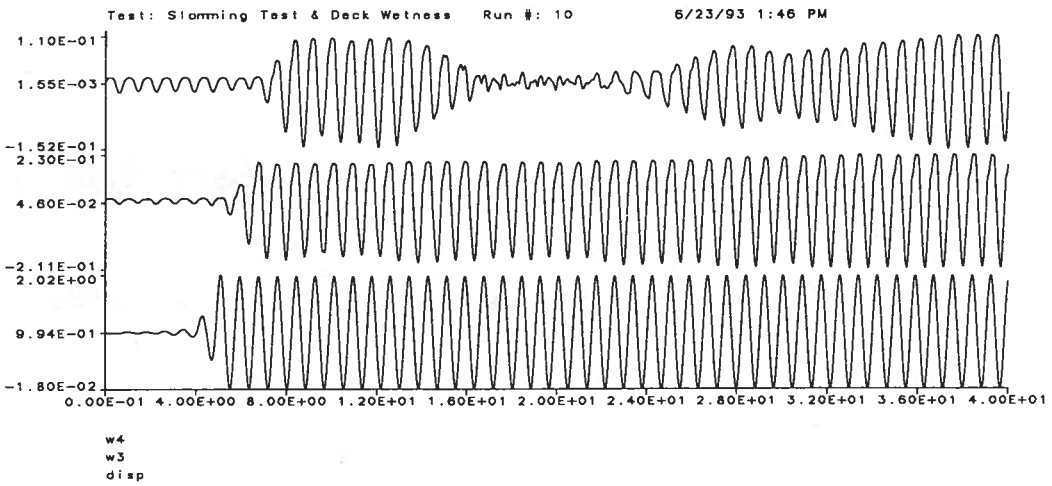

(a) Time-History Acquisitions

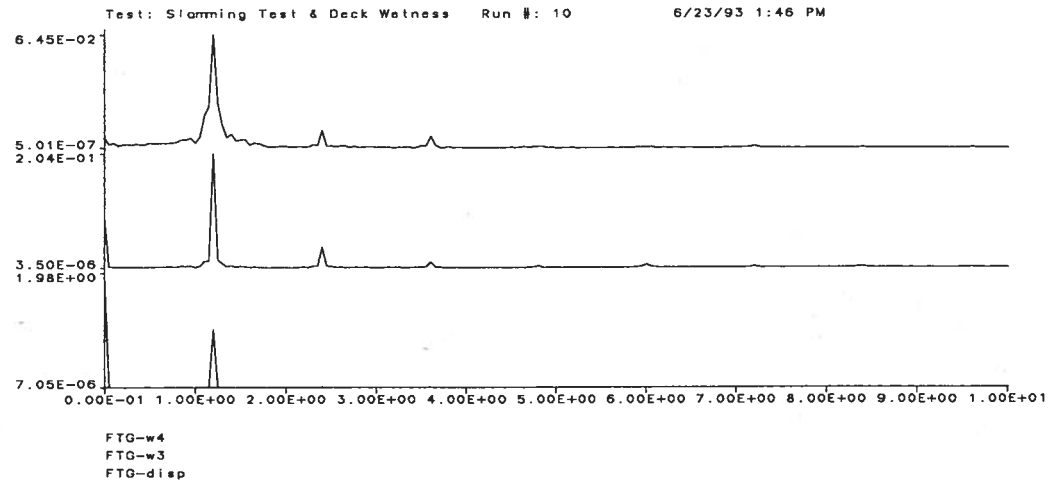

(b) Gains of the FFT Analyses

Figure B.12: Run 10, $f_1 = 1.202\,Hz$, $A_1 = 1.001\,in$, $\alpha = 6$

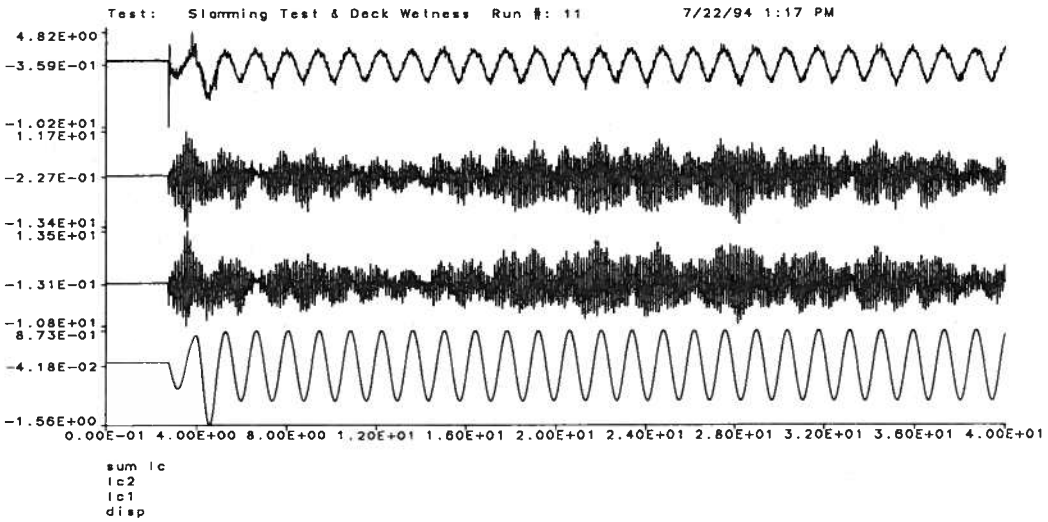

(a) Time-History Acquisitions

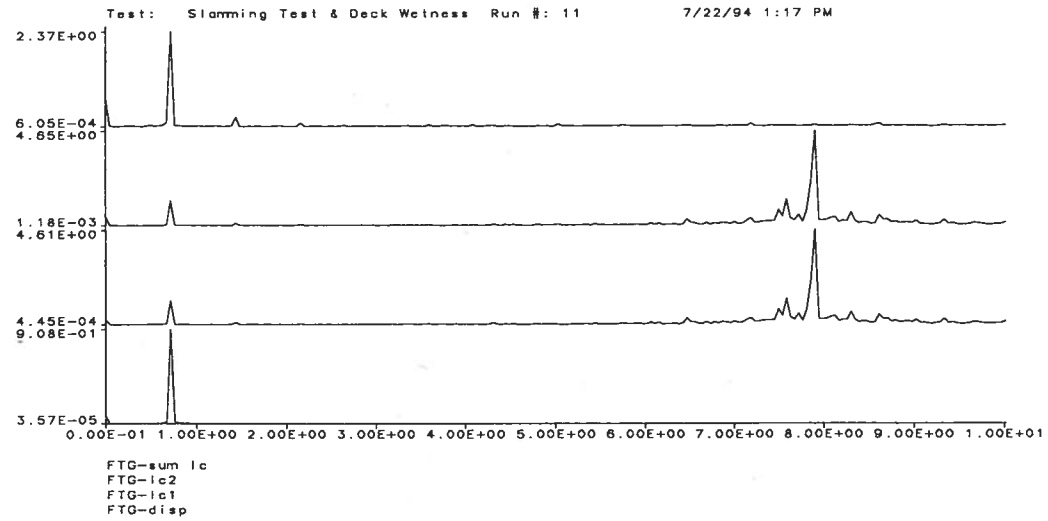

(b) Gains of the FFT Analyses

Figure B.13: Run 11, $f_1 = 0.719\,Hz$, $A_1 = 0.908\,in$, $\alpha = 6$

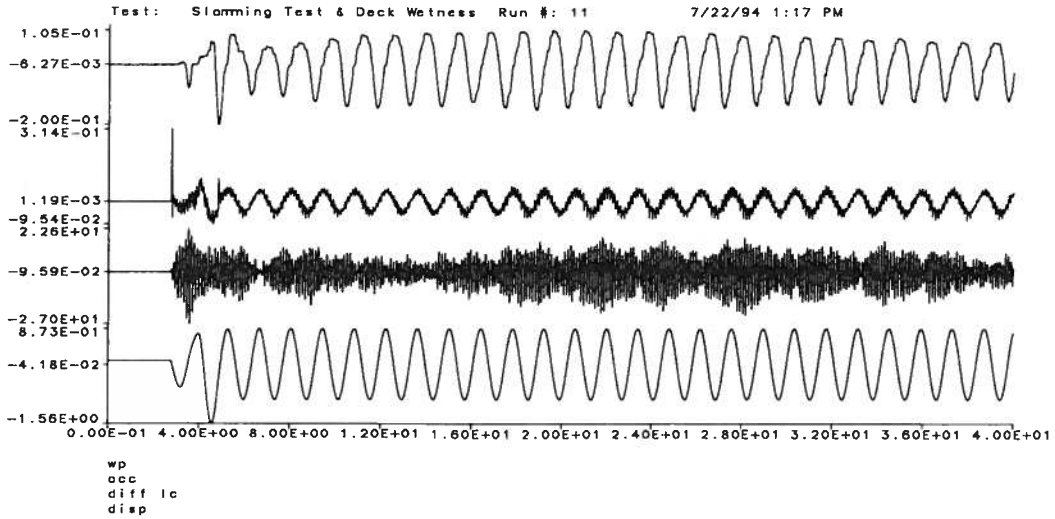

(a) Time-History Acquisitions

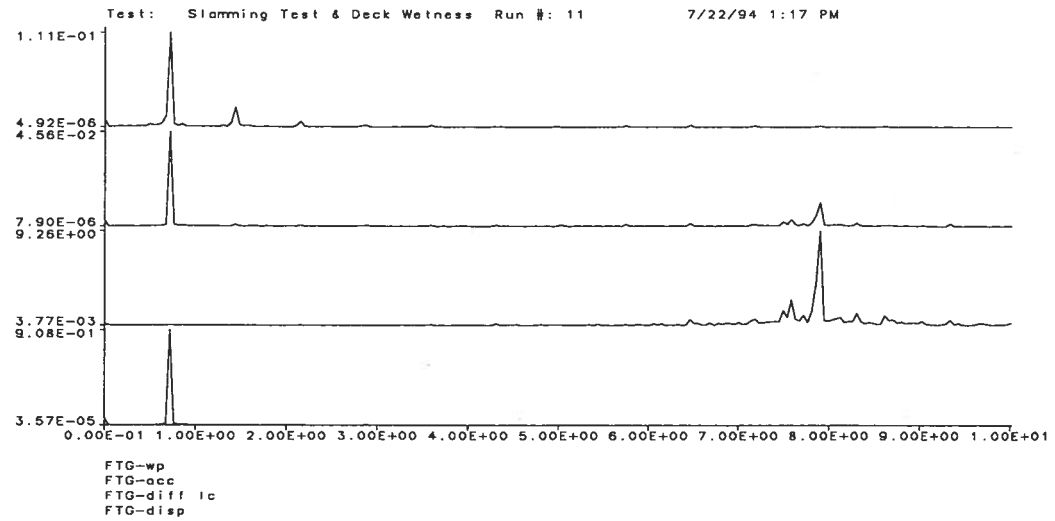

(b) Gains of the FFT Analyses

Figure B.14: Run 11, $f_1 = 0.719\,Hz$, $A_1 = 0.908\,in$, $\alpha = 6$

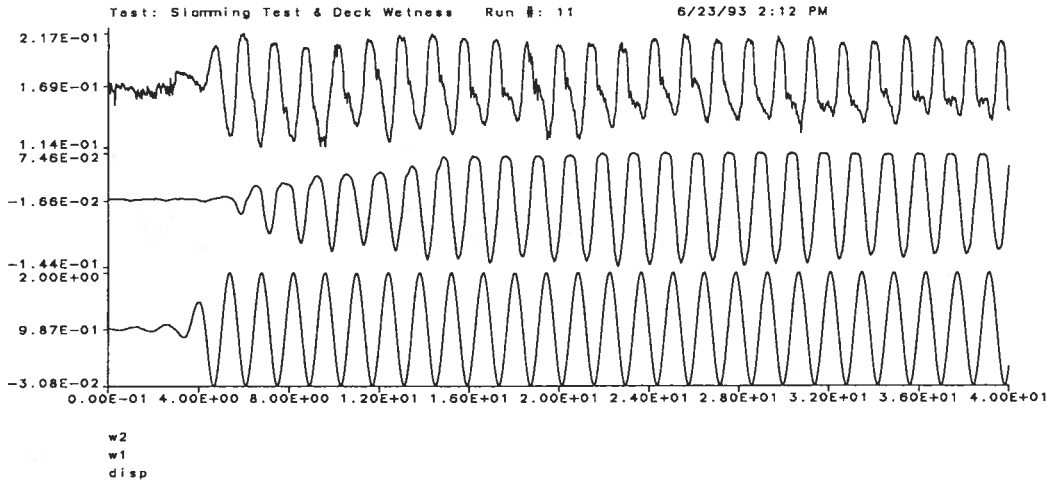

(a) Time-History Acquisitions

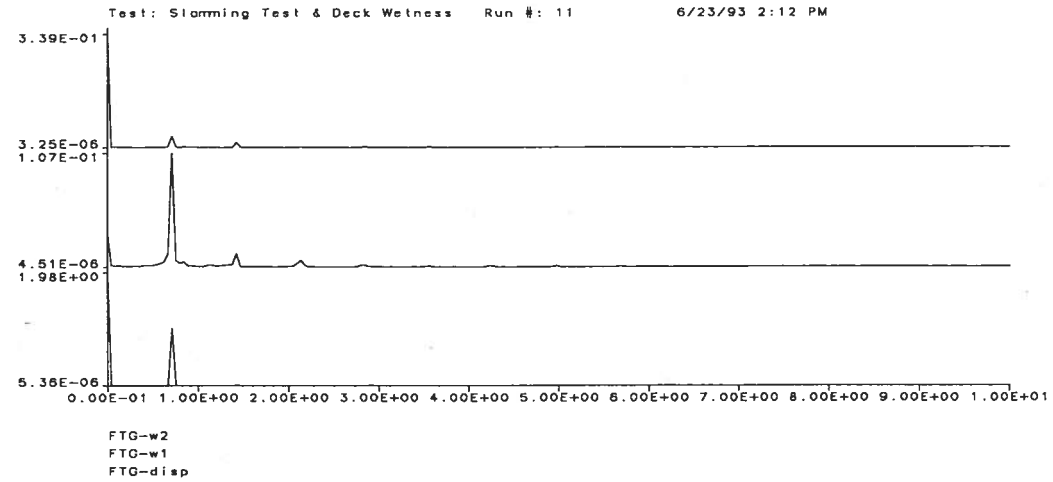

(b) Gains of the FFT Analyses

Figure B.15: Run 11, $f_1 = 0.712\,Hz$, $A_1 = 1.006\,in$, $\alpha = 6$

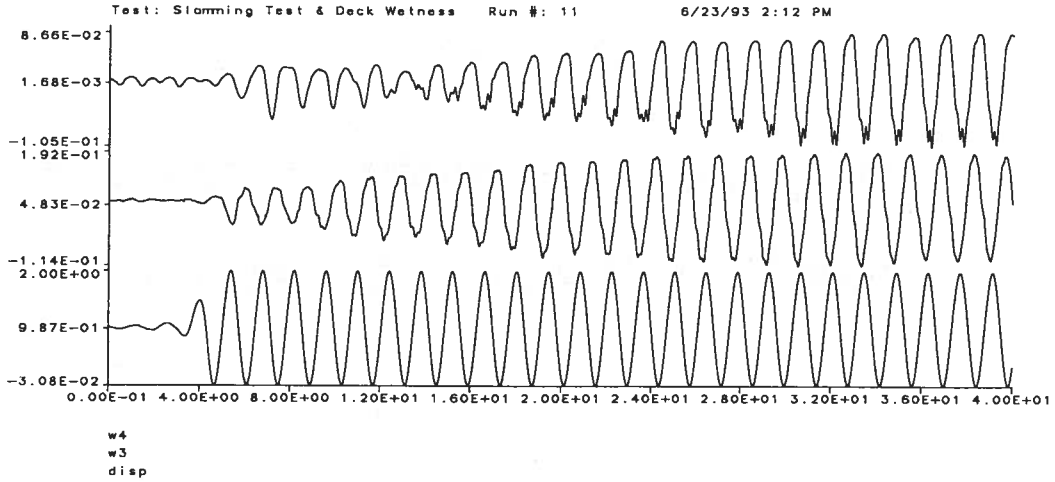

(a) Time-History Acquisitions

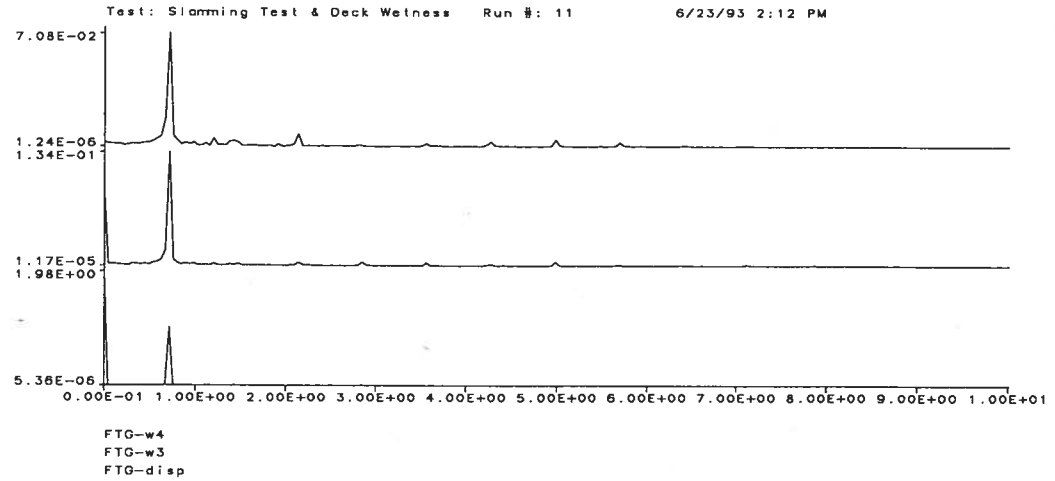

(b) Gains of the FFT Analyses

Figure B.16: Run 11, $f_1 = 0.712\,Hz$, $A_1 = 1.006\,in$, $\alpha = 6$

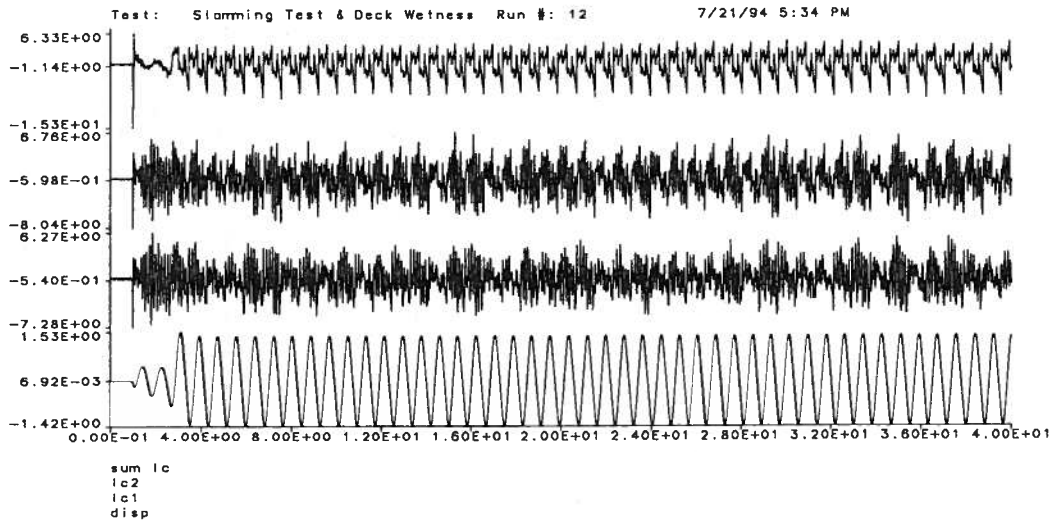

(a) Time-History Acquisitions

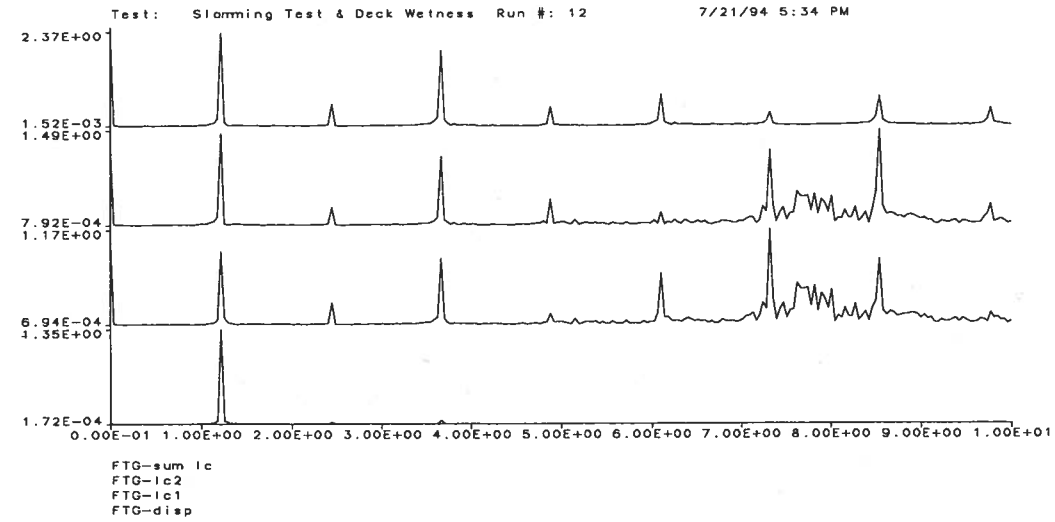

(b) Gains of the FFT Analyses

Figure B.17: Run 12, $f_1 = 1.221\,Hz$, $A_1 = 1.357\,in$, $\alpha = 6$

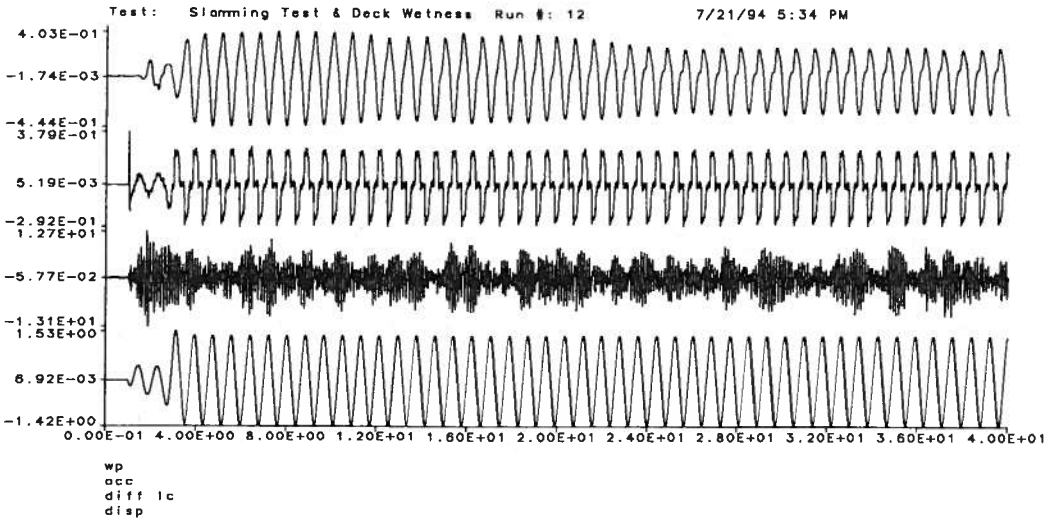

(a) Time-History Acquisitions

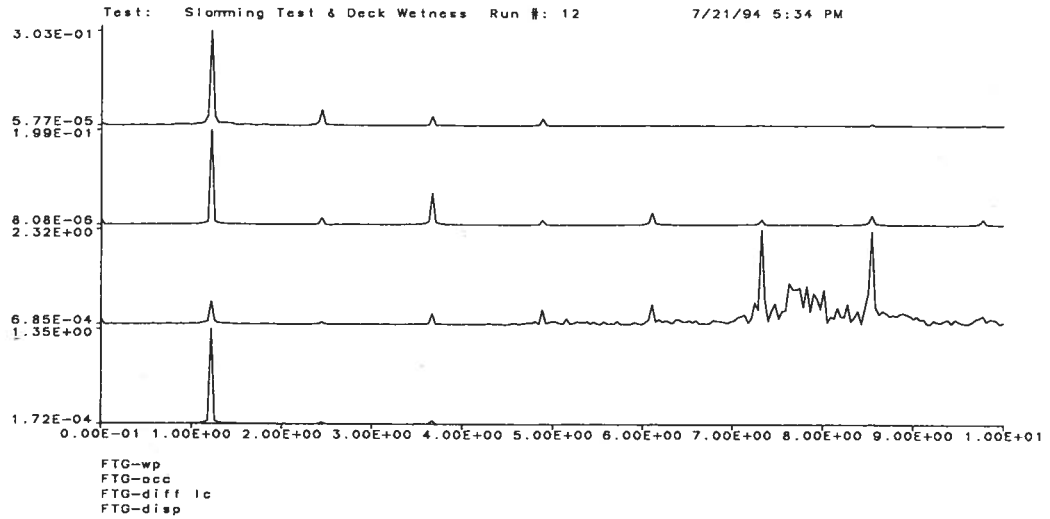

(b) Gains of the FFT Analyses

Figure B.18: Run 12, $f_1 = 1.221\,Hz$, $A_1 = 1.357\,in$, $\alpha = 6$

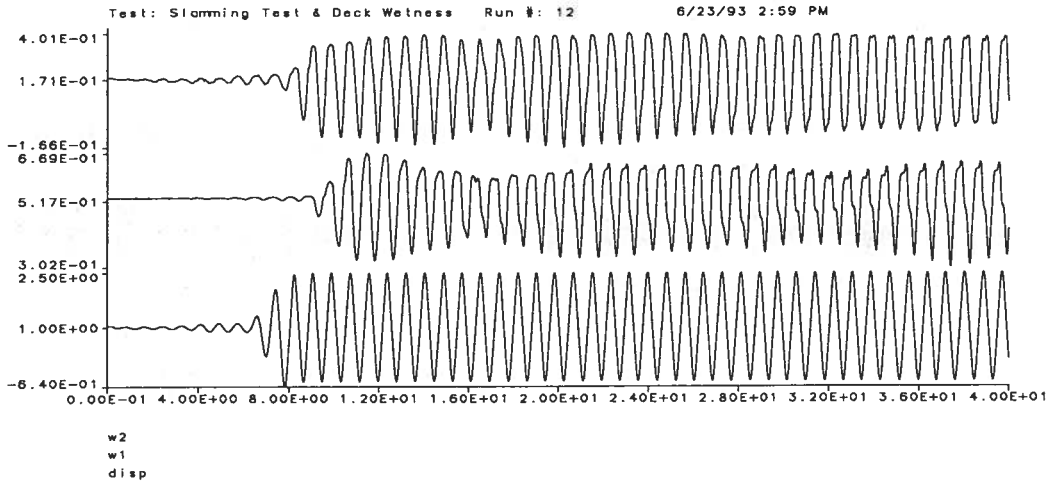

(a) Time-History Acquisitions

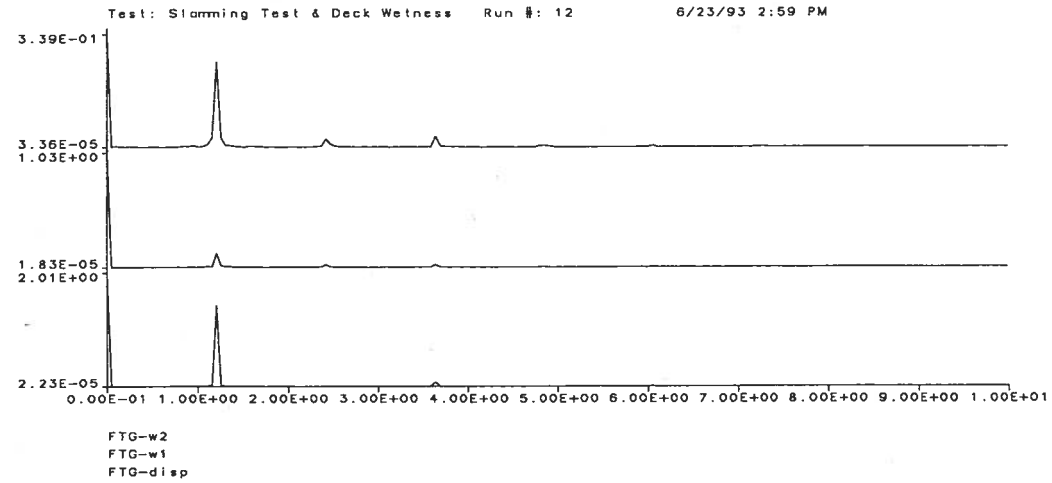

(b) Gains of the FFT Analyses

Figure B.19: Run 12, $f_1 = 1.210\,Hz$, $A_1 = 1.431\,in$, $\alpha = 6$

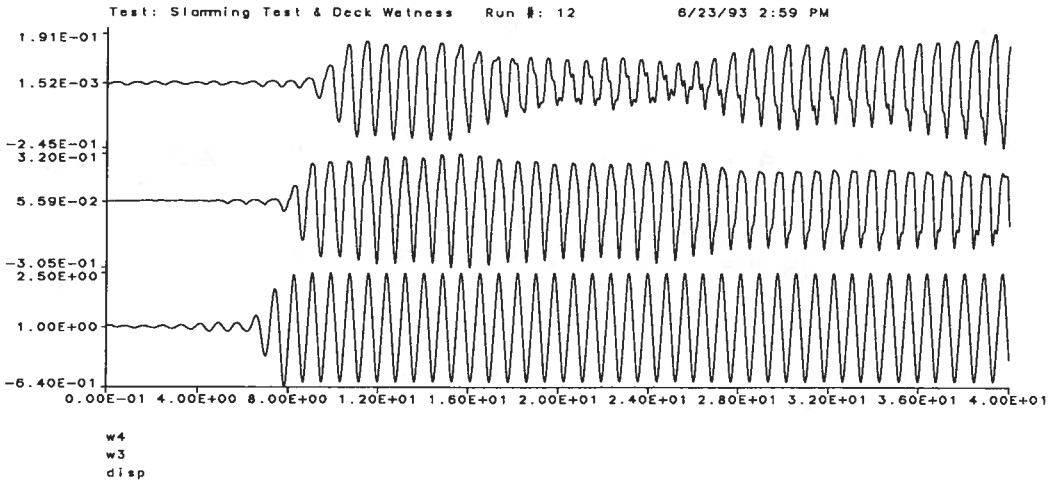

(a) Time-History Acquisitions

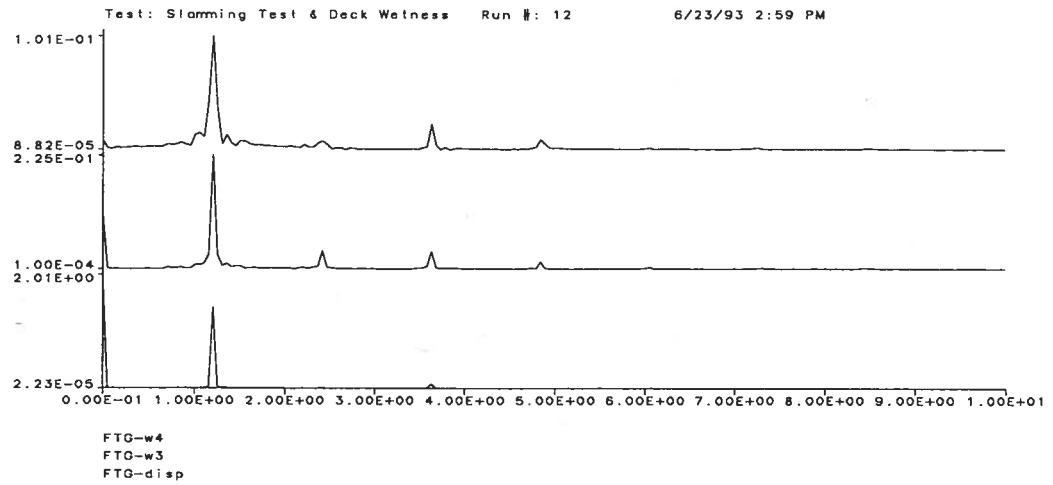

(b) Gains of the FFT Analyses

Figure B.20: Run 12, $f_1 = 1.210\,Hz$, $A_1 = 1.431\,in$, $\alpha = 6$

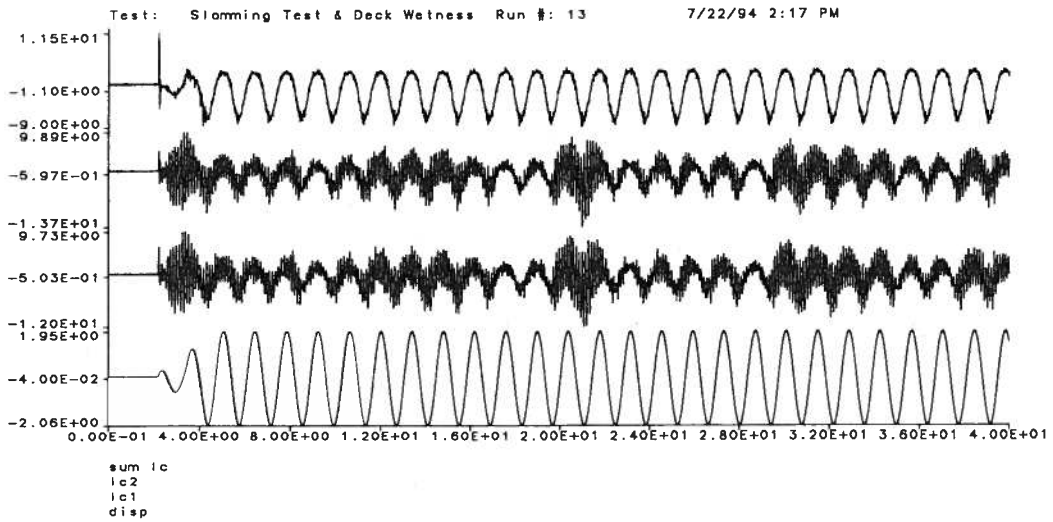

(a) Time-History Acquisitions

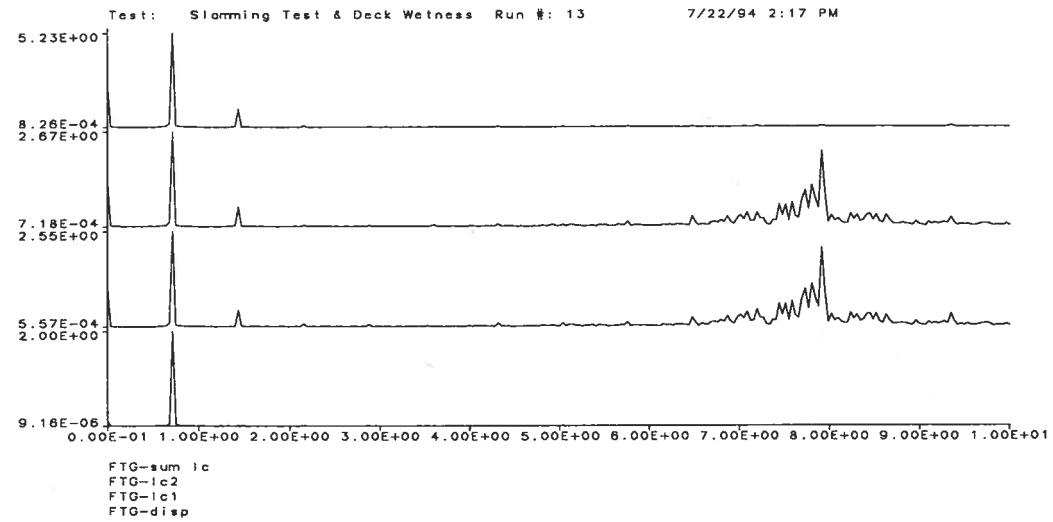

(b) Gains of the FFT Analyses

Figure B.21: Run 13, $f_1 = 0.720\,Hz$, $A_1 = 1.997\,in$, $\alpha = 6$

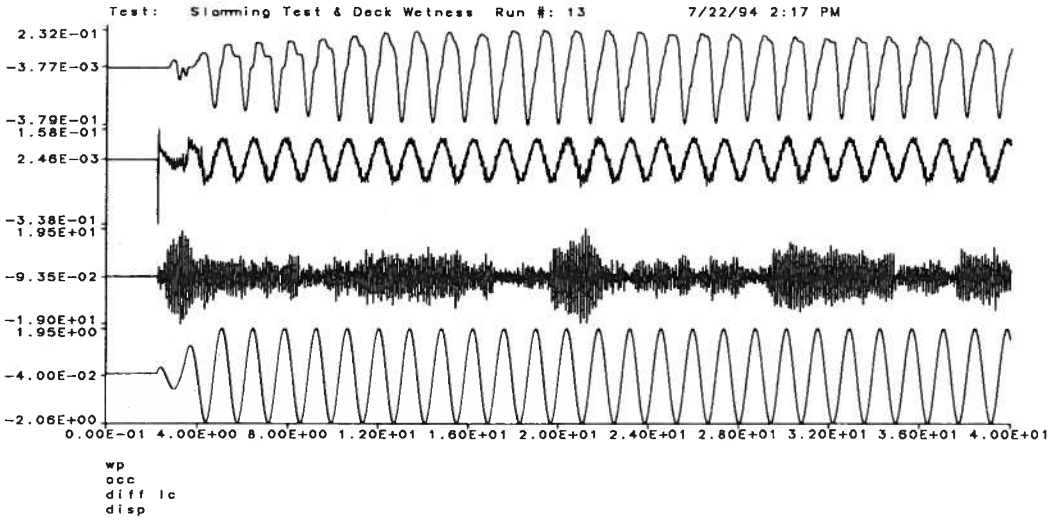

(a) Time-History Acquisitions

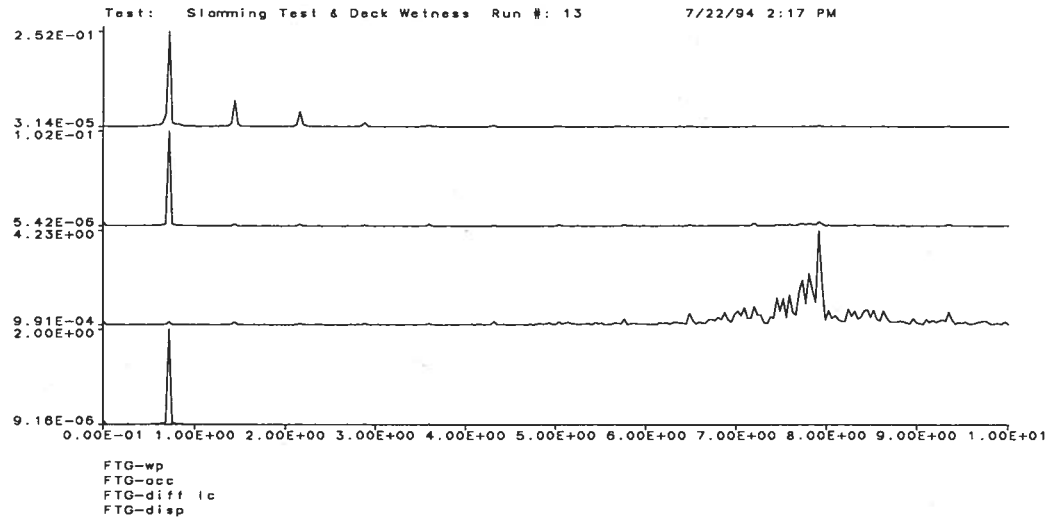

(b) Gains of the FFT Analyses

Figure B.22: Run 13, $f_1 = 0.720\,Hz$, $A_1 = 1.997\,in$, $\alpha = 6$

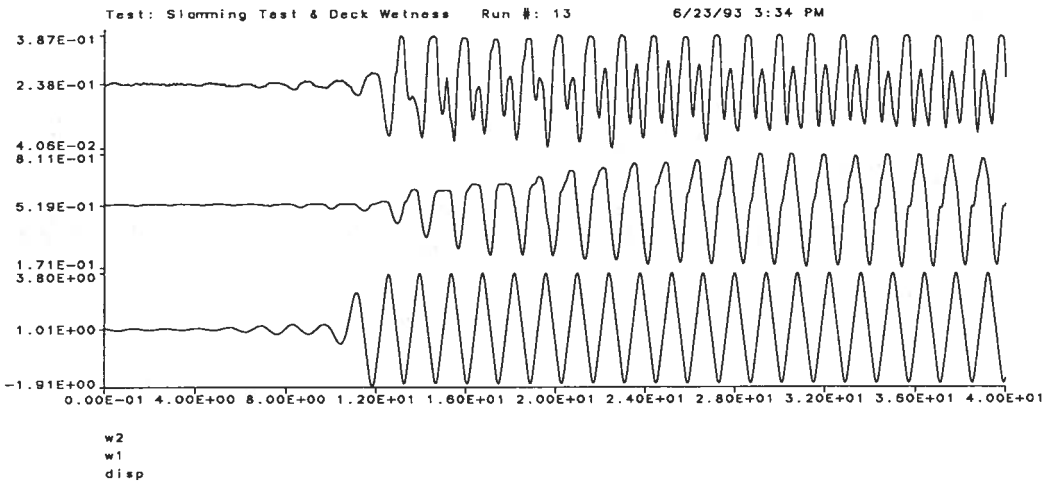

(a) Time-History Acquisitions

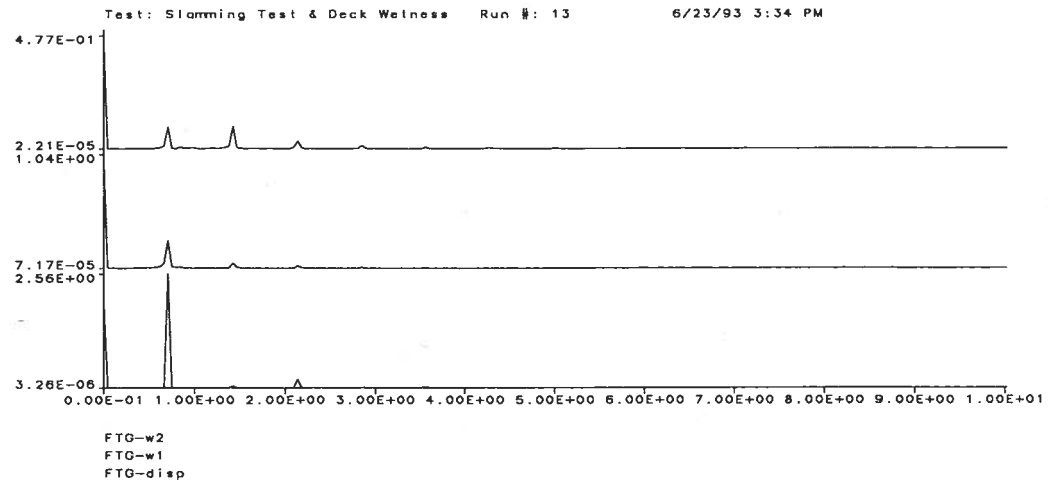

(b) Gains of the FFT Analyses

Figure B.23: Run 13, $f_1 = 0.713\,Hz$, $A_1 = 2.560\,in$, $\alpha = 6$

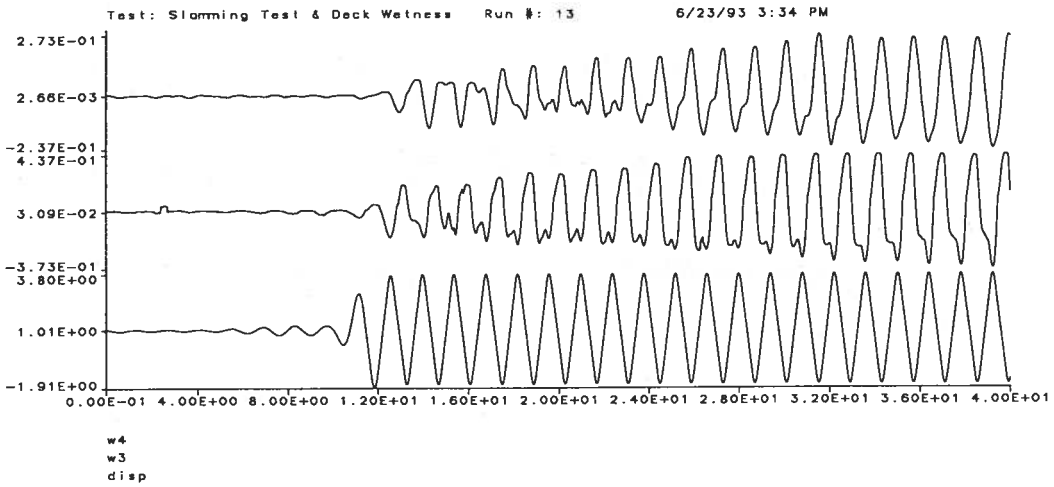

(a) Time-History Acquisitions

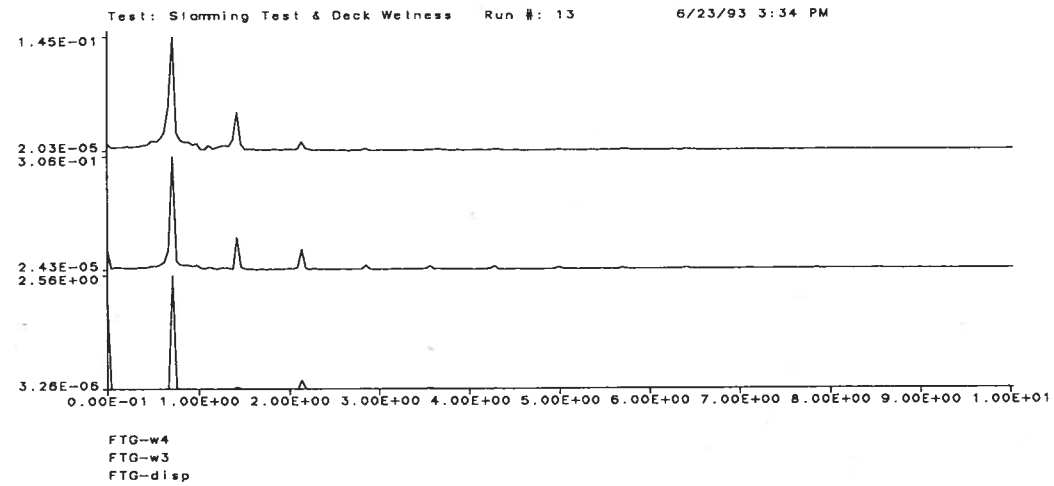

(b) Gains of the FFT Analyses

Figure B.24: Run 13, $f_1 = 0.713\,Hz$, $A_1 = 2.560\,in$, $\alpha = 6$

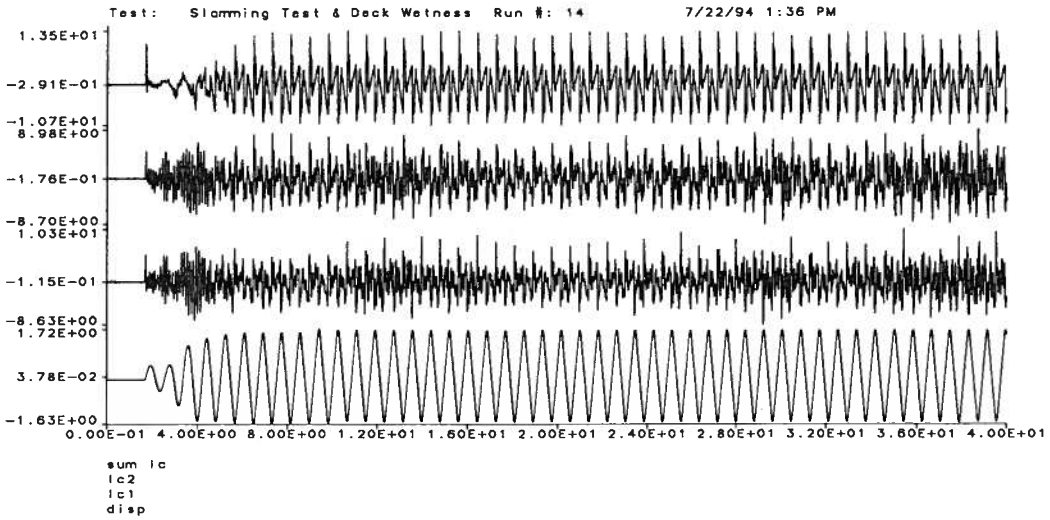

(a) Time-History Acquisitions

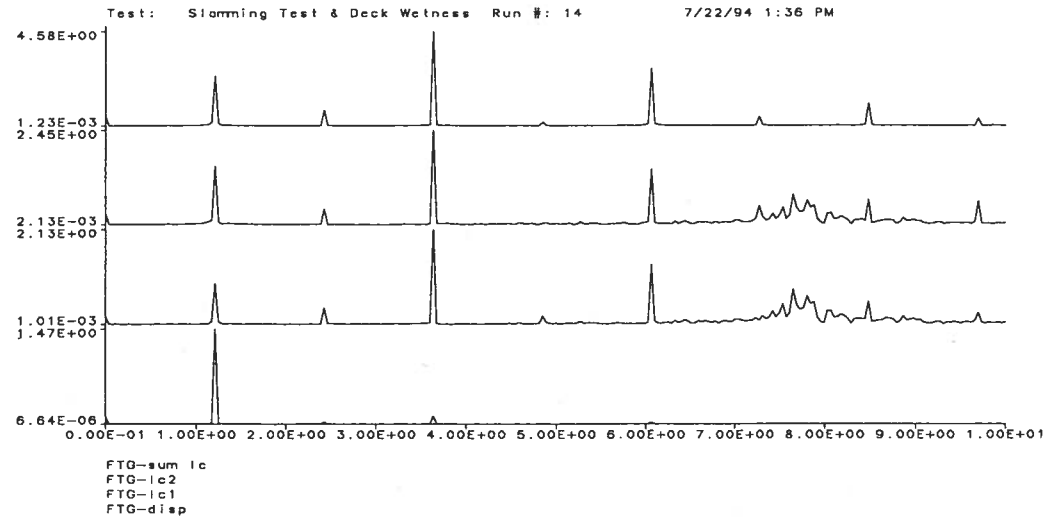

(b) Gains of the FFT Analyses

Figure B.25: Run 14, $f_1 = 1.213\,Hz$, $A_1 = 1.471\,in$, $\alpha = 6$

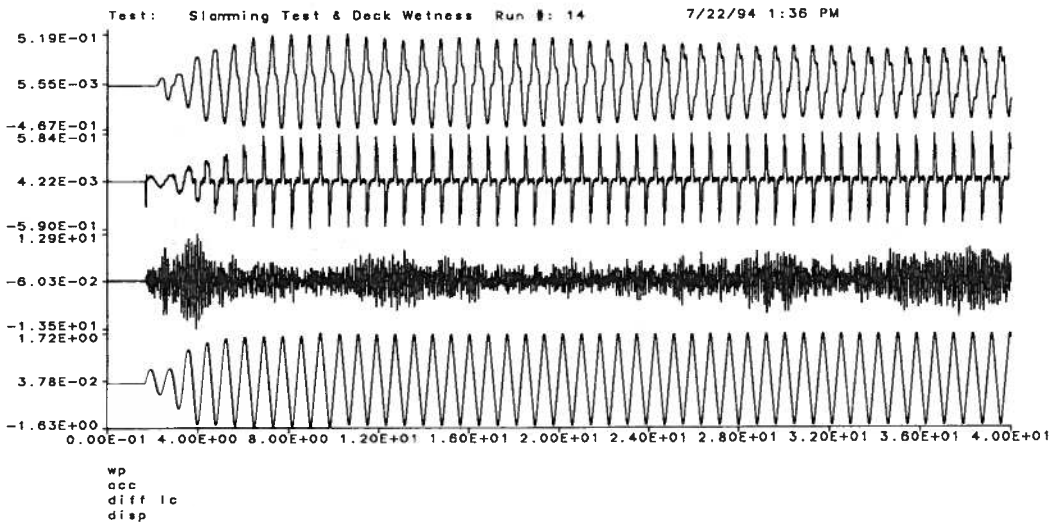

(a) Time-History Acquisitions

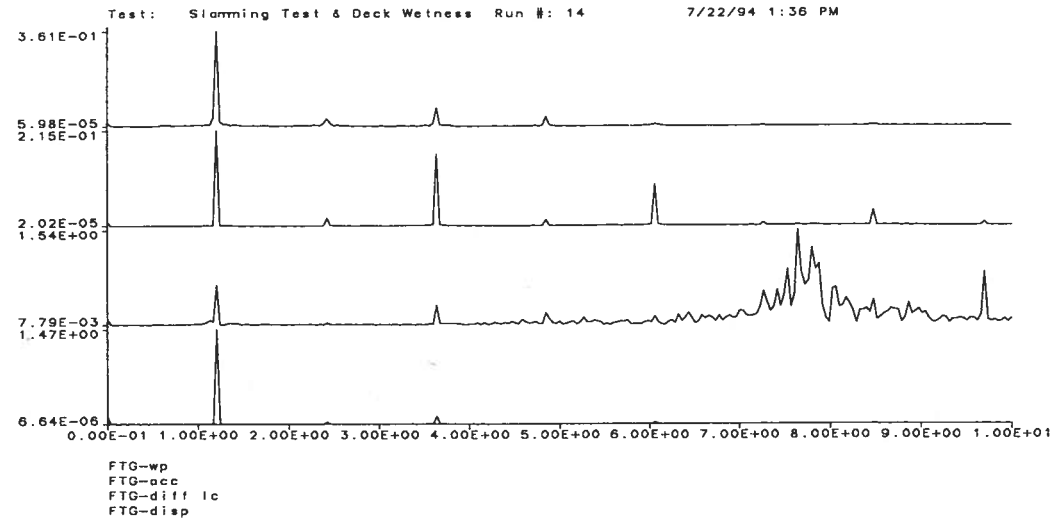

(b) Gains of the FFT Analyses

Figure B.26: Run 14, $f_1 = 1.213\,Hz$, $A_1 = 1.471\,in$, $\alpha = 6$

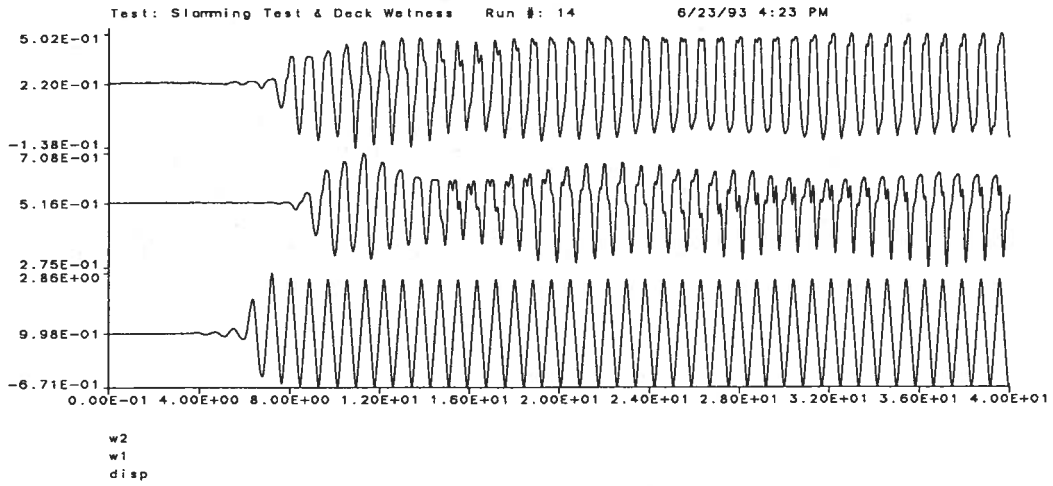

(a) Time-History Acquisitions

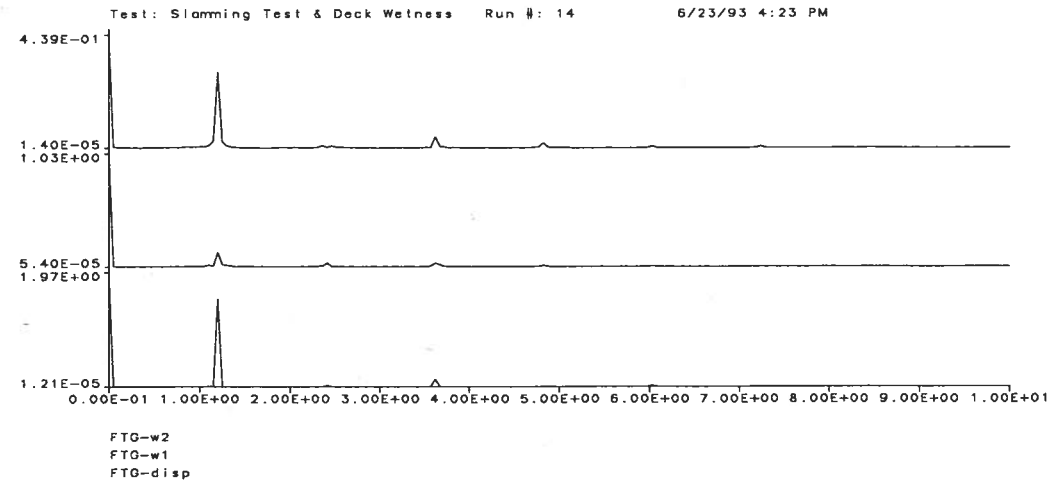

(b) Gains of the FFT Analyses

Figure B.27: Run 14, $f_1 = 1.206\,Hz$, $A_1 = 1.515\,in$, $\alpha = 6$

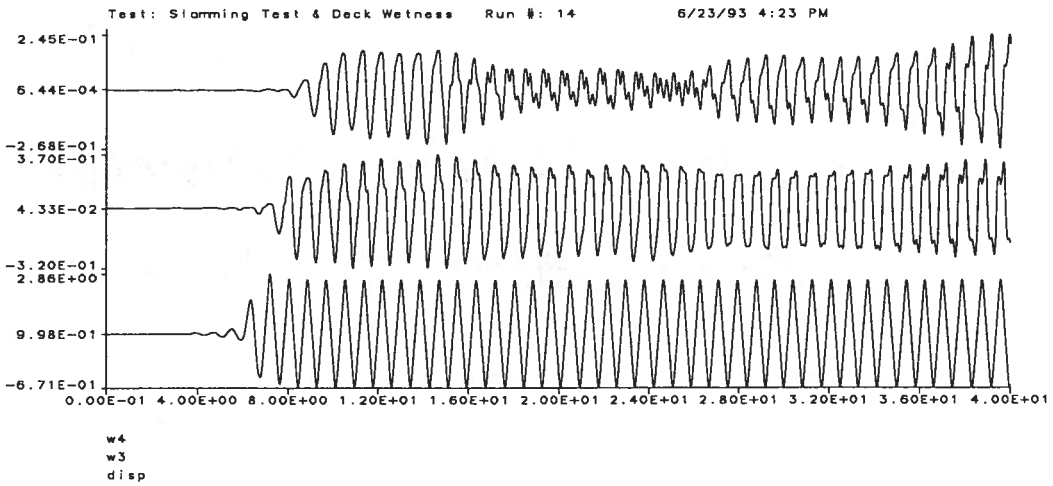

(a) Time-History Acquisitions

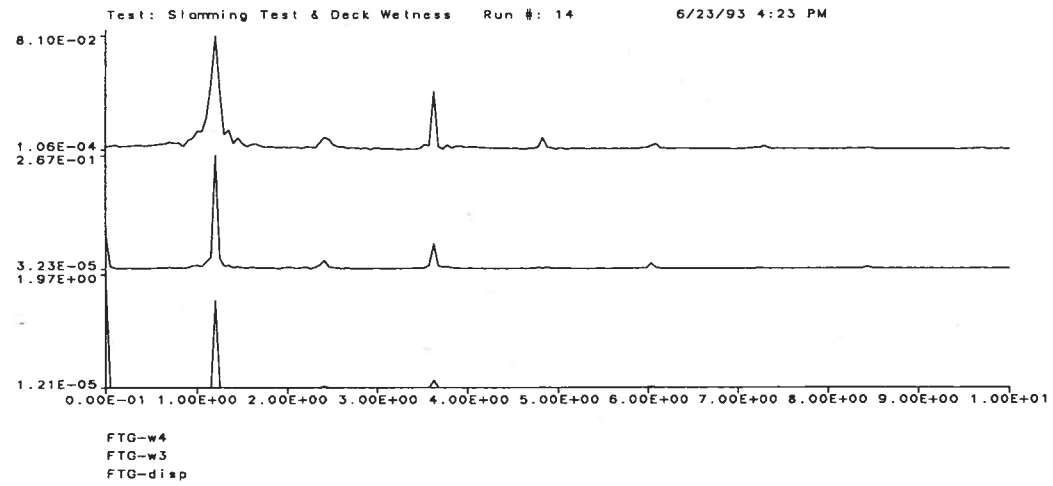

(b) Gains of the FFT Analyses

Figure B.28: Run 14, $f_1 = 1.206\,Hz$, $A_1 = 1.515\,in$, $\alpha = 6$

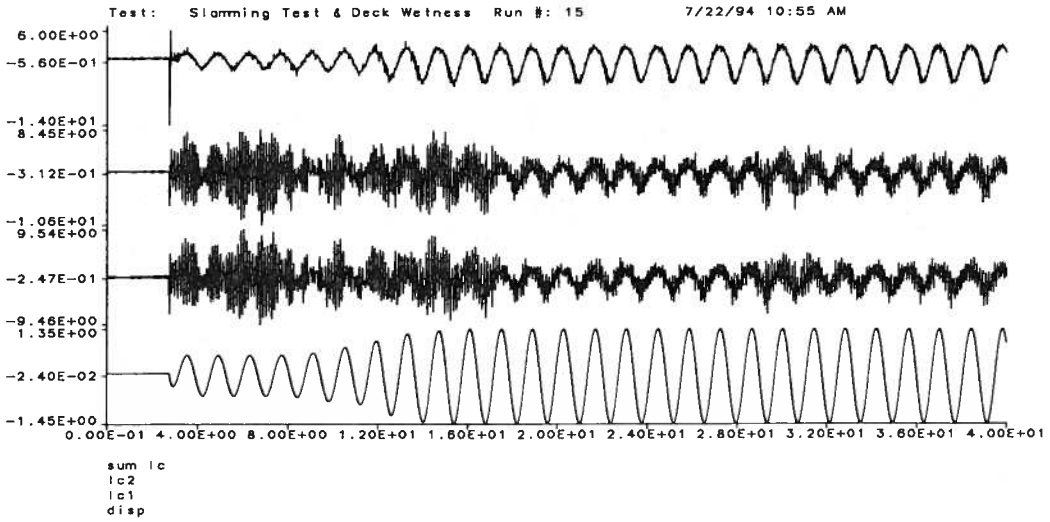

(a) Time-History Acquisitions

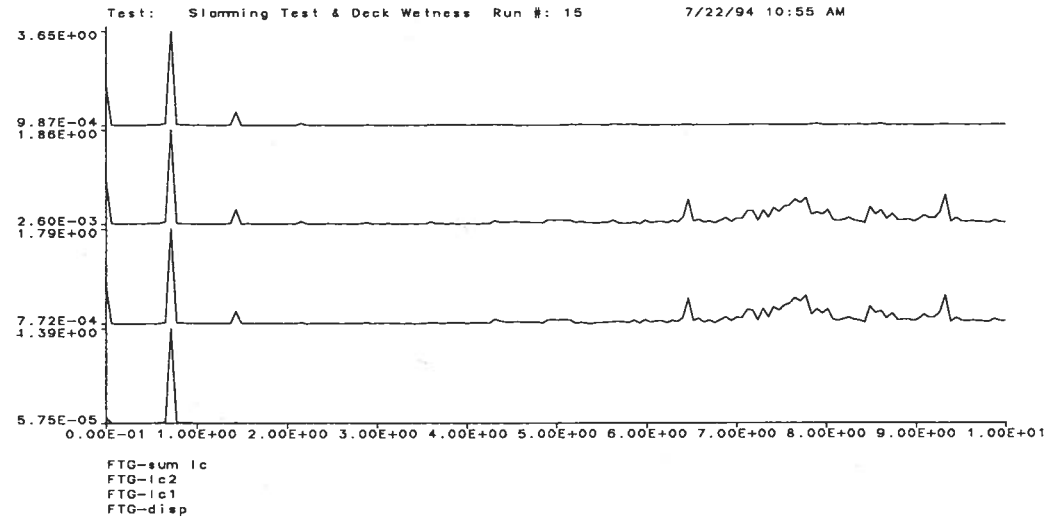

(b) Gains of the FFT Analyses

Figure B.29: Run 15, $f_1 = 0.718\,Hz$, $A_1 = 1.393\,in$, $\alpha = 6$

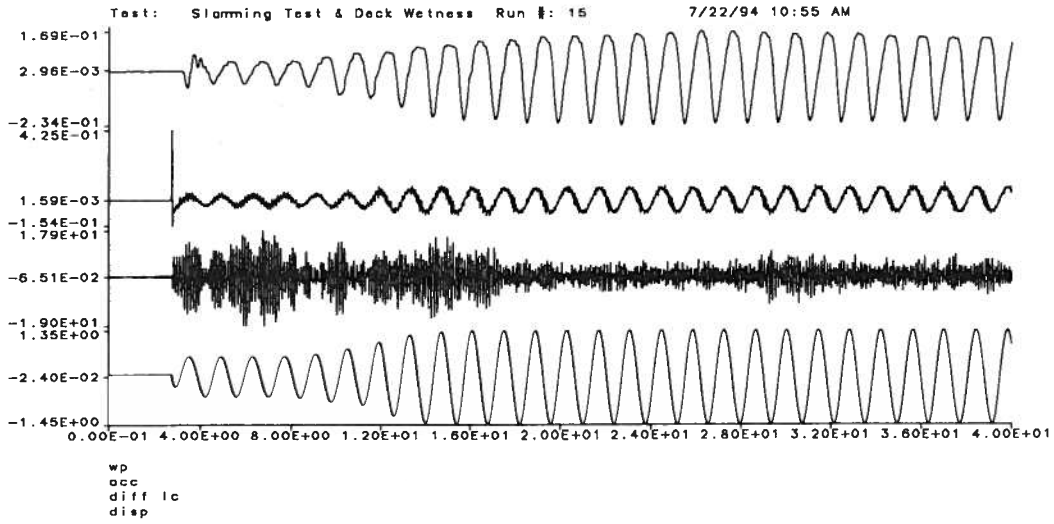

(a) Time-History Acquisitions

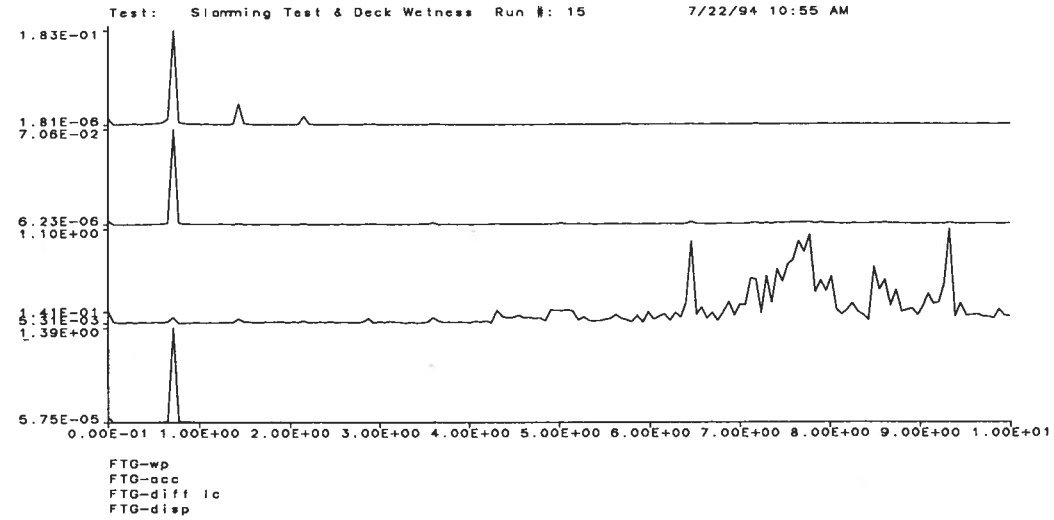

(b) Gains of the FFT Analyses

Figure B.30: Run 15, $f_1 = 0.718\,Hz$, $A_1 = 1.393\,in$, $\alpha = 6$

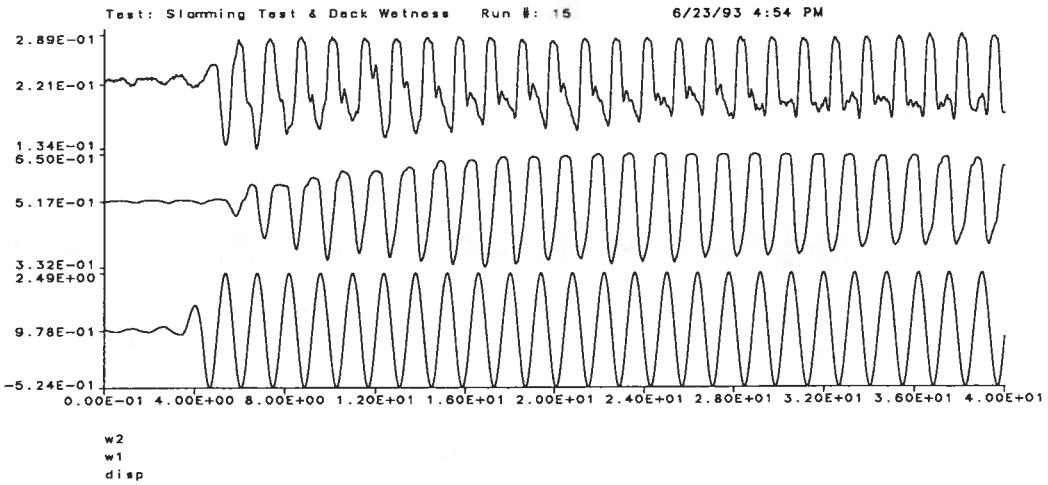

(a) Time-History Acquisitions

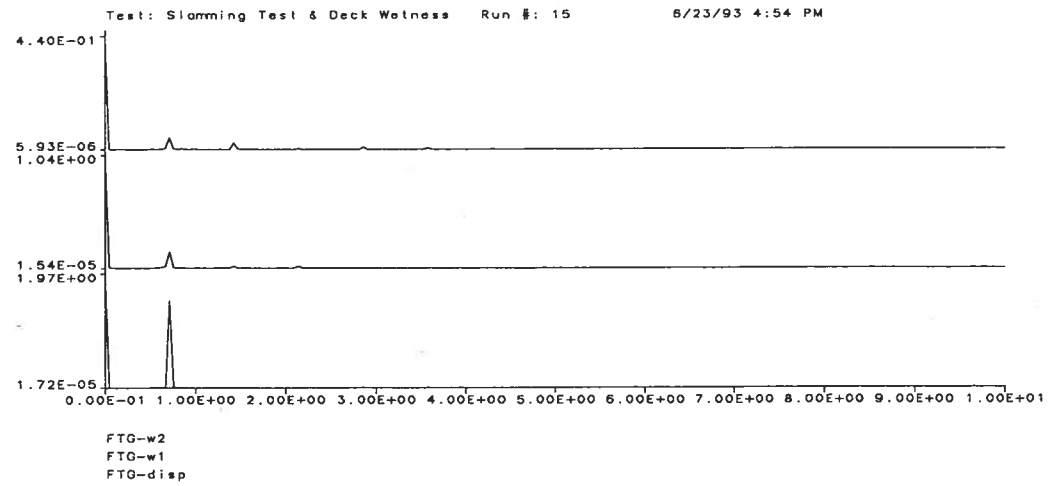

(b) Gains of the FFT Analyses

Figure B.31: Run 15, $f_1 = 0.714\,Hz$, $A_1 = 1.502\,in$, $\alpha = 6$

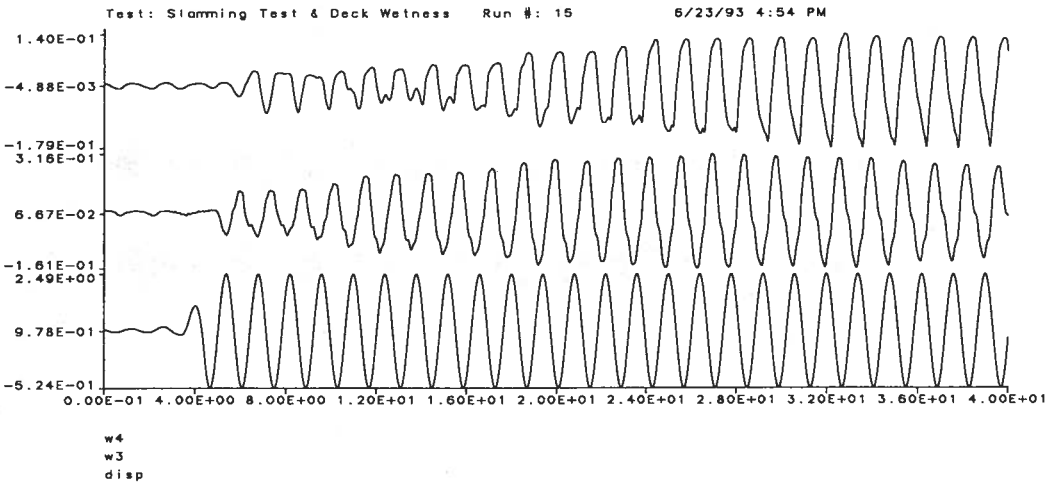

(a) Time-History Acquisitions

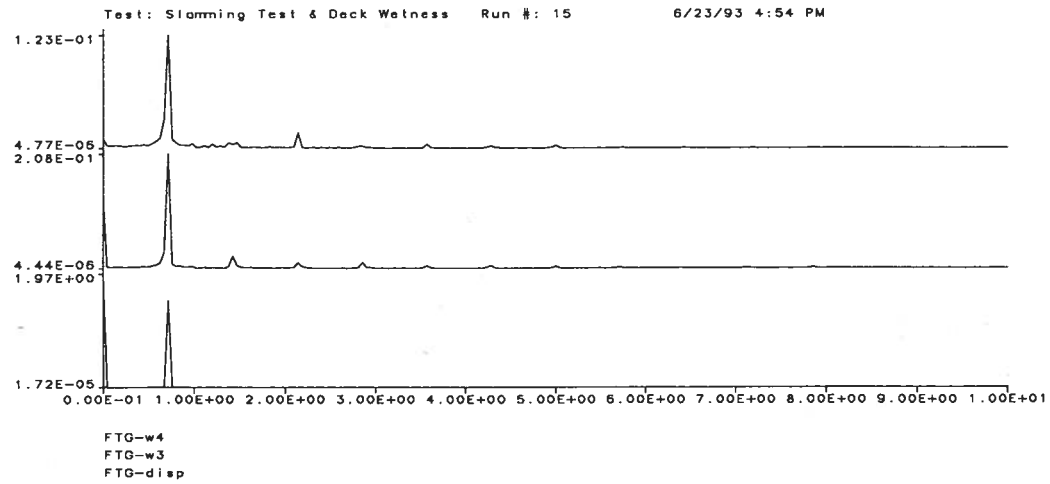

(b) Gains of the FFT Analyses

Figure B.32: Run 15, $f_1 = 0.714\,Hz$, $A_1 = 1.502\,in$, $\alpha = 6$

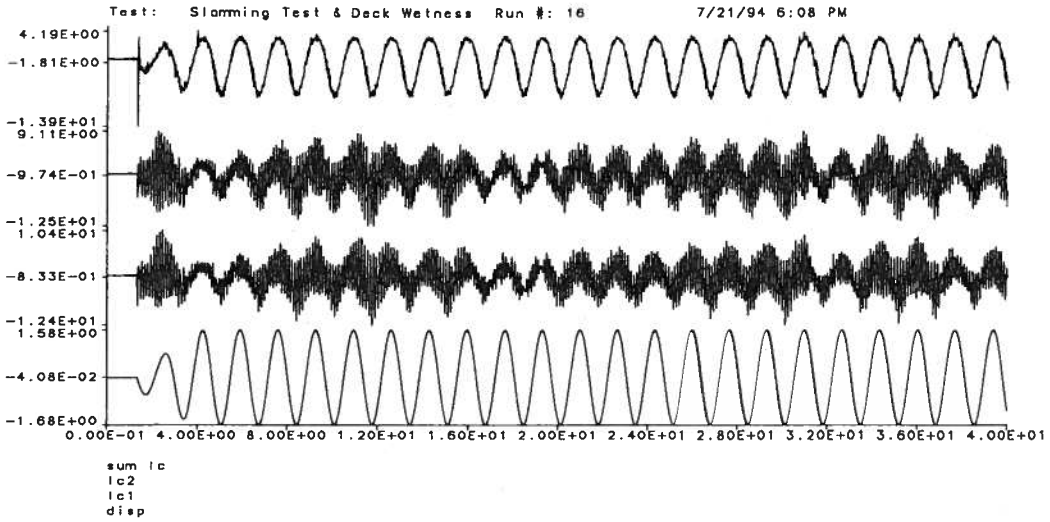

(a) Time-History Acquisitions

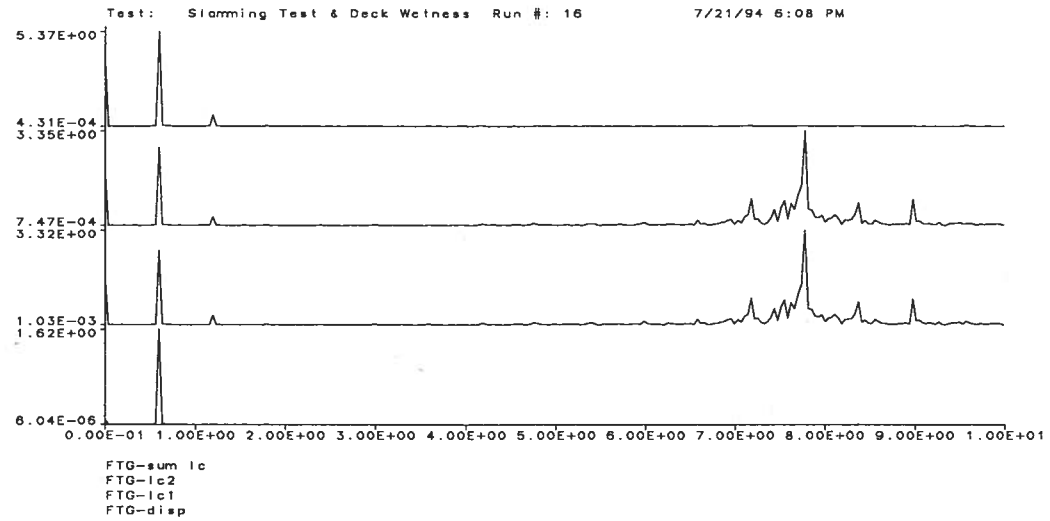

(b) Gains of the FFT Analyses

Figure B.33: Run 16, $f_1 = 0.599\,Hz$, $A_1 = 1.623\,in$, $\alpha = 6$

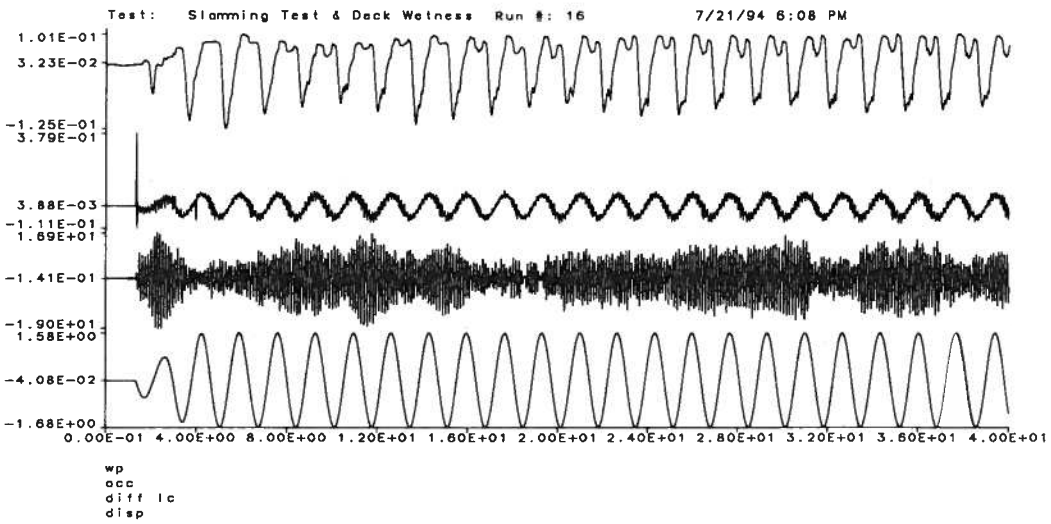

(a) Time-History Acquisitions

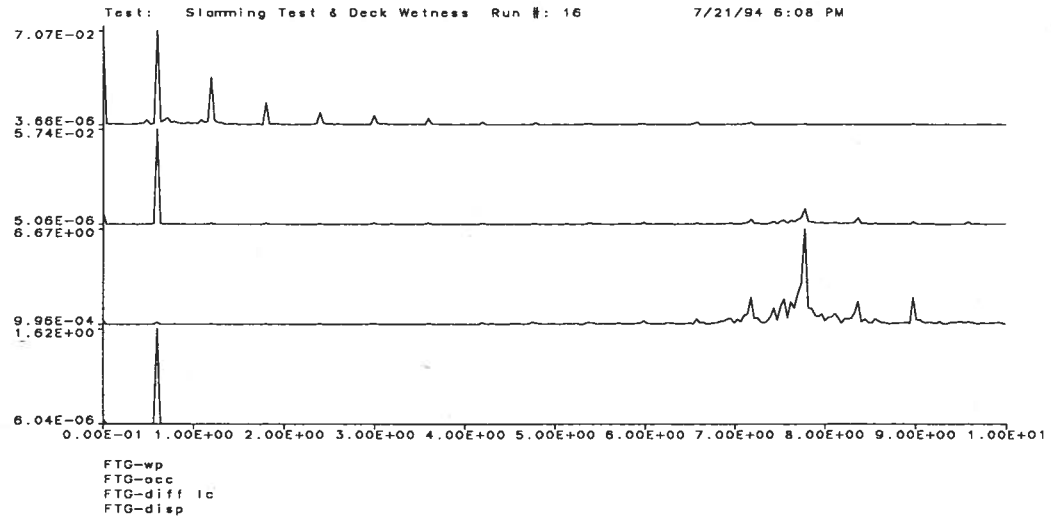

(b) Gains of the FFT Analyses

Figure B.34: Run 16, $f_1 = 0.599\,Hz$, $A_1 = 1.623\,in$, $\alpha = 6$

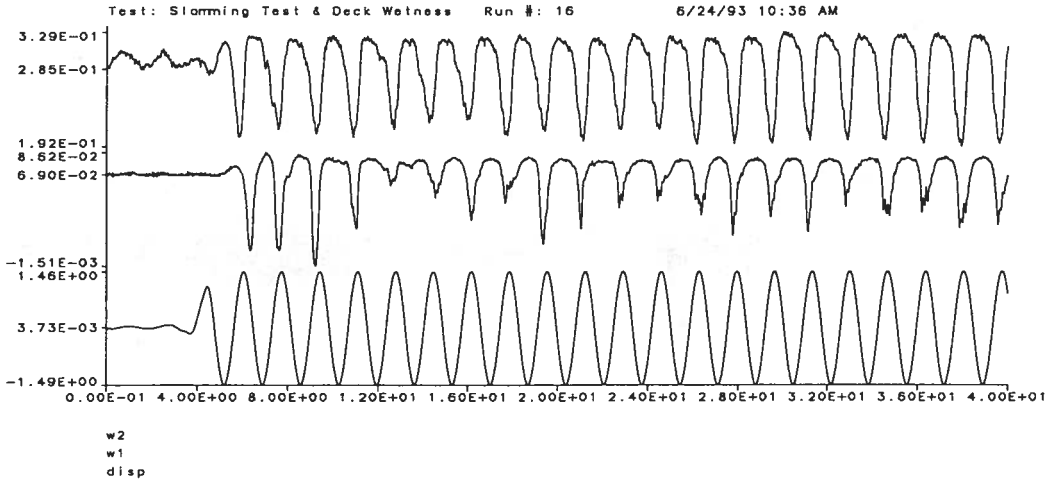

(a) Time-History Acquisitions

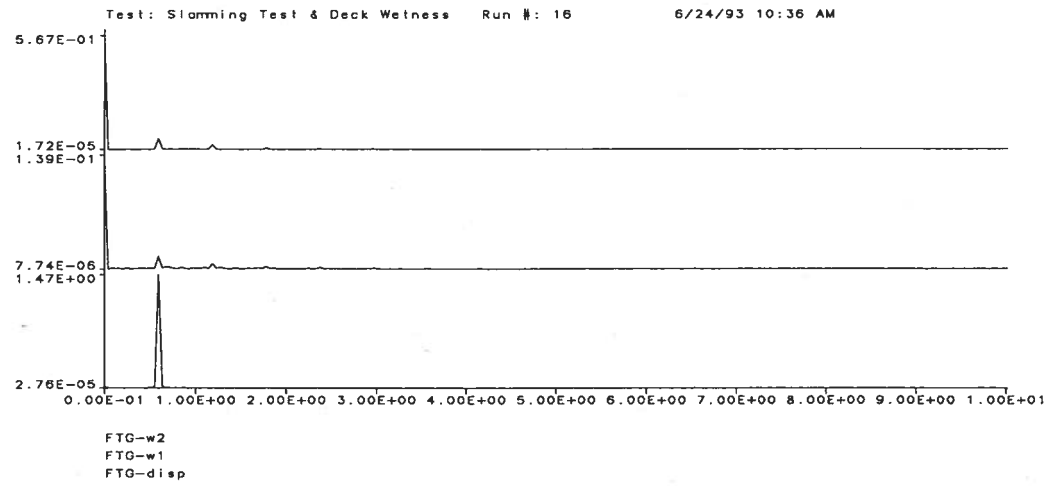

(b) Gains of the FFT Analyses

Figure B.35: Run 16, $f_1 = 0.594\,Hz$, $A_1 = 1.470\,in$, $\alpha = 6$

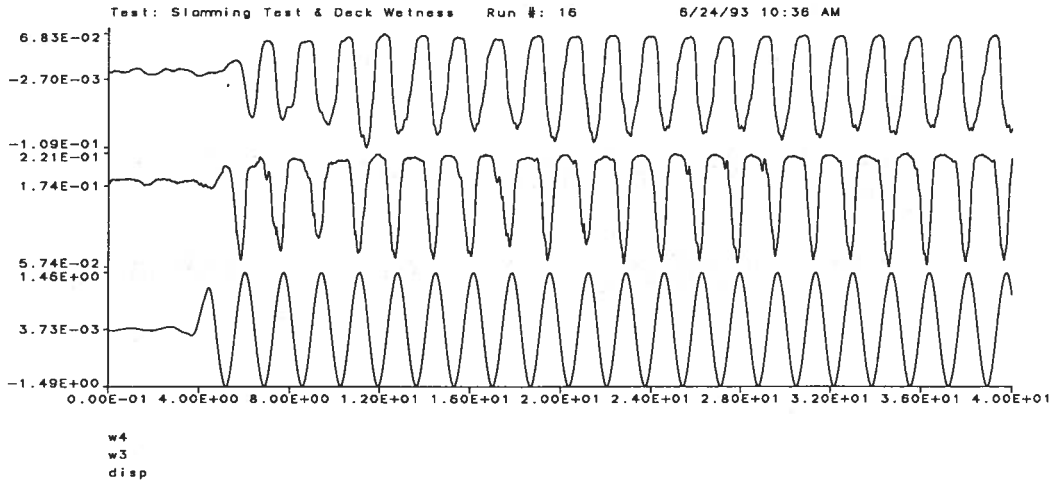

(a) Time-History Acquisitions

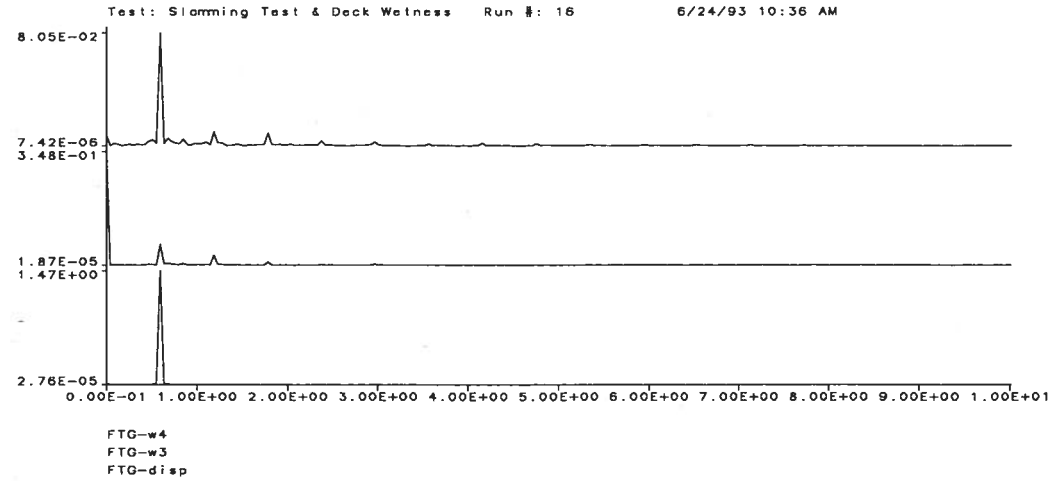

(b) Gains of the FFT Analyses

Figure B.36: Run 16, $f_1 = 0.594\,Hz$, $A_1 = 1.470\,in$, $\alpha = 6$

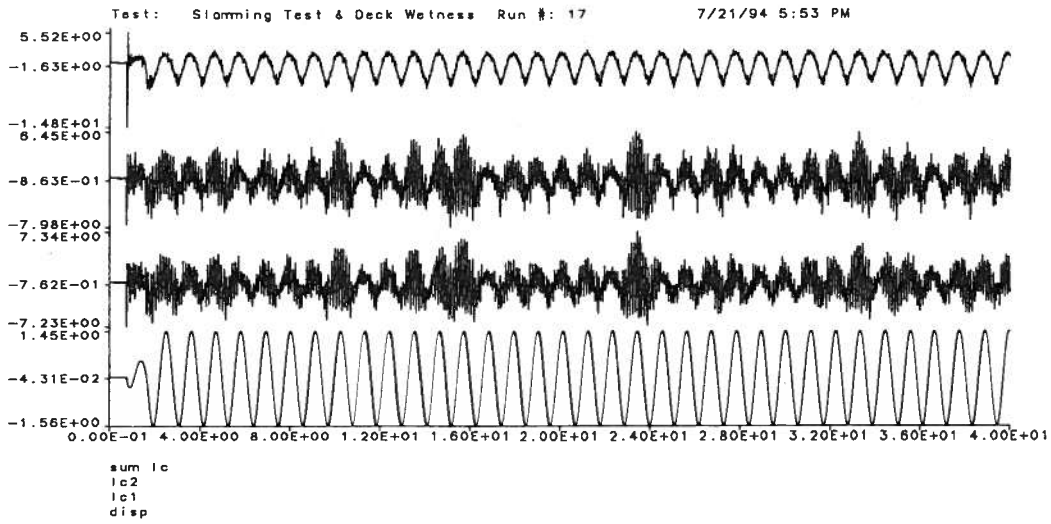

(a) Time-History Acquisitions

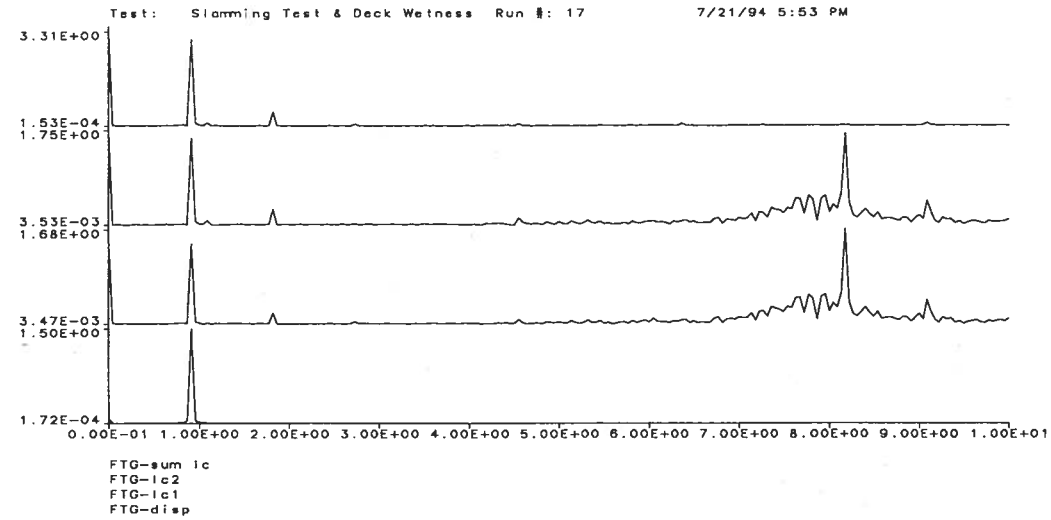

(b) Gains of the FFT Analyses

Figure B.37: Run 17, $f_1 = 0.909\,Hz$, $A_1 = 1.503\,in$, $\alpha = 6$

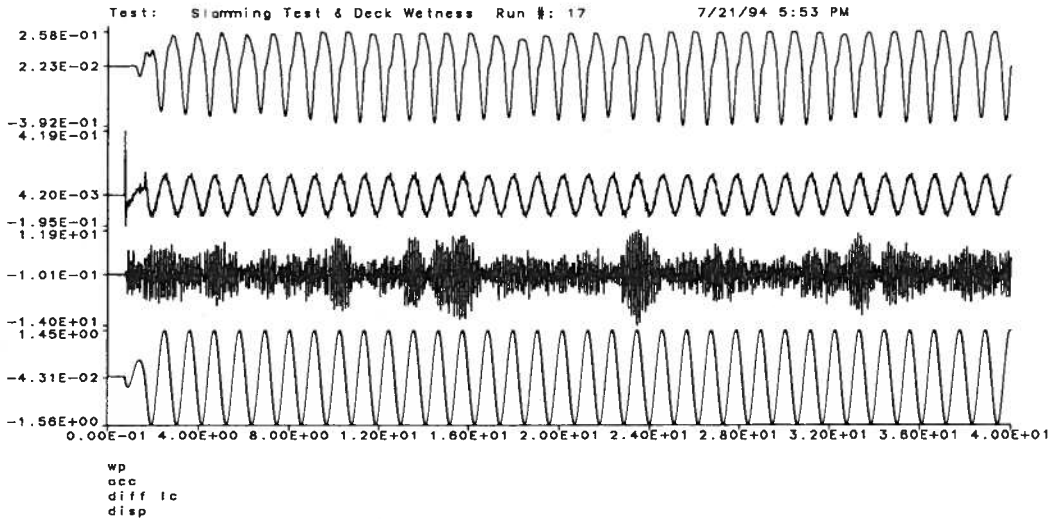

(a) Time-History Acquisitions

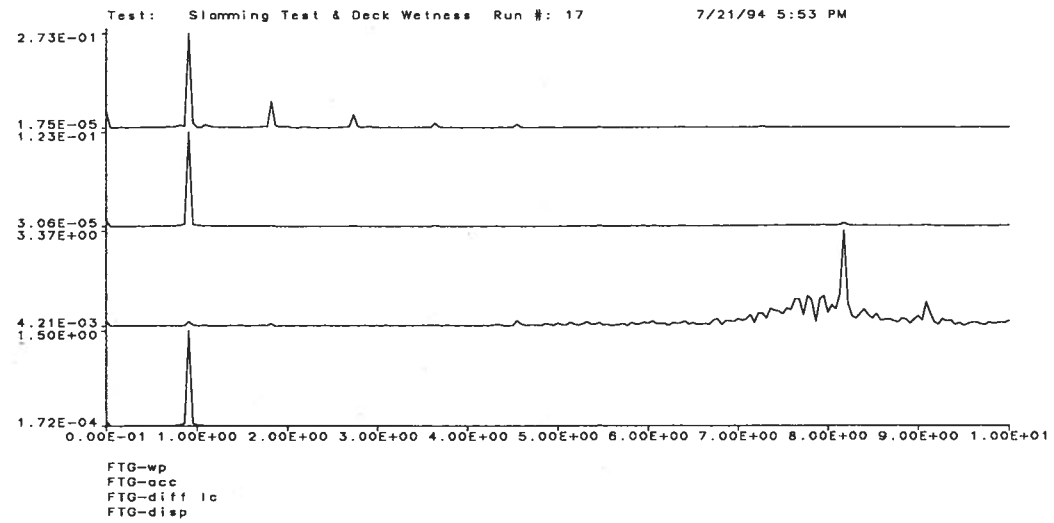

(b) Gains of the FFT Analyses

Figure B.38: Run 17, $f_1 = 0.909\,Hz$, $A_1 = 1.503\,in$, $\alpha = 6$

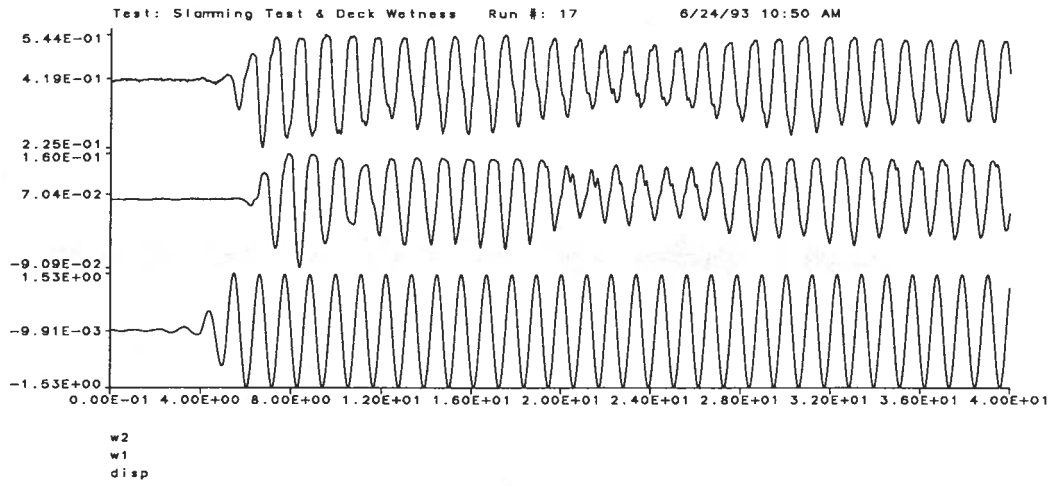

(a) Time-History Acquisitions

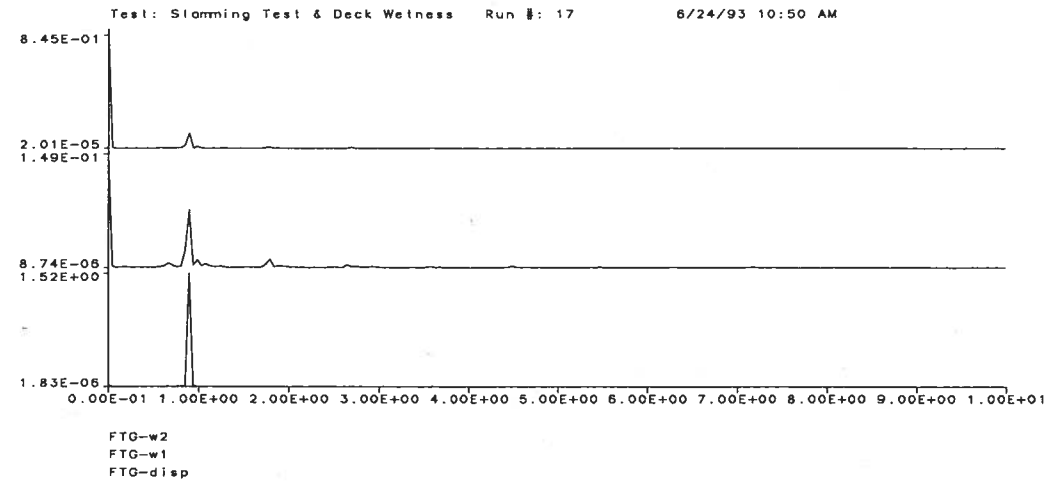

(b) Gains of the FFT Analyses

Figure B.39: Run 17, $f_1 = 0.895\,Hz$, $A_1 = 1.520\,in$, $\alpha = 6$

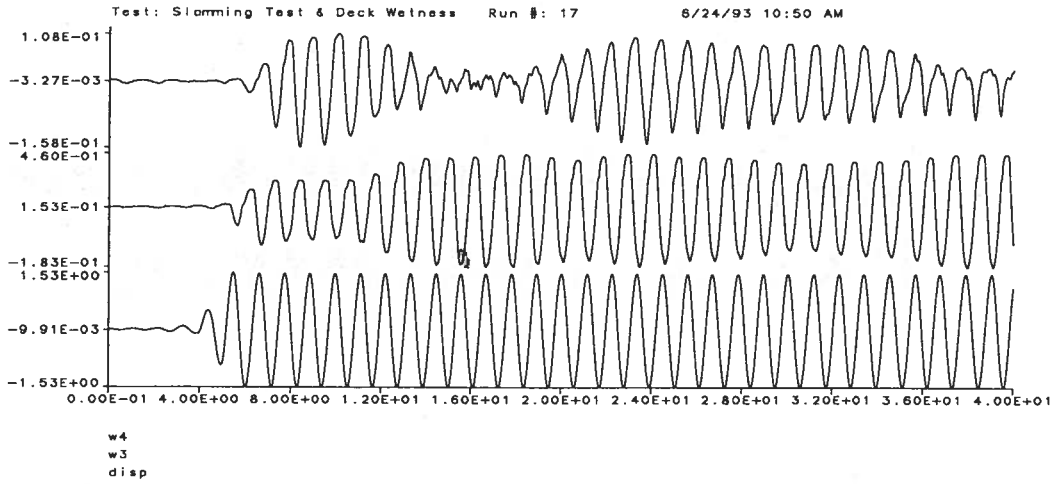

(a) Time-History Acquisitions

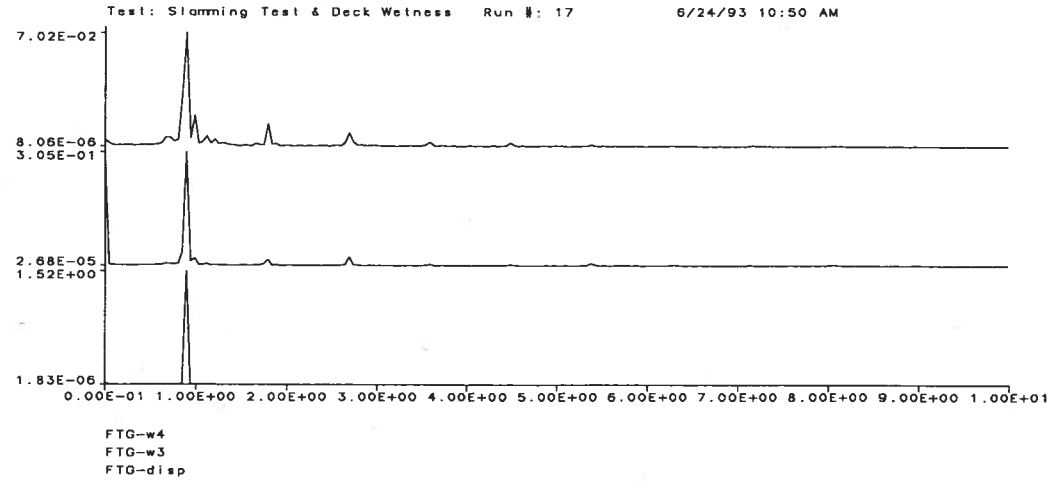

(b) Gains of the FFT Analyses

Figure B.40: Run 17, $f_1 = 0.895\,Hz$, $A_1 = 1.520\,in$, $\alpha = 6$

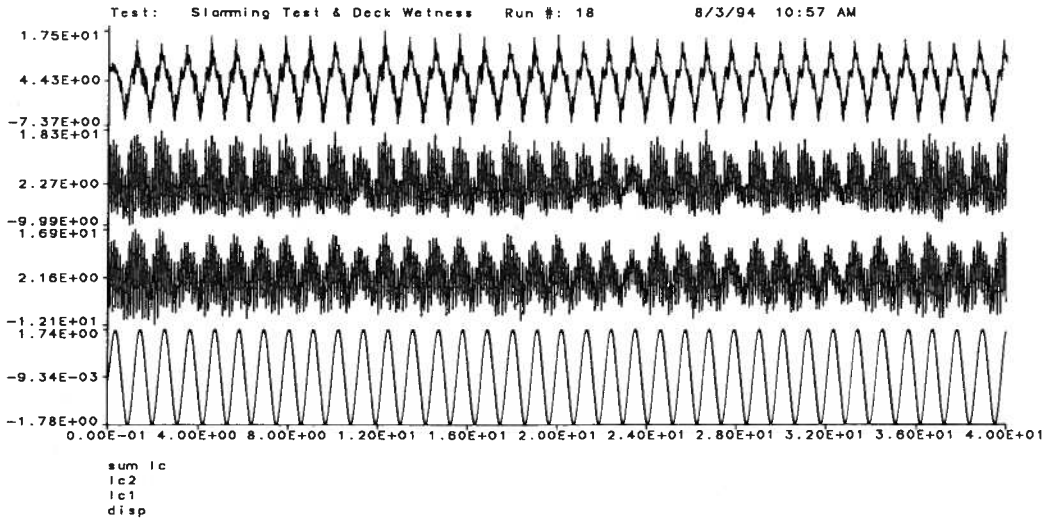

(a) Time-History Acquisitions

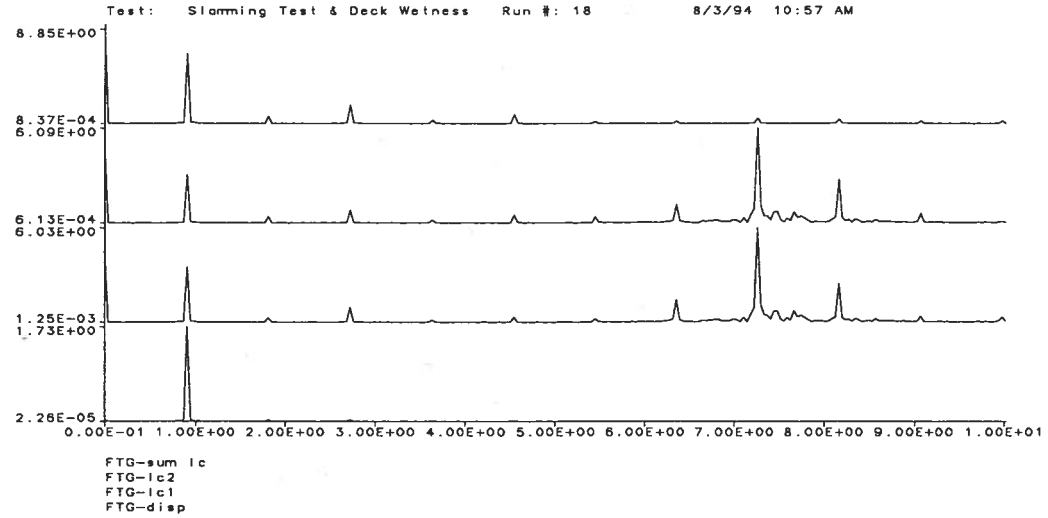

(b) Gains of the FFT Analyses

Figure B.41: Run 18, $f_1 = 0.908\,Hz$, $A_1 = 1.732\,in$, $\alpha = 6$

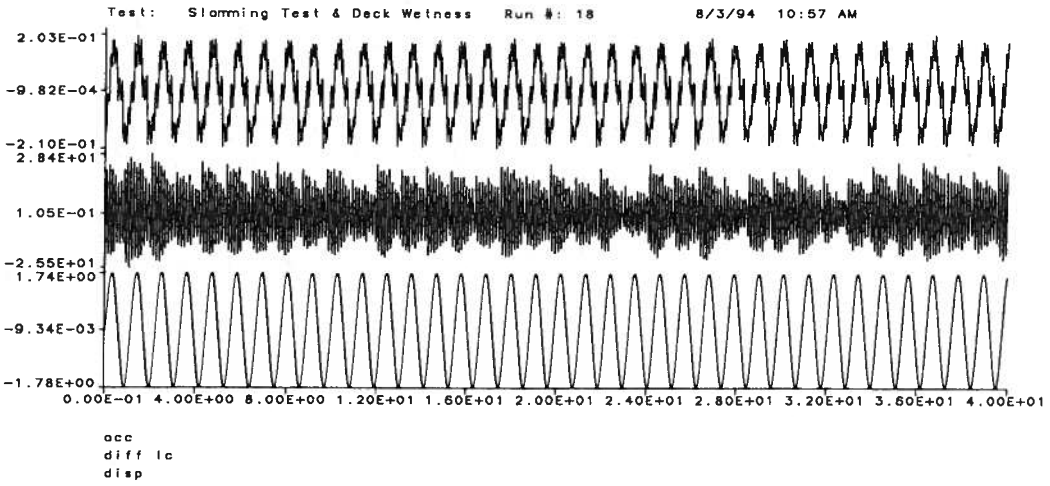

(a) Time-History Acquisitions

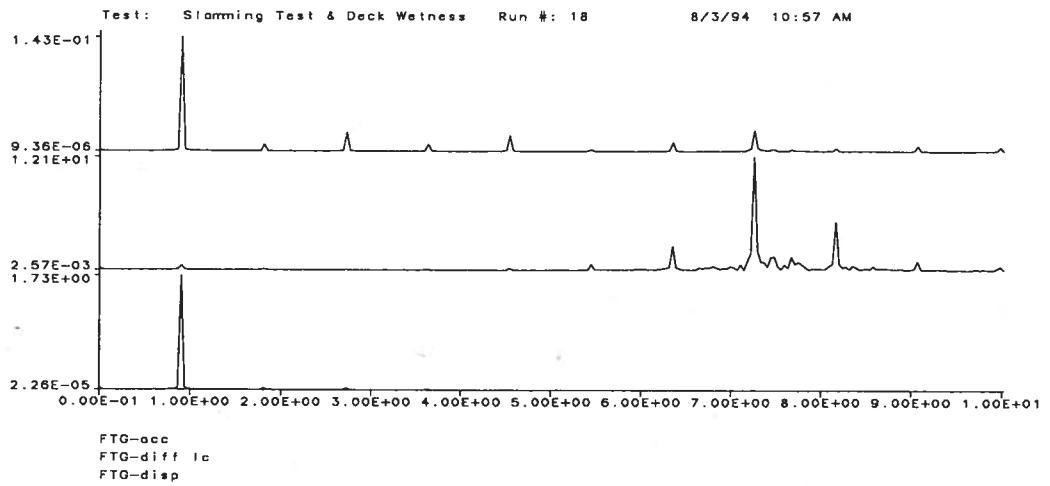

(b) Gains of the FFT Analyses

Figure B.42: Run 18, $f_1 = 0.908\,Hz$, $A_1 = 1.732\,in$, $\alpha = 6$

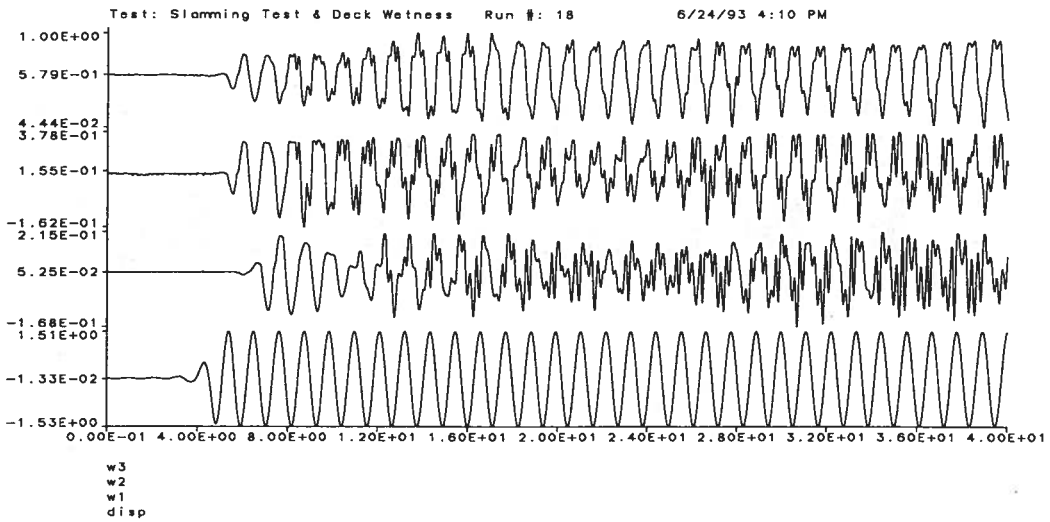

(a) Time-History Acquisitions

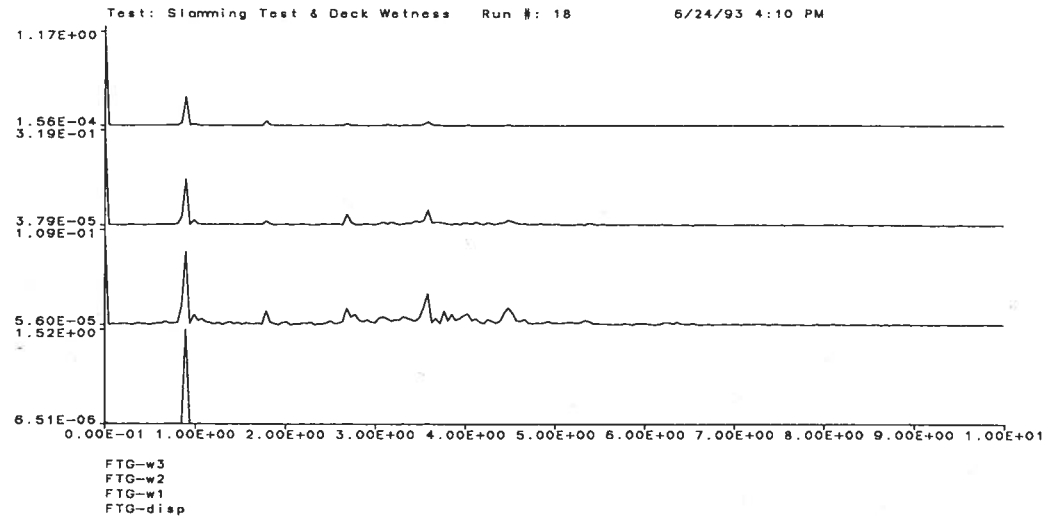

(b) Gains of the FFT Analyses

Figure B.43: Run 18, $f_1 = 0.895\,Hz$, $A_1 = 1.523\,in$, $\alpha = 6$

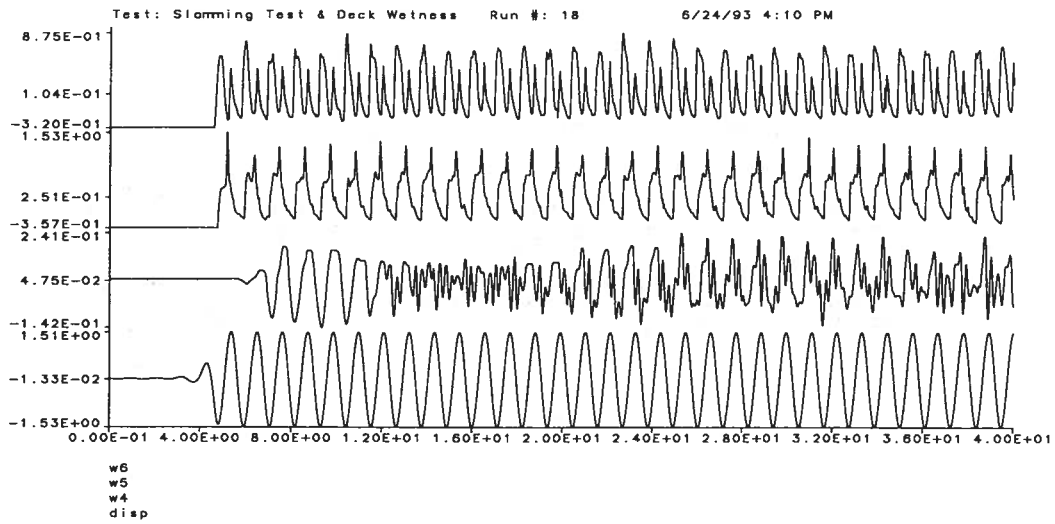

(a) Time-History Acquisitions

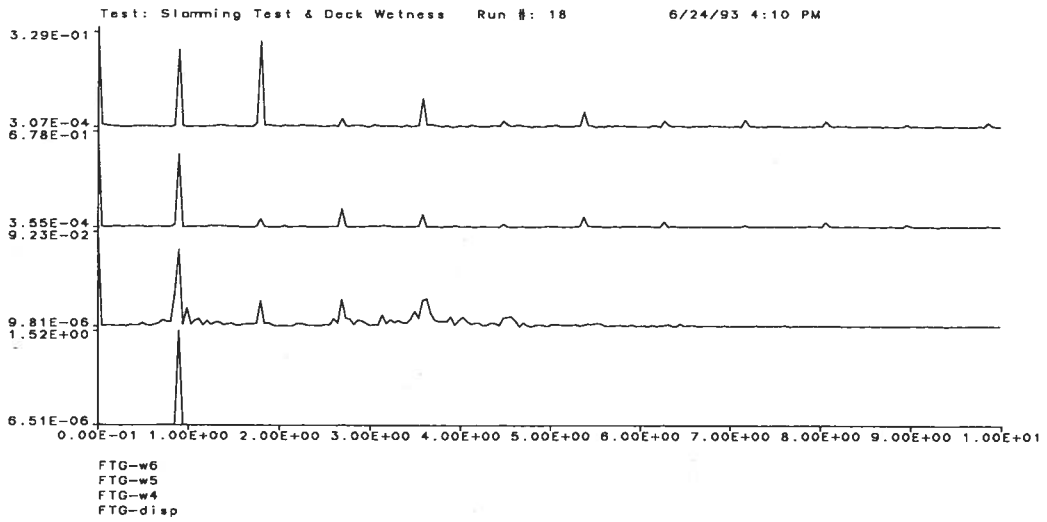

(b) Gains of the FFT Analyses

Figure B.44: Run 18, $f_1 = 0.895\,Hz$, $A_1 = 1.523\,in$, $\alpha = 6$

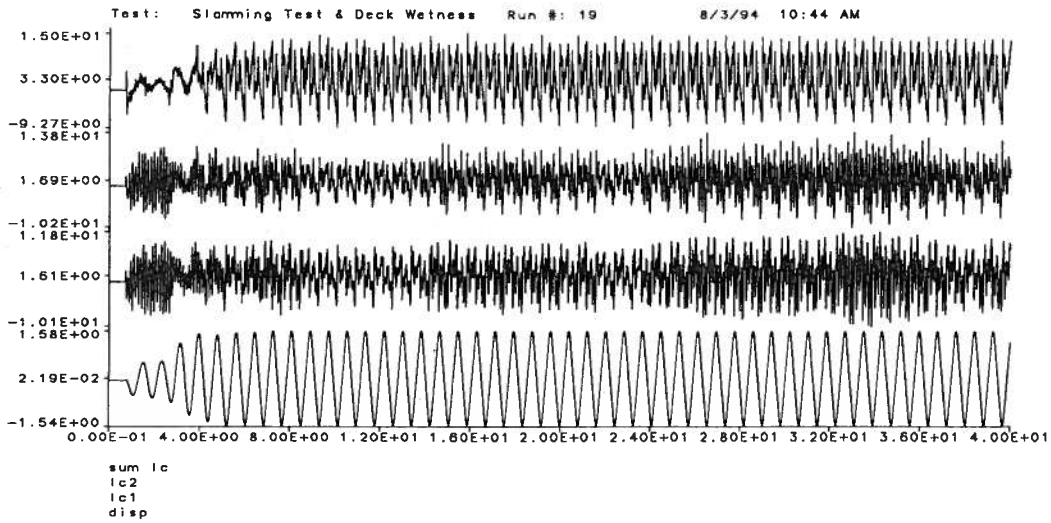

(a) Time-History Acquisitions

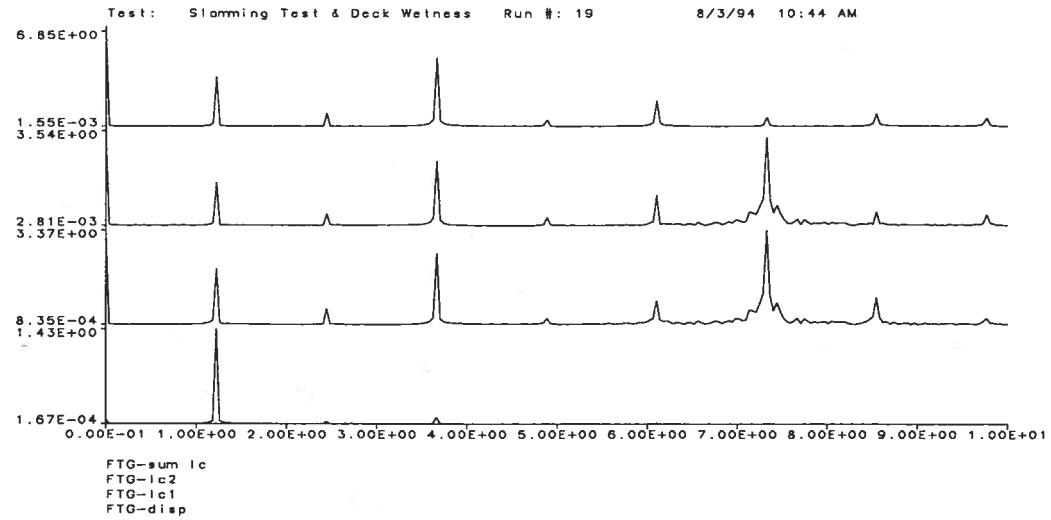

(b) Gains of the FFT Analyses

Figure B.45: Run 19, $f_1 = 1.221\,Hz$, $A_1 = 1.435\,in$, $\alpha = 6$

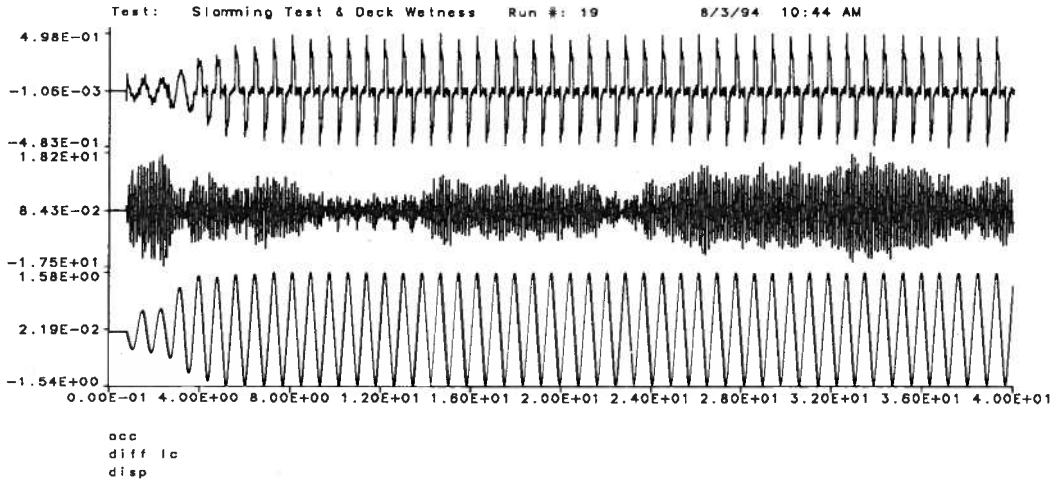

(a) Time-History Acquisitions

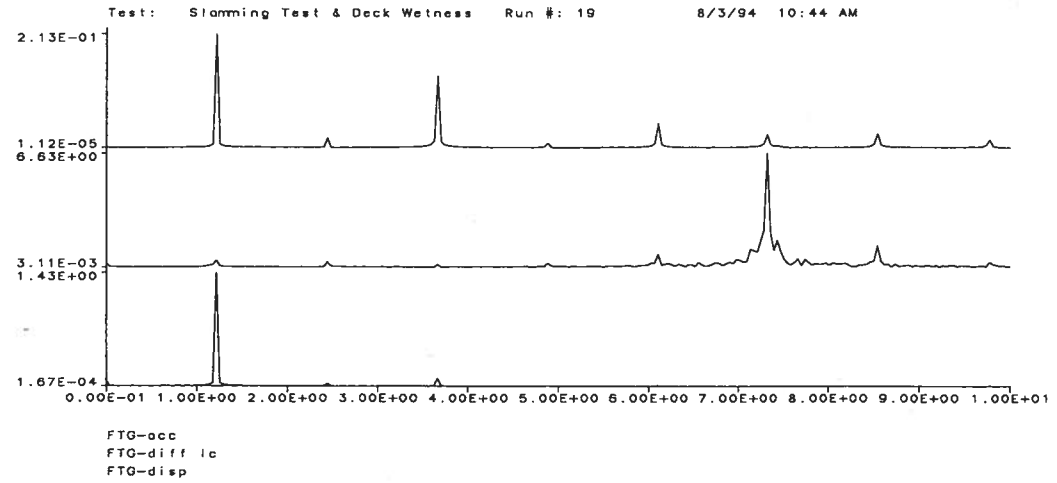

(b) Gains of the FFT Analyses

Figure B.46: Run 19, $f_1 = 1.221\,Hz$, $A_1 = 1.435\,in$, $\alpha = 6$

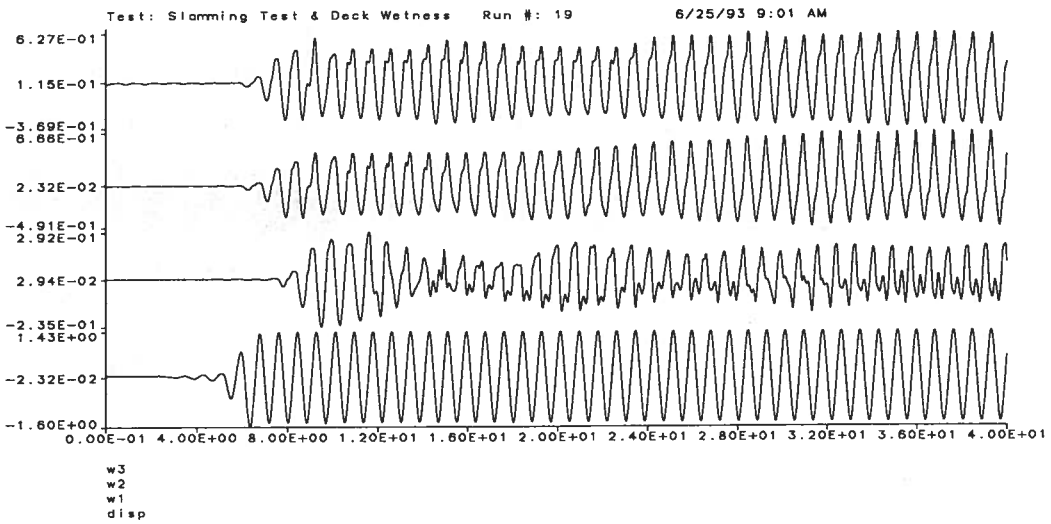

(a) Time-History Acquisitions

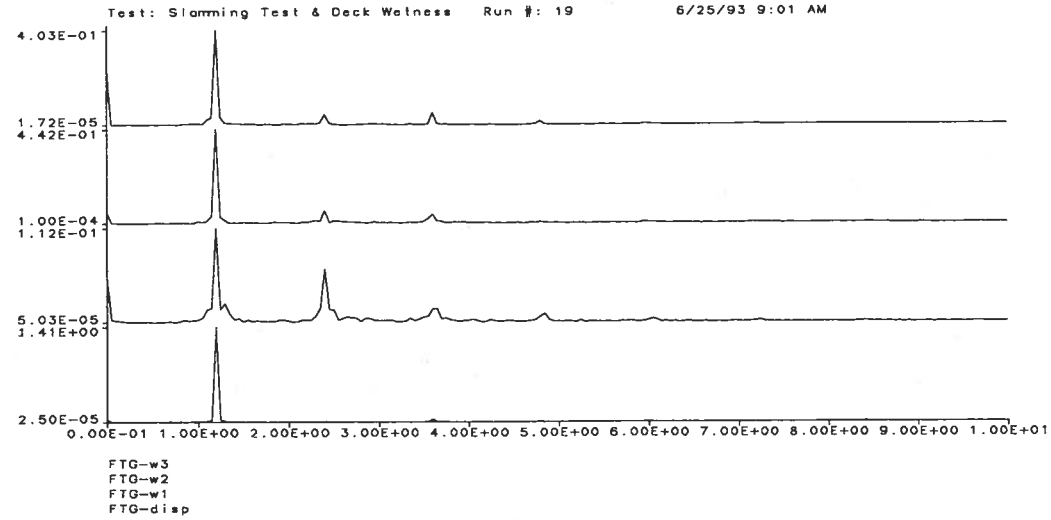

(b) Gains of the FFT Analyses

Figure B.47: Run 19, $f_1 = 1.198\,Hz$, $A_1 = 1.411\,in$, $\alpha = 6$

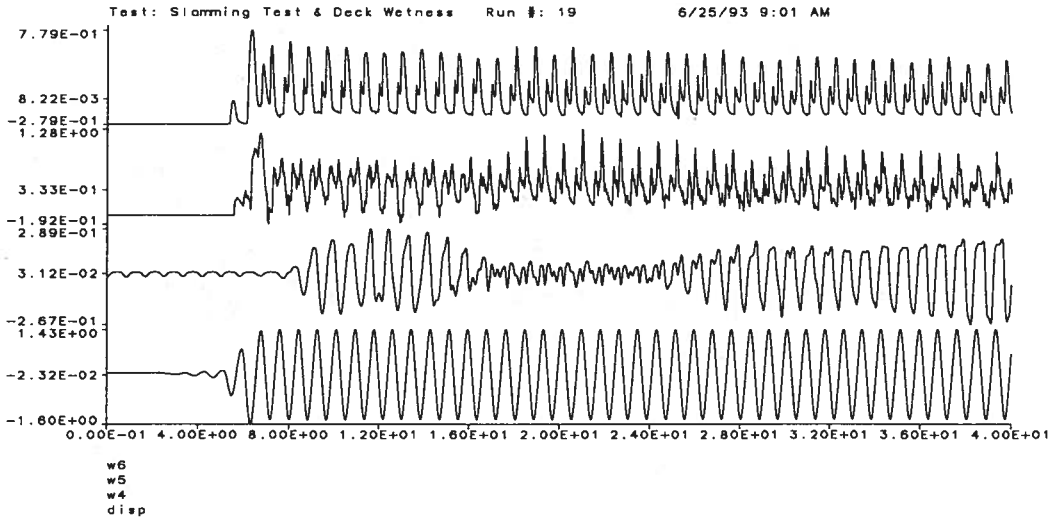

(a) Time-History Acquisitions

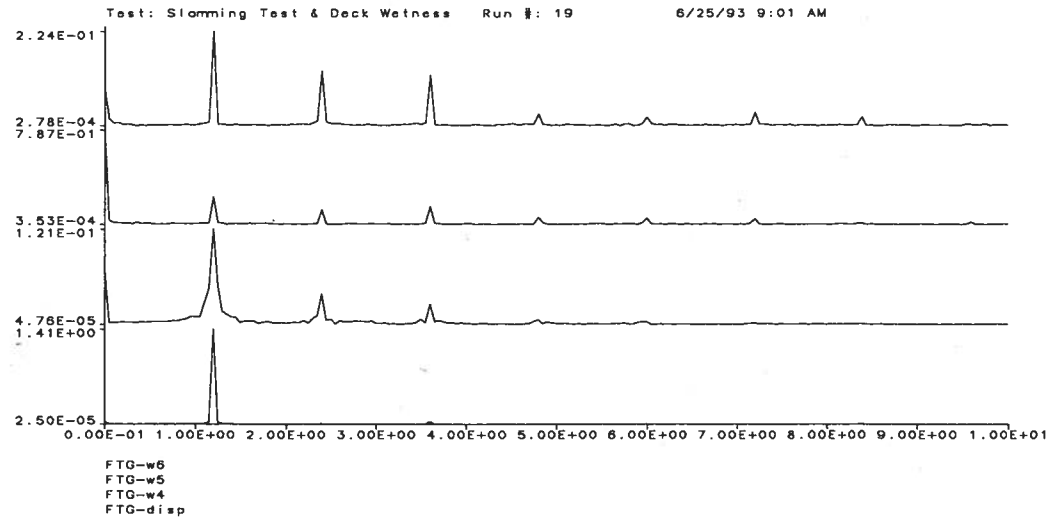

(b) Gains of the FFT Analyses

Figure B.48: Run 19, $f_1 = 1.198\,Hz$, $A_1 = 1.411\,in$, $\alpha = 6$

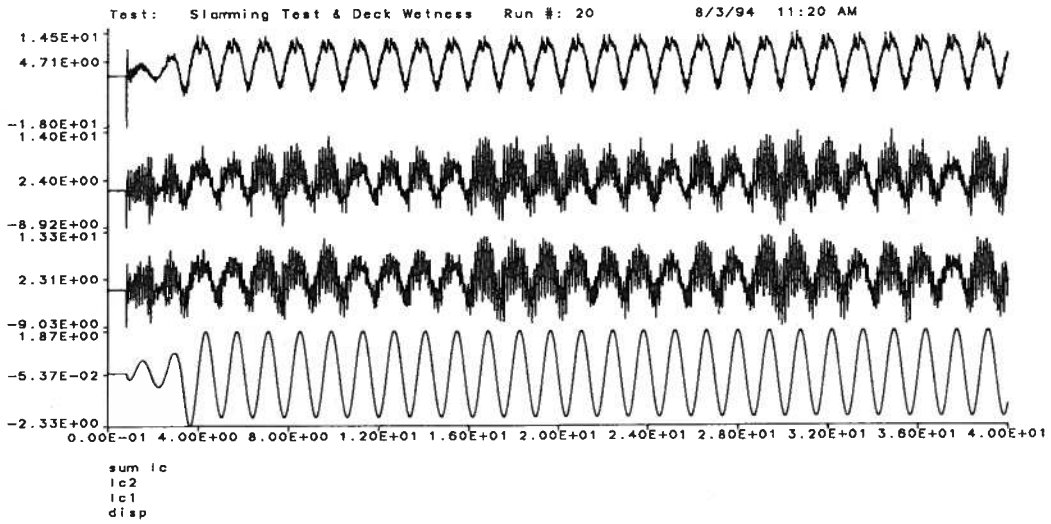

(a) Time-History Acquisitions

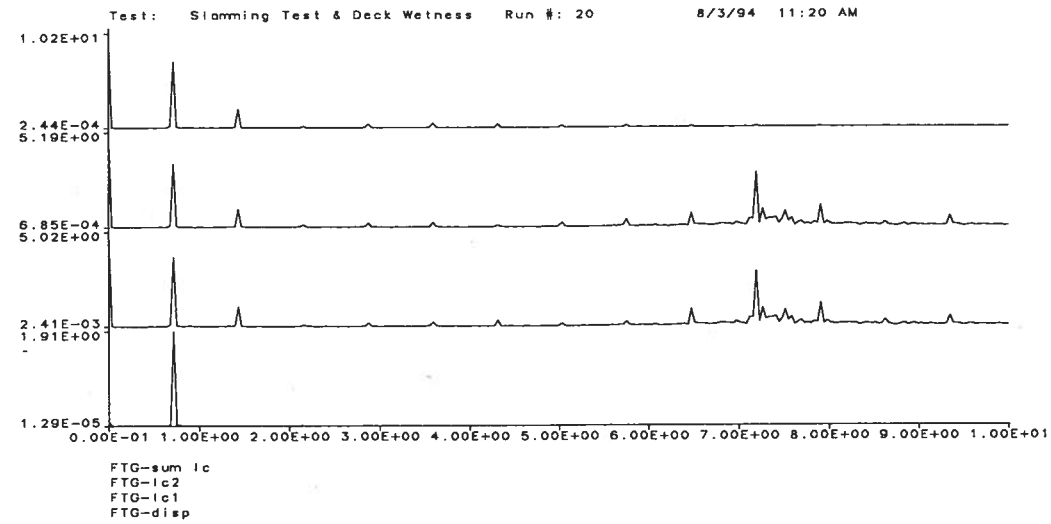

(b) Gains of the FFT Analyses

Figure B.49: Run 20, $f_1 = 0.720\,Hz$, $A_1 = 1.908\,in$, $\alpha = 6$

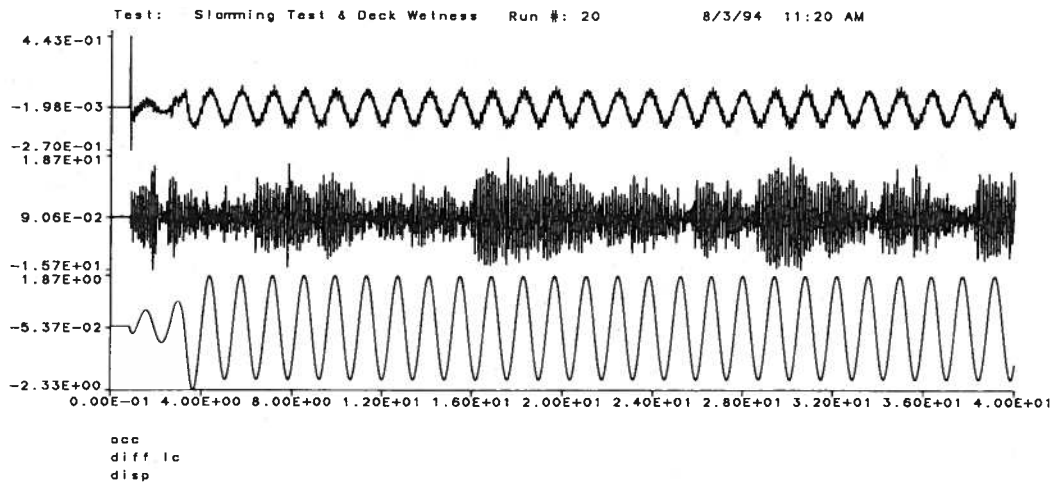

(a) Time-History Acquisitions

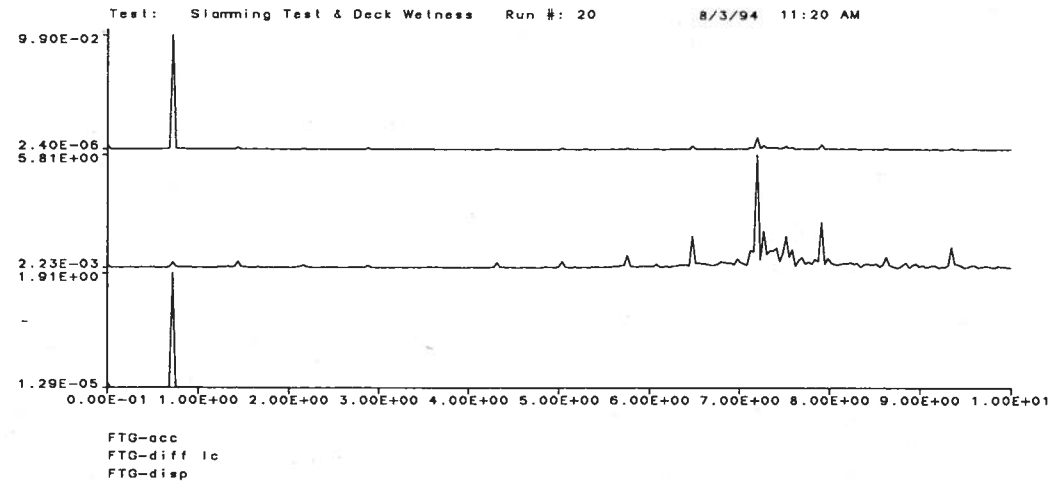

(b) Gains of the FFT Analyses

Figure B.50: Run 20, $f_1 = 0.720\,Hz$, $A_1 = 1.908\,in$, $\alpha = 6$

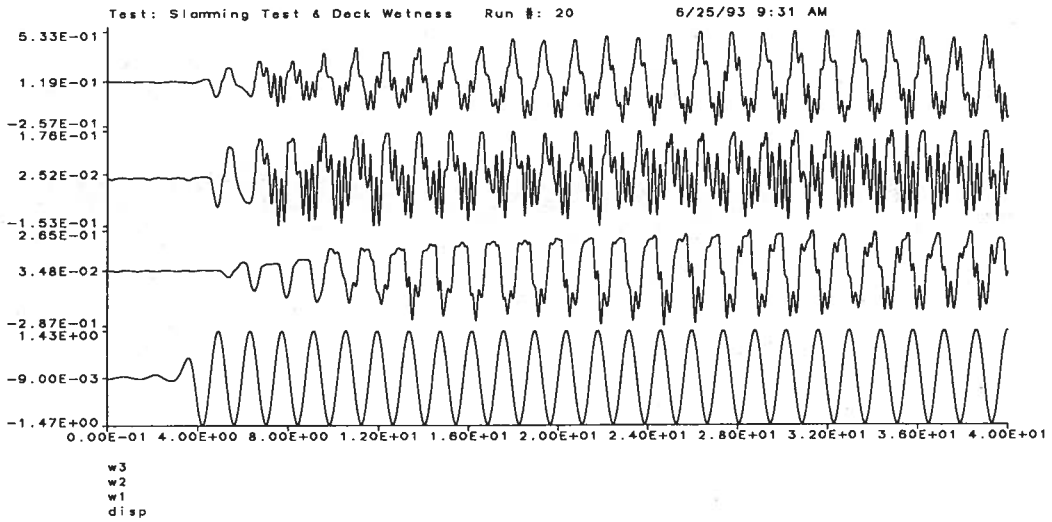

(a) Time-History Acquisitions

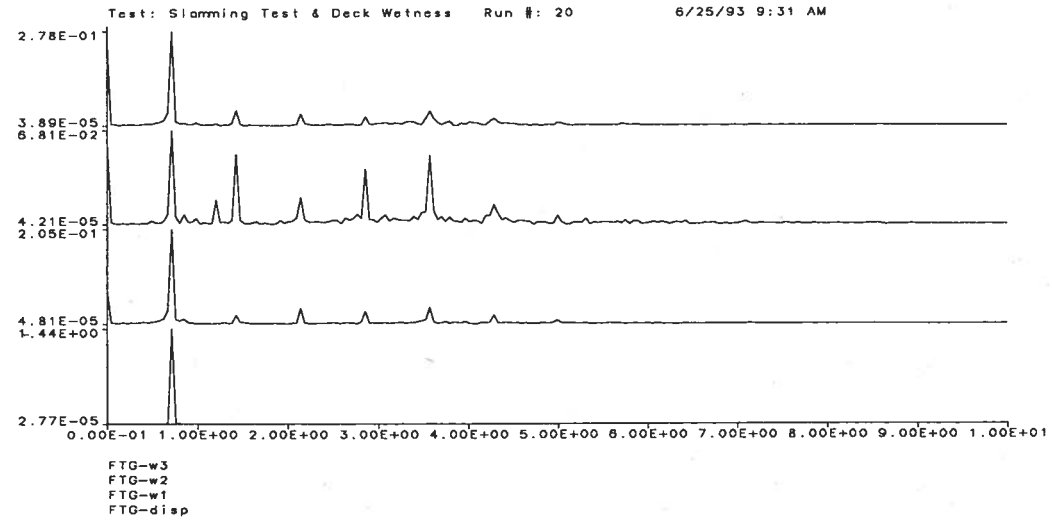

(b) Gains of the FFT Analyses

Figure B.51: Run 20, $f_1 = 0.713\,Hz$, $A_1 = 1.435\,in$, $\alpha = 6$

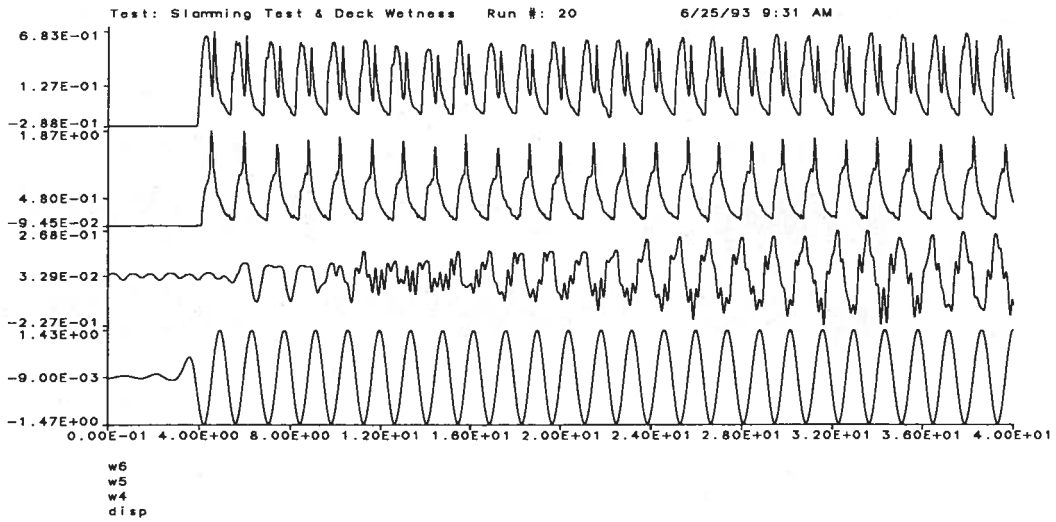

(a) Time-History Acquisitions

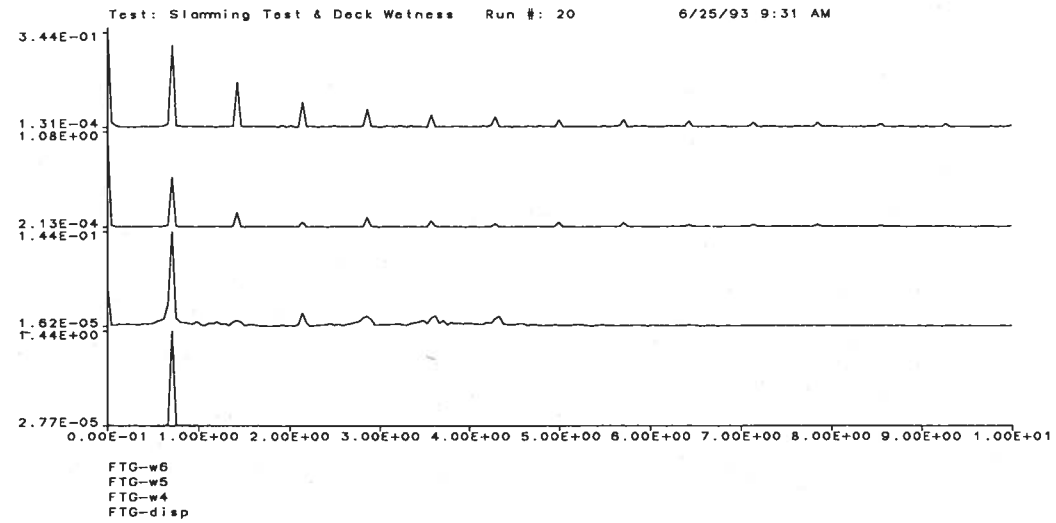

(b) Gains of the FFT Analyses

Figure B.52: Run 20, $f_1 = 0.713\,Hz$, $A_1 = 1.435\,in$, $\alpha = 6$

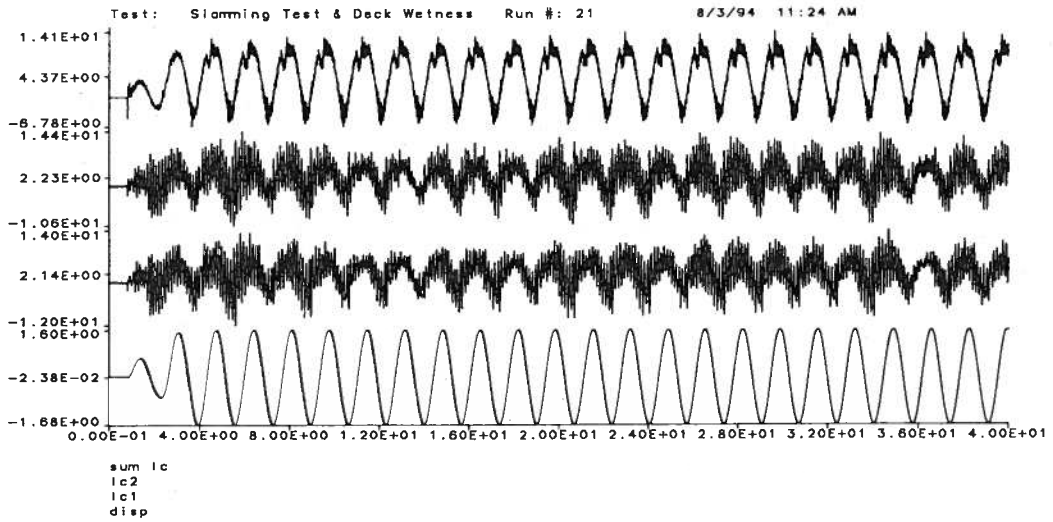

(a) Time-History Acquisitions

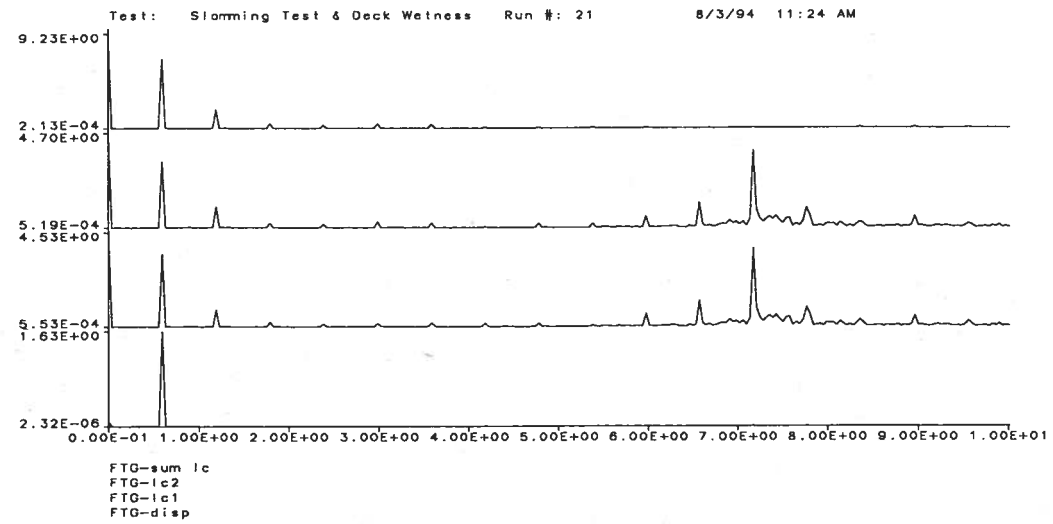

(b) Gains of the FFT Analyses

Figure B.53: Run 21, $f_1 = 0.598\,Hz$, $A_1 = 1.632\,in$, $\alpha = 6$

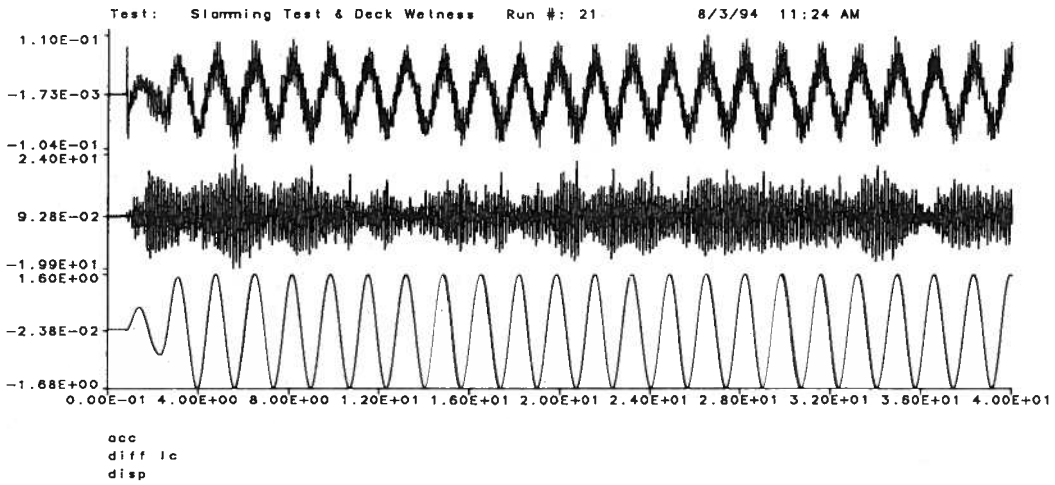

(a) Time-History Acquisitions

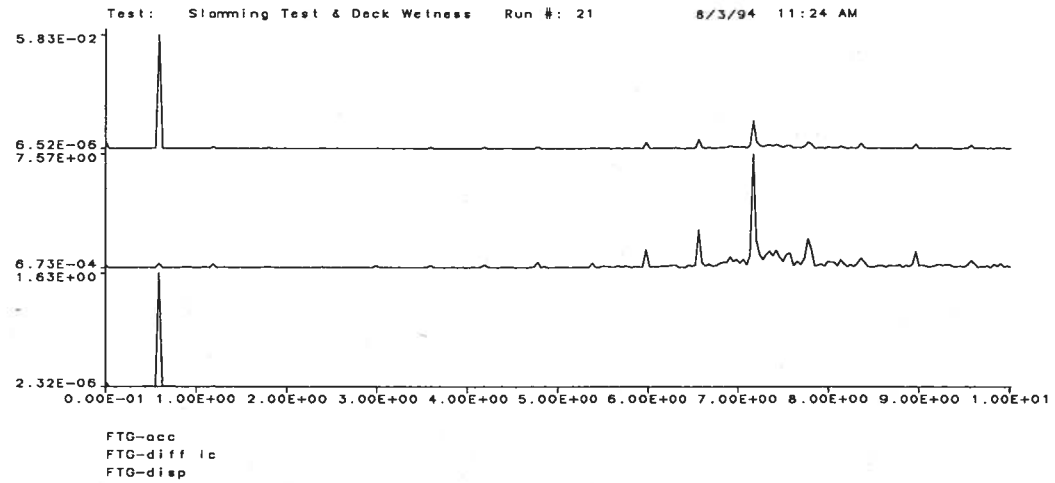

(b) Gains of the FFT Analyses

Figure B.54: Run 21, $f_1 = 0.598\,Hz$, $A_1 = 1.632\,in$, $\alpha = 6$

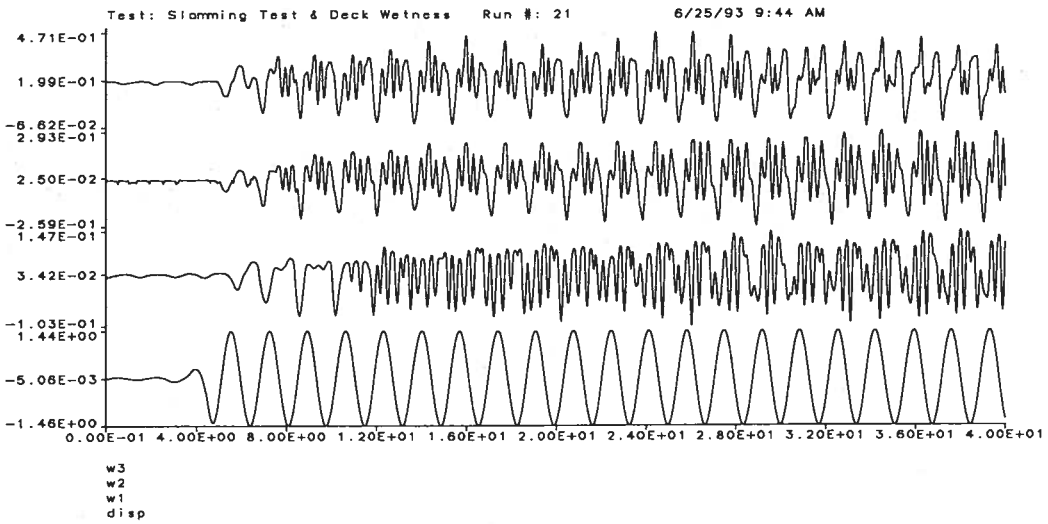

(a) Time-History Acquisitions

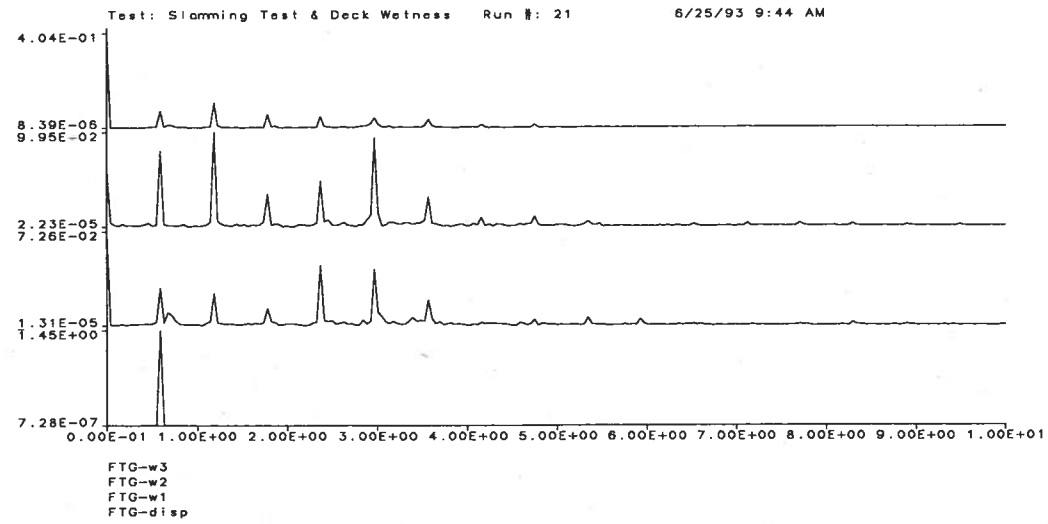

(b) Gains of the FFT Analyses

Figure B.55: Run 21, $f_1 = 0.593\,Hz$, $A_1 = 1.447\,in$, $\alpha = 6$

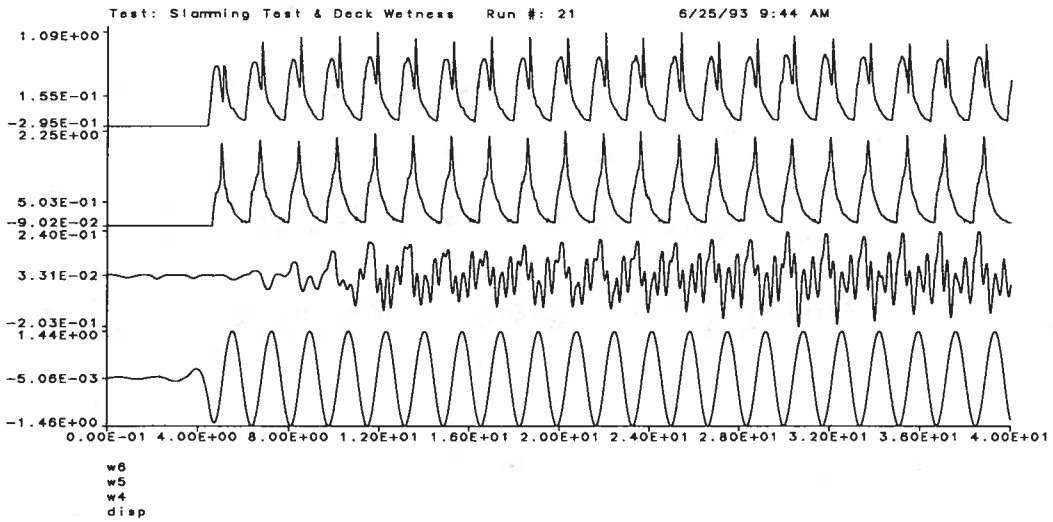

(a) Time-History Acquisitions

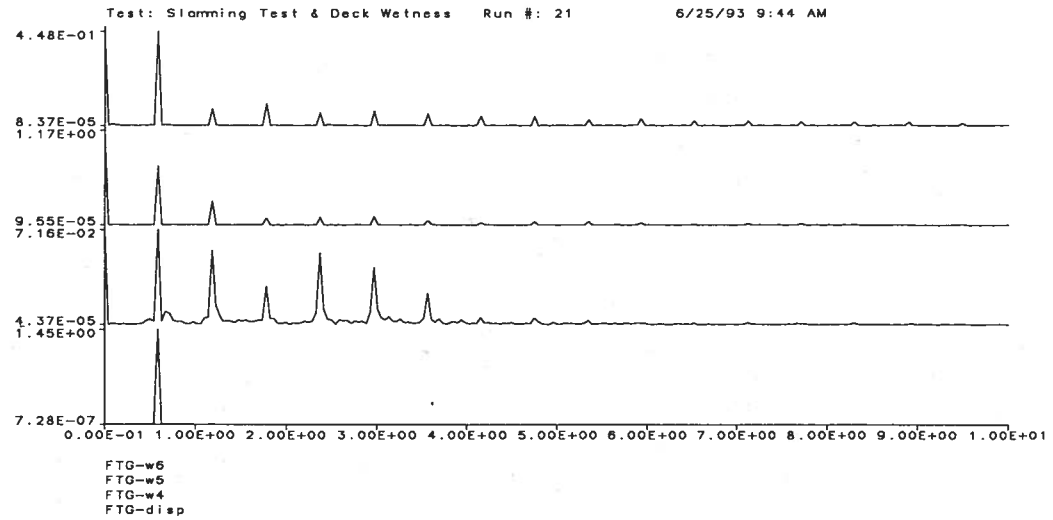

(b) Gains of the FFT Analyses

Figure B.56: Run 21, $f_1 = 0.593\,Hz$, $A_1 = 1.447\,in$, $\alpha = 6$

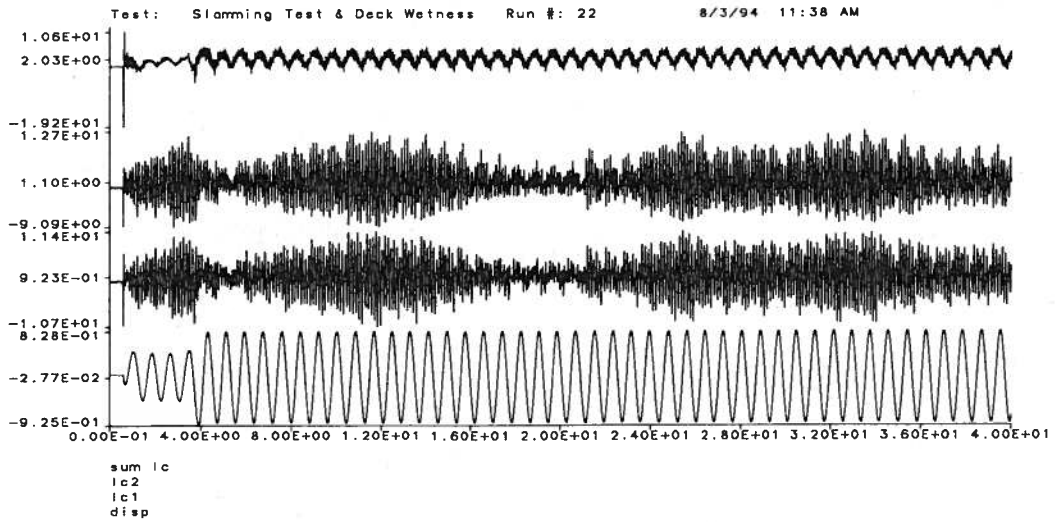

(a) Time-History Acquisitions

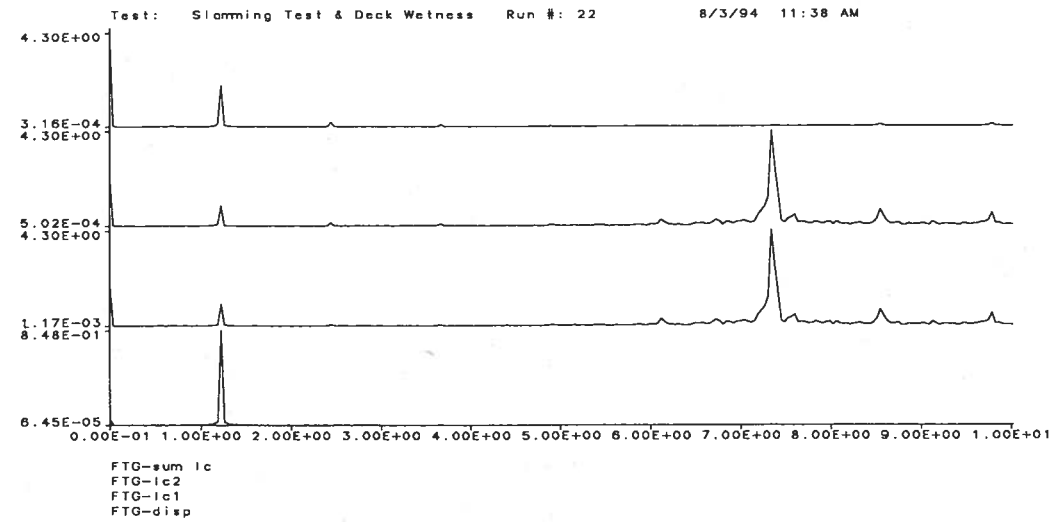

(b) Gains of the FFT Analyses

Figure B.57: Run 22, $f_1 = 1.223\,Hz$, $A_1 = 0.848\,in$, $\alpha = 6$

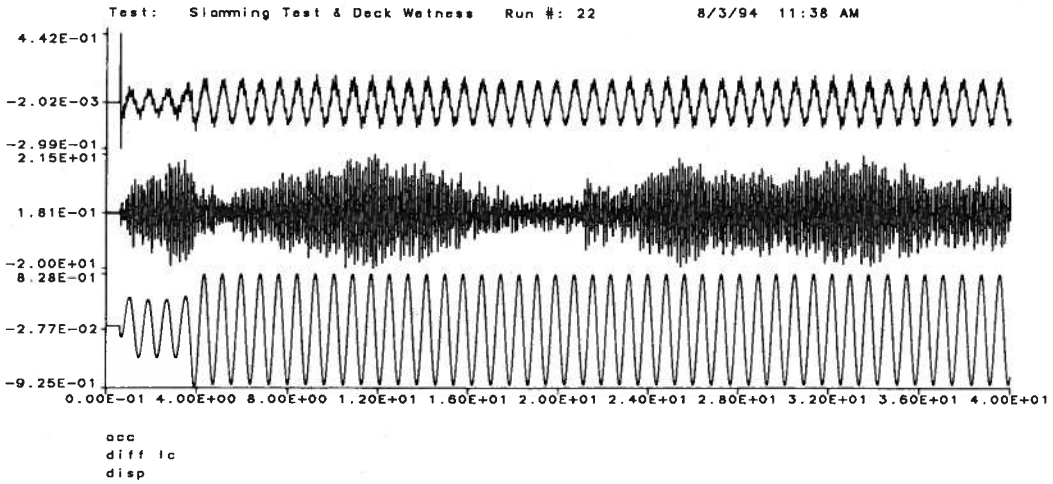

(a) Time-History Acquisitions

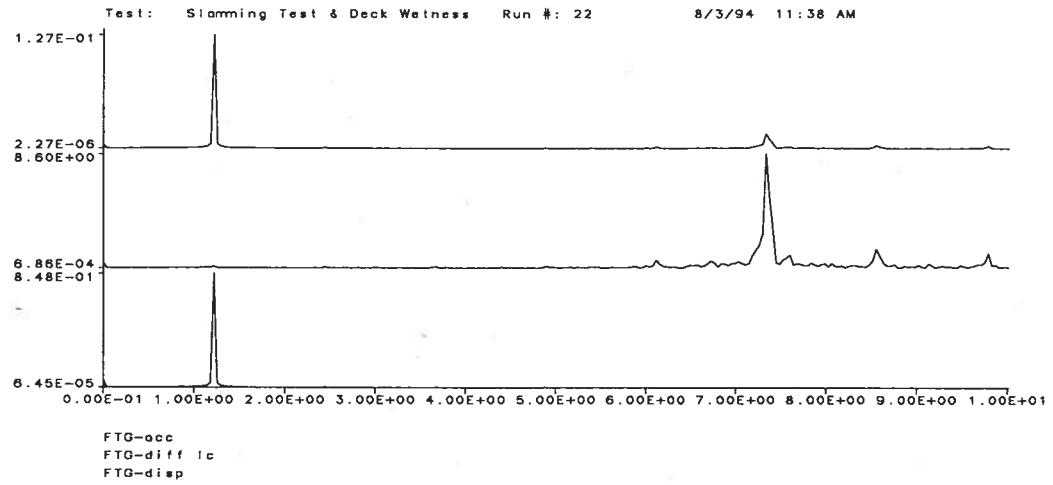

(b) Gains of the FFT Analyses

Figure B.58: Run 22, $f_1 = 1.223\,Hz$, $A_1 = 0.848\,in$, $\alpha = 6$

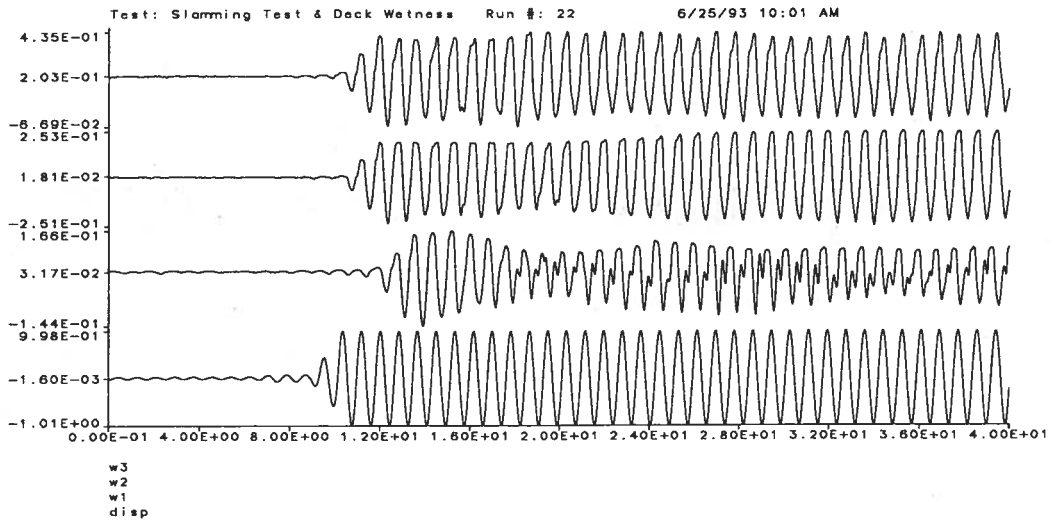

(a) Time-History Acquisitions

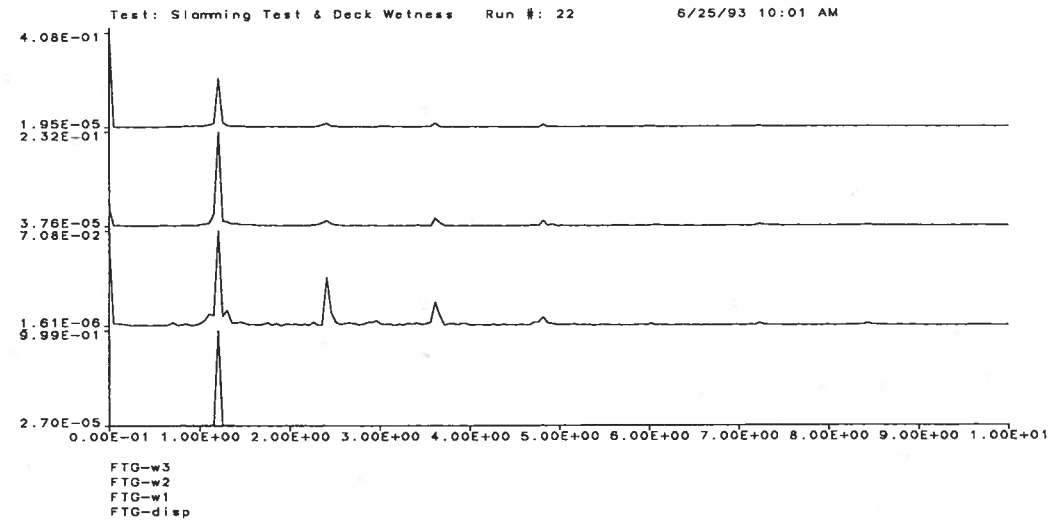

(b) Gains of the FFT Analyses

Figure B.59: Run 22, $f_1 = 1.205\,Hz$, $A_1 = 0.999\,in$, $\alpha = 6$

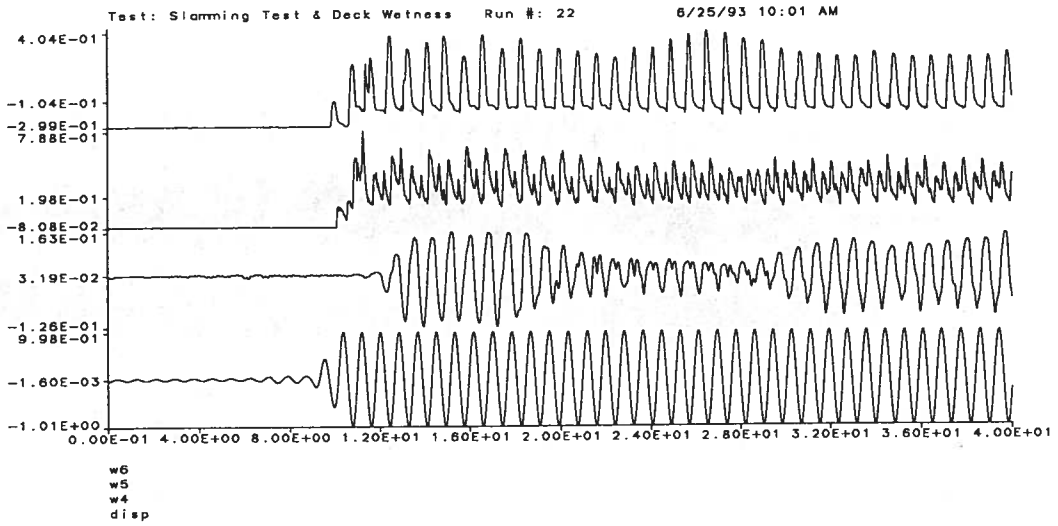

(a) Time-History Acquisitions

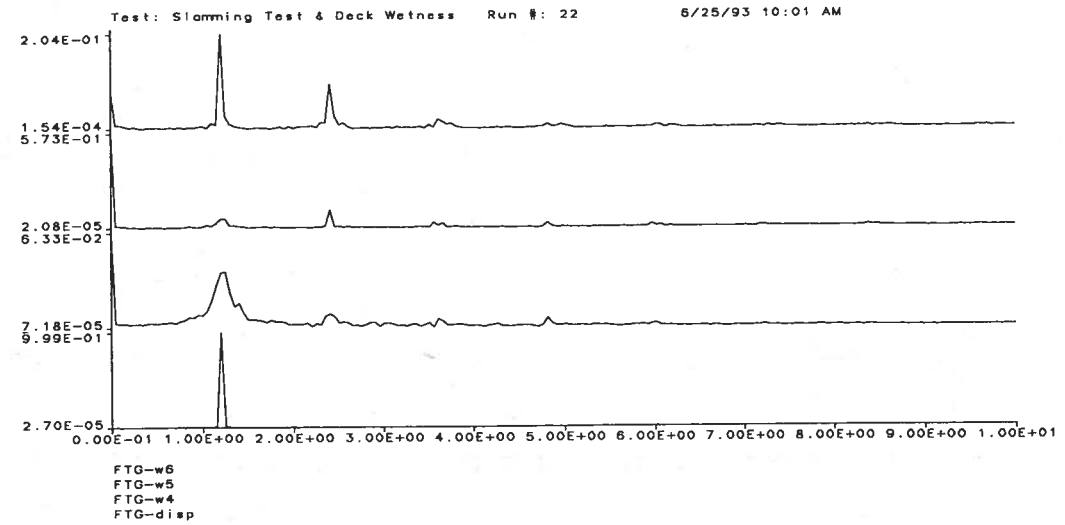

(b) Gains of the FFT Analyses

Figure B.60: Run 22, $f_1 = 1.205\,Hz$, $A_1 = 0.999\,in$, $\alpha = 6$

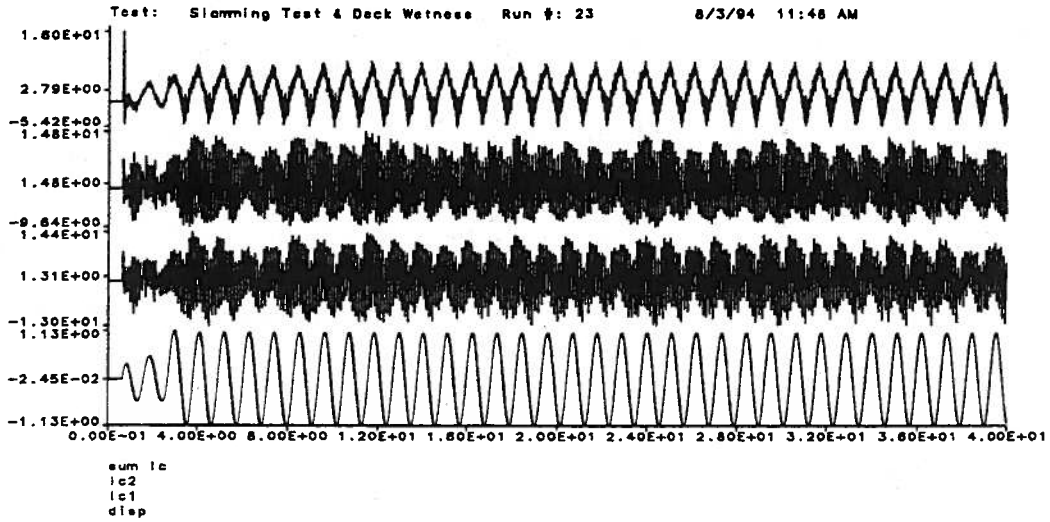

(a) Time-History Acquisitions

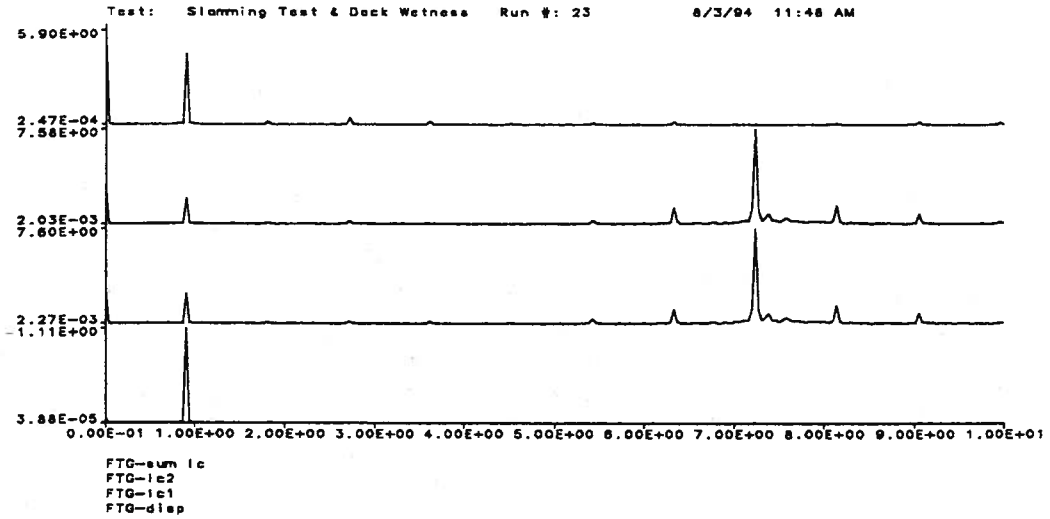

(b) Gains of the FFT Analyses

Figure B.61: Run 23, $f_1 = 0.905\,Hz$, $A_1 = 1.110\,in$, $\alpha = 6$

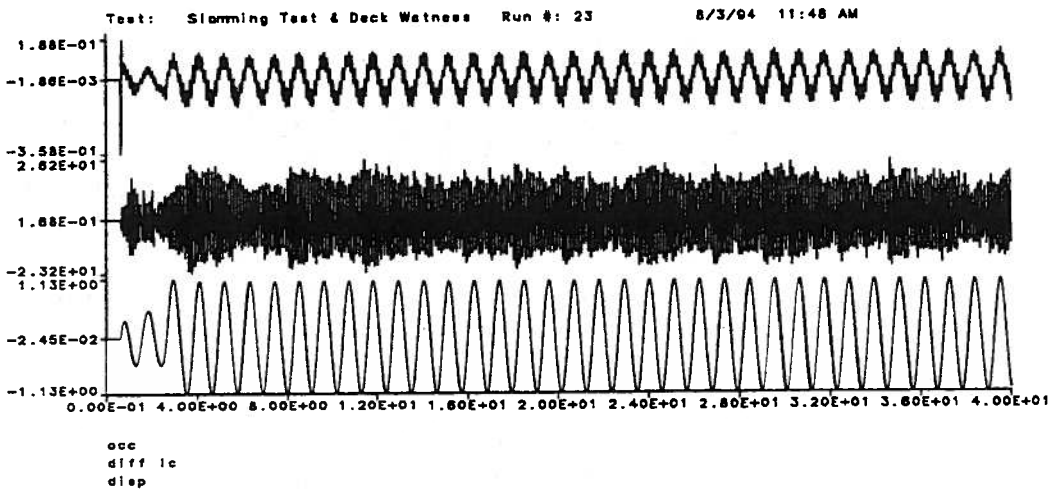

(a) Time-History Acquisitions

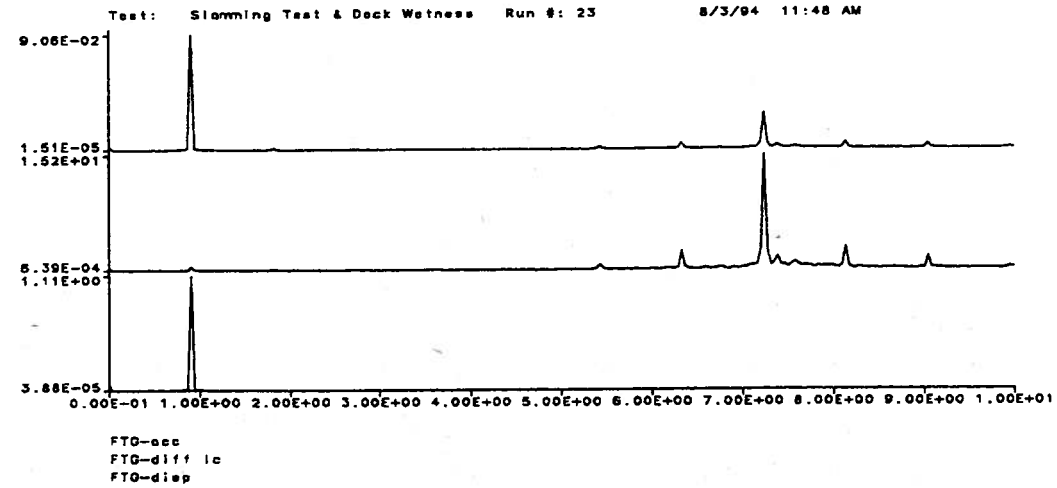

(b) Gains of the FFT Analyses

Figure B.62: Run 23, $f_1 = 0.905\,Hz$, $A_1 = 1.110\,in$, $\alpha = 6$

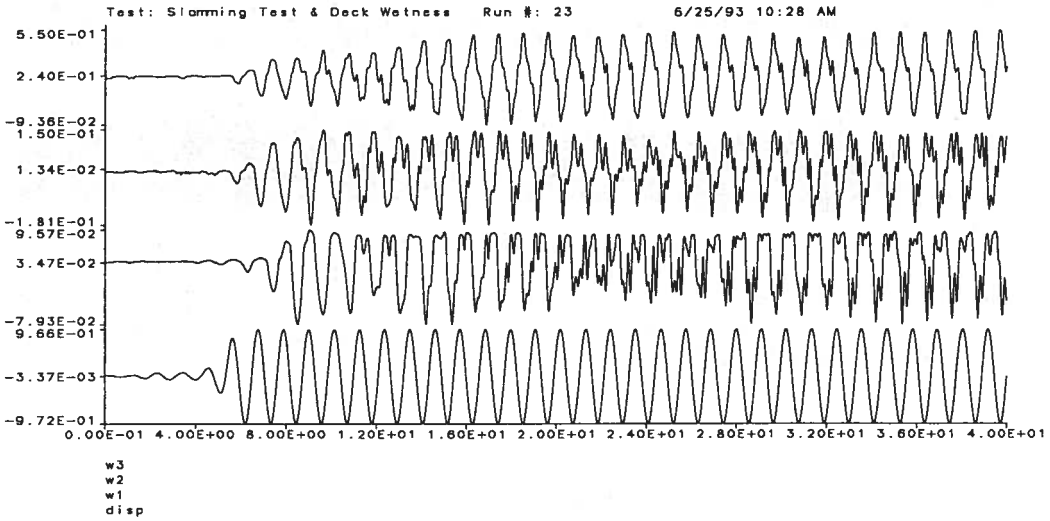

(a) Time-History Acquisitions

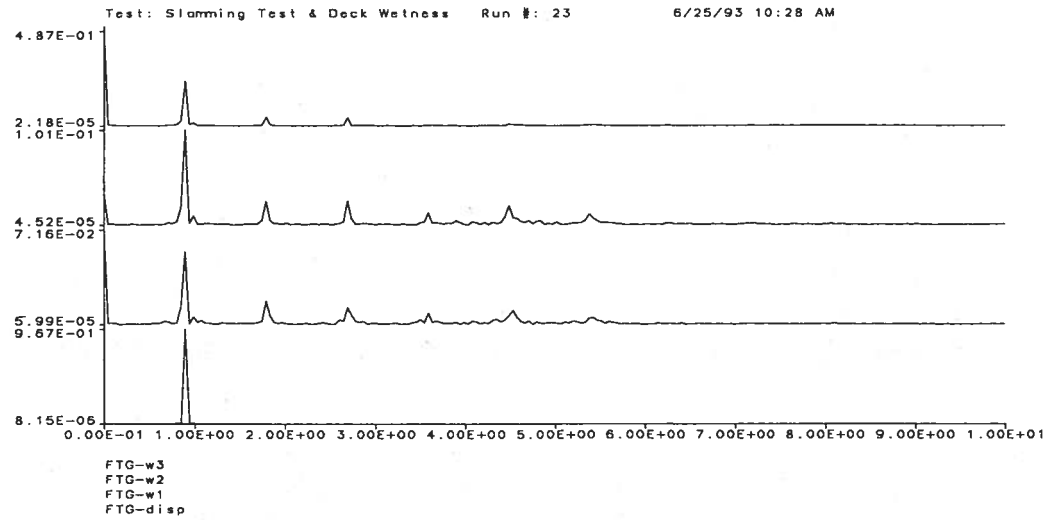

(b) Gains of the FFT Analyses

Figure B.63: Run 23, $f_1 = 0.896\,Hz$, $A_1 = 0.967\,in$, $\alpha = 6$

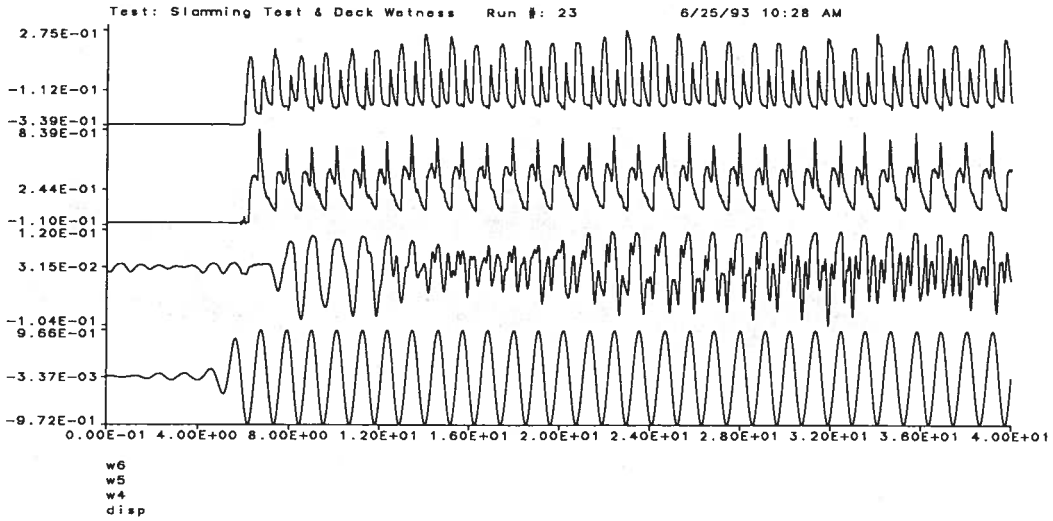

(a) Time-History Acquisitions

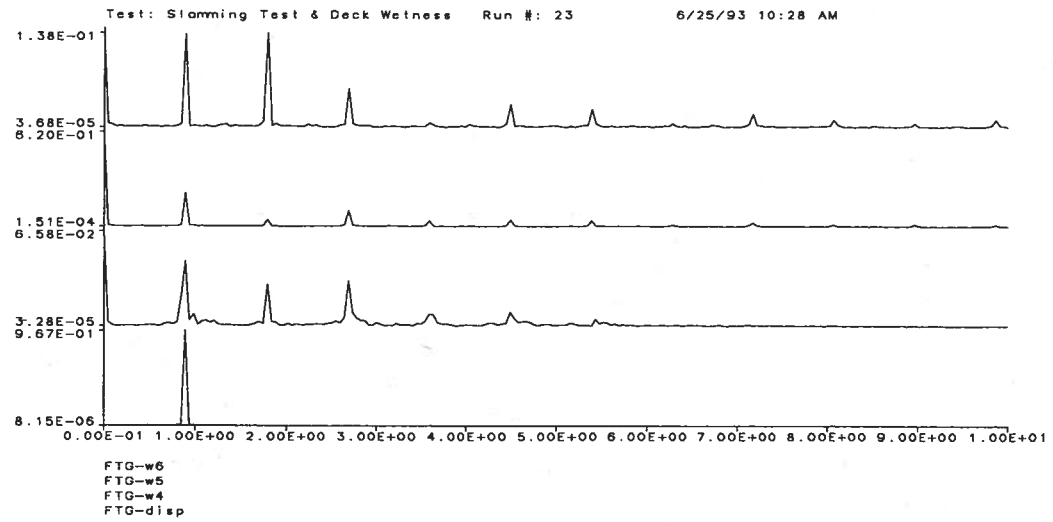

(b) Gains of the FFT Analyses

Figure B.64: Run 23, $f_1 = 0.896\,Hz$, $A_1 = 0.967\,in$, $\alpha = 6$

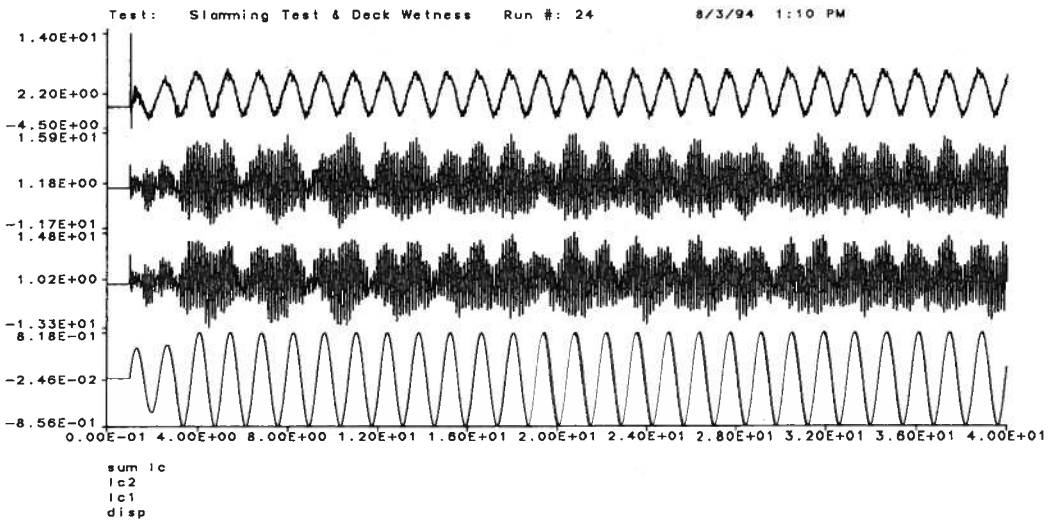

(a) Time-History Acquisitions

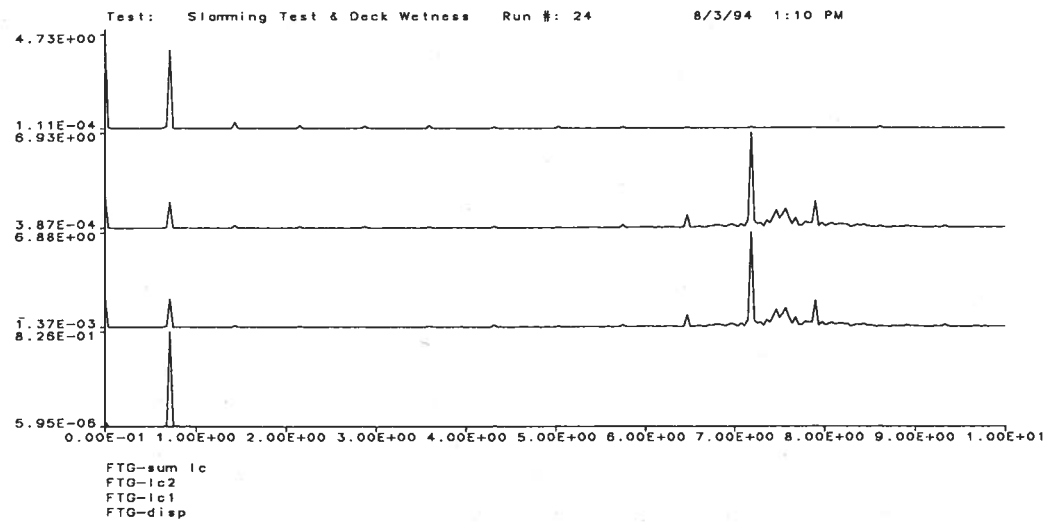

(b) Gains of the FFT Analyses

Figure B.65: Run 24, $f_1 = 0.719\,Hz$, $A_1 = 0.825\,in$, $\alpha = 6$

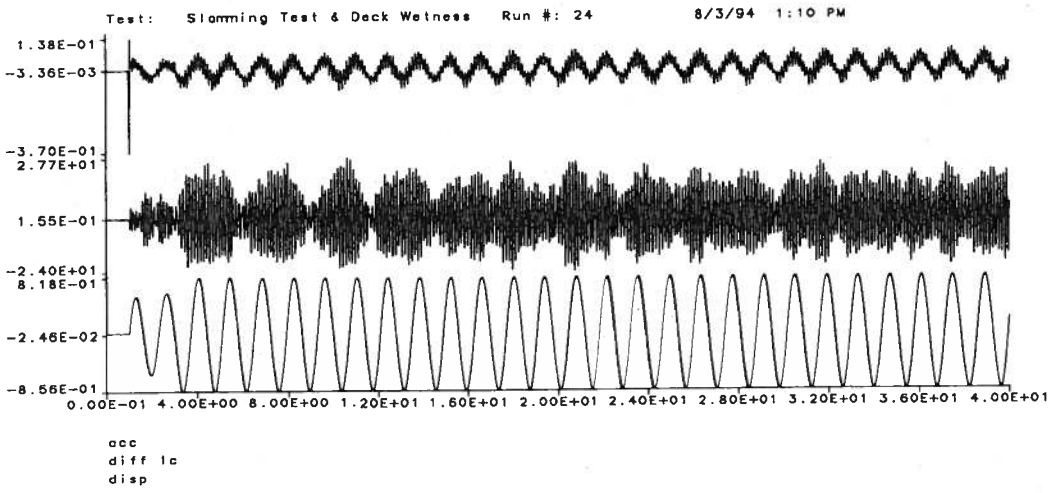

(a) Time-History Acquisitions

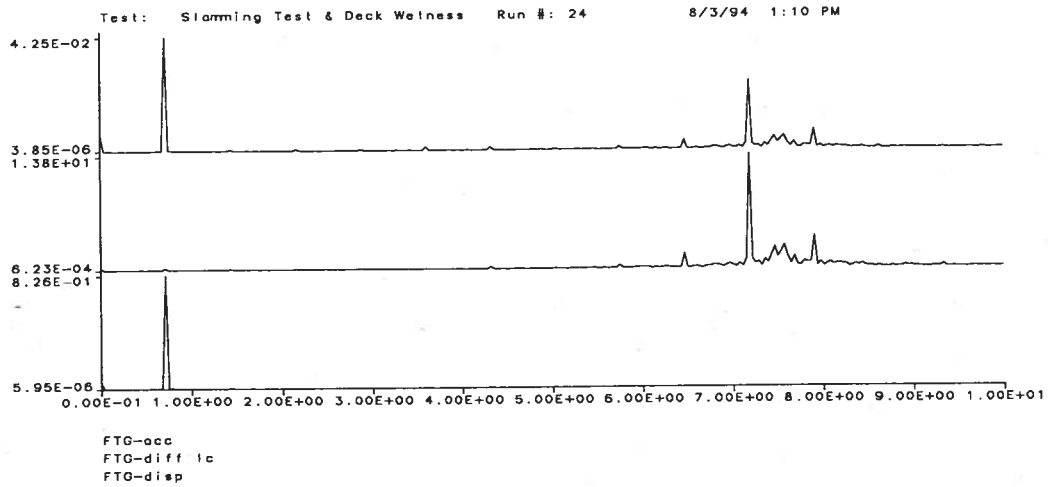

(b) Gains of the FFT Analyses

Figure B.66: Run 24, $f_1 = 0.719\,Hz$, $A_1 = 0.825\,in$, $\alpha = 6$

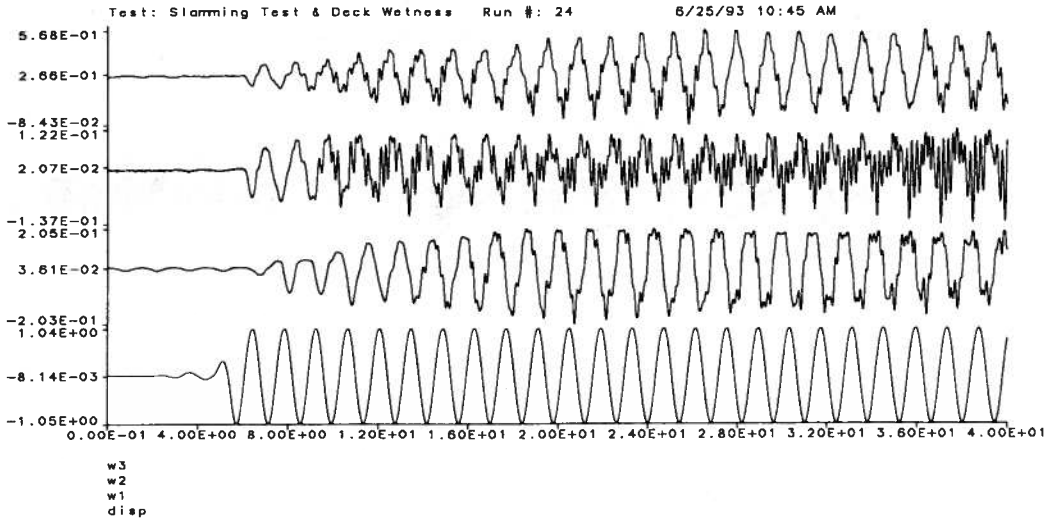

(a) Time-History Acquisitions

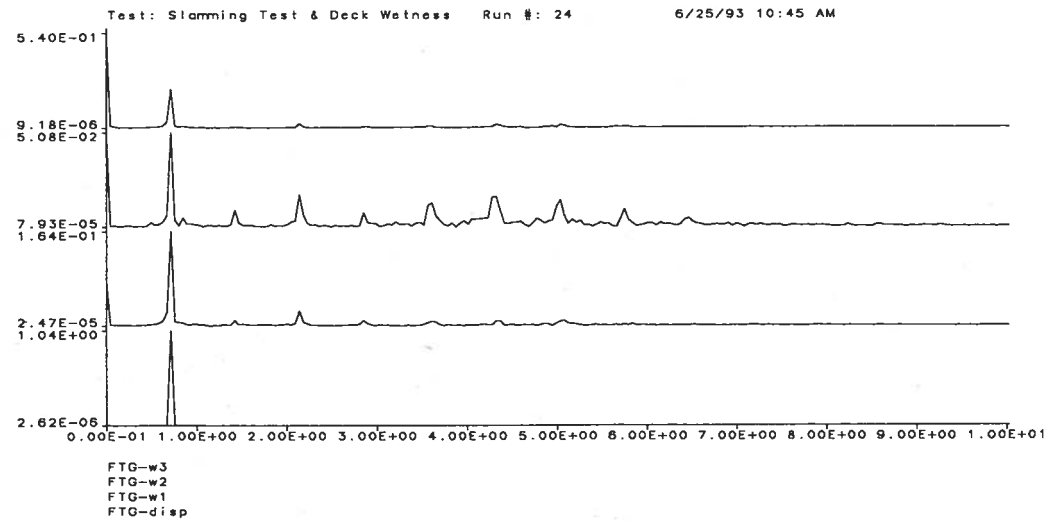

(b) Gains of the FFT Analyses

Figure B.67: Run 24, $f_1 = 0.713\,Hz$, $A_1 = 1.043\,in$, $\alpha = 6$

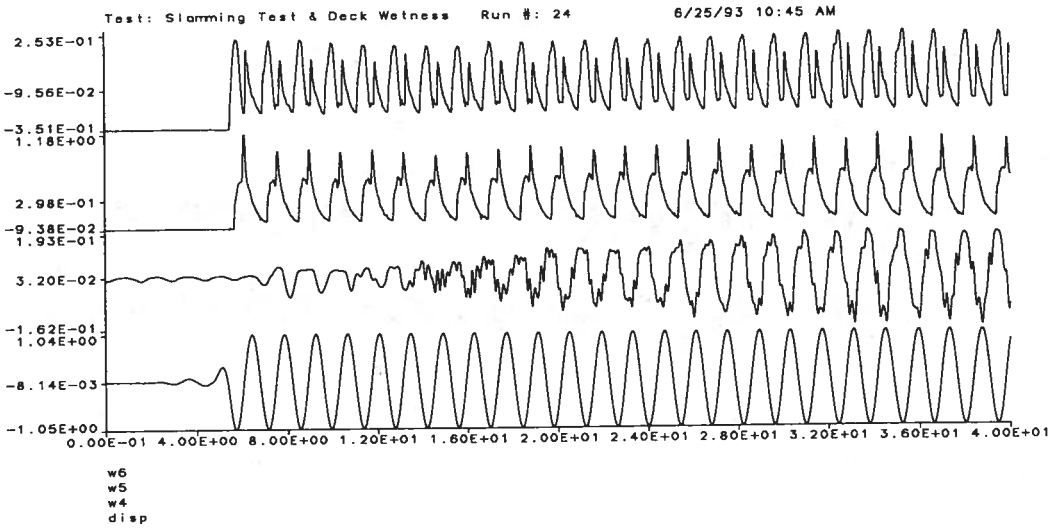

(a) Time-History Acquisitions

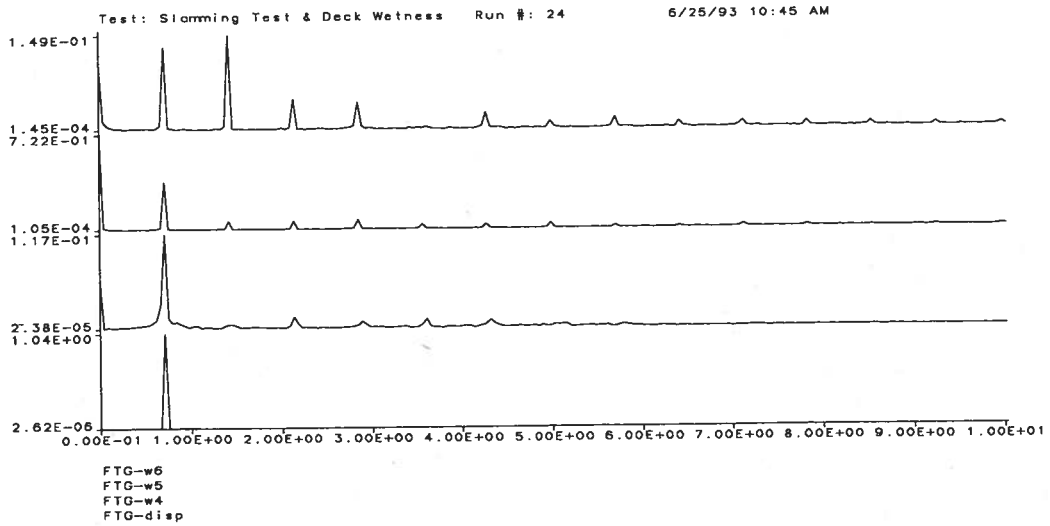

(b) Gains of the FFT Analyses

Figure B.68: Run 24, $f_1 = 0.713\,Hz$, $A_1 = 1.043\,in$, $\alpha = 6$

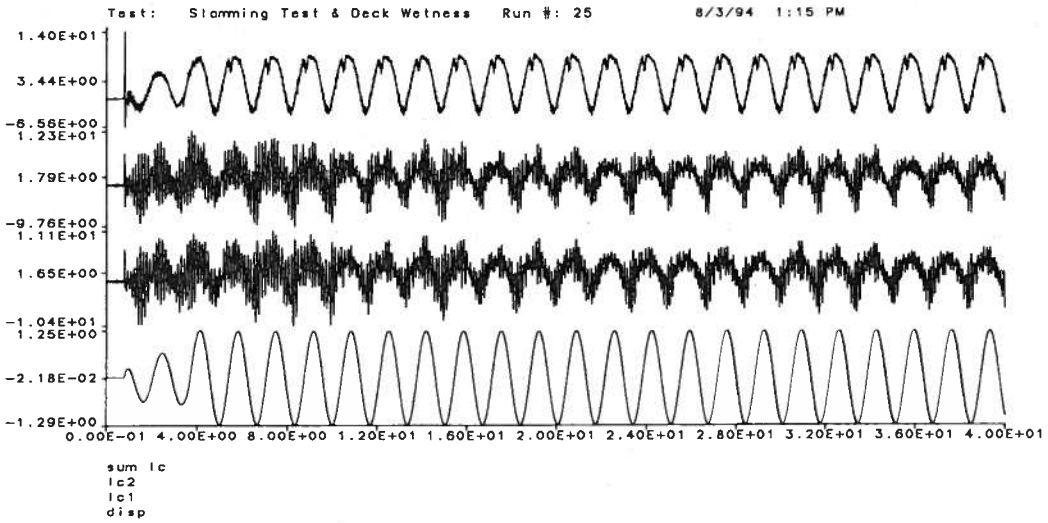

(a) Time-History Acquisitions

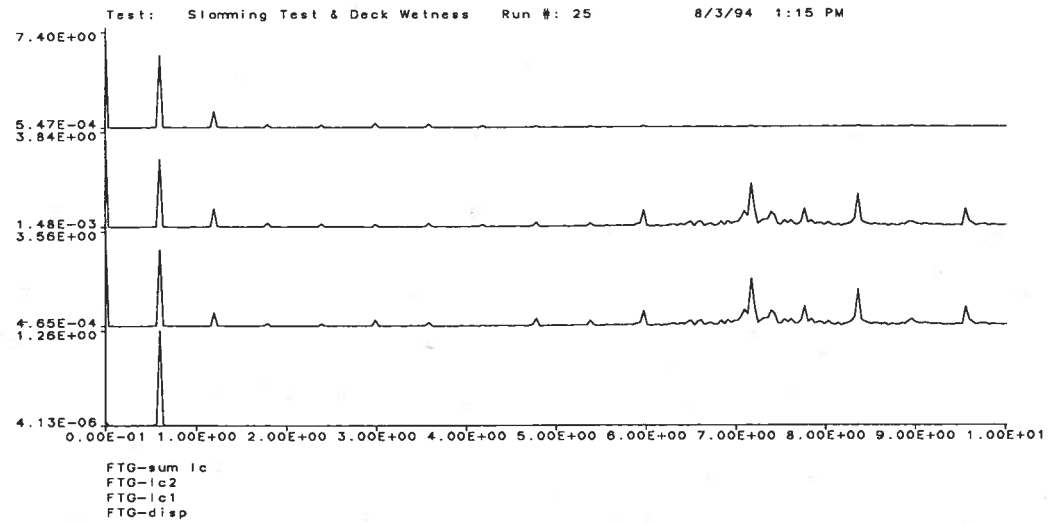

(b) Gains of the FFT Analyses

Figure B.69: Run 25, $f_1 = 0.598\,Hz$, $A_1 = 1.257\,in$, $\alpha = 6$

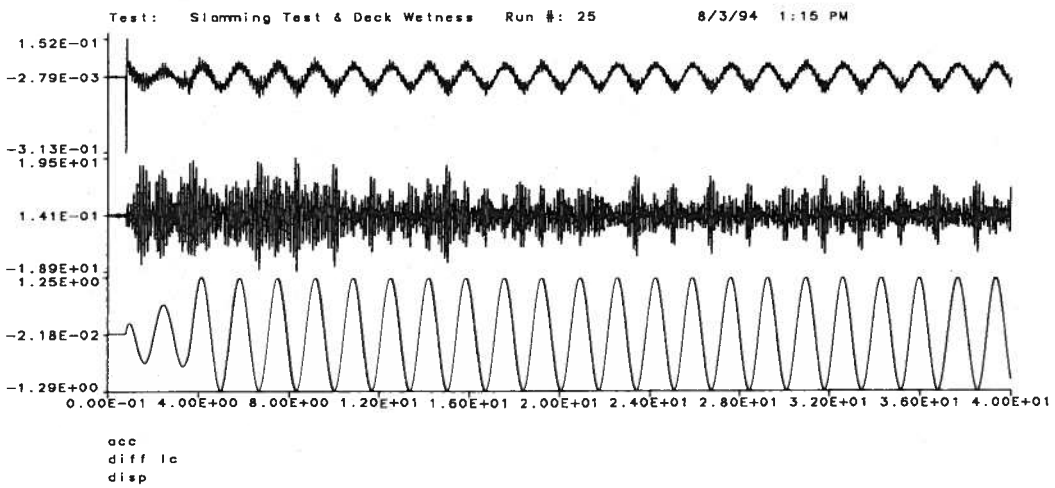

(a) Time-History Acquisitions

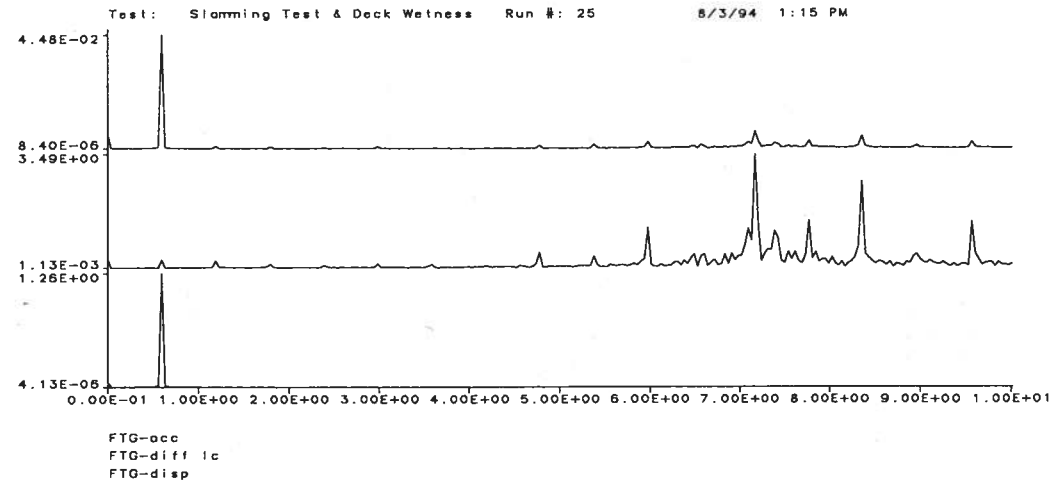

(b) Gains of the FFT Analyses

Figure B.70: Run 25, $f_1 = 0.598\,Hz$, $A_1 = 1.257\,in$, $\alpha = 6$

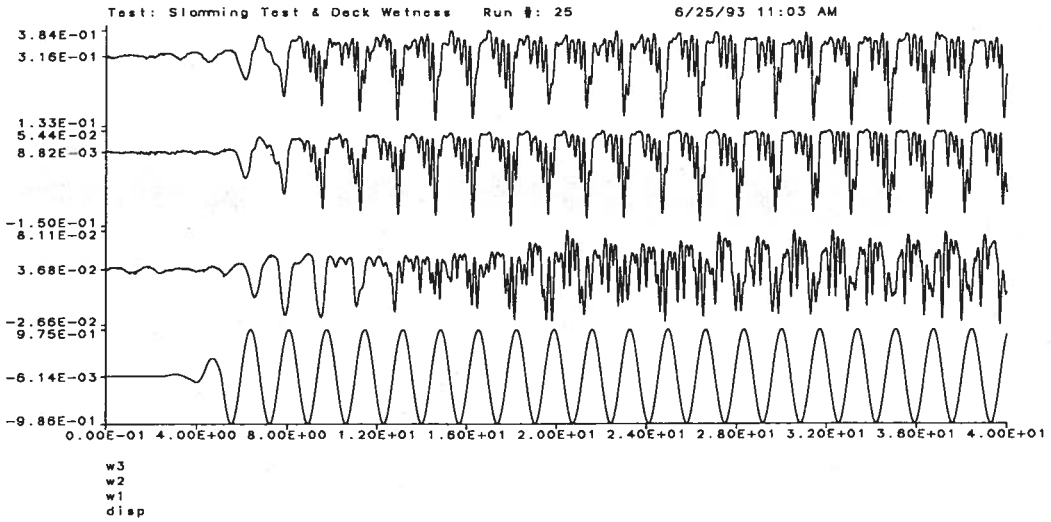

(a) Time-History Acquisitions

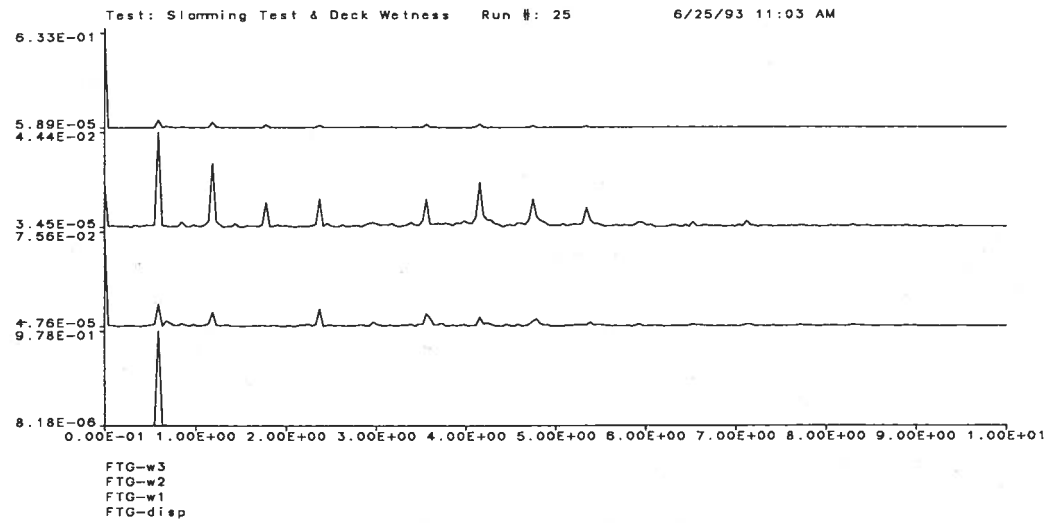

(b) Gains of the FFT Analyses

Figure B.71: Run 25, $f_1 = 0.593\,Hz$, $A_1 = 0.978\,in$, $\alpha = 6$

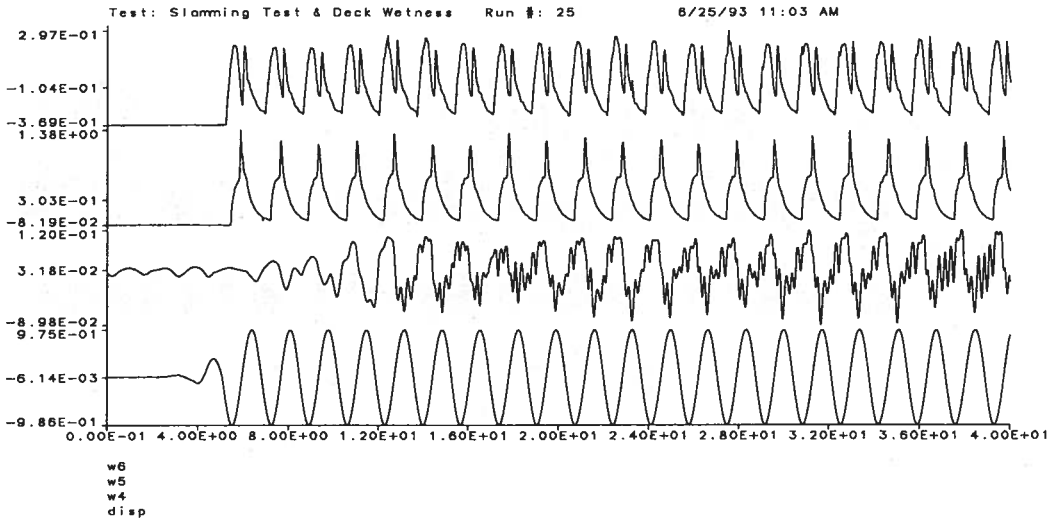

(a) Time-History Acquisitions

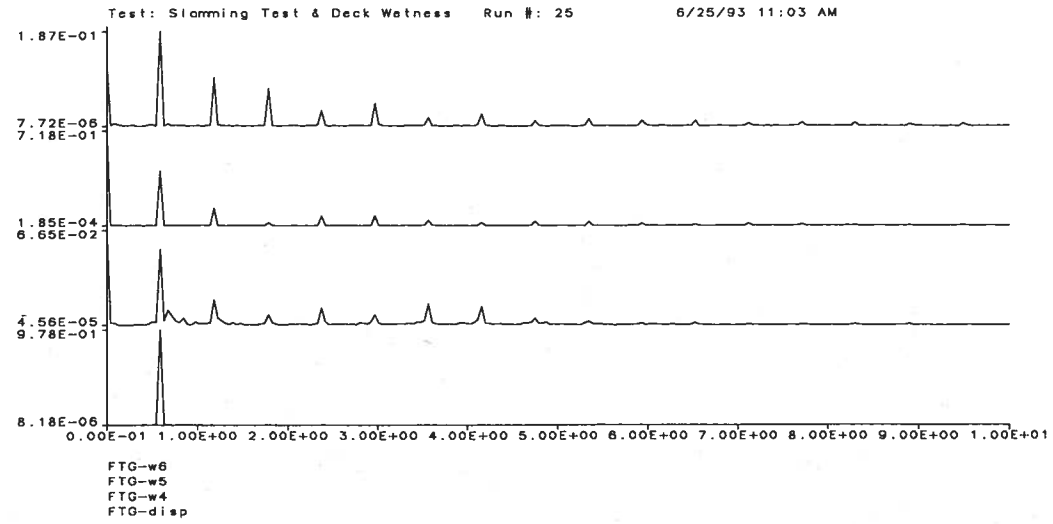

(b) Gains of the FFT Analyses

Figure B.72: Run 25, $f_1 = 0.593\,Hz$, $A_1 = 0.978\,in$, $\alpha = 6$

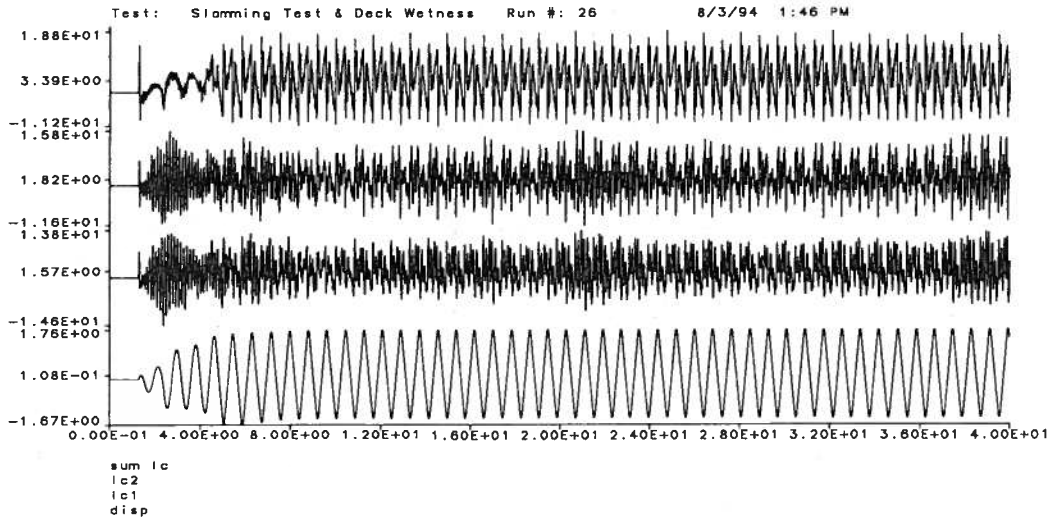

(a) Time-History Acquisitions

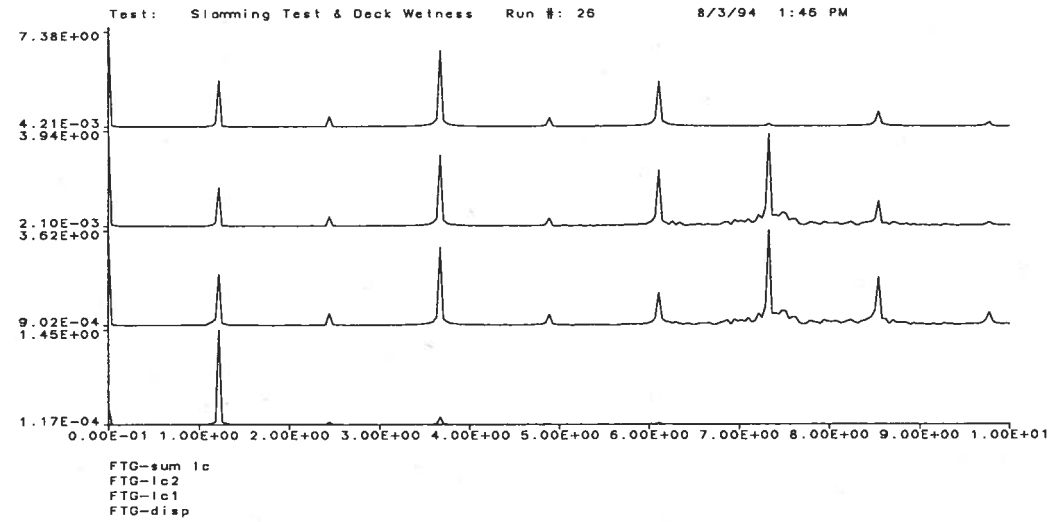

(b) Gains of the FFT Analyses

Figure B.73: Run 26, $f_1 = 1.222\,Hz$, $A_1 = 1.455\,in$, $\alpha = 6$

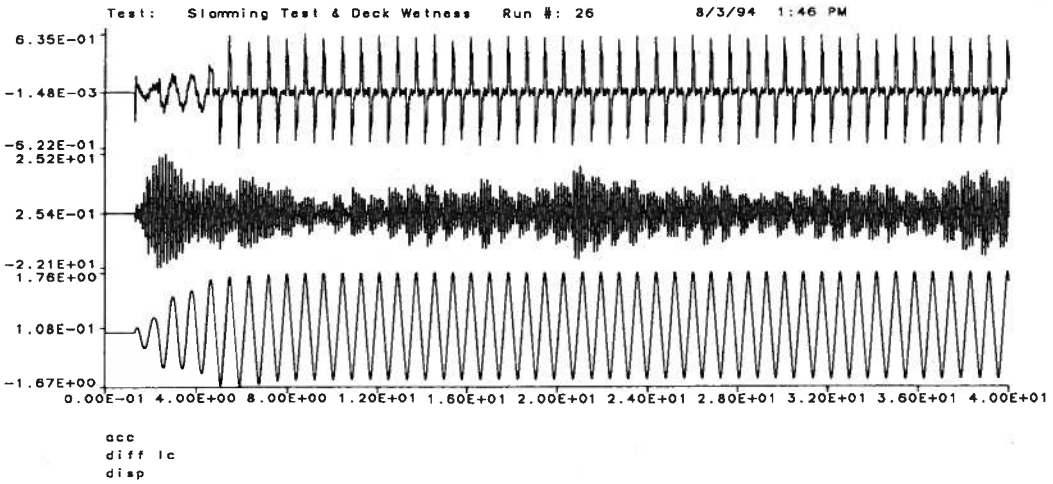

(a) Time-History Acquisitions

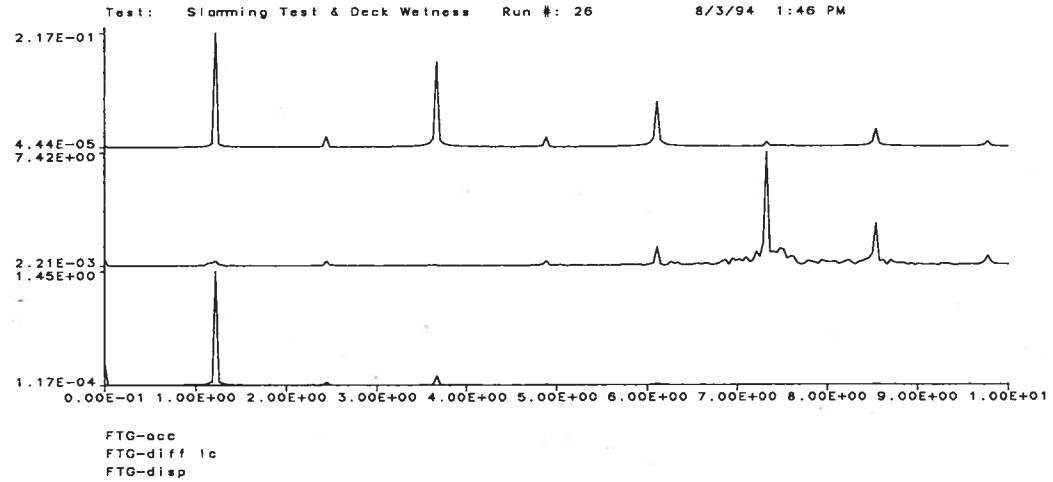

(b) Gains of the FFT Analyses

Figure B.74: Run 26, $f_1 = 1.222\,Hz$, $A_1 = 1.455\,in$, $\alpha = 6$

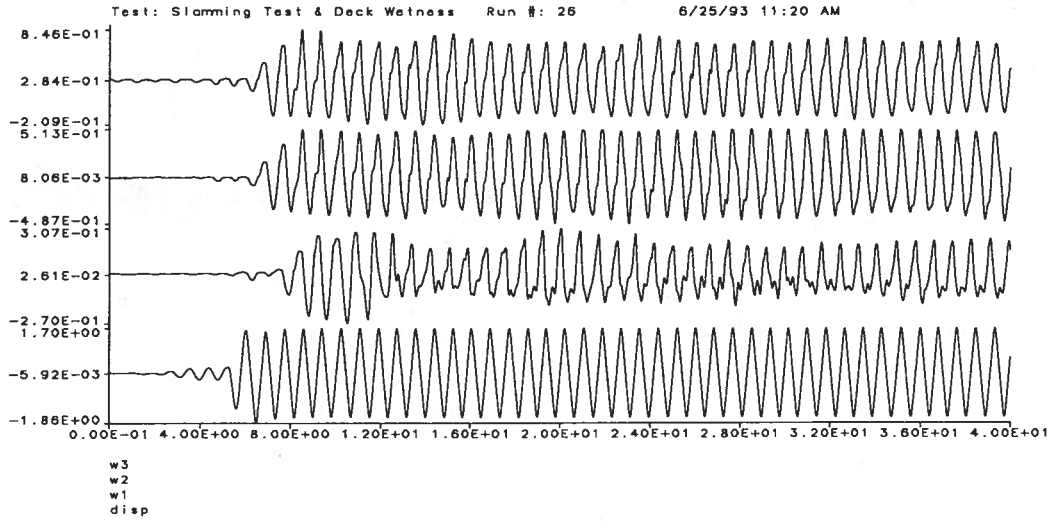

(a) Time-History Acquisitions

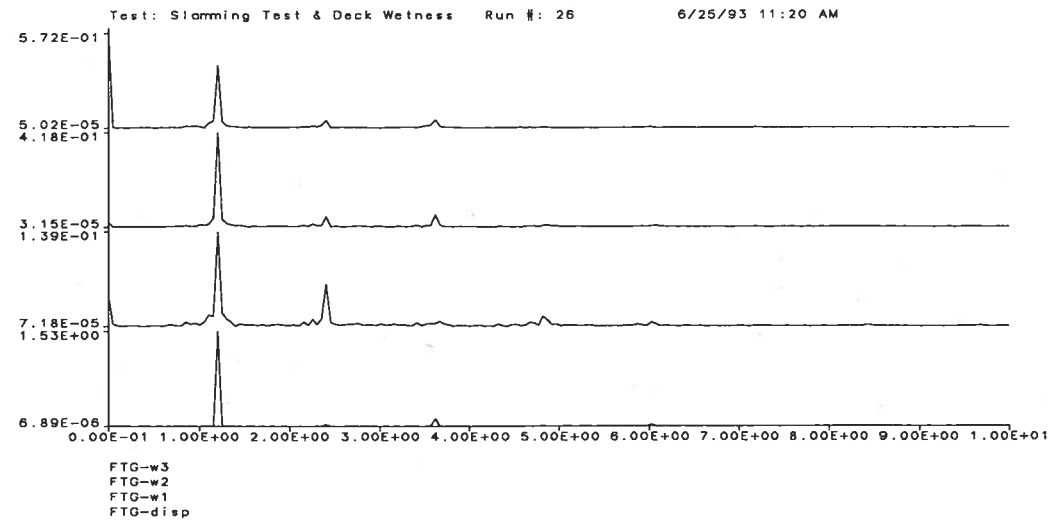

(b) Gains of the FFT Analyses

Figure B.75: Run 26, $f_1 = 1.205\,Hz$, $A_1 = 1.529\,in$, $\alpha = 6$

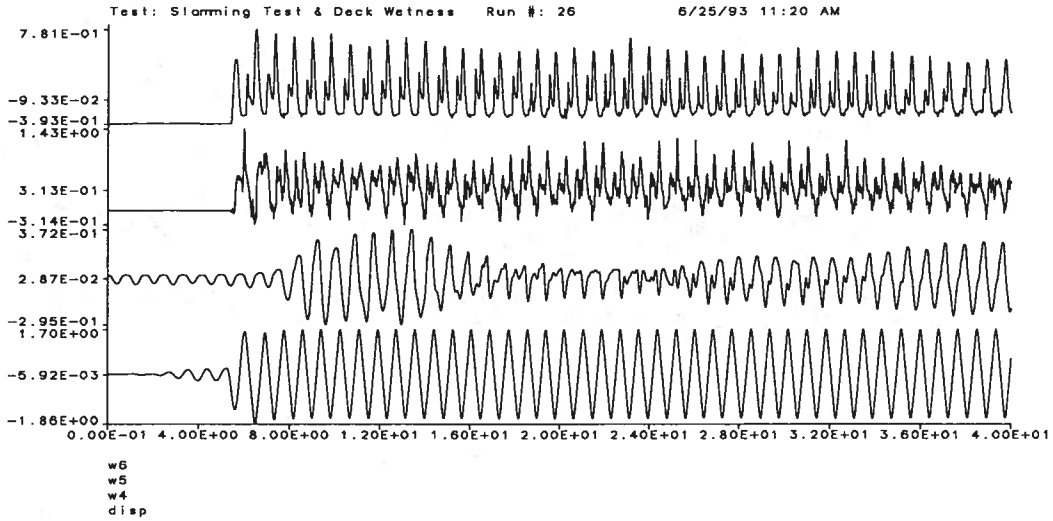

(a) Time-History Acquisitions

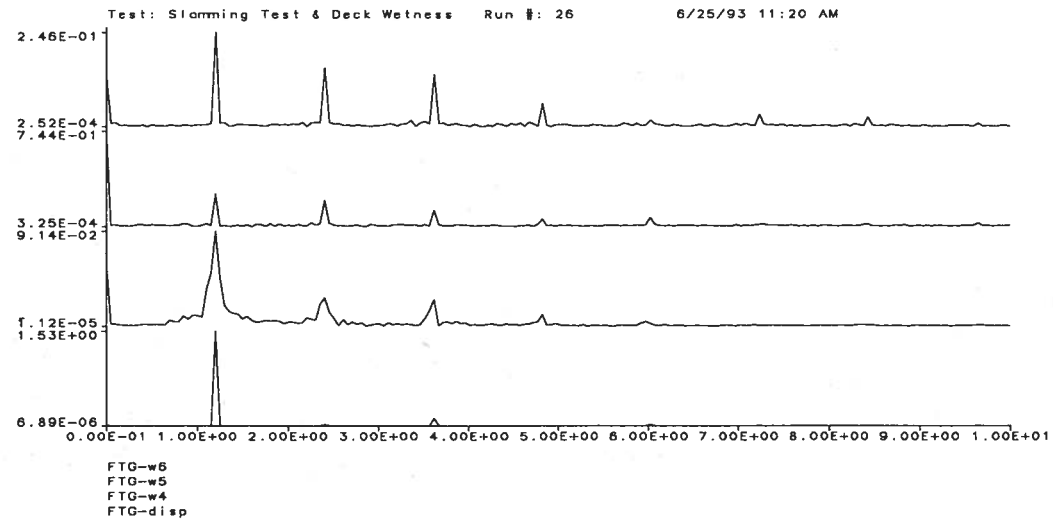

(b) Gains of the FFT Analyses

Figure B.76: Run 26, $f_1 = 1.205\,Hz$, $A_1 = 1.529\,in$, $\alpha = 6$

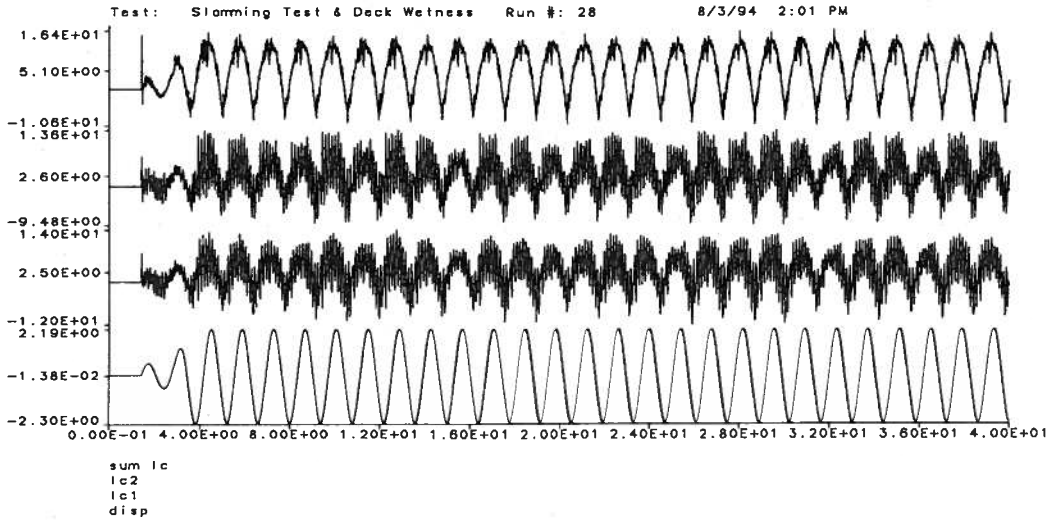

(a) Time-History Acquisitions

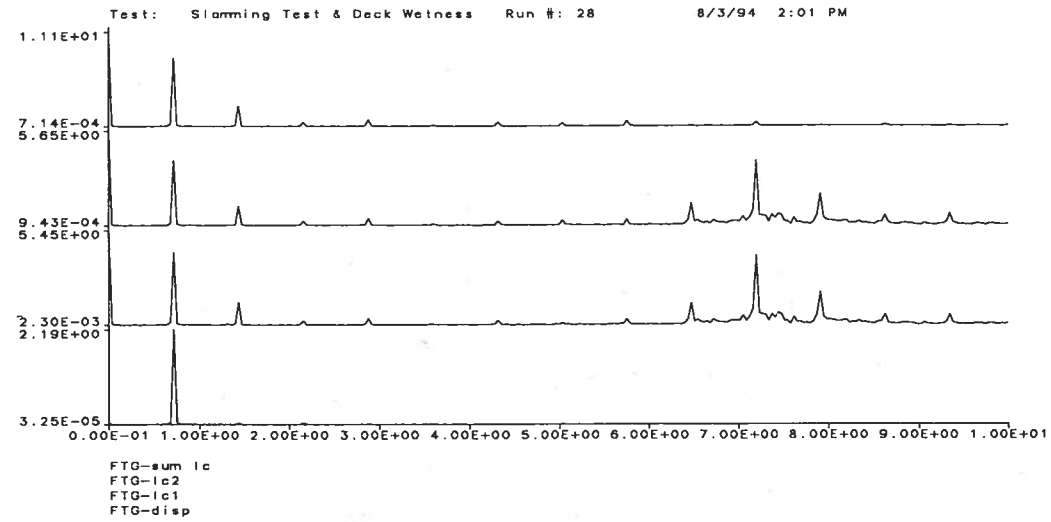

(b) Gains of the FFT Analyses

Figure B.77: Run 28, $f_1 = 0.719\,Hz$, $A_1 = 2.189\,in$, $\alpha = 6$

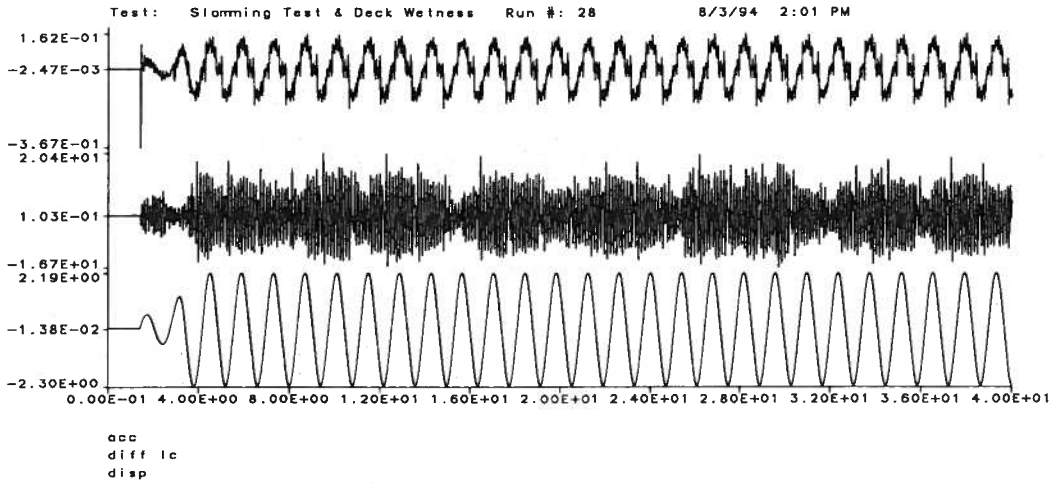

(a) Time-History Acquisitions

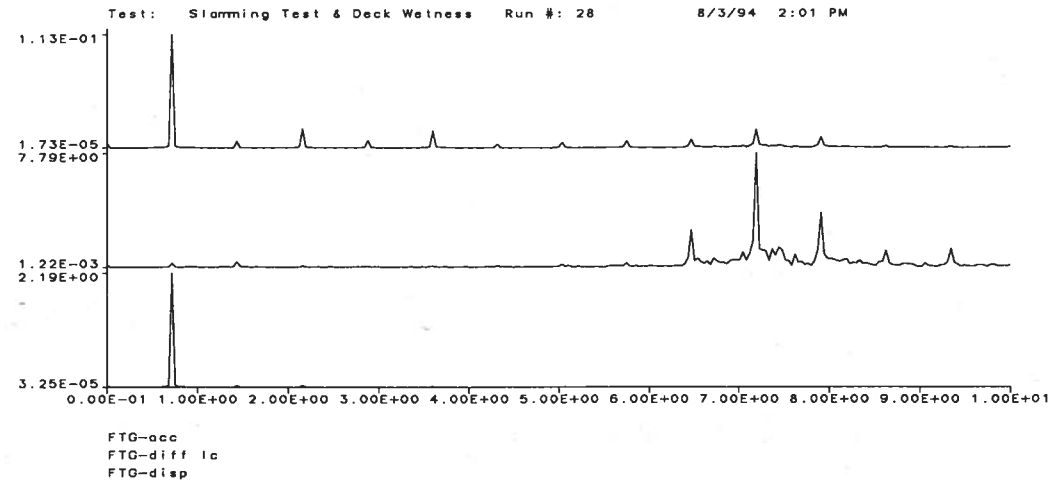

(b) Gains of the FFT Analyses

Figure B.78: Run 28, $f_1 = 0.719\,Hz$, $A_1 = 2.189\,in$, $\alpha = 6$

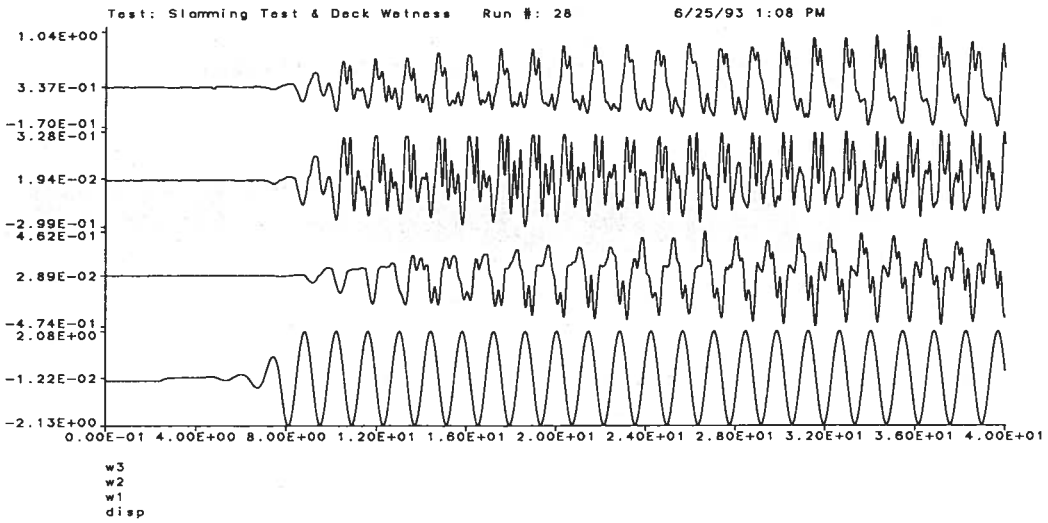

(a) Time-History Acquisitions

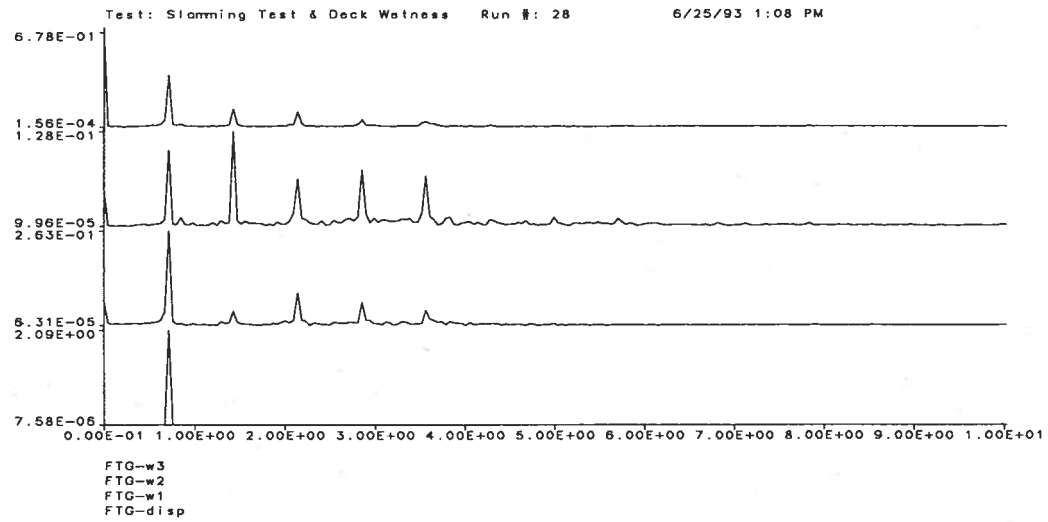

(b) Gains of the FFT Analyses

Figure B.79: Run 28, $f_1 = 0.713\,Hz$, $A_1 = 2.089\,in$, $\alpha = 6$

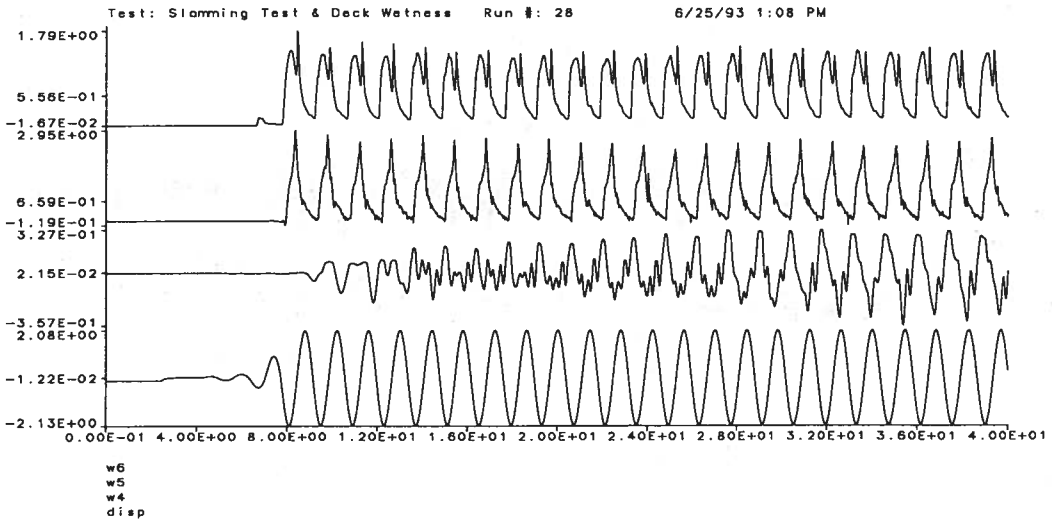

(a) Time-History Acquisitions

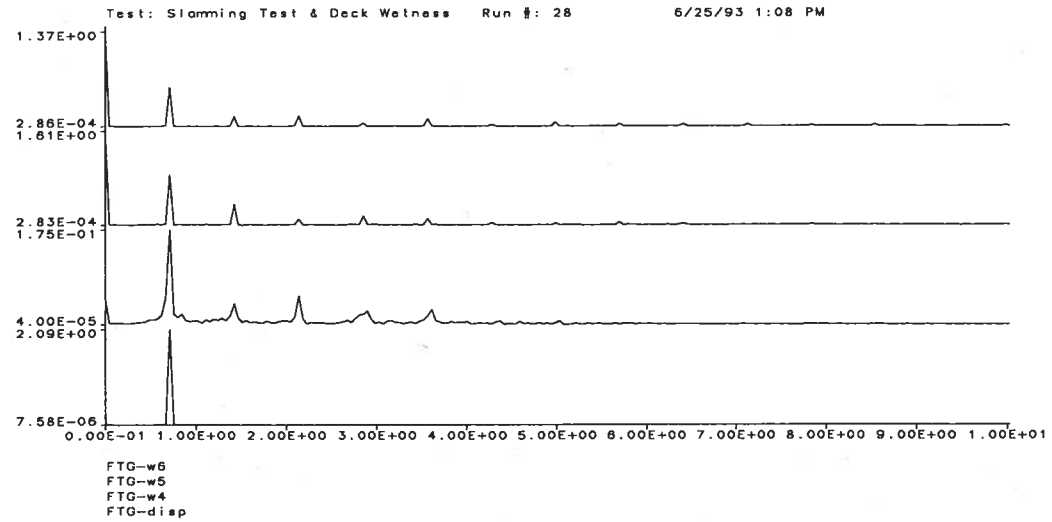

(b) Gains of the FFT Analyses

Figure B.80: Run 28, $f_1 = 0.713\,Hz$, $A_1 = 2.089\,in$, $\alpha = 6$

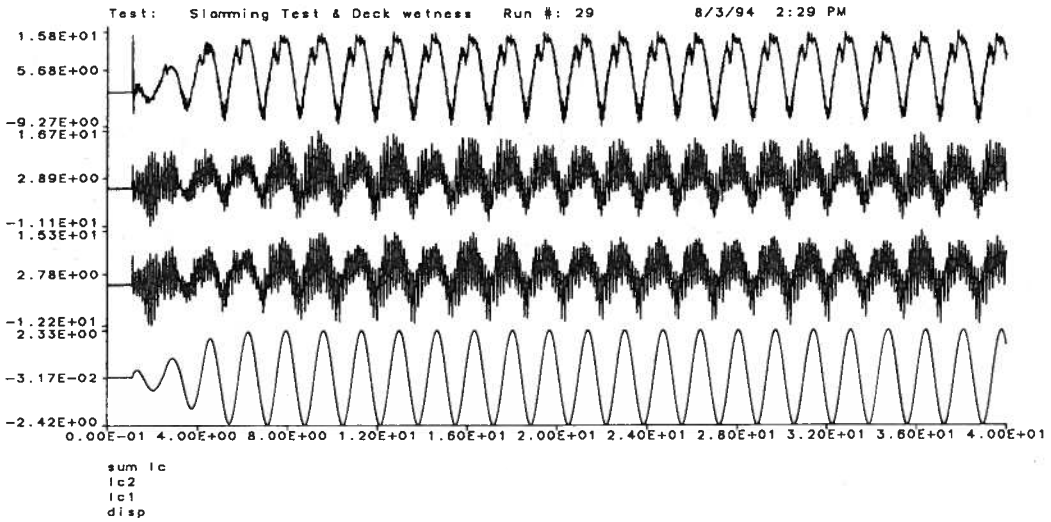

(a) Time-History Acquisitions

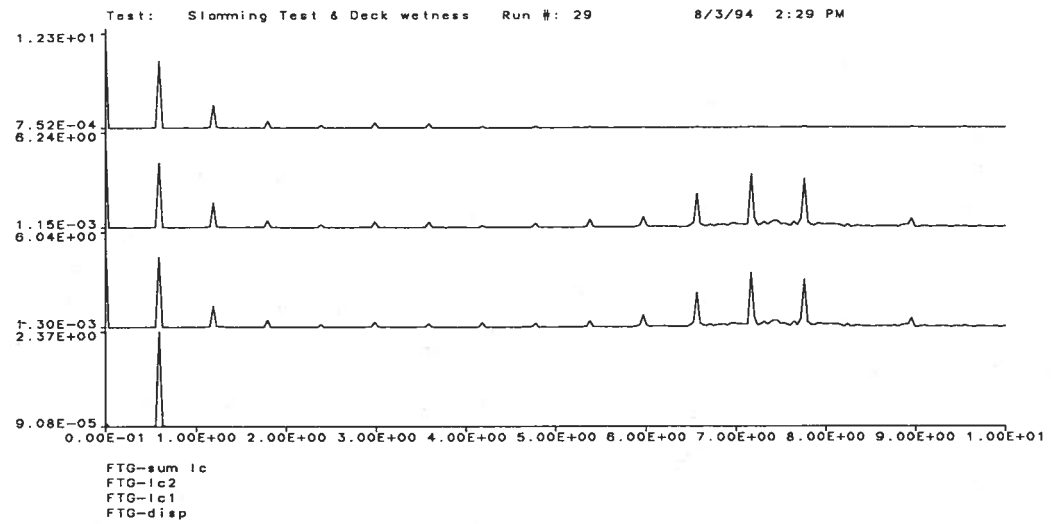

(b) Gains of the FFT Analyses

Figure B.81: Run 29, $f_1 = 0.597\,Hz$, $A_1 = 2.372\,in$, $\alpha = 6$

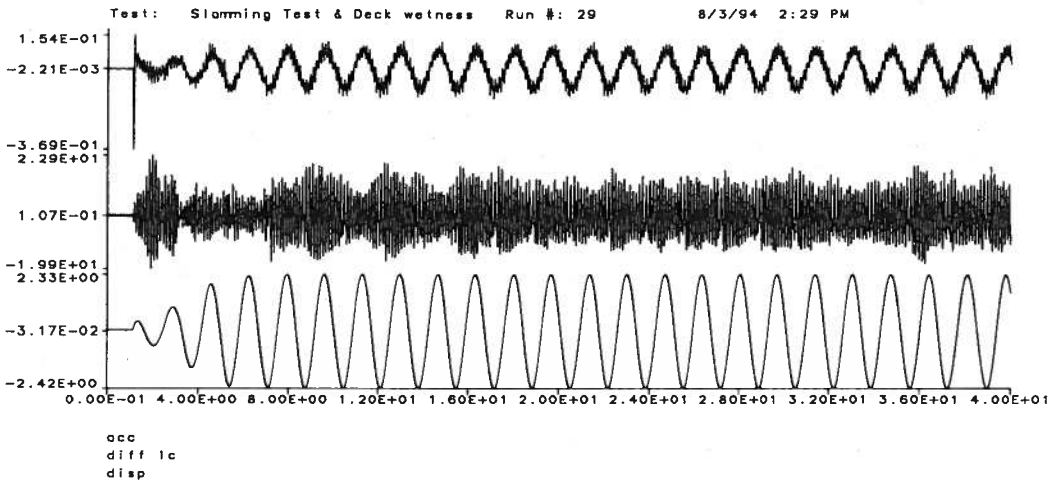

(a) Time-History Acquisitions

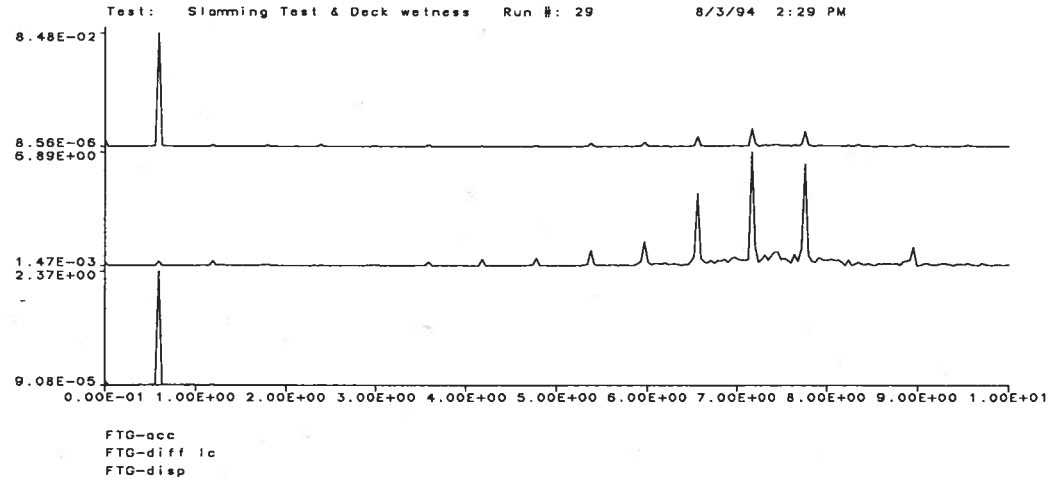

(b) Gains of the FFT Analyses

Figure B.82: Run 29, $f_1 = 0.597\,Hz$, $A_1 = 2.372\,in$, $\alpha = 6$

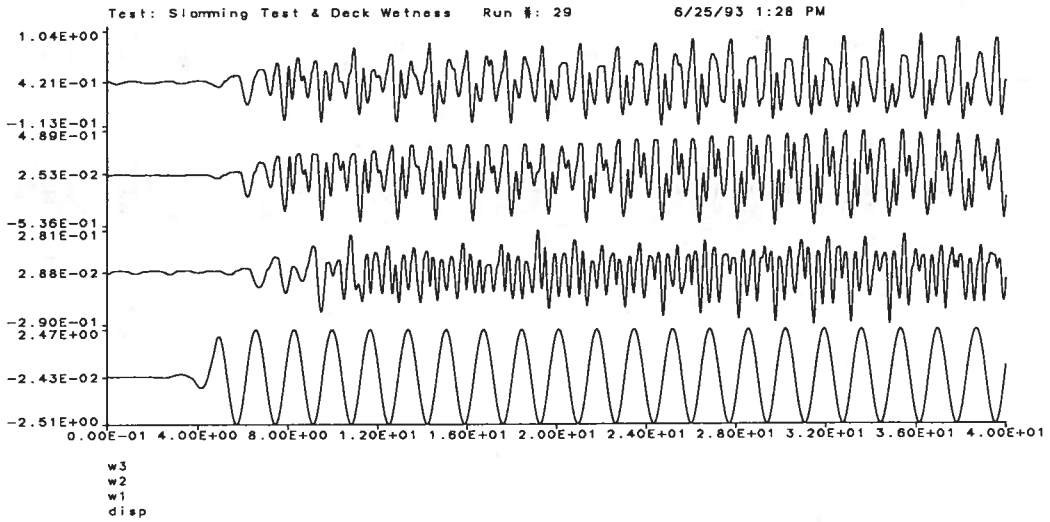

(a) Time-History Acquisitions

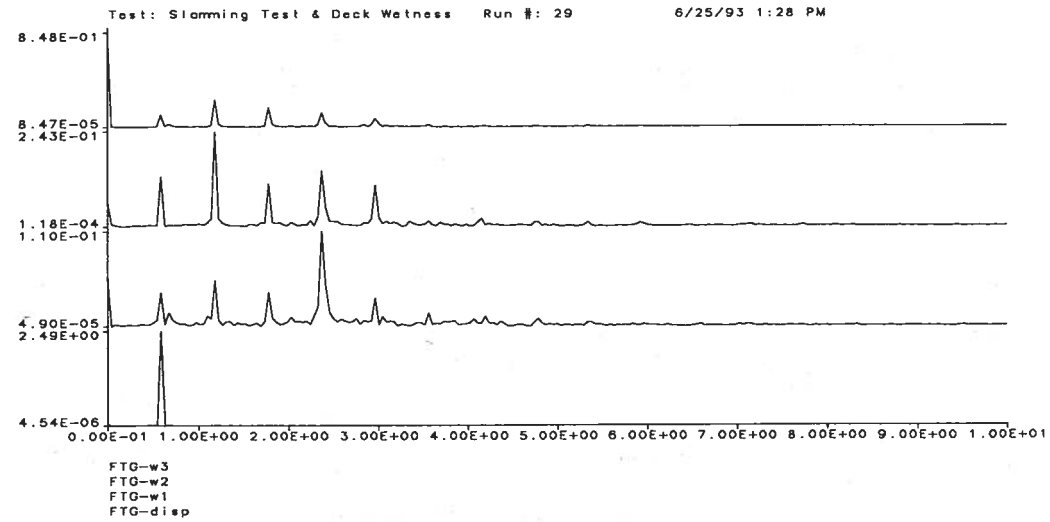

(b) Gains of the FFT Analyses

Figure B.83: Run 29, $f_1 = 0.593\,Hz$, $A_1 = 2.493\,in$, $\alpha = 6$

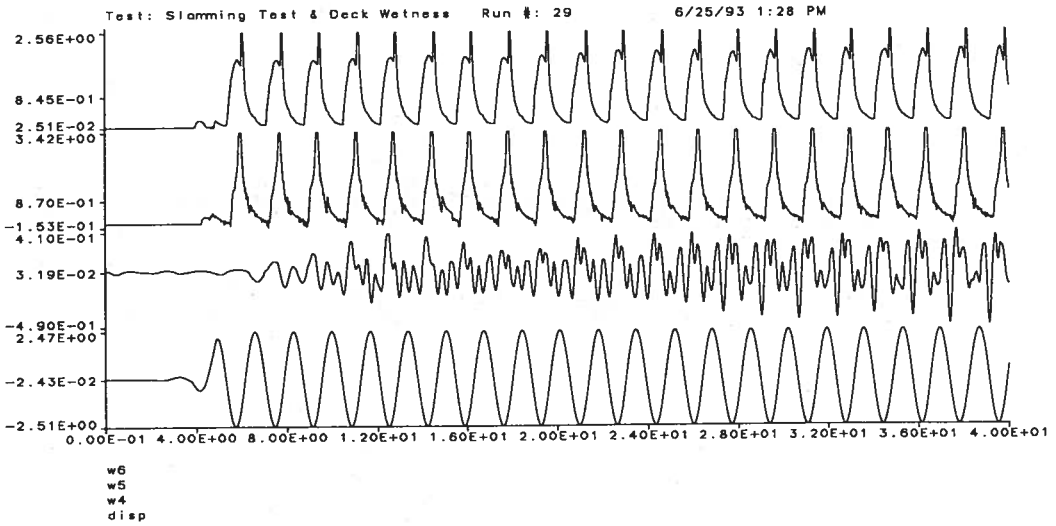

(a) Time-History Acquisitions

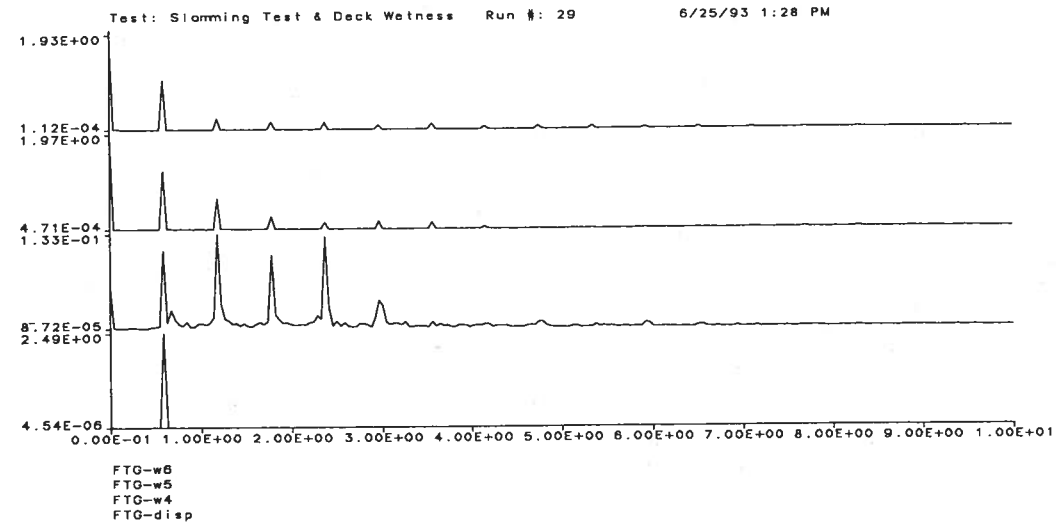

(b) Gains of the FFT Analyses

Figure B.84: Run 29, $f_1 = 0.593\,Hz$, $A_1 = 2.493\,in$, $\alpha = 6$

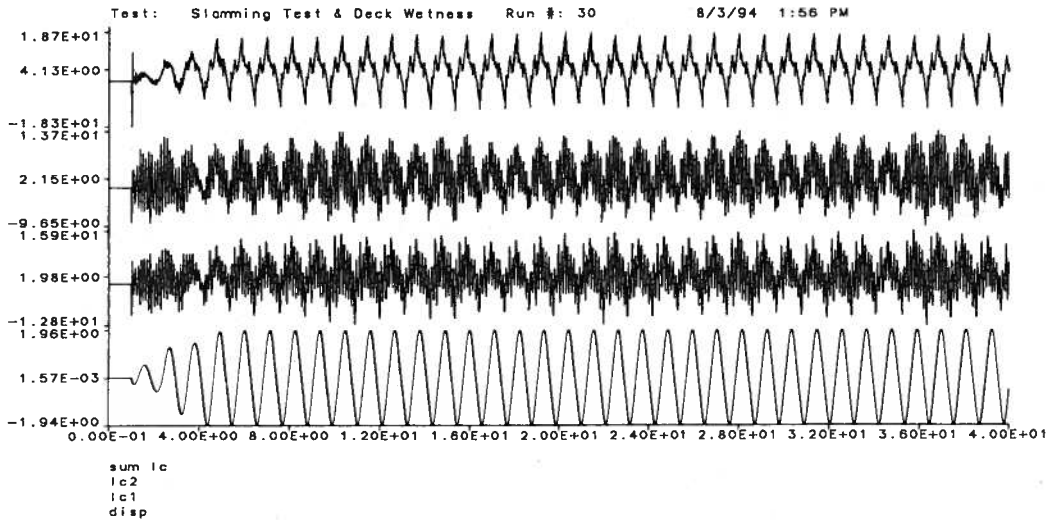

(a) Time-History Acquisitions

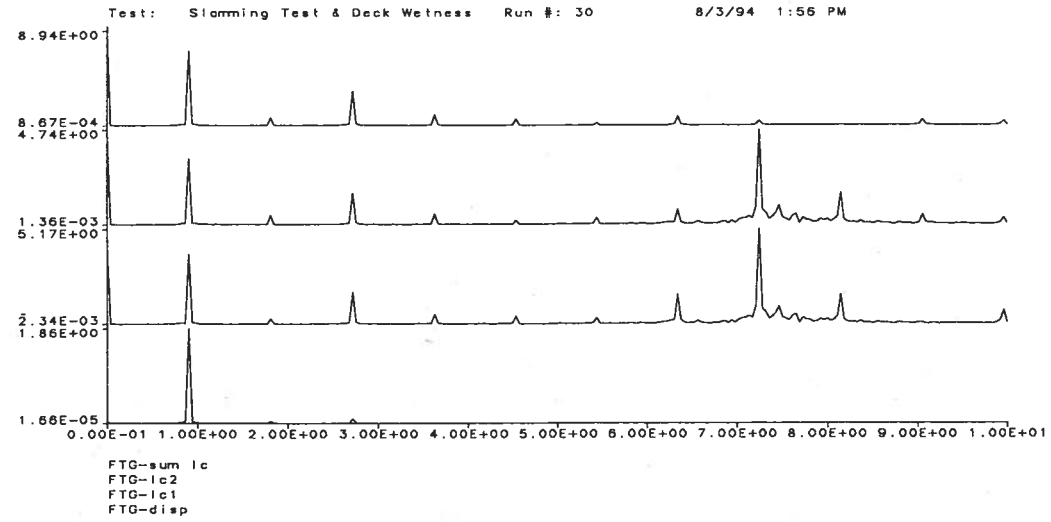

(b) Gains of the FFT Analyses

Figure B.85: Run 30, $f_1 = 0.905\,Hz$, $A_1 = 1.858\,in$, $\alpha = 6$

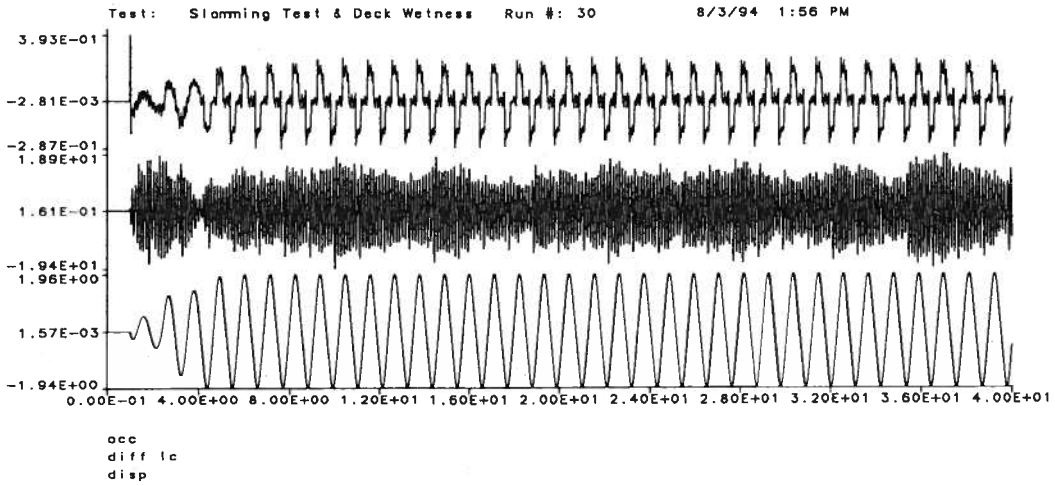

(a) Time-History Acquisitions

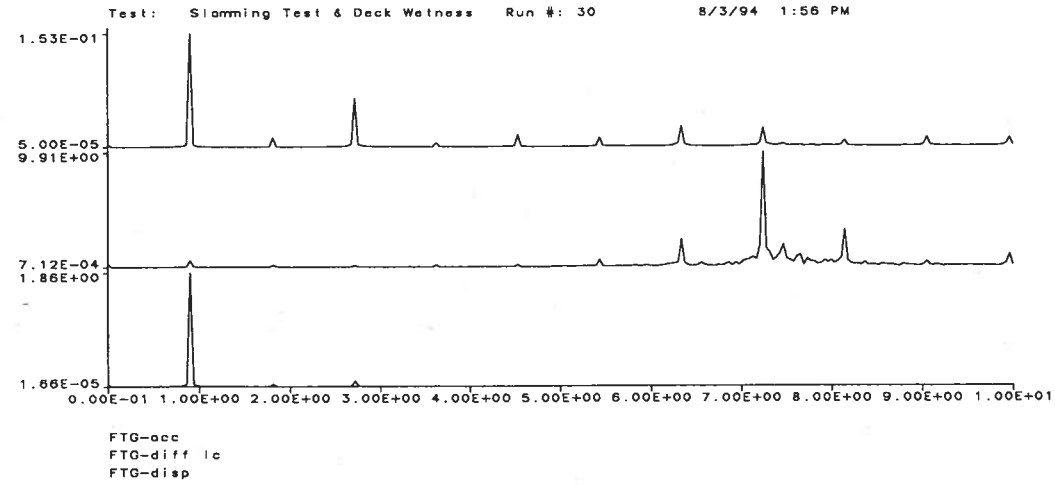

(b) Gains of the FFT Analyses

Figure B.86: Run 30, $f_1 = 0.905\,Hz$, $A_1 = 1.858\,in$, $\alpha = 6$

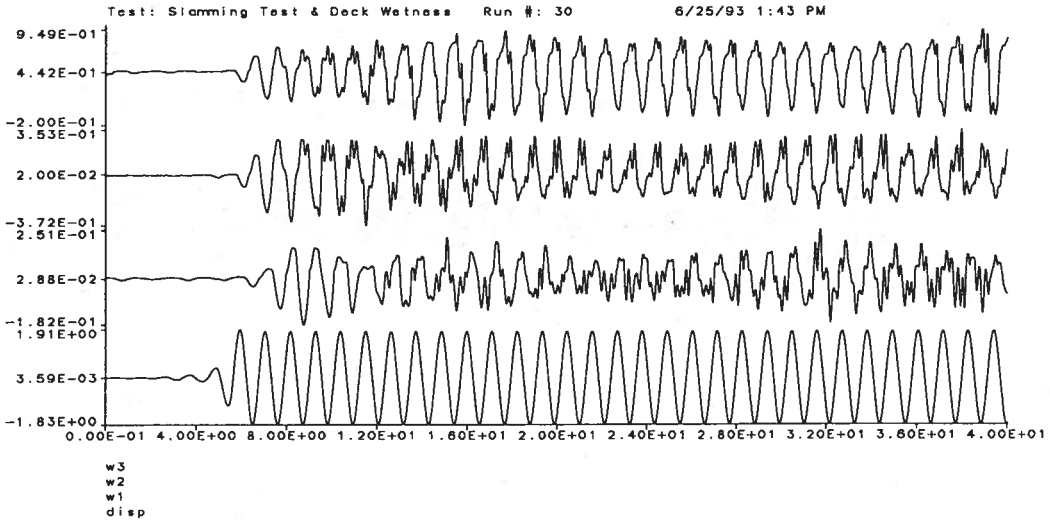

(a) Time-History Acquisitions

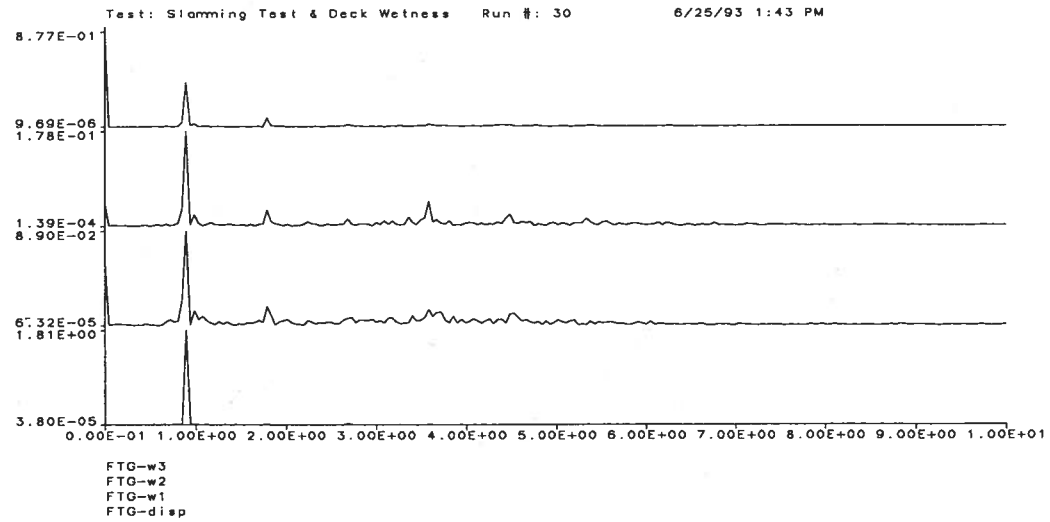

(b) Gains of the FFT Analyses

Figure B.87: Run 30, $f_1 = 0.896\,Hz$, $A_1 = 1.810\,in$, $\alpha = 6$

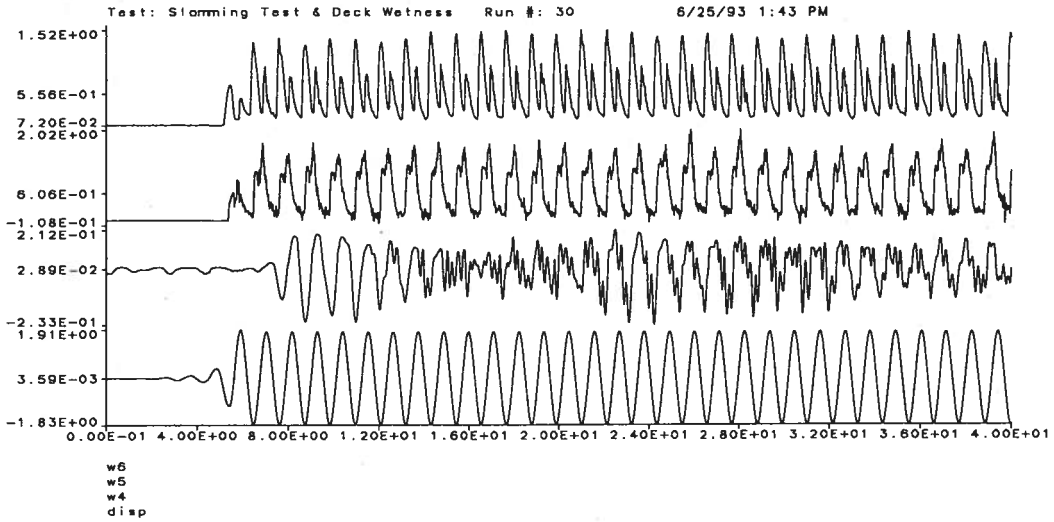

(a) Time-History Acquisitions

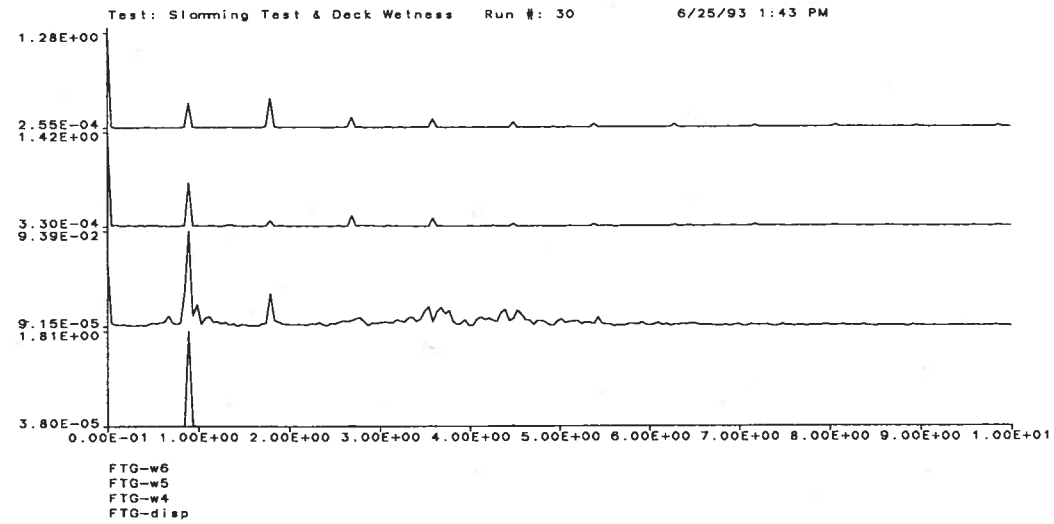

(b) Gains of the FFT Analyses

Figure B.88: Run 30, $f_1 = 0.896\,Hz$, $A_1 = 1.810\,in$, $\alpha = 6$

Appendix C

Tables of Fourier Coefficients

Table C.1: Run 06, Nondimensional Fourier Coefficients: Gain and Phase

j	$\omega(j)$	$A(j)$	$\phi_A(j)$	$F_{hy}(j)$	$\phi_{hy}(j)$
0	.00000E+00	.48202E-02	.31416E+01	.50215E-02	.00000E+00
1	.11455E+01	.62585E-01	-.24928E+01	.25074E-01	.40721E+00
2	.22910E+01	.31106E-03	-.22239E+01	.16795E-02	.64201E+00
3	.34365E+01	.13747E-03	.10606E+01	.69292E-03	.33300E+00
4	.45820E+01	.11005E-03	.28877E+01	.37624E-04	.20536E+01
5	.57274E+01	.76090E-04	.28662E+01	.70011E-03	.19485E+01
6	.68729E+01	.37675E-04	.80989E+00	.13470E-03	-.75459E+00
j	$\omega(j)$	$F_{dy}(j)$	$\phi_{dy}(j)$	$F_{st}(j)$	$\phi_{st}(j)$
0	.00000E+00	.25752E-02	.31416E+01	.75967E-02	.00000E+00
1	.11455E+01	.82588E-02	-.16817E+01	.30034E-01	.64843E+00
2	.22910E+01	.16976E-02	-.12310E+01	.27202E-02	.12802E+01
3	.34365E+01	.73160E-03	.38183E+00	.52003E-04	-.20518E+01
4	.45820E+01	.14048E-03	.24893E+01	.10755E-03	-.50408E+00
5	.57274E+01	.72302E-03	.19983E+01	.42173E-04	-.17165E+00
6	.68729E+01	.12660E-03	-.71978E+00	.92893E-05	-.12488E+01
j	$\omega(j)$	$F_{lc}(j)$	$\phi_{lc}(j)$	$F_{in}(j)$	$\phi_{in}(j)$
0	.00000E+00	.55035E-02	.31416E+01	.48205E-03	.31416E+01
1	.11455E+01	.12761E-01	-.29936E+01	.13153E-01	.65855E+00
2	.22910E+01	.15569E-02	-.25673E+01	.16433E-03	.13377E+01
3	.34365E+01	.78257E-03	-.30018E+01	.16799E-03	.23671E+01
4	.45820E+01	.82483E-04	-.21884E+01	.73524E-04	-.26620E+01
5	.57274E+01	.67301E-03	-.12843E+01	.68198E-04	.30655E+01
6	.68729E+01	.22391E-03	.24793E+01	.90635E-04	.26167E+01

Table C.2: Run 07, Nondimensional Fourier Coefficients: Gain and Phase

j	$\omega(j)$	$A(j)$	$\phi_A(j)$	$F_{hy}(j)$	$\phi_{hy}(j)$
0	.00000E+00	.93139E-02	.31416E+01	.10530E-01	.00000E+00
1	.75453E+00	.57902E-01	-.24848E+01	.25380E-01	.54775E+00
2	.15091E+01	.25362E-03	-.20924E+01	.14069E-02	.10576E+01
3	.22636E+01	.11947E-03	.12529E+00	.65603E-03	.48061E+00
4	.30181E+01	.83265E-04	.24726E+01	.30020E-04	-.90723E+00
5	.37727E+01	.24757E-04	.76313E+00	.48769E-03	.18289E+01
6	.45272E+01	.10654E-05	.22365E+01	.14401E-03	.11996E-01
j	$\omega(j)$	$F_{dy}(j)$	$\phi_{dy}(j)$	$F_{st}(j)$	$\phi_{st}(j)$
0	.00000E+00	.15043E-02	.00000E+00	.90254E-02	.00000E+00
1	.75453E+00	.39980E-02	-.17236E+01	.28124E-01	.65664E+00
2	.15091E+01	.10518E-02	-.15060E+01	.23589E-02	.13037E+01
3	.22636E+01	.70682E-03	.45784E+00	.53097E-04	-.29689E+01
4	.30181E+01	.42856E-04	.25252E+01	.72131E-04	-.73600E+00
5	.37727E+01	.49547E-03	.18224E+01	.84033E-05	-.17044E+01
6	.45272E+01	.13595E-03	.10125E-01	.80651E-05	.43539E-01
j	$\omega(j)$	$F_{lc}(j)$	$\phi_{lc}(j)$	$F_{in}(j)$	$\phi_{in}(j)$
0	.00000E+00	.10950E-01	.31416E+01	.42049E-03	.31416E+01
1	.75453E+00	.20158E-01	-.26220E+01	.52606E-02	.65599E+00
2	.15091E+01	.13623E-02	-.21233E+01	.70406E-04	.19225E+01
3	.22636E+01	.67916E-03	-.27680E+01	.75079E-04	.23106E+01
4	.30181E+01	.69433E-04	-.31166E+01	.56899E-04	-.26791E+01
5	.37727E+01	.43332E-03	-.13466E+01	.56561E-04	.20919E+01
6	.45272E+01	.12363E-03	.29344E+01	.35594E-04	.86778E+00

Table C.3: Run 08, Nondimensional Fourier Coefficients: Gain and Phase

j	$\omega(j)$	$A(j)$	$\phi_A(j)$	$F_{hy}(j)$	$\phi_{hy}(j)$
0	.00000E+00	.10315E-02	.00000E+00	.13226E-01	.00000E+00
1	.11295E+01	.12013E+00	.15640E+01	.47964E-01	-.18010E+01
2	.22591E+01	.21482E-02	.12333E+01	.61427E-02	.24950E+01
3	.33886E+01	.48016E-02	-.16412E+01	.16226E-02	-.10966E+01
4	.45182E+01	.64822E-04	.13839E+01	.79427E-03	.24870E+01
5	.56477E+01	.52920E-03	-.11141E+01	.55868E-03	-.91457E+00
6	.67773E+01	.25729E-03	-.10208E+01	.65478E-03	-.19182E+01
j	$\omega(j)$	$F_{dy}(j)$	$\phi_{dy}(j)$	$F_{st}(j)$	$\phi_{st}(j)$
0	.00000E+00	.41483E-02	.31416E+01	.17374E-01	.00000E+00
1	.11295E+01	.14934E-01	.23826E+01	.56977E-01	-.15727E+01
2	.22591E+01	.65155E-02	.76344E+00	.96437E-02	-.30581E+01
3	.33886E+01	.39887E-02	-.13579E+01	.24572E-02	.16123E+01
4	.45182E+01	.11124E-02	.25892E+01	.33234E-03	-.30599E+00
5	.56477E+01	.80625E-03	-.90979E+00	.24759E-03	.22426E+01
6	.67773E+01	.78500E-03	-.18890E+01	.13189E-03	.13982E+01
j	$\omega(j)$	$F_{lc}(j)$	$\phi_{lc}(j)$	$F_{in}(j)$	$\phi_{in}(j)$
0	.00000E+00	.14627E-01	.31416E+01	.14013E-02	.31416E+01
1	.11295E+01	.24452E-01	.11041E+01	.24861E-01	-.15685E+01
2	.22591E+01	.69430E-02	-.89073E+00	.17806E-02	-.18771E+01
3	.33886E+01	.11197E-01	.16097E+01	.97500E-02	.15395E+01
4	.45182E+01	.16259E-02	-.39118E+00	.88357E-03	-.15488E+00
5	.56477E+01	.37019E-02	.21202E+01	.31469E-02	.21013E+01
6	.67773E+01	.23484E-02	.18013E+01	.18351E-02	.19975E+01

Table C.4: Run 09, Nondimensional Fourier Coefficients: Gain and Phase

j	$\omega(j)$	$A(j)$	$\phi_A(j)$	$F_{hy}(j)$	$\phi_{hy}(j)$
0	.00000E+00	.12808E-01	.31416E+01	.24836E-01	.00000E+00
1	.75453E+00	.13186E+00	.16592E+01	.58077E-01	-.15550E+01
2	.15091E+01	.48557E-03	.36643E+00	.73185E-02	.30497E+01
3	.22636E+01	.35698E-03	.10492E+01	.34637E-03	-.97699E+00
4	.30181E+01	.84560E-04	.69273E+00	.24073E-03	-.29870E+01
5	.37727E+01	.22447E-03	.17031E+01	.26396E-03	-.27434E+01
6	.45272E+01	.14594E-03	.42956E+00	.23113E-03	.22675E+00
j	$\omega(j)$	$F_{dy}(j)$	$\phi_{dy}(j)$	$F_{st}(j)$	$\phi_{st}(j)$
0	.00000E+00	.25707E-02	.31416E+01	.27407E-01	.00000E+00
1	.75453E+00	.78712E-02	.22259E+01	.64565E-01	-.14822E+01
2	.15091E+01	.38974E-02	.72296E+00	.10387E-01	-.29569E+01
3	.22636E+01	.35171E-03	-.53618E+00	.15270E-03	-.23615E+01
4	.30181E+01	.14567E-03	.59418E+00	.37767E-03	-.28221E+01
5	.37727E+01	.26762E-03	.30018E+01	.14131E-03	-.14166E+01
6	.45272E+01	.37794E-03	.31222E+00	.14897E-03	-.26965E+01
j	$\omega(j)$	$F_{lc}(j)$	$\phi_{lc}(j)$	$F_{in}(j)$	$\phi_{in}(j)$
0	.00000E+00	.25491E-01	.31416E+01	.65491E-03	.31416E+01
1	.75453E+00	.45986E-01	.15656E+01	.12139E-01	-.14751E+01
2	.15091E+01	.71293E-02	-.99461E-01	.19701E-03	-.29543E+01
3	.22636E+01	.49438E-03	.23266E+01	.16244E-03	.26776E+01
4	.30181E+01	.36936E-03	.26360E+00	.13268E-03	.46237E+00
5	.37727E+01	.46598E-04	-.12373E+00	.22477E-03	-.26399E+01
6	.45272E+01	.27605E-03	.29721E+01	.10911E-03	.20149E+01

Table C.5: Run 10, Nondimensional Fourier Coefficients: Gain and Phase

j	$\omega(j)$	$A(j)$	$\phi_A(j)$	$F_{hy}(j)$	$\phi_{hy}(j)$
0	.00000E+00	.91666E-02	.31416E+01	.77915E-02	.00000E+00
1	.15397E+01	.69752E-01	.21671E+01	.23898E-01	-.14971E+01
2	.30795E+01	.42090E-03	.11070E+01	.85197E-03	.31085E+01
3	.46192E+01	.31306E-03	.26143E+01	.23504E-03	.69417E+00
4	.61589E+01	.31580E-04	.17427E+01	.52671E-04	.28138E+00
5	.76987E+01	.13785E-03	.84475E+00	.36377E-03	-.10968E+01
6	.92384E+01	.16248E-03	-.29547E+01	.83963E-03	-.25679E+01
j	$\omega(j)$	$F_{dy}(j)$	$\phi_{dy}(j)$	$F_{st}(j)$	$\phi_{st}(j)$
0	.00000E+00	.31386E-02	.31416E+01	.10930E-01	.00000E+00
1	.15397E+01	.17755E-01	.29035E+01	.33863E-01	-.97460E+00
2	.30795E+01	.31509E-02	.14503E+01	.33351E-02	-.19486E+01
3	.46192E+01	.23673E-03	.13016E+01	.14111E-03	-.58434E+00
4	.61589E+01	.10909E-03	.15676E+01	.10700E-03	-.10819E+01
5	.76987E+01	.35391E-03	-.94782E+00	.54296E-04	-.24109E+01
6	.92384E+01	.90414E-03	-.25902E+01	.67385E-04	.26940E+00
j	$\omega(j)$	$F_{lc}(j)$	$\phi_{lc}(j)$	$F_{in}(j)$	$\phi_{in}(j)$
0	.00000E+00	.85180E-02	.31416E+01	.72650E-03	.31416E+01
1	.15397E+01	.13690E-01	.15539E+00	.26555E-01	-.95743E+00
2	.30795E+01	.76758E-03	-.39183E+00	.30064E-03	-.20631E+01
3	.46192E+01	.44541E-03	-.21208E+01	.23521E-03	-.17945E+01
4	.61589E+01	.17700E-03	.22057E+01	.16628E-03	.19040E+01
5	.76987E+01	.34198E-03	-.26574E+01	.50180E-03	-.18466E+01
6	.92384E+01	.40684E-03	-.57205E+00	.76731E-03	-.20638E+01

Table C.6: Run 11, Nondimensional Fourier Coefficients: Gain and Phase

j	$\omega(j)$	$A(j)$	$\phi_A(j)$	$F_{hy}(j)$	$\phi_{hy}(j)$
0	.00000E+00	.10304E-01	.31416E+01	.76423E-02	.00000E+00
1	.90724E+00	.58213E-01	.11278E+01	.24745E-01	-.22138E+01
2	.18145E+01	.18129E-03	-.95503E+00	.17395E-02	.17806E+01
3	.27217E+01	.10808E-03	-.95553E+00	.55727E-03	-.14373E+01
4	.36290E+01	.70129E-04	-.19434E+01	.15614E-03	-.13595E+01
5	.45362E+01	.50248E-04	.94480E+00	.37745E-03	.98725E+00
6	.54435E+01	.13997E-04	.22071E+01	.16215E-03	.16128E+01
j	$\omega(j)$	$F_{dy}(j)$	$\phi_{dy}(j)$	$F_{st}(j)$	$\phi_{st}(j)$
0	.00000E+00	.19098E-02	.31416E+01	.95521E-02	.00000E+00
1	.90724E+00	.63955E-02	.20041E+01	.28345E-01	-.20139E+01
2	.18145E+01	.11278E-02	-.10133E+00	.23450E-02	.22562E+01
3	.27217E+01	.60367E-03	-.13806E+01	.56875E-04	.23499E+01
4	.36290E+01	.21943E-03	-.15632E+01	.73633E-04	.11351E+01
5	.45362E+01	.40203E-03	.99926E+00	.25015E-04	-.19602E+01
6	.54435E+01	.16373E-03	.15845E+01	.48764E-05	-.27843E+01
j	$\omega(j)$	$F_{lc}(j)$	$\phi_{lc}(j)$	$F_{in}(j)$	$\phi_{in}(j)$
0	.00000E+00	.81063E-02	.31416E+01	.46406E-03	.31416E+01
1	.90724E+00	.17337E-01	.83828E+00	.76363E-02	-.20094E+01
2	.18145E+01	.16663E-02	-.14315E+01	.14054E-03	.27692E+01
3	.27217E+01	.60821E-03	.15946E+01	.81658E-04	.75103E+00
4	.36290E+01	.13051E-03	.13022E+01	.72524E-04	-.37908E+00
5	.45362E+01	.31200E-03	-.22783E+01	.78044E-04	.15041E+01
6	.54435E+01	.25008E-03	-.18210E+01	.10569E-03	-.22788E+01

Table C.7: Run 12, Nondimensional Fourier Coefficients: Gain and Phase

j	$\omega(j)$	$A(j)$	$\phi_A(j)$	$F_{hy}(j)$	$\phi_{hy}(j)$
0	.00000E+00	.65297E-03	.00000E+00	.48637E-02	.00000E+00
1	.15413E+01	.87014E-01	-.23633E+01	.32052E-01	.26080E+00
2	.30826E+01	.16010E-02	-.39073E+00	.17701E-02	.31388E+00
3	.46239E+01	.31375E-02	-.90532E+00	.27284E-02	-.72586E+00
4	.61652E+01	.22577E-03	-.13888E+01	.18519E-02	-.96717E+00
5	.77065E+01	.49204E-03	-.21570E+01	.14634E-02	-.17734E+01
6	.92478E+01	.16394E-03	.64077E+00	.56197E-03	.42225E+00
j	$\omega(j)$	$F_{dy}(j)$	$\phi_{dy}(j)$	$F_{st}(j)$	$\phi_{st}(j)$
0	.00000E+00	.46875E-02	.31416E+01	.95512E-02	.00000E+00
1	.15413E+01	.20852E-01	-.14877E+01	.41213E-01	.78208E+00
2	.30826E+01	.53546E-02	-.11314E+01	.54251E-02	.16806E+01
3	.46239E+01	.42924E-02	-.75864E+00	.15680E-02	.23259E+01
4	.61652E+01	.20811E-02	-.93722E+00	.23662E-03	.24409E+01
5	.77065E+01	.16857E-02	-.18001E+01	.22624E-03	.11680E+01
6	.92478E+01	.60672E-03	.35160E+00	.60865E-04	.27833E+01
j	$\omega(j)$	$F_{lc}(j)$	$\phi_{lc}(j)$	$F_{in}(j)$	$\phi_{in}(j)$
0	.00000E+00	.67705E-02	.31416E+01	.19068E-02	.31416E+01
1	.15413E+01	.17246E-01	.20171E+01	.33480E-01	.79166E+00
2	.30826E+01	.40476E-02	-.30963E+01	.23876E-02	.29888E+01
3	.46239E+01	.13892E-01	.23271E+01	.11177E-01	.23055E+01
4	.61652E+01	.34921E-02	.22730E+01	.16592E-02	.23831E+01
5	.77065E+01	.57351E-02	.12043E+01	.42979E-02	.11488E+01
6	.92478E+01	.24217E-02	-.29442E+01	.18781E-02	-.30110E+01

Table C.8: Run 13, Nondimensional Fourier Coefficients: Gain and Phase

j	$\omega(j)$	$A(j)$	$\phi_A(j)$	$F_{hy}(j)$	$\phi_{hy}(j)$
0	.00000E+00	.10626E-01	.31416E+01	.21768E-01	.00000E+00
1	.90877E+00	.12812E+00	.29189E+01	.54880E-01	-.39467E+00
2	.18175E+01	.61804E-03	.28338E+01	.75391E-02	-.10228E+01
3	.27263E+01	.18054E-03	-.17615E+01	.37520E-03	-.30452E+01
4	.36351E+01	.13004E-03	-.55017E+00	.17087E-03	.98205E+00
5	.45438E+01	.98900E-04	.19755E+01	.32811E-03	-.23604E+01
6	.54526E+01	.11562E-03	.19735E+01	.24007E-03	.26083E+01
j	$\omega(j)$	$F_{dy}(j)$	$\phi_{dy}(j)$	$F_{st}(j)$	$\phi_{st}(j)$
0	.00000E+00	.34968E-02	.31416E+01	.25264E-01	.00000E+00
1	.90877E+00	.12590E-01	-.25210E+01	.62442E-01	-.22252E+00
2	.18175E+01	.55488E-02	-.27343E+01	.99678E-02	-.43906E+00
3	.27263E+01	.46000E-03	-.29674E+01	.90753E-04	.50165E+00
4	.36351E+01	.35279E-03	-.41350E+00	.36420E-03	.22479E+01
5	.45438E+01	.30762E-03	-.25546E+01	.64915E-04	-.12064E+01
6	.54526E+01	.34706E-03	.23633E+01	.12814E-03	-.12498E+01
j	$\omega(j)$	$F_{lc}(j)$	$\phi_{lc}(j)$	$F_{in}(j)$	$\phi_{in}(j)$
0	.00000E+00	.22576E-01	.31416E+01	.80833E-03	.31416E+01
1	.90877E+00	.38189E-01	.26652E+01	.17104E-01	-.21148E+00
2	.18175E+01	.73003E-02	.20876E+01	.33262E-03	-.26855E+00
3	.27263E+01	.64354E-03	-.15815E+00	.29591E-03	-.48308E+00
4	.36351E+01	.33804E-03	-.20100E+01	.17098E-03	-.18606E+01
5	.45438E+01	.36431E-03	.17352E+01	.31953E-03	.27282E+01
6	.54526E+01	.41059E-03	-.45208E+00	.17242E-03	-.33886E+00

Table C.9: Run 14, Nondimensional Fourier Coefficients: Gain and Phase

j	$\omega(j)$	$A(j)$	$\phi_A(j)$	$F_{hy}(j)$	$\phi_{hy}(j)$
0	.00000E+00	.16463E-01	.00000E+00	.44495E-04	.00000E+00
1	.15320E+01	.94363E-01	.20400E+01	.29805E-01	-.15946E+01
2	.30639E+01	.18781E-02	.25118E+01	.26601E-02	.27302E+01
3	.45959E+01	.75681E-02	-.17991E+00	.65289E-02	.97101E-01
4	.61278E+01	.43646E-03	.97797E+00	.23291E-02	-.15914E+01
5	.76598E+01	.15599E-02	-.25662E+01	.45387E-02	-.26087E+01
6	.91917E+01	.14302E-03	.31245E+01	.28182E-02	.23368E+01
j	$\omega(j)$	$F_{dy}(j)$	$\phi_{dy}(j)$	$F_{st}(j)$	$\phi_{st}(j)$
0	.00000E+00	.37505E-02	.31416E+01	.37950E-02	.00000E+00
1	.15320E+01	.21935E-01	.27509E+01	.42878E-01	-.10968E+01
2	.30639E+01	.67334E-02	.14746E+01	.64273E-02	-.20714E+01
3	.45959E+01	.10026E-01	.23978E-01	.35468E-02	.30307E+01
4	.61278E+01	.30256E-02	-.14763E+01	.76051E-03	.20249E+01
5	.76598E+01	.52362E-02	-.25943E+01	.70103E-03	.64033E+00
6	.91917E+01	.30699E-02	.23676E+01	.26754E-03	-.44329E+00
j	$\omega(j)$	$F_{lc}(j)$	$\phi_{lc}(j)$	$F_{in}(j)$	$\phi_{in}(j)$
0	.00000E+00	.14593E-02	.31416E+01	.14148E-02	.31416E+01
1	.15320E+01	.17590E-01	-.11349E+00	.35939E-01	-.10855E+01
2	.30639E+01	.56520E-02	-.38024E+00	.29944E-02	-.35257E+00
3	.45959E+01	.33099E-01	.30528E+01	.26709E-01	.30076E+01
4	.61278E+01	.14132E-02	.27626E+01	.22612E-02	-.22167E+01
5	.76598E+01	.19654E-01	.62740E+00	.15142E-01	.65569E+00
6	.91917E+01	.31452E-02	-.44478E+00	.11150E-02	.65332E+00

Table C.10: Run 15, Nondimensional Fourier Coefficients: Gain and Phase

j	$\omega(j)$	$A(j)$	$\phi_A(j)$	$F_{hy}(j)$	$\phi_{hy}(j)$
0	.00000E+00	.11037E-01	.31416E+01	.10346E-01	.00000E+00
1	.90616E+00	.89360E-01	.13074E+01	.38122E-01	-.20220E+01
2	.18123E+01	.43880E-03	-.51646E+00	.39064E-02	.20378E+01
3	.27185E+01	.19795E-03	.62927E-02	.50830E-03	-.15227E+01
4	.36246E+01	.58617E-04	.14536E+01	.13948E-03	.61767E+00
5	.45308E+01	.14902E-03	.43583E+00	.32146E-03	.91975E+00
6	.54370E+01	.30375E-04	-.24332E+01	.12227E-03	.28396E+01
j	$\omega(j)$	$F_{dy}(j)$	$\phi_{dy}(j)$	$F_{st}(j)$	$\phi_{st}(j)$
0	.00000E+00	.53088E-02	.31416E+01	.15654E-01	.00000E+00
1	.90616E+00	.93870E-02	.21682E+01	.43571E-01	-.18341E+01
2	.18123E+01	.29023E-02	.30658E+00	.52254E-02	.26181E+01
3	.27185E+01	.53340E-03	-.13838E+01	.76474E-04	.29256E+01
4	.36246E+01	.15954E-03	-.11434E-01	.94462E-04	.20773E+01
5	.45308E+01	.40015E-03	.79308E+00	.90849E-04	-.28119E+01
6	.54370E+01	.12751E-03	-.30177E+01	.53037E-04	.13850E+01
j	$\omega(j)$	$F_{lc}(j)$	$\phi_{lc}(j)$	$F_{in}(j)$	$\phi_{in}(j)$
0	.00000E+00	.10816E-01	.31416E+01	.47045E-03	.31416E+01
1	.90616E+00	.26643E-01	.10330E+01	.11806E-01	-.18255E+01
2	.18123E+01	.38043E-02	-.11139E+01	.10929E-03	.23978E+01
3	.27185E+01	.60965E-03	.15480E+01	.10876E-03	.12106E+01
4	.36246E+01	.15383E-03	-.23249E+01	.32457E-04	-.13091E+01
5	.45308E+01	.19579E-03	-.29204E+01	.21278E-03	.15530E+01
6	.54370E+01	.19781E-03	-.58482E+00	.87343E-04	-.98621E+00

Table C.11: Run 16, Nondimensional Fourier Coefficients: Gain and Phase

j	$\omega(j)$	$A(j)$	$\phi_A(j)$	$F_{hy}(j)$	$\phi_{hy}(j)$
0	.00000E+00	.22607E-02	.00000E+00	.88742E-02	.00000E+00
1	.75604E+00	.10411E+00	-.27156E+01	.48745E-01	.34424E+00
2	.15121E+01	.70231E-03	-.25807E+01	.47351E-02	.55184E+00
3	.22681E+01	.12037E-03	-.52584E+00	.31237E-03	-.59290E+00
4	.30241E+01	.44843E-05	-.27033E+01	.49845E-04	.16858E+01
5	.37802E+01	.81083E-04	-.12459E+01	.33098E-03	.44885E+00
6	.45362E+01	.14812E-03	-.11204E+01	.15532E-03	-.20466E+01
j	$\omega(j)$	$F_{dy}(j)$	$\phi_{dy}(j)$	$F_{st}(j)$	$\phi_{st}(j)$
0	.00000E+00	.38206E-02	.31416E+01	.12695E-01	.00000E+00
1	.75604E+00	.39962E-02	-.12895E+01	.49158E-01	.42546E+00
2	.15121E+01	.27713E-02	-.17937E+01	.69614E-02	.84031E+00
3	.22681E+01	.40850E-03	-.92612E+00	.15257E-03	.14817E+01
4	.30241E+01	.21163E-03	.16553E+01	.16182E-03	-.14957E+01
5	.37802E+01	.32383E-03	.28420E+00	.54315E-04	.18058E+01
6	.45362E+01	.22839E-03	-.16010E+01	.11076E-03	.21895E+01
j	$\omega(j)$	$F_{lc}(j)$	$\phi_{lc}(j)$	$F_{in}(j)$	$\phi_{in}(j)$
0	.00000E+00	.10102E-01	.31416E+01	.12275E-02	.31416E+01
1	.75604E+00	.39204E-01	-.28195E+01	.95893E-02	.43471E+00
2	.15121E+01	.46391E-02	-.25814E+01	.10359E-03	.17061E+00
3	.22681E+01	.36261E-03	.23331E+01	.88151E-04	.14726E+01
4	.30241E+01	.12286E-04	-.28217E+01	.48850E-04	.19346E+01
5	.37802E+01	.21210E-03	-.28013E+01	.12230E-03	.63789E+00
6	.45362E+01	.27964E-03	.82329E+00	.13653E-03	.51306E+00

Table C.12: Run 17, Nondimensional Fourier Coefficients: Gain and Phase

j	$\omega(j)$	$A(j)$	$\phi_A(j)$	$F_{hy}(j)$	$\phi_{hy}(j)$
0	.00000E+00	.49489E-02	.31416E+01	.10808E-01	.00000E+00
1	.11478E+01	.96389E-01	.13636E+01	.41470E-01	-.20153E+01
2	.22956E+01	.50265E-03	-.29630E+00	.37110E-02	.20498E+01
3	.34434E+01	.26520E-03	.53561E+00	.39161E-03	-.11079E+01
4	.45912E+01	.56076E-04	-.39698E+00	.21924E-03	-.37017E+00
5	.57390E+01	.10928E-03	.25326E+01	.61786E-03	.23763E+01
6	.68868E+01	.10968E-03	-.12383E+01	.39037E-03	.48135E+00
j	$\omega(j)$	$F_{dy}(j)$	$\phi_{dy}(j)$	$F_{st}(j)$	$\phi_{st}(j)$
0	.00000E+00	.34911E-02	.31416E+01	.14300E-01	.00000E+00
1	.11478E+01	.11451E-01	.23837E+01	.46299E-01	-.17778E+01
2	.22956E+01	.38928E-02	.23890E+00	.59829E-02	.27339E+01
3	.34434E+01	.42007E-03	-.91992E+00	.81262E-04	-.29408E+01
4	.45912E+01	.40559E-03	-.61871E+00	.20048E-03	.22505E+01
5	.57390E+01	.66371E-03	.23719E+01	.45945E-04	-.82950E+00
6	.68868E+01	.39892E-03	.31984E+00	.64238E-04	.21044E+01
j	$\omega(j)$	$F_{lc}(j)$	$\phi_{lc}(j)$	$F_{in}(j)$	$\phi_{in}(j)$
0	.00000E+00	.12222E-01	.31416E+01	.14134E-02	.31416E+01
1	.11478E+01	.22188E-01	.89494E+00	.20513E-01	-.17647E+01
2	.22956E+01	.35378E-02	-.11208E+01	.20256E-03	.25803E+01
3	.34434E+01	.52696E-03	.19046E+01	.14749E-03	.15558E+01
4	.45912E+01	.52976E-04	-.22569E+01	.20893E-03	-.61357E+00
5	.57390E+01	.59149E-03	-.75251E+00	.27475E-04	.20983E+01
6	.68868E+01	.24553E-03	-.27970E+01	.15089E-03	.70511E+00

Table C.13: Run 18, Nondimensional Fourier Coefficients: Gain and Phase

j	$\omega(j)$	$A(j)$	$\phi_A(j)$	$F_{hy}(j)$	$\phi_{hy}(j)$
0	.00000E+00	.15497E-01	.00000E+00	.18527E-01	.00000E+00
1	.11466E+01	.11107E+00	.16450E+01	.64308E-01	-.21427E+01
2	.22933E+01	.18573E-02	.17124E+01	.37259E-02	.19535E+01
3	.34399E+01	.15830E-02	-.13920E+01	.96256E-02	-.55111E+00
4	.45866E+01	.53035E-03	.23465E+01	.37977E-02	-.80220E+00
5	.57332E+01	.62626E-03	-.11109E+01	.28605E-02	-.71019E+00
6	.68799E+01	.28269E-05	-.23278E+01	.11207E-02	-.31062E+01
j	$\omega(j)$	$F_{dy}(j)$	$\phi_{dy}(j)$	$F_{st}(j)$	$\phi_{st}(j)$
0	.00000E+00	.77864E-01	.00000E+00	.59337E-01	.31416E+01
1	.11466E+01	.38526E-01	-.29161E+01	.45543E-01	-.15105E+01
2	.22933E+01	.18851E-01	.30596E+01	.17501E-01	.10950E+00
3	.34399E+01	.85752E-02	-.45949E+00	.13401E-02	-.11765E+01
4	.45866E+01	.37093E-02	-.17927E+01	.35687E-02	.25154E+00
5	.57332E+01	.24266E-02	-.70062E+00	.43471E-03	-.76368E+00
6	.68799E+01	.22147E-02	-.28896E+01	.11458E-02	.46376E+00
j	$\omega(j)$	$F_{lc}(j)$	$\phi_{lc}(j)$	$F_{in}(j)$	$\phi_{in}(j)$
0	.00000E+00	.18208E-01	.31416E+01	.31875E-03	.00000E+00
1	.11466E+01	.47761E-01	.68625E+00	.23906E-01	-.14811E+01
2	.22933E+01	.50382E-02	-.13455E+01	.14786E-02	-.17515E+01
3	.34399E+01	.12459E-01	.23538E+01	.38362E-02	.17247E+01
4	.45866E+01	.23184E-02	.23384E+01	.14793E-02	-.80068E+00
5	.57332E+01	.59710E-02	.22840E+01	.31694E-02	.21511E+01
6	.68799E+01	.13101E-02	.25767E+00	.32885E-03	.11078E+01

Table C.14: Run 19, Nondimensional Fourier Coefficients: Gain and Phase

j	$\omega(j)$	$A(j)$	$\phi_A(j)$	$F_{hy}(j)$	$\phi_{hy}(j)$
0	.00000E+00	.98626E-02	.00000E+00	.43162E-01	.31416E+01
1	.15413E+01	.92012E-01	-.19787E+01	.45632E-01	.57147E+00
2	.30826E+01	.21002E-02	.11066E+01	.46910E-02	-.83565E-01
3	.46239E+01	.62513E-02	.30871E+00	.13555E-01	.47439E+00
4	.61652E+01	.26365E-03	.29368E+01	.20892E-02	.28394E+01
5	.77065E+01	.65859E-03	.23433E+01	.60303E-02	.24249E+01
6	.92478E+01	.33399E-03	-.22978E+01	.32771E-02	.24022E+01
j	$\omega(j)$	$F_{dy}(j)$	$\phi_{dy}(j)$	$F_{st}(j)$	$\phi_{st}(j)$
0	.00000E+00	.46338E-02	.00000E+00	.47796E-01	.31416E+01
1	.15413E+01	.24848E-01	-.39696E+00	.37614E-01	.11471E+01
2	.30826E+01	.13573E-01	.20343E+01	.16507E-01	-.86216E+00
3	.46239E+01	.14897E-01	.42869E+00	.14915E-02	-.31410E+01
4	.61652E+01	.30831E-02	.23051E+01	.16683E-02	-.15280E+01
5	.77065E+01	.64857E-02	.24366E+01	.46125E-03	-.55087E+00
6	.92478E+01	.32083E-02	.21572E+01	.79538E-03	-.25187E+01
j	$\omega(j)$	$F_{lc}(j)$	$\phi_{lc}(j)$	$F_{in}(j)$	$\phi_{in}(j)$
0	.00000E+00	.43315E-01	.00000E+00	.15313E-03	.00000E+00
1	.15413E+01	.26195E-01	.28123E+01	.35831E-01	.11817E+01
2	.30826E+01	.69075E-02	-.28516E+01	.30630E-02	-.22586E+01
3	.46239E+01	.36173E-01	-.27350E+01	.22668E-01	-.27756E+01
4	.61652E+01	.35421E-02	-.29900E+00	.14529E-02	-.29444E+00
5	.77065E+01	.13614E-01	-.72386E+00	.75839E-02	-.72956E+00
6	.92478E+01	.47918E-02	.25719E+00	.40794E-02	.99747E+00

Table C.15: Run 20, Nondimensional Fourier Coefficients: Gain and Phase

j	$\omega(j)$	$A(j)$	$\phi_A(j)$	$F_{hy}(j)$	$\phi_{hy}(j)$
0	.00000E+00	.53083E-02	.31416E+01	.77118E-01	.31416E+01
1	.90877E+00	.12240E+00	-.35968E+00	.63628E-01	.21009E+01
2	.18175E+01	.49380E-03	-.16256E+01	.14384E-01	-.26903E+01
3	.27263E+01	.22116E-03	.67554E+00	.11618E-02	.14668E+01
4	.36351E+01	.22173E-03	.10101E+01	.27081E-02	.64529E+00
5	.45438E+01	.43068E-04	-.16858E+00	.34690E-02	-.14251E+01
6	.54526E+01	.17638E-04	-.15038E+01	.25511E-02	-.29429E+01
j	$\omega(j)$	$F_{dy}(j)$	$\phi_{dy}(j)$	$F_{st}(j)$	$\phi_{st}(j)$
0	.00000E+00	.20052E-01	.31416E+01	.57066E-01	.31416E+01
1	.90877E+00	.40176E-01	.13244E+01	.44893E-01	.27788E+01
2	.18175E+01	.18983E-01	-.14997E+01	.19094E-01	.24166E+01
3	.27263E+01	.13530E-02	.15230E+01	.20382E-03	-.12923E+01
4	.36351E+01	.61345E-02	.12871E+01	.42838E-02	-.14664E+01
5	.45438E+01	.31644E-02	-.13647E+01	.36433E-03	-.19765E+01
6	.54526E+01	.39280E-02	-.26362E+01	.16826E-02	.98090E+00
j	$\omega(j)$	$F_{lc}(j)$	$\phi_{lc}(j)$	$F_{in}(j)$	$\phi_{in}(j)$
0	.00000E+00	.77684E-01	.00000E+00	.56546E-03	.00000E+00
1	.90877E+00	.52001E-01	-.12457E+01	.16544E-01	.27950E+01
2	.18175E+01	.14604E-01	.44447E+00	.24103E-03	.22577E-01
3	.27263E+01	.10754E-02	-.17757E+01	.14198E-03	.23340E+01
4	.36351E+01	.28889E-02	-.25215E+01	.19408E-03	-.28810E+01
5	.45438E+01	.34316E-02	.17137E+01	.38660E-04	-.11727E+01
6	.54526E+01	.26421E-02	.22252E+00	.10995E-03	.80745E+00

Table C.16: Run 21, Nondimensional Fourier Coefficients: Gain and Phase

j	$\omega(j)$	$A(j)$	$\phi_A(j)$	$F_{hy}(j)$	$\phi_{hy}(j)$
0	.00000E+00	.54245E-02	.31416E+01	.69884E-01	.31416E+01
1	.75528E+00	.10465E+00	-.67230E+00	.56732E-01	.18302E+01
2	.15106E+01	.40534E-03	-.22521E+01	.13323E-01	-.31410E+01
3	.22659E+01	.24738E-03	-.37246E+00	.32185E-02	-.24544E-01
4	.30211E+01	.20734E-03	-.15729E+00	.21840E-02	-.20495E+01
5	.37764E+01	.13235E-03	-.95699E+00	.33326E-02	.21538E+01
6	.45317E+01	.65777E-04	-.14876E+01	.27224E-02	.18476E+00
j	$\omega(j)$	$F_{dy}(j)$	$\phi_{dy}(j)$	$F_{st}(j)$	$\phi_{st}(j)$
0	.00000E+00	.20925E-01	.31416E+01	.48960E-01	.31416E+01
1	.75528E+00	.34418E-01	.11000E+01	.38647E-01	.24663E+01
2	.15106E+01	.18939E-01	-.21058E+01	.16693E-01	.17923E+01
3	.22659E+01	.32400E-02	-.55387E-01	.10189E-03	.17436E+01
4	.30211E+01	.23761E-02	-.19418E+00	.36509E-02	-.27242E+01
5	.37764E+01	.29918E-02	.20778E+01	.41671E-03	.27297E+01
6	.45317E+01	.23828E-02	.71389E+00	.13746E-02	-.88071E+00
j	$\omega(j)$	$F_{lc}(j)$	$\phi_{lc}(j)$	$F_{in}(j)$	$\phi_{in}(j)$
0	.00000E+00	.70532E-01	.00000E+00	.64709E-03	.00000E+00
1	.75528E+00	.49329E-01	-.14314E+01	.97505E-02	.24809E+01
2	.15106E+01	.13447E-01	-.43668E-02	.14089E-03	-.48984E+00
3	.22659E+01	.31939E-02	.30836E+01	.10994E-03	.13043E+01
4	.30211E+01	.22280E-02	.11117E+01	.61767E-04	.18793E+01
5	.37764E+01	.33334E-02	-.98717E+00	.23342E-05	.24154E+00
6	.45317E+01	.26714E-02	-.29286E+01	.91675E-04	-.78204E+00

Table C.17: Run 22, Nondimensional Fourier Coefficients: Gain and Phase

j	$\omega(j)$	$A(j)$	$\phi_A(j)$	$F_{hy}(j)$	$\phi_{hy}(j)$
0	.00000E+00	.65468E-02	.31416E+01	.34316E-01	.31416E+01
1	.15444E+01	.54402E-01	.43332E+00	.26147E-01	.30400E+01
2	.30889E+01	.22047E-03	.22759E+00	.12911E-02	-.17250E+01
3	.46333E+01	.87392E-04	.22433E+01	.69507E-03	.21515E+01
4	.61778E+01	.74737E-04	-.12963E+01	.27472E-03	.20944E+01
5	.77222E+01	.11435E-03	.22934E+01	.82594E-04	.26658E+01
6	.92667E+01	.10210E-03	-.16871E+01	.27884E-02	.55135E+00
j	$\omega(j)$	$F_{dy}(j)$	$\phi_{dy}(j)$	$F_{st}(j)$	$\phi_{st}(j)$
0	.00000E+00	.97429E-02	.31416E+01	.24573E-01	.31416E+01
1	.15444E+01	.13605E-01	.22178E+01	.19611E-01	-.27099E+01
2	.30889E+01	.78464E-02	.77579E+00	.89148E-02	-.22791E+01
3	.46333E+01	.11229E-02	.17715E+01	.54255E-03	-.18653E+01
4	.61778E+01	.14419E-02	-.14880E+01	.16944E-02	.17228E+01
5	.77222E+01	.25521E-03	-.12775E+01	.31823E-03	.20517E+01
6	.92667E+01	.25143E-02	.77732E+00	.65700E-03	-.47891E+00
j	$\omega(j)$	$F_{lc}(j)$	$\phi_{lc}(j)$	$F_{in}(j)$	$\phi_{in}(j)$
0	.00000E+00	.34969E-01	.00000E+00	.65325E-03	.00000E+00
1	.15444E+01	.13736E-01	-.10417E+01	.21184E-01	-.26920E+01
2	.30889E+01	.15150E-02	.14288E+01	.22459E-03	.14985E+01
3	.46333E+01	.69949E-03	-.10579E+01	.47456E-04	-.25016E+01
4	.61778E+01	.23861E-03	-.68994E+00	.97889E-04	.10738E+01
5	.77222E+01	.21011E-03	-.29632E+01	.28019E-03	.31397E+01
6	.92667E+01	.10326E-03	.27011E+01	.27333E-02	.58297E+00

Table C.18: Run 23, Nondimensional Fourier Coefficients: Gain and Phase

j	$\omega(j)$	$A(j)$	$\phi_A(j)$	$F_{hy}(j)$	$\phi_{hy}(j)$
0	.00000E+00	.79935E-03	.31416E+01	.39726E-01	.31416E+01
1	.11420E+01	.71180E-01	-.20254E+01	.44099E-01	.57158E+00
2	.22841E+01	.18744E-03	.11234E+01	.11784E-02	.45264E+00
3	.34261E+01	.12346E-03	.24158E+01	.31425E-02	.13861E+01
4	.45681E+01	.43767E-04	-.13560E+01	.18490E-02	-.12455E+01
5	.57102E+01	.14226E-03	-.12597E+01	.74005E-03	.25817E+01
6	.68522E+01	.13645E-03	.20194E+00	.91892E-03	.14968E+01
j	$\omega(j)$	$F_{dy}(j)$	$\phi_{dy}(j)$	$F_{st}(j)$	$\phi_{st}(j)$
0	.00000E+00	.48465E-02	.31416E+01	.34879E-01	.31416E+01
1	.11420E+01	.25010E-01	-.29053E-01	.27394E-01	.11137E+01
2	.22841E+01	.11428E-01	.21272E+01	.11609E-01	-.91327E+00
3	.34261E+01	.31493E-02	.14001E+01	.44368E-04	-.33202E+00
4	.45681E+01	.13443E-02	.42699E+00	.23938E-02	-.18383E+01
5	.57102E+01	.66525E-03	.26309E+01	.82380E-04	.21731E+01
6	.68522E+01	.16268E-02	.94531E+00	.97180E-03	-.27146E+01
j	$\omega(j)$	$F_{lc}(j)$	$\phi_{lc}(j)$	$F_{in}(j)$	$\phi_{in}(j)$
0	.00000E+00	.40399E-01	.00000E+00	.67282E-03	.00000E+00
1	.11420E+01	.32258E-01	-.28220E+01	.15168E-01	.11305E+01
2	.22841E+01	.13672E-02	-.27923E+01	.22983E-03	.29338E+01
3	.34261E+01	.31714E-02	-.17777E+01	.75929E-04	-.29461E+01
4	.45681E+01	.18349E-02	.18820E+01	.29575E-04	-.17808E+00
5	.57102E+01	.70456E-03	-.45320E+00	.84809E-04	.14953E+01
6	.68522E+01	.96811E-03	-.20092E+01	.34535E-03	.30259E+01

Table C.19: Run 24, Nondimensional Fourier Coefficients: Gain and Phase

j	$\omega(j)$	$A(j)$	$\phi_A(j)$	$F_{hy}(j)$	$\phi_{hy}(j)$
0	.00000E+00	.26433E-02	.31416E+01	.38847E-01	.31416E+01
1	.90790E+00	.52932E-01	-.15097E+01	.34452E-01	.10778E+01
2	.18158E+01	.61008E-04	.17223E+01	.22059E-02	.18157E+01
3	.27237E+01	.10521E-03	.28961E+01	.10030E-02	.17309E+01
4	.36316E+01	.16114E-03	-.30109E+01	.83719E-03	-.68674E+00
5	.45395E+01	.20159E-03	-.13763E+01	.93514E-03	.28295E+01
6	.54474E+01	.20744E-03	.79044E-02	.46451E-03	.53958E+00
j	$\omega(j)$	$F_{dy}(j)$	$\phi_{dy}(j)$	$F_{st}(j)$	$\phi_{st}(j)$
0	.00000E+00	.13554E-01	.31416E+01	.25293E-01	.31416E+01
1	.90790E+00	.20373E-01	.53652E+00	.19973E-01	.16313E+01
2	.18158E+01	.92026E-02	.30232E+01	.86677E-02	.12184E+00
3	.27237E+01	.11633E-02	.17494E+01	.16163E-03	-.12767E+01
4	.36316E+01	.13929E-02	-.24157E+01	.17345E-02	.22907E+00
5	.45395E+01	.10011E-02	.27075E+01	.13515E-03	-.14352E+01
6	.54474E+01	.22784E-03	-.30410E+01	.67770E-03	.39619E+00
j	$\omega(j)$	$F_{lc}(j)$	$\phi_{lc}(j)$	$F_{in}(j)$	$\phi_{in}(j)$
0	.00000E+00	.39867E-01	.00000E+00	.10205E-02	.00000E+00
1	.90790E+00	.28707E-01	-.21967E+01	.71036E-02	.16432E+01
2	.18158E+01	.22652E-02	-.13520E+01	.83195E-04	-.21158E+01
3	.27237E+01	.10687E-02	-.14719E+01	.91298E-04	-.22087E+01
4	.36316E+01	.78775E-03	.25193E+01	.72005E-04	-.14689E+01
5	.45395E+01	.10922E-02	-.17975E+00	.20627E-03	.46168E+00
6	.54474E+01	.48367E-03	-.30002E+01	.18848E-03	.20111E+01

Table C.20: Run 25, Nondimensional Fourier Coefficients: Gain and Phase

j	$\omega(j)$	$A(j)$	$\phi_A(j)$	$F_{hy}(j)$	$\phi_{hy}(j)$
0	.00000E+00	.29768E-02	.31416E+01	.58864E-01	.31416E+01
1	.75453E+00	.80626E-01	-.30718E+01	.46895E-01	-.54958E+00
2	.15091E+01	.35867E-03	-.12234E+01	.89443E-02	-.14772E+01
3	.22636E+01	.15145E-03	-.15853E+01	.18190E-02	-.43920E+00
4	.30181E+01	.34425E-04	-.27569E+01	.15228E-02	.15093E+01
5	.37727E+01	.39221E-04	-.13243E+01	.23422E-02	-.27403E+01
6	.45272E+01	.11483E-04	.31379E+00	.19622E-02	-.11628E+01
j	$\omega(j)$	$F_{dy}(j)$	$\phi_{dy}(j)$	$F_{st}(j)$	$\phi_{st}(j)$
0	.00000E+00	.20292E-01	.31416E+01	.38573E-01	.31416E+01
1	.75453E+00	.28204E-01	-.12220E+01	.30416E-01	.66161E-01
2	.15091E+01	.15581E-01	-.47938E+00	.13102E-01	-.30100E+01
3	.22636E+01	.17264E-02	-.46985E+00	.10736E-03	.76256E-01
4	.30181E+01	.26570E-02	.28293E+01	.27148E-02	.26214E+00
5	.37727E+01	.21767E-02	-.27210E+01	.17102E-03	-.29876E+01
6	.45272E+01	.22466E-02	-.64021E+00	.11215E-02	-.27198E+01
j	$\omega(j)$	$F_{lc}(j)$	$\phi_{lc}(j)$	$F_{in}(j)$	$\phi_{in}(j)$
0	.00000E+00	.59844E-01	.00000E+00	.97944E-03	.00000E+00
1	.75453E+00	.41091E-01	.24843E+01	.74857E-02	.81757E-01
2	.15091E+01	.90670E-02	.16547E+01	.15058E-03	.10411E+01
3	.22636E+01	.17236E-02	.26713E+01	.11014E-03	.69441E-01
4	.30181E+01	.14781E-02	-.16223E+01	.47160E-04	.11901E+01
5	.37727E+01	.24419E-02	.37373E+00	.11961E-03	-.19692E+00
6	.45272E+01	.19745E-02	.19824E+01	.14253E-04	.25140E+01

Table C.21: Run 26, Nondimensional Fourier Coefficients: Gain and Phase

j	$\omega(j)$	$A(j)$	$\phi_A(j)$	$F_{hy}(j)$	$\phi_{hy}(j)$
0	.00000E+00	.22042E-01	.00000E+00	.56993E-01	.31416E+01
1	.15429E+01	.93334E-01	-.27806E+01	.46324E-01	-.21152E+00
2	.30857E+01	.23754E-02	-.42320E+00	.37485E-02	-.18316E+01
3	.46286E+01	.74645E-02	-.20661E+01	.16370E-01	-.19127E+01
4	.61715E+01	.48807E-03	.35321E+00	.24425E-02	-.44493E+00
5	.77144E+01	.13507E-02	-.15452E+01	.10974E-01	-.14123E+01
6	.92572E+01	.67506E-04	-.21451E+01	.27132E-02	.57440E-01
j	$\omega(j)$	$F_{dy}(j)$	$\phi_{dy}(j)$	$F_{st}(j)$	$\phi_{st}(j)$
0	.00000E+00	.39978E-02	.31416E+01	.52995E-01	.31416E+01
1	.15429E+01	.24557E-01	-.12879E+01	.40859E-01	.34597E+00
2	.30857E+01	.13771E-01	.51215E+00	.16607E-01	-.24672E+01
3	.46286E+01	.17187E-01	-.19505E+01	.10343E-02	.54919E+00
4	.61715E+01	.30666E-02	-.74023E+00	.10188E-02	.16291E+01
5	.77144E+01	.12266E-01	-.14083E+01	.12924E-02	.17669E+01
6	.92572E+01	.24593E-02	.36056E+00	.82028E-03	-.10509E+01
j	$\omega(j)$	$F_{lc}(j)$	$\phi_{lc}(j)$	$F_{in}(j)$	$\phi_{in}(j)$
0	.00000E+00	.57608E-01	.00000E+00	.61503E-03	.00000E+00
1	.15429E+01	.25904E-01	.20293E+01	.36423E-01	.37979E+00
2	.30857E+01	.57167E-02	.18976E+01	.33261E-02	.25725E+01
3	.46286E+01	.43464E-01	.11615E+01	.27153E-01	.11208E+01
4	.61715E+01	.49501E-02	-.30548E+01	.31027E-02	-.26443E+01
5	.77144E+01	.25363E-01	.17033E+01	.14395E-01	.16834E+01
6	.92572E+01	.14989E-02	.27884E+01	.14665E-02	.47768E+00

Table C.22: Run 28, Nondimensional Fourier Coefficients: Gain and Phase

j	$\omega(j)$	$A(j)$	$\phi_A(j)$	$F_{hy}(j)$	$\phi_{hy}(j)$
0	.00000E+00	.45881E-02	.31416E+01	.82986E-01	.31416E+01
1	.90790E+00	.14043E+00	.43014E+00	.72253E-01	.29088E+01
2	.18158E+01	.19620E-02	-.89161E+00	.16584E-01	-.11280E+01
3	.27237E+01	.24157E-02	.12001E+01	.17728E-02	.28427E+01
4	.36316E+01	.75401E-03	-.22173E+01	.43471E-02	-.20818E+01
5	.45395E+01	.83550E-03	-.85447E+00	.24573E-02	.26538E+01
6	.54474E+01	.88297E-04	-.24439E+01	.31560E-02	.22267E+01
j	$\omega(j)$	$F_{dy}(j)$	$\phi_{dy}(j)$	$F_{st}(j)$	$\phi_{st}(j)$
0	.00000E+00	.18381E-01	.31416E+01	.64605E-01	.31416E+01
1	.90790E+00	.44226E-01	.21365E+01	.50974E-01	-.27241E+01
2	.18158E+01	.22005E-01	.54380E-01	.21974E-01	-.23139E+01
3	.27237E+01	.15051E-02	.28265E+01	.26903E-03	.29339E+01
4	.36316E+01	.88238E-02	-.17465E+01	.49308E-02	.16894E+01
5	.45395E+01	.20298E-02	.29038E+01	.70199E-03	.18569E+01
6	.54474E+01	.48085E-02	.23579E+01	.17296E-02	-.54276E+00
j	$\omega(j)$	$F_{lc}(j)$	$\phi_{lc}(j)$	$F_{in}(j)$	$\phi_{in}(j)$
0	.00000E+00	.83865E-01	.00000E+00	.87975E-03	.00000E+00
1	.90790E+00	.58680E-01	-.43672E+00	.18972E-01	-.26975E+01
2	.18158E+01	.17652E-01	.20149E+01	.10680E-02	.20353E+01
3	.27237E+01	.35100E-02	-.14377E+01	.32021E-02	-.19646E+01
4	.36316E+01	.55018E-02	.95342E+00	.12662E-02	.58050E+00
5	.45395E+01	.77113E-03	.13934E+01	.27911E-02	.23876E+01
6	.54474E+01	.34787E-02	-.75486E+00	.62028E-03	.19070E+00

Table C.23: Run 29, Nondimensional Fourier Coefficients: Gain and Phase

j	$\omega(j)$	$A(j)$	$\phi_A(j)$	$F_{hy}(j)$	$\phi_{hy}(j)$
0	.00000E+00	.57326E-02	.31416E+01	.93186E-01	.31416E+01
1	.75378E+00	.15217E+00	-.14544E+01	.74592E-01	.10472E+01
2	.15076E+01	.34284E-03	.13123E+01	.21802E-01	.13746E+01
3	.22613E+01	.24273E-03	-.25320E+01	.65166E-02	-.29576E+01
4	.30151E+01	.41177E-03	.31310E+01	.24721E-02	.78713E+00
5	.37689E+01	.42920E-04	.26859E+01	.49719E-02	-.20831E+01
6	.45227E+01	.11473E-03	-.28669E+01	.40914E-02	.12189E+01
j	$\omega(j)$	$F_{dy}(j)$	$\phi_{dy}(j)$	$F_{st}(j)$	$\phi_{st}(j)$
0	.00000E+00	.23510E-01	.31416E+01	.69675E-01	.31416E+01
1	.75378E+00	.44724E-01	.23375E+00	.54593E-01	.16848E+01
2	.15076E+01	.24116E-01	.24041E+01	.22695E-01	.22966E+00
3	.22613E+01	.65139E-02	-.28096E+01	.96336E-03	.18316E+01
4	.30151E+01	.33652E-02	-.29481E+01	.55881E-02	.44353E+00
5	.37689E+01	.47967E-02	-.21463E+01	.35522E-03	-.10595E+01
6	.45227E+01	.24614E-02	.17028E+01	.22292E-02	.67940E+00
j	$\omega(j)$	$F_{lc}(j)$	$\phi_{lc}(j)$	$F_{in}(j)$	$\phi_{in}(j)$
0	.00000E+00	.94049E-01	.00000E+00	.86298E-03	.00000E+00
1	.75378E+00	.63903E-01	-.22296E+01	.14184E-01	.16996E+01
2	.15076E+01	.21948E-01	-.17714E+01	.17616E-03	-.23566E+01
3	.22613E+01	.65503E-02	.15398E+00	.19914E-03	-.12318E+01
4	.30151E+01	.25904E-02	-.22617E+01	.26279E-03	-.12037E+01
5	.37689E+01	.49950E-02	.10371E+01	.10934E-03	-.31073E+00
6	.45227E+01	.41363E-02	-.18671E+01	.23289E-03	-.51840E+00

Table C.24: Run 30, Nondimensional Fourier Coefficients: Gain and Phase

j	$\omega(j)$	$A(j)$	$\phi_A(j)$	$F_{hy}(j)$	$\phi_{hy}(j)$
0	.00000E+00	.14502E-02	.00000E+00	.69958E-01	.31416E+01
1	.11432E+01	.11918E+00	.27616E+01	.69220E-01	-.10413E+01
2	.22864E+01	.24440E-02	-.22564E+01	.33970E-02	-.24300E+01
3	.34295E+01	.55081E-02	.19750E+01	.15036E-01	.28447E+01
4	.45727E+01	.36868E-03	.18668E+01	.72910E-02	-.29134E+01
5	.57159E+01	.46542E-03	-.13666E+01	.18584E-02	-.14165E+01
6	.68591E+01	.26898E-03	-.28867E+00	.14078E-02	-.23938E+01
j	$\omega(j)$	$F_{dy}(j)$	$\phi_{dy}(j)$	$F_{st}(j)$	$\phi_{st}(j)$
0	.00000E+00	.12969E-01	.31416E+01	.56989E-01	.31416E+01
1	.11432E+01	.42834E-01	-.17282E+01	.45176E-01	-.39625E+00
2	.22864E+01	.20228E-01	-.97282E+00	.20128E-01	.23372E+01
3	.34295E+01	.15510E-01	.27649E+01	.13071E-02	-.15370E+01
4	.45727E+01	.75237E-02	.29192E+01	.33168E-02	-.14994E+01
5	.57159E+01	.21229E-02	-.15230E+01	.33864E-03	.99570E+00
6	.68591E+01	.25457E-02	-.23283E+01	.11446E-02	.89380E+00
j	$\omega(j)$	$F_{lc}(j)$	$\phi_{lc}(j)$	$F_{in}(j)$	$\phi_{in}(j)$
0	.00000E+00	.70631E-01	.00000E+00	.67357E-03	.00000E+00
1	.11432E+01	.51853E-01	.17867E+01	.25526E-01	-.36419E+00
2	.22864E+01	.54345E-02	.69402E+00	.20389E-02	.66470E+00
3	.34295E+01	.23838E-01	-.65023E+00	.11034E-01	-.11412E+01
4	.45727E+01	.74555E-02	.98690E-01	.96799E-03	-.12369E+01
5	.57159E+01	.45222E-02	.18651E+01	.26946E-02	.19616E+01
6	.68591E+01	.16840E-02	.22013E+01	.20647E-02	.29452E+01

The University of Michigan is an equal opportunity/ affirmative action employer. Under applicable federal and state laws, including Title IX of the Education Amendments of 1972, the University does not discriminate on the basis of sex, race, or other prohibited matters in employment, in educational programs and activities, or in admissions. Inquiries or complaints may be addressed to the University's Director of Affirmative Action and Title IX Compliance: Dr. Gwendolyn C. Baker, 5072 Administration Building, 763-0235.